



Delft University of Technology

Towards the Integration of Additive Manufacturing for Freeform Steel and Glass Façade Construction

Tramontini, L.M.

DOI

[10.71690/abe.2024.08](https://doi.org/10.71690/abe.2024.08)

Publication date

2024

Document Version

Final published version

Citation (APA)

Tramontini, L. M. (2024). *Towards the Integration of Additive Manufacturing for Freeform Steel and Glass Façade Construction*. [Dissertation (TU Delft), Delft University of Technology]. A+BE | Architecture and the Built Environment. <https://doi.org/10.71690/abe.2024.08>

Important note

To cite this publication, please use the final published version (if applicable).
Please check the document version above.

Copyright

Other than for strictly personal use, it is not permitted to download, forward or distribute the text or part of it, without the consent of the author(s) and/or copyright holder(s), unless the work is under an open content license such as Creative Commons.

Takedown policy

Please contact us and provide details if you believe this document breaches copyrights.
We will remove access to the work immediately and investigate your claim.



Towards the Integration of Additive Manufacturing for Freeform Steel and Glass Façade Construction

Lia Tramontini

Towards the Integration of Additive Manufacturing for Freeform Steel and Glass Façade Construction

Lia Tramontini



24#08

Design | Sirene Ontwerpers, Véro Crickx

Cover photo | Structural node fabricated using laser powder bed fusion by Lia Tramontini

Keywords | Freeform architecture, Façades, Additive manufacturing, Mass-customized fabrication

ISBN 978-94-6366-848-4

ISSN 2212-3202

© 2024 Lia Tramontini

This dissertation is open access at <https://doi.org/10.7480/abe.2024.08>

Attribution 4.0 International (CC BY 4.0)

This is a human-readable summary of (and not a substitute for) the license that you'll find at:
<https://creativecommons.org/licenses/by/4.0/>

You are free to:

Share — copy and redistribute the material in any medium or format

Adapt — remix, transform, and build upon the material

for any purpose, even commercially.

This license is acceptable for Free Cultural Works.

The licensor cannot revoke these freedoms as long as you follow the license terms.

Under the following terms:

Attribution — You must give appropriate credit, provide a link to the license, and indicate if changes were made. You may do so in any reasonable manner, but not in any way that suggests the licensor endorses you or your use.

Unless otherwise specified, all the photographs in this thesis were taken by the author. For the use of illustrations effort has been made to ask permission for the legal owners as far as possible. We apologize for those cases in which we did not succeed. These legal owners are kindly requested to contact the author.

Towards the Integration of Additive Manufacturing for Freeform Steel and Glass Façade Construction

Dissertation

for the purpose of obtaining the degree of doctor
at Delft University of Technology
by the authority of the Rector Magnificus, prof.dr.ir. T.H.J.J. van der Hagen
chair of the Board for Doctorates
to be defended publicly on
Thursday 18 April 2024 at 15:00 o'clock

by

Lia Marie TRAMONTINI
Master of Science in Architecture, Urbanism and Building Sciences,
Delft University of Technology, Netherlands
born in Sudbury, Canada

This dissertation has been approved by the promotor.

Composition of the doctoral committee:

Rector Magnificus,	chairperson
Prof. Dr.-Ing. U. Knaack	Delft University of Technology, promotor
Dr. M. Turrin	Delft University of Technology, promotor
Prof. Dr.-Ing T. Klein †	Delft University of Technology, promotor

Independent members:

Prof. Dr.-Ing. M. Overend	Delft University of Technology
Dr.-Ing. M. Oppe	knippershelbig GmbH
Associate Prof. Dr. B. Peters	University of Toronto
Associate Prof. Dr.-Ing. J.C.U. Wurm	Katholieke Universiteit Leuven
Prof.-Ing. J. O'Callaghan	Delft University of Technology, reserve member

Other members:

Dr.-Ing. A. Luna Navarro	Delft University of Technology
--------------------------	--------------------------------

This study was financed by the following organizations:

- La Fondation Baxter et Alma Ricard
- Jansen AG

Cette étude a été financée par les organisations suivantes :

- La Fondation Baxter et Alma Ricard
- Jansen AG

Dédié à Maman et Papa,

*Merci pour votre encouragement et soutien constants et indéfectibles.
Chaque réussite et chaque succès futur reposent
sur les fondations que vous m'avez données.*

*Thank you for a lifetime of unwavering encouragement and support.
Every current achievement and future success is built
on the foundation you've given me.*

Contents

List of Tables	13
List of Figures	14
List of Acronyms	21
Summary	23
Samenvatting	27
Résumé	31

1	Introduction	35
---	---------------------	----

1.1	Background	35
1.1.1	Freeform steel and glass façades	35
1.1.2	Typical steel and glass façade construction	36
1.1.3	Systemized façade construction	38
1.1.4	Additive manufacturing	39
1.2	Problem statement	41
1.2.1	Complexity of freeform steel and glass façade design and construction	41
1.2.2	Geometrical complexity at nodal conditions	41
1.2.3	Quality façade performance	42
1.2.4	Additive Manufacturing: an opportunity	43
1.2.5	The AM learning curve	43
1.3	Research objective and questions	45
1.3.1	Aim	45
1.3.2	Research questions	45
1.4	Research strategy	47
1.4.1	Research methods and organization	47
1.5	Research impact	50
1.5.1	Societal relevance	50
1.5.2	Scientific relevance	51

2 Freeform Steel and Glass Façade Construction 53

A review of detailed design strategies for the construction of freeform steel and glass façade precedents

- 2.1 **Introduction** 54
 - 2.1.1 Previous research 55
 - 2.1.2 Precedents selection 57
- 2.2 **Structural node typologies** 66
 - 2.2.1 Multi-axis: hollow 68
 - 2.2.2 Multi-axis: solid 70
 - 2.2.3 Multi-axis: built-up 71
 - 2.2.4 Single-axis: faceted 72
 - 2.2.5 Single-axis: cylindrical 73
 - 2.2.6 Single-axis: bisecting 74
 - 2.2.7 Stacked connection 76
 - 2.2.8 Direct connection 77
- 2.3 **Enclosure system typologies** 78
 - 2.3.1 Direct glazing 78
 - 2.3.2 Secondary profile 80
 - 2.3.3 Offset point-supports 81
 - 2.3.4 Cassette system 83
 - 2.3.5 Mega-panel system 85
 - 2.3.6 Variations in joining methods for the interior drainage layer 86
- 2.4 **Opportunities for the use of additive manufacturing in freeform steel and glass façade construction** 90
 - 2.4.1 Opportunities for AM structural nodes 90
 - 2.4.2 Opportunities for AM in the enclosure system 95
- 2.5 **Conclusion** 99

3 Additively Manufactured Nodes and Connections 103

A literature review on the use of additive manufacturing for façade nodes and connections

- 3.1 **Introduction** 104
- 3.2 **Literature selection and overview** 104
- 3.3 **Literature review findings** 106
 - 3.3.1 Use of AM in façades 106
 - 3.3.2 AM nodes and connections 106
- 3.4 **Identification of research gaps** 116
 - 3.4.1 Gasket nodes 116
 - 3.4.2 Systemized topology 117
 - 3.4.3 Metal printing technologies 118
 - 3.4.4 AM in the AEC industry 119
- 3.5 **Conclusion** 120

4 Additive Manufacturing for Structural Nodes 123

Methods, materials, design, and analysis

- 4.1 **Introduction** 124
- 4.2 **Metal additive manufacturing methods** 125
 - 4.2.1 Overview of metal additive manufacturing methods 125
 - 4.2.2 Preliminary comparison of metal AM methods 129
 - 4.2.3 Selection of metal AM methods 131
- 4.3 **Material properties of stainless steel 316L fabricated using PBF-L, DED-L, and DED-GMA** 132
 - 4.3.1 Summary of requirements for steel structures per Eurocode standards 132
 - 4.3.2 Mechanical properties of AM SS316L 135
 - 4.3.2.1 Ductility 142
 - 4.3.2.2 Fracture toughness 145
 - 4.3.2.3 Fatigue strength 148
 - 4.3.2.4 Ultimate tensile strength, yield strength/0.2% proof strength, and elastic modulus 150
 - 4.3.3 Discussion on the mechanical properties of AM SS316L 152

4.4 **Design guidelines for metal DED and PBF additive manufacturing** 154

4.5 **Design, fabrication, and analysis of AM structural nodes** 158

4.5.1 Design boundary conditions 159

4.5.2 Structural node designs 162

4.5.2.1 Design of benchmark CNC-milled node 162

4.5.2.2 Design of DED-GMA node 163

4.5.2.3 Design of DED-L node 164

4.5.2.4 Design of PBF-L node 165

4.5.3 Node fabrication 166

4.5.3.1 Benchmark CNC node fabrication simulation 166

4.5.3.2 DED-GMA node fabrication process 167

4.5.3.3 DED-L node fabrication process 170

4.5.3.4 PBF-L node fabrication process 172

4.6 **Results and discussion** 176

4.6.1 Fabrication times and material usage 177

4.6.2 Reflection on the design and fabrication of nodes 180

4.6.2.1 Reflection on the design and fabrication of the CNC node 180

4.6.2.2 Reflection on the design and fabrication of DED nodes 183

4.6.2.3 Reflection on the design and fabrication of the PBF-L node 190

4.6.2.4 General reflection 193

4.6.3 Recommendations 196

4.7 **Conclusion** 197

5 **Additive Manufacturing for Gasket Nodes** 201

Materials, methods, and proof of concept

5.1 **Introduction** 202

5.2 **Materials for AM gaskets** 203

5.2.1 Performance requirements for gaskets 203

5.2.2 AM elastomeric materials 207

5.3 **Printing methods for AM gasket nodes** 209

5.4 **Design, fabrication and analysis of gasket nodes** 212

5.4.1 Preliminary prototypes 212

5.4.2 Final gasket node prototype 214

5.4.3 Evaluation of AM gasket node solution 218

5.5 Conclusion 220

6 Additive Manufacturing in Practice 223

A case study for the integration of AM into the design, engineering, and execution of freeform steel and glass façade construction

6.1 Introduction 224

6.2 The case study 227

6.3 Interdisciplinary collaboration for the design and development of structural nodes 230

6.3.1 Overall façade design 230

6.3.2 Structural node design 234

6.3.3 Digital fabrication design 244

6.3.4 Entwined interests of project stakeholders 245

6.4 Design and development of node gaskets 249

6.5 Interdisciplinary digital workflows in AM FFSGF 252

6.5.1 Architectural design and rationalization 254

6.5.2 Global parameter integration 256

6.5.3 Overall structural analysis 257

6.5.4 Local structural analysis 257

6.5.5 Local parameter integration and fabrication 258

6.5.6 CAM modelling 260

6.6 Reflection and discussion 261

6.6.1 Reflection on the proposed project workflows 261

6.6.1.1 Overall design and connection design 261

6.6.1.2 Structural node design and refinement 262

6.6.1.3 Prototyping 264

6.6.1.4 Digital fabrication design 266

6.6.1.5 Gasket node design 266

6.6.2	Reflection on the proposed digital workflow	267
6.6.3	Recommendations for the interdisciplinary development of AM parts for buildings	270

6.7	Conclusion	272
-----	-------------------	-----

7	Conclusion	275
---	-------------------	-----

7.1	Introduction	275
7.2	Research Sub-questions	276
7.3	Main Research Question	281
7.4	General Conclusions	283
7.4.1	Limitations of the research	283
7.4.2	Future Research	284
7.5	Final Remarks	291

	Bibliography	293
	Appendix A	301
	Curriculum Vitae	306
	Publications	307

List of Tables

2.1	Cases studies for the exploration of structural and enclosure system typologies	58	4.11	Parameters and simulated fabrication time for CNC milled node	167
2.2	Relative ranking of structural node typologies	91	4.12	Process parameters for DED-GMA node additive manufacturing	168
2.3	Rubric explaining relative node rankings	92	4.13	Process parameters for DED-L node additive manufacturing	170
2.4	Comparison of node solutions for internal drainage layer	98	4.14	Process parameters for DED-L node subtractive operations	171
3.1	Search keywords by category	105	4.15	Process parameters for PBF-L node additive manufacturing	173
3.2	Summary of AM structural node precedents	108	4.16	Comparison of AM node size and surface roughness	177
4.1	Most relevant Eurocode standards for the design of structural nodes	133	5.1	Classification requirements for gaskets per EN 12365-1 [203]	205
4.2	Material requirements for steel structures	134	5.2	Elastomeric compression seal gaskets and accessories physical requirements per ASTM C864-05 [204]	206
4.3	Properties and printing variables from literature for PBF-L samples	136	5.3	Summary of selection of AM elastomeric materials	207
4.4	Properties and printing variables from literature for DED-L samples	138	5.4	Material properties of AM elastomeric materials	208
4.5	Properties and printing variables from literature for DED-GMA samples	140	5.5	Benchmark features for design and fabrication of AM gaskets	212
4.6	Summary of toughness values from literature	146	5.6	Comparison of features of AM node gasket to current construction methods	219
4.7	Summary of fatigue strength values from literature	148	6.1	AM-related entwined interests of project stakeholders for the development of AM structural nodes	246
4.8	Key strengths and limitations of DED and PBF additive manufacturing	154			
4.9	Relevant design guidelines for DED and PBF additive manufacturing	155			
4.10	Applied load cases for structural node verification	161			

List of Figures

- 1.1 a) Archetypal system layers for typical stick-built dry-sealed steel and glass façade system. b) Schematic façade system design for typical steel and glass façade highlighting the different layers in the schematic assembly for two incoming branches (Branches A and B from 1.1a) and denoting the key system interfaces. (Image by author) 37
- 1.2 Semantic network of AM design potentials. Different printable features achievable using AM are grouped by type of complexity (green) and linked to various value-creation and cost-saving opportunities (blue) to highlight different routes for the potential advantages of AM solutions (Image after source: [21]) 40
- 1.3 Schematic illustration of U-angles (left), V-angles (middle) and W-angles (right) typical at nodes in freeform construction (Image by author) 42
- 1.4 Summary of problem statement for the use of AM in FFSGF construction. (Image by author) 44
- 1.5 Chapter organization and corresponding sub-questions. (Image by author) 48
- 2.1 Categorization of structural node typologies (Image by author) 66
- 2.2 Structural system categorization by axis: a) Multi-axis node; b) Single-axis node; c) No node component (Image by author) 67
- 2.3 Structural system categorization by profile end condition: a) examples of standard member end conditions; b) examples of non-standard member end conditions; c) example of continuous members. (Image by author) 68
- 2.4 Node sub-component assembly for Westfield Shopping Center roof (Image courtesy of ©Seele) 69
- 2.5 Standard end connection with end plate and opening in profile for access to fix and tension bolts (Image source: [10]) 69
- 2.6 CNC-machined node with simple geometry from DZ Bank Berlin (Image source: [113]) 70
- 2.7 CNC-machined node with end-face connection from shopping center in Bratislava. (Image source: [92]) 70
- 2.8 CNC-machined node with splice connection from 34th street Canopies. (Image courtesy of TrussWorks Intl) 70
- 2.9 Built-up node with end-face and splice connections from A2 Cockpit in Utrecht. (Image courtesy of ONL) 72
- 2.10 Faceted single-axis node in single-layer configuration (Image source: [30]) 73
- 2.11 Faceted single-axis node in double-layer configuration (Image source: [30]) 73
- 2.12 Cylindrical nodes of Ex Unione Militare by Stahlbau Pichler (Image courtesy of Guido Ranieri Da Re) 74
- 2.13 Hotel Dieu courtyard roof cylindrical nodes by Roschmann Group (Image source: [101]) 74
- 2.14 Single-Axis bisecting node from British Museum, London. (Image source: [27]) 75
- 2.15 Schubert Club Band Shell: a) detail with and without cable housing unit; and b) overall toroidal geometry. (Image source: [35]) 76

- 2.16 Directly welded node from BMW Welt façade, a true freeform geometry requiring complex cutting and welding of profiles (Image courtesy of Frank Dinger) 77
- 2.17 Structural node of the Sage at Gateshead façade – a geometrically optimal surface divided into quad panels) constructed using traditional steel framing methods (Image source: [47]) 77
- 2.18 Categorization of enclosure system typologies (Image by author) 78
- 2.19 Schematic illustration showing the key elements and interfaces in the direct glazing typology with a sample detail for reference (Image by author) 79
- 2.20 Schematic illustration showing the key elements and interfaces in the secondary profile typology with a sample detail for reference (Image by author) 80
- 2.21 Offset support of Mansueto Library (Image source: [122] (CC BY-SA 2.0)) 81
- 2.22 Cylindrical node on steel structure of King's Cross Station. (Image courtesy of Barrie Tate) 81
- 2.23 Schematic illustration showing the key elements and interfaces in offset point-support typology with a sample detail for reference (Image by author) 82
- 2.24 Salvador Dali Museum Façade by Novum Structures. (Image courtesy of ©Salvador Dali Museum, Inc., St. Petersburg, FL.) 83
- 2.25 Façade from Town Hall Alphen aan den Rijn which has a unidirectional support structure consisting of columns. (Image by author) 83
- 2.26 Schematic illustration showing the key elements and interfaces in cassette system typology with a sample detail for reference (Image by author) 84
- 2.27 Outer appearance of Smithsonian Kogod Courtyard roof (Image source: [48]) 85
- 2.28 Schematic representation of planar quadrilateral panel relative to non-planar quadrilateral reference geometry (Image by author) 85
- 2.29 Mega-panel for construction of Hyatt Capital Gate (©Jeff Schofield - Image courtesy of Synthesize Architecture) 86
- 2.30 Single-layer cut and joined joint Ex-Unione Militare (Image courtesy of Guido Ranieri Da Re) 87
- 2.31 Multi-layered cut and joined drainage system in Hotel Dieu Courtyard roof (Image courtesy of Pierre Chassagne) 87
- 2.32 Circular gasket applied on aluminium adaptor profile in Gardens by the Bay (Image courtesy of YKK AP Façades) 88
- 2.33 Smithsonian Kogod Courtyard roof cassette system detail (Image source: [54]) 89
- 2.34 Smithsonian Kogod Courtyard roof internal drainage connection (Image courtesy of Foster + Partners) 89
- 2.35 Relative fabrication efficiency, geometrical flexibility, and material efficiency of structural node typologies (Image by author) 93
- 2.36 Example illustrating the definition of the minimum node radius and the impact of increasing node radius on misalignments between structural later and outer faces in single-axis nodes. (Image by author) 95
- 3.1 Number of collected articles by AM façade elements, material and 3D printing strategy (Image by author) 107
- 3.2 a) Vertical panel edge connection with a tolerance of 1mm. b) Horizontal panel edge connection with a tolerance of 2mm. (Image source: [128]) 109

- 3.3 Rendering of Nematox I façade node by Holger Strauss [129]; the first AM structural node for freeform metal and glass construction. Design for stick-built aluminium façade system and equipped with standard connections, and integrated screw channel and gasket rebates. (Image source: [129]) 110
- 3.4 Nematox II, additively manufactured using PBF-L technology and mounted to AA-100 façade system by Alcoa (Image source: [129]) 110
- 3.5 3D Printed stainless steel node for timber canopy, prototyped at full-scale using SLM. (Image source: [130]) 111
- 3.6 3D Printed ABS node using FFF for aluminium pipe and lycra canopy. (Image source: [132]) 111
- 3.7 3D Printed stainless steel node for steel and glass canopy, prototyped at 25% scale using BJ. (Image source: [4]) 112
- 3.8 Exploded detail of the proposed glazing connection for 3F3D node. (Image source: [4]) 112
- 3.9 Additively manufactured prototypes of structural nodes: unsmoothed transitional node with the end of each member closed for bolt-connection (left); BESO node (right). (Image source: [133]) 113
- 3.10 Process used for the manufacturing of the AM sand moulds and cast "Smart nodes" for Galleria mall in Gwanggyo (Image source: [112]) 114
- 3.11 Design for N-AM_Li3 node system for aluminium and glass façade system and connection to commercial system. (Image source: [134]) 115
- 3.12 a) Aluminium façade system with exposed profile. b) Steel Façade system with continuous gasket (Images Source: [10]) 117
- 4.1 Range of metal AM printing methods. AM methods can be broadly organized into families, which can be further subdivided by the nature of the base material, heat source/binder, machine operations, etc. (Image by author) 126
- 4.2 Comparison of range of build volumes for different metal AM methods. (Data source:[146], image by author) 130
- 4.3 Comparison of range machine costs for different metal AM methods. (Data source:[146], image by author) 130
- 4.4 Sample strength values for AM SS316L for different metal AM methods. (Data source: [146], image by author) 130
- 4.5 Schematic illustration of a) PBF-L; b) DED-L; c) DED-GMA printing processes (Image by author) 131
- 4.6 Ductility by elongation at fracture (EF) values from literature relative to benchmark values and EC3 requirements (Image by author) 142
- 4.7 Ductility by ratio of ultimate tensile strength (f_u) to yield strength (f_y) values calculated from literature compared to EC3 requirement and benchmark f_u/f_y ratio calculated from 0,2% proof strength and f_u values from [138] (Image by author) 143
- 4.8 Comparison of S–N curves for different PBF-L production routes with wrought material at stress ratio $R = 0$ (Image Source: [153]) 149
- 4.9 Comparison of S-N curves of DED-L(Powder) and DED-L(Wire) at stress ratio $R = -1$ (Image Source: [171]) 149
- 4.10 Ultimate tensile strength, yield strength, and elastic modulus values from literature (Image by author) 151
- 4.11 Schematic load configurations A and B applied to nodes for FEA validation (Image by author) 161
- 4.12 Benchmark CNC node design (Image by author) 162

4.13	DED-GMA node design (Image by author)	163	4.29	Comparison of node surface area and volume based on different profile dimensions and node configurations showing the impact these variables can have on the weight of solid nodes and fabrication metrics related to surface area and volume (Image by author)	183
4.14	DED-L node design (Image by author)	164	4.30	End connection alternatives explored during the development of DED-GMA node: increasing thickness with simple path planning (left) and flat end face with multiple steps and orientations (right). (Image by author w/ photo courtesy of Mx3D)	184
4.15	PBF-L node design (Image by author)	165	4.31	Relative size of node arms and DED-GMA torch (Image courtesy of Mx3D)	185
4.16	Order of additive operations for AM process of DED-GMA node (Image by author)	168	4.32	Relative amount of solid (printing) volume vs hollow for DED-L nodes in different configurations: uneven arm distribution (left) and compact (right). (Image by author)	189
4.17	DED-GMA node during printing process (Image courtesy of Mx3D)	169	4.33	Peak yield strength of four scanning speed specimens under different loading strain rates. (Image Source: [193])	191
4.18	Final DED-GMA node after surface finishing (Image courtesy of Jansen AG)	169	5.1	Silicone additive manufacturing technology by Spectroplast. (Image Source:[217])	209
4.19	Main additive operations and movements axes for DED-L node. (Image by author)	171	5.2	Digital light synthesis printing technology by Carbon 3D.(Image Source:[219])	210
4.20	DED-L node after substrate removal, before polishing (Image by author)	172	5.3	Drop on demand technology by ACEO. (Image Source:[221])	211
4.21	PBF-L node on substrate (Image by author)	174	5.4	Gasket prototype printed in EPU 40 by Sculpteo using digital light synthesis printing technology. (Image by author)	213
4.22	EDM process on PBF-L node (Image by author)	175	5.5	Gasket prototype printed in True Silicone A60 by Spectroplast using silicone additive manufacturing technology. (Image by author)	213
4.23	Close-up of EDM process (Image by author)	175	5.6	Gasket prototype printed in Silicone GP Shore A 60 by ACEO using drop on demand printing technology. (Image by author)	213
4.24	PBF-L node with difficult to remove support structure (Image by author)	175	5.7	Gasket prototype printed in TPU-70A by Protolabs using powder bed fusion printing technology. (Image by author)	213
4.25	Leftover support structures after removal effort with CNC milling (Image by author)	175			
4.26	Relative surface roughness of PBF-L node (left); DED-L node (middle); and DED-GMA node (right). (Image by author)	177			
4.27	Fabrication time comparison for different nodes (Image by author)	178			
4.28	Material usage comparison for different nodes (Image by author)	179			

- 5.8 First gasket design installed in a mock-up (Image courtesy of Jansen AG) 214
- 5.9 Final node gasket prototype design (Image by author) 214
- 5.10 Base geometry for gasket node modelling. (Image by author) 215
- 5.11 Modelling of gasket crown with variable cross-section spanning space between base and glazing plane. (Image by author) 216
- 5.12 Proposed gasket node design and functional features showing interfaces with structural node and incoming gasket profiles (Image by author) 216
- 5.13 Top view of printed AM gasket node prototype (Image by author) 217
- 5.14 Detailed view of node identifier and triangular protrusion for interface with structural node (Image by author) 217
- 5.15 Detailed view of connection detail in AM gasket node prototype (Image by author) 217
- 6.1 Interdisciplinary responsibilities in freeform steel and glass façade construction (Image by author) 225
- 6.2 Exterior view of freeform façade for Glasstec 2022 (Image courtesy of Jansen AG) 228
- 6.3 Interior view of freeform façade for Glasstec 2022 (Image courtesy of Jansen AG) 228
- 6.4 Detail view of additively manufactured structural node in freeform façade for Glasstec 2022 (Image courtesy of Jansen AG) 229
- 6.5 Detail view of additively manufactured structural node and gasket node in freeform façade (Image by author) 229
- 6.6 Workflow for interdisciplinary collaboration for the design of freeform steel and glass façades (Image by author) 231
- 6.7 Façade schematic design and rationalization showing overall dimensions and positive and negative critical panel angles (Image by author) 233
- 6.8 Workflow for the design and fabrication of AM structural nodes for freeform steel and glass façades, a continuation of the workflow diagram in Figure 6.6 (Image by author) 235
- 6.9 Initial schematic design options for DED-GMA node including proposed printing sequence and Printing Orientation (PO) (Image by author) 237
- 6.10 Proposed qualitative structural improvements to initial schematic DED-GMA node design (Image Source: knippershelbig GmbH) 237
- 6.11 DED-GMA node design iteration following feedback on manufacturability from AM fabricator (Image by author) 237
- 6.12 Final iteration of DED-GMA node which was printed and installed in the mock-up wall (Image by author) 237
- 6.13 FEA model of template node for preliminary structural validation of DED-GMA node (Image courtesy of knippershelbig GmbH) 238
- 6.14 FEA model of first iteration of PBF-L node installed in the first full-scale mock-up (Image by author) 238
- 6.15 FEA model of second iteration of PBF-L node (Image by author) 238
- 6.16 FEA model of third iteration of PBF-L node (Image by author) 238
- 6.17 Preliminary prototype for DED-GMA node with excessive warping (Image courtesy of Mx3D) 239
- 6.18 Preliminary prototype for DED-L node with undesirable surface texture (Image by author) 239

- 6.19 Preliminary prototype for PBF-L node with difficult to remove support structures (Image by author) 239
- 6.20 First prototype using DED-GMA (Image courtesy of Jansen AG) 241
- 6.21 End-condition iterations to improve surface quality by integrating contour paths, printing solid end conditions without integrated boring holes, and subdividing the path planning for the solid infill (Image courtesy of Jansen AG) 241
- 6.22 Sample iteration of end condition using less material but more complex path planning that requires several changes of printing orientation which are visible in the surface texture (Image courtesy of Mx3D) 241
- 6.23 DED-GMA node in first full-scale mock-up assembly (Image courtesy of Jansen AG) 242
- 6.24 DED-L node in first full-scale mock-up assembly (Image courtesy of Jansen AG) 242
- 6.25 PBF-L node in first full-scale mock-up assembly (Image courtesy of Jansen AG) 242
- 6.26 Full-scale mock-up with 3 metal AM nodes fabricated using DED-GMA (top), PBF-L (middle), and DED- (bottom) (Image courtesy of Jansen AG) 243
- 6.27 Top-down decision-making approach for structural node design (Image by author) 245
- 6.28 Workflow for the design and fabrication of AM gasket nodes for freeform steel and glass façades, a continuation of the workflow diagram in Figure 6.6 (Image by author) 251
- 6.29 Digital workflow for interdisciplinary collaboration for the design and construction during the development of the Glasstec project. (Image by author) 253
- 6.30 Screenshot of digital data from GPI model fed back to AD&R model for node size optimization. (Image by author) 255
- 6.31 Screenshots of GPI model for quick visualization of project with different profile dimensions. (Image by author) 256
- 6.32 Geometric node “building blocks” that are output from GPI model and input for LPIF model (Image by author) 259
- 6.33 Geometric node data that is output from LSA model and used FEA validation and CAM fabrication (Image by author) 259
- 6.34 Exploded view of simplified LPIF model (Image by author) 260
- 6.35 2D CAD output from LPIF model for the fabrication of the insulated glazing showing the individual panel dimensions and the relative set-out of the interior and exterior panes (Image by author) 260

List of Acronyms

AD&R	Architectural Design & Rationalization
AEC	Architecture, Engineering and Construction
AM	Additive Manufacturing
BESO	Bi-Evolutionary Structural Optimization
BIM	Building Information Modeling
BJ	Binder Jetting
BTF	Buy-to-Fly
CAM	Computer Aided Manufacturing
CLIP	Continuous Liquid Interface Production
DED	Directed Energy Deposition
DED-GMA	Gas Metal Arc Directed Energy Deposition
DED-L	Laser-based Directed Energy Deposition
DfAM	Design for Additive Manufacturing
(C)DLP	(Continuous) Digital Light Projection
DLS	Digital Light Synthesis
DMLS	Direct Metal Laser Sintering
EC3	Eurocode 3
EPU	Elastomeric Polyurethane
EDM	Electrical Discharge Machining
EF	Elongation at Fracture
FFF	Fused Filament Fabrication
FFSGF	Freeform Steel and Glass Façade(s)
GPI	Global Parameter Integration
HIP	Hot Isostatic Pressing
IGU	Insulated Glazing Unit
LCA	Life Cycle Analysis
LPIF	Local Parameter Integration & Fabrication
LSA	Local Structural Analysis
ME	Metal Extrusion
MJ	Material Jetting
NPJ	Nanoparticle Jetting
OSA	Overall Structural Analysis
PBF	Powder Bed Fusion

>>>

PBF-L	Laser-based Powder Bed Fusion
PDM	Project Delivery Method
PO	Printing Orientation
PQ	Planar Quadrilateral
RT	Rapid Tooling
SAM	Silicone Additive Manufacturing
SL	Stereolithography
SLM	Selective Laser Melting
SS316L	Stainless Steel grade 1.4404 (AISI 316L)
TPU	Thermoplastic Polyurethane
VP	Vat Polymerization
WAAM	Wire and Arc Additive Manufacturing

Summary

The dissertation 'Towards the integration of Additive Manufacturing for Freeform Steel and Glass Façade Construction' explores the use of Additive Manufacturing (AM) as a means of improving the design and construction of Freeform Steel and Glass Façades (FFSGF). This type of construction involves the design, fabrication, and assembly of complex components, which requires close interdisciplinary collaboration to realize the architectural vision of the designer and achieve good façade performance while also striving for efficiency in design, material use, fabrication, construction, and cost.

Recent developments in additive manufacturing technology are making AM a more efficient, reliable, and accessible fabrication strategy for a range of different industries, scales, and materials. As such, it is quickly becoming an increasingly tenable fabrication method for the construction industry, and in particular, for the fabrication of mass-customized components such as those common in freeform construction. Therefore, seeing AM as an opportunity to improve on current fabrication strategies, this dissertation aims to answer the following question:

How can additive manufacturing be effectively utilized to develop node solutions that support freeform steel and glass façade construction?

The object of the research is to facilitate the integration of AM into the design and construction of future freeform steel and glass façades through the detailed exploration of different AM technologies for key components of freeform steel and glass façade assemblies. The research considers the impact of the use of AM over the entire design and construction process as well as on the roles and responsibilities of the different disciplines involved.

The first two chapters of this research (Chapters 2 and 3) comprise the background analysis to identify key opportunities and metrics by which existing solutions can potentially be improved upon. The research begins with identifying key opportunities for the use of AM by studying existing freeform steel and glass façade construction strategies. These are classified into general typologies for which the strengths and limitations are discussed. Following this, a literature review on the use of AM in façades is used to understand the extent to which AM technology has already been explored in this context.

Chapters 4 and 5 explore the design and development of two key components, namely a structural node and gasket node, respectively. Background research for these explorations comprise an overview of different possible AM methods, an overview of relevant design for additive manufacturing guidelines, and an assessment of the mechanical properties of the additively manufactured materials. Following this, physical prototypes are designed and printed using different AM technologies. For the structural node, three different nodes are designed per the design guidelines of selected metal AM methods. The three node prototypes are manufactured, and compared in terms of their fabrication efficiency and material efficiency. For the gasket node, a preliminary benchmark node design is printed using four different elastomeric AM methods and materials. A final node gasket is then designed, manufactured, and qualitatively compared to existing gasket solutions.

Chapter 6 discusses the integration of the product development undertaken in the previous two chapters in the larger context of a construction project. It is a case study outlining the way in which the design, development, and fabrication of AM products was conducted over the course of an interdisciplinary collaboration between a designer, an engineering team, and an execution team, for the realization of a full-scale freeform steel and glass façade. This chapter also outlines the digital strategy that was used to facilitate the interdisciplinary collaboration.

The dissertation concludes by discussing the main research question and proposing future research directions. The systemization of AM node design is recognized as a crucial aspect that can streamline the development process, facilitate standardization, and support the creation of libraries of interchangeable AM nodes. Limitations of the scope of research, such as the focus on specific AM methods and materials, are acknowledged. Areas for future research are identified including the further exploration of AM methods and materials, the development of AM components, the investigation of interdisciplinary design for AM, and the analysis of the role and impact of AM in sustainable construction practices. The study highlights the potential of AM in FFSGF construction, but it also emphasizes the importance of further exploration and optimization for AM to be effectively integrated as a viable and sustainable building practice.

AM technology has revolutionary potential when it comes to the fabrication of complex parts. As this technology continues to advance, it is quickly becoming a more accessible means of fabrication for the construction industry. That being said, its use, particularly for the realization of structural components, adds a layer of complexity to the already complex interdisciplinary undertaking that is the design and construction of freeform steel and glass façades. Unlocking the full potential of this revolutionary technology for these applications requires building a body of

knowledge at the intersection of design, engineering, construction, and AM that building industry professionals can refer to in order to help facilitate the design and realization of additively manufactured parts and products. This dissertation aims to contribute to that growing body of knowledge.

Samenvatting

Het proefschrift 'Richting integratie van 'additive manufacturing' in de constructie van vrije-vorm façades in staal en glas' verkent de toepassing van 'additive manufacturing' (hierna AM) voor het verbeteren van ontwerp en constructie van vrije-vorm façades in staal en glas. Deze bouwmethode omvat het ontwerpen, vervaardigen en monteren van complexe onderdelen, waarbij nauwe multidisciplinaire samenwerking tussen ontwerpers, ingenieurs en fabrikanten vereist is om zowel een architectonische visie als goede façadeprestaties te realiseren, en tegelijkertijd te streven naar efficiëntie op het gebied van ontwerp, materiaal, productie en kosten.

Recente ontwikkelingen in AM-technologie hebben van AM een efficiëntere, meer betrouwbare en toegankelijke productiemethode gemaakt voor verschillende industrieën, schaalgroottes en materialen. Hierdoor wordt AM steeds vaker erkend als een werkbare productiemethode voor de bouwsector, met name voor massamaatwerkproductie van onderdelen die kenmerkend is voor vrije-vormconstructies. Door AM te zien als een mogelijkheid om huidige productiestrategieën te verbeteren, tracht dit proefschrift de volgende vraag te beantwoorden:

Hoe kan 'additive manufacturing' effectief worden ingezet in het ontwikkelen van knoopverbindingen die bijdragen aan de constructie van vrije-vorm façades in staal en glas?

Dit onderzoek richt zich op de integratie van AM in ontwerp en constructie om toekomstige vrije-vorm façades in staal en glas mogelijk te maken, door middel van een gedetailleerde verkenning van verschillende AM technologieën voor sleutelementen die horen bij vrije-vorm façadestelsels in staal en glas. Het onderzoek bestudeert de impact van de toepassing van AM in het gehele ontwerp- en constructieproces, alsmede de functies en verantwoordelijkheden die horen bij de betrokken disciplines.

De eerste twee hoofdstukken van dit onderzoek (Hoofdstukken 2 en 3) bestaan uit een achtergrondstudie waarin de belangrijkste kansen worden onderscheiden, en de bestaande gegevens worden geïdentificeerd waarop de huidige oplossingen verbeterd kunnen worden. Het onderzoek begint met het identificeren van kansen voor de toepassing van AM door bestaande constructiemethoden van vrije-vorm façades in staal en glas te bestuderen. Deze worden ingedeeld in generieke

typologieën aan de hand waarvan voor- en nadelen worden beschreven. Vervolgens wordt een literatuurstudie uitgevoerd om te leren in hoeverre AM-technologie in deze context al is onderzocht en toegepast.

Hoofdstukken 4 en 5 verkennen het ontwerp en de ontwikkeling van twee sleutelementen: de constructieve knoop en de afdichtingsknoop. Achtergrondonderzoek voor deze verkenningen bestaat uit een overzicht van verschillende mogelijke AM-methoden, een overzicht van relevante ontwerp-voor-AM-richtlijnen, en een beoordeling van de mechanische eigenschappen van AM-gefabriceerde materialen. Vervolgens zijn fysieke prototypen ontworpen en geprint. Voor de constructieve knoop zijn drie verschillende ontwerpen gemaakt volgens de ontwerprichtlijnen van de gekozen metalen AM-methoden. De drie prototypen zijn gefabriceerd en vergeleken op het gebied van productie-efficiëntie en materiaalefficiëntie. Voor de afdichtingsknoop is een referentieknoop geprint middels vier verschillende elastomere printmethoden. Een laatste afdichtingsknoop is ontworpen, geproduceerd en vergeleken met bestaande afdichtingsoplossingen.

Hoofdstuk 6 beschrijft de integratie van de productontwikkeling van de voorgaande twee hoofdstukken in de grotere context van een bouwproject. Dit hoofdstuk dient als een case study die schetst hoe ontwerp, ontwikkeling en productie van de AM-producten wordt uitgevoerd bij de interdisciplinaire samenwerking tussen ontwerpers, ingenieurs en uitvoerders, voor de realisatie van een vrije-vorm façade in staal en glas op ware grootte. Dit hoofdstuk schetst tevens de digitale strategie die is gebruikt om die interdisciplinaire samenwerking mogelijk te maken.

Het proefschrift eindigt met een reflectie op de hoofdvraag, en stelt potentiële onderzoeksrichtingen voor. De systematisering van het ontwerp van AM-knopen wordt cruciaal geacht in het stroomlijnen van het ontwikkelproces, het bewerkstelligen van standaardisatie, en het ondersteunen van bibliotheken met uitwisselbare AM-knopen. Beperkingen van de scope van het onderzoek – zoals de focus op specifieke AM-methoden en -materialen – worden onderkend. Toekomstige onderzoeksgebieden zijn: het verder verkennen van AM-methoden en materialen, doorontwikkelen van AM-onderdelen, bestuderen van interdisciplinaire ontwerpmethodes voor AM, en het analyseren van de implicaties betreffende duurzaamheid. De studie onderstreept de potentie van AM in vrije-vorm façades in staal en glas, maar benadrukt de vraag naar meer verkenning, optimalisatie en integratie in duurzame bouwpraktijken.

AM-technologie heeft de potentie revolutionair te worden als het gaat om de productie van complexe onderdelen. Naargelang de technologie zich verder ontwikkelt kan deze snel een toegankelijker productiemethode voor de bouw

worden. Tegelijkertijd voegt de toepassing ervan een extra laag aan complexiteit toe aan een al complexe, interdisciplinaire bezigheid die het ontwerpen en bouwen van vrije-vorm façades in staal en glas is. Om het volledige potentieel van deze revolutionaire technologie voor deze toepassingen te benutten dient een kennisdomein opgebouwd te worden op het snijvlak tussen ontwerp, engineering, productie en AM die vakmensen uit de industrie kunnen raadplegen, om hen te faciliteren in het ontwerpproces van AM-gefabriceerde onderdelen en producten. Dit proefschrift tracht bij te dragen aan dat groeiende kennisdomein.

Résumé

La thèse « Vers l'intégration de la fabrication additive pour la construction de façades de forme libre en acier et verre » explore l'utilisation de la Fabrication Additive (FA) comme moyen d'améliorer le design et la construction de façades de forme libre en acier et verre. Ce type de façade implique le design, la fabrication et l'assemblage de composants complexes, ce qui nécessite une collaboration multidisciplinaire entre architectes, ingénieurs, et fabricants afin de réaliser une vision architecturale et atteindre de bonnes performances de façade tout en visant à être efficace dans le design, l'utilisation des matériaux, le processus de fabrication et les coûts.

Les développements récents de la technologie de (FA) rendent celle-ci une stratégie de fabrication plus efficace, fiable et accessible pour une gamme d'industries, d'échelles, et de matériaux. Comme telle, la FA devient rapidement une méthode de fabrication de plus en plus tenable pour l'industrie de construction et, en particulier, pour la fabrication de composants personnalisés en masse, tels que ceux courants dans la construction de façades de forme libre. Par conséquent, voyant la FA comme une opportunité d'améliorer les stratégies de fabrication actuelles, cette thèse vise à répondre à la question suivante:

Comment la fabrication additive peut-elle être utilisée efficacement pour développer des solutions de nœuds qui soutiennent la construction de façades de forme libre en acier et verre?

Cette recherche vise à faciliter l'intégration de la FA dans le design et la construction de façades de forme libre en acier et verre par l'exploration de diverses technologies de FA pour des composants clés de leurs assemblages. La recherche prend en compte l'impact de l'utilisation de la FA sur l'ensemble du processus de conception et de construction ainsi que sur les rôles et responsabilités des différentes disciplines impliquées.

Les deux premiers chapitres de cette thèse (chapitres 2 et 3) comprennent l'analyse de fond pour identifier des opportunités pour l'amélioration des solutions existantes. La recherche commence par l'identification des opportunités clés pour l'utilisation de la FA en étudiant les méthodes courantes de construction de façades de forme libre en acier et verre. Celles-ci sont classées en typologies dont les forces et les limites

sont discutées. Ensuite, une revue de la littérature sur l'utilisation de la FA pour l'exécution de façades est effectuée afin d'évaluer dans quelle mesure la technologie de FA a déjà été explorée dans ce contexte.

Les chapitres 4 et 5 explorent le design et le développement de deux composants clés : le nœud structurel et le nœud d'étanchéité. La recherche de base pour ces explorations comprend un aperçu de diverses technologies de FA ainsi que des directives de conception pertinentes, et une évaluation des propriétés mécaniques des matériaux fabriqués de manière additive. Pour le nœud structurel, trois nœuds différents sont conçus selon les directives de conception des technologies de FA métallique sélectionnés. Ces trois nœuds sont fabriqués et comparés en termes d'efficacité de fabrication et d'efficacité matérielle. Quant au nœud d'étanchéité, un nœud de référence est imprimé en utilisant quatre différents procédés de FA pour élastomères. Par la suite, un nœud d'étanchéité final est conçu, fabriqué et comparé qualitativement aux solutions d'étanchéité courantes.

Le chapitre 6 aborde l'intégration du développement des produits entrepris dans les deux chapitres précédents au sein du contexte élargi d'un projet de construction. Il s'agit d'une étude de cas décrivant la manière dont le design, le développement et la fabrication des produits FA ont été entrepris dans le cadre d'une collaboration interdisciplinaire pour la réalisation d'une façade de forme libre en acier et verre à l'échelle réelle. Ce chapitre présente également la stratégie numérique qui a été utilisée pour faciliter la collaboration interdisciplinaire.

La thèse se termine par l'examen de la question de recherche principale et la proposition de pistes pour de futures recherches. La systématisation du design des nœuds pour la FA est reconnue comme un aspect crucial pouvant accélérer le processus de développement, faciliter la standardisation, et soutenir la création de bibliothèques de nœuds FA interchangeables. Les limites de la portée de la recherche sont également reconnues, telles que l'accent mis sur des méthodes et des matériaux de FA spécifiques. Les axes de recherche futurs comprennent l'exploration d'autres méthodes et matériaux de FA, le développement continu des composants de FA, l'étude du design interdisciplinaire de la FA et l'analyse des implications en matière de durabilité. L'étude souligne le potentiel de la FA pour la construction des façades de forme libre en acier et verre, mais souligne également l'importance de la poursuite de l'exploration et de l'optimisation pour que la FA soit intégrée de manière efficace en tant que pratique de construction viable et durable.

La technologie de FA a un potentiel révolutionnaire en ce qui concerne la fabrication de pièces complexes. À mesure que cette technologie progresse, elle devient rapidement un moyen de fabrication plus accessible pour l'industrie de

la construction. Cependant, son utilisation, en particulier pour la réalisation de composants structurels, ajoute un niveau de complexité à une entreprise déjà complexe et interdisciplinaire que représente le design et la construction de façades de forme libre. Afin d'exploiter pleinement le potentiel de cette technologie révolutionnaire pour ce type d'application, il faut créer un corpus de connaissances à l'intersection du design, de l'ingénierie, de la construction, et de la FA, auquel les professionnels du secteur du bâtiment peuvent s'appuyer afin de faciliter le processus de conception de produits FA. Cette thèse vise à contribuer à ce corpus de connaissances en expansion.



British Museum courtyard roof (Image by author)

1 Introduction

The dissertation '*Towards the integration of Additive Manufacturing for Freeform Steel and Glass Façade Construction*' investigates the potential of AM in supporting construction industry professionals in the development of mass-customized node products for freeform steel and glass façades.

This first chapter provides an introduction to the topics addressed throughout the dissertation, starting with background information and the problem definition. This is followed by the formulation of a main research question and supporting sub-questions, and subsequently the strategies and methods used to address these questions. This chapter concludes with a discussion on the societal and scientific impact of this research.

1.1 Background

1.1.1 Freeform steel and glass façades

As its etymological root suggests, the façade is in essence the “face” of the building. A building’s façade contributes its identity and character from its curb-side presence to its silhouette in a cityscape. In addition to this, the façade is responsible for the essential task of separating the indoor environment from the outdoor environment, filtering exterior energy and mass flows e.g. light, air, moisture, sound. The façade, thus integral to so many aspects of the experience and performance of every building, is a focal point of architectural design and engineering.

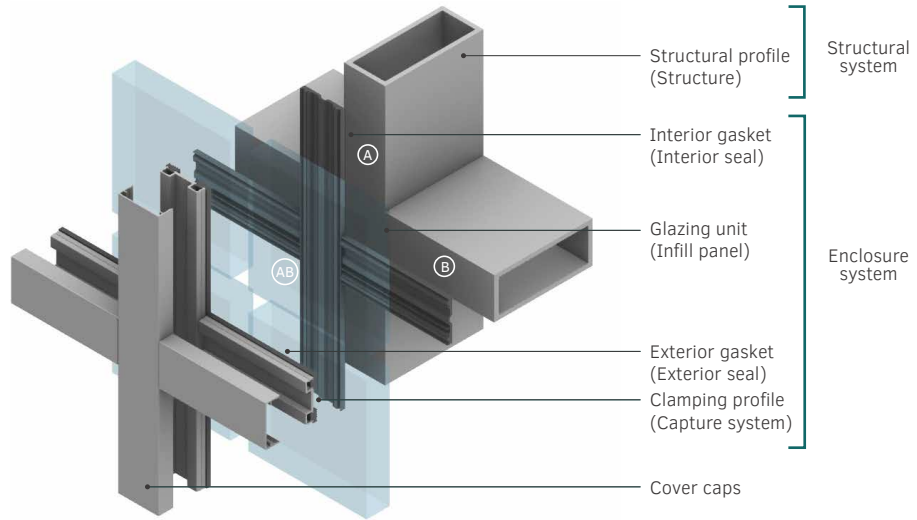
Over the past several decades, the design and construction of freeform high-transparency façades have become increasingly popular. Reasons for using freeform geometry are many. In some cases, for example, freeform geometry is a means to achieving structural optimization in widespan structures [1-3]. In some cases, it is the result of generating forms that span or envelop other infrastructural objects [4, 5]. In some cases, it is a design instrument for the architect to, for instance, express movement [6, 7], imitate nature [8-12], symbolize something [13, 14], and/or give the building a strong identity [7, 11, 12, 14, 15].

The choice of steel for the main load-bearing structure over other materials such as aluminium is the norm for two main reasons: first, because its high strength and stiffness enable the use of slimmer profiles which helps to contribute to the overall transparency of the envelope; and second, the weldability of steel makes it a good option where complex interfaces have to be connected, and where the required load transfer is substantial and intricate.

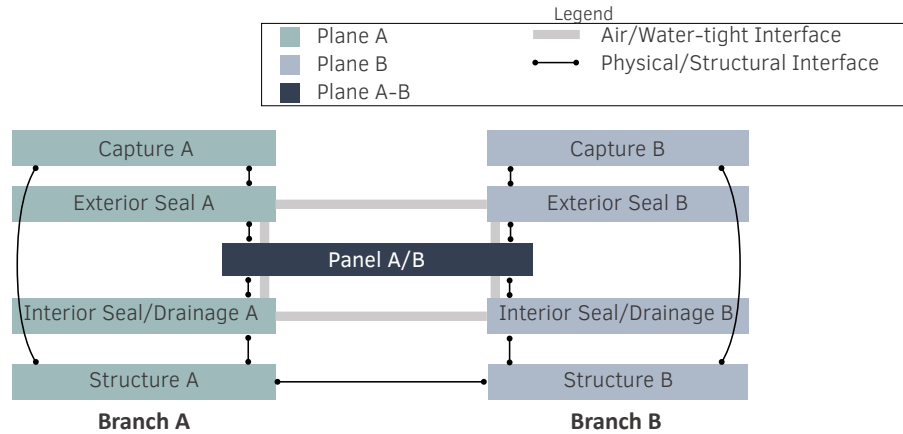
1.1.2 Typical steel and glass façade construction

In glass façade construction, there are two main construction typologies: stick-built façades, and unitized façades [16]. Stick built façades generally consists of mullions and transoms that are either assembled on-site or preassembled in prefabricated ladders that are shipped to the site and subsequently assembled and glazed [16]. In unitized façades, module-size units are preassembled with integrated glazing units and mounted on a supporting structure. The majority of Freeform Steel and Glass Façades (FFSGF) are based on stick-built façade construction.

Figure 1.1a illustrates an archetypal configuration of a stick-built steel and glass curtain-wall façade. The entire system is supported by the load-bearing structure. The glazing unit is sandwiched between two sealing planes. The glazing is captured along edges with a clamping profile, which compresses the gasket profiles between the infill panel and structural profiles, and ties the whole to the main load-bearing structure [17]. The system is then outfitted with a cover cap. Figure 1.1b schematically illustrates the key interfaces and connections between components for two adjacent branches bordering a glazed unit for a typical stick-built curtain wall assembly, whether it be wet or dry sealed. Components generally interface with components within the same layer in other branches, as well as with adjacent layers within the same branch. The proper functioning of the façade relies not only on the components that make up the assembly, but also crucially on the integrity of these interfaces.



a)



b)

FIG. 1.1 a) Archetypal system layers for typical stick-built dry-sealed steel and glass façade system. b) Schematic façade system design for typical steel and glass façade highlighting the different layers in the schematic assembly for two incoming branches (Branches A and B from 1.1a) and denoting the key system interfaces. (Image by author)

For example, structural profiles must be interconnected in such a way that allows for the effective transfer of forces between members. They must also be arranged in such a way that their outer faces provide a supporting surface for the application of the interior gasket layer. Likewise, interior gaskets must be carefully cut, connected, and fused to one another in order to provide a continuous drainage plane. They must also be continuously compressed between the adjacent structural profile and glass around the entire perimeter of the glazing unit in order to provide an air- and water-tight seal.

1.1.3 Systemized façade construction

In addition to their performance-related requirements, façades also need to respond to several other demands of the construction industry. Such demands include cost-effectiveness and the ability to respond to project timelines. In order to meet the range of façade requirements, the industry has by-and-large adopted systemized façades as the norm [18]. The term “systemized façade” in the context of this research refers to façade systems developed as “system products” as defined in [19]:

“A system product is developed as [an] integral system, and built up from various functional elements and components, of which the characteristics are not yet completely determined. The system is developed to be composed in all of its functional parts to act in the application situation as a coherent whole. The system knows one level of system design and another level of application design. The system product is suitable to be applied to divers situations in various compositions and/or executions. A system product needs amplifying engineering information for its components and composition to make its final engineering possible in view of the application and to be accurately manufactured for this application purpose. Amplification (or choice parameters) may be derived from dimensions, sometimes from colour finishing or, for instance, type preserving, but will never change the design of the system as such. The technical core of the system product remains unchanged.”

It is acknowledged that the term “systemized façade” is also sometimes used to refer to unitized façade construction, however in the context of this dissertation, it is only used according to the definition from [19]. Systemized façades have a number of key advantages that make them a logical solution:

- façade assemblies undergo comprehensive performance testing by the system-house using full-scale performance mock-ups such that the tolerances and technical requirements are reliably consistent for all future applications;
- façade assemblies consist of catalogues of products where typical design variables such as profile dimensions can be interchanged without changing the technical core of the façade system [19];
- catalogues of products have standardized interfaces to which enable a “predictable scope and sequence of construction” [18];
- catalogues of products have predetermined performance limitations which can be selected based on specific project requirements facilitating design and engineering;
- and products can be mass-manufactured and stored in order to respond to quick project lead times.

The terms "systemized nodes" and "systemized products" are also used in this dissertation to refer to nodes and products developed as integral parts of systemized façades. Amplification or choice parameters for systemized nodes and products can be implemented through parametric design and modelling.

1.1.4 Additive manufacturing

Additive Manufacturing (AM) is defined as “the process of joining materials to make objects from 3D model data, usually layer upon layer, as opposed to subtractive manufacturing methodologies” [20]. This relatively new and innovative family of manufacturing technologies provides a number of advantages that are unprecedented in more traditional manufacturing methods. As shown below in Figure 1.2 [21], these advantages can be categorized into different types of complexity that are achievable with AM, and in some cases, unique to the technology: form complexity; hierarchical complexity, functional complexity, and material complexity. These levels of complexity can be leveraged to create value in AM products to offset the relatively high cost of AM processes through additional product value, improvement to sustainability, reduced production lead times, indirect value propositions, and reduced overall costs.

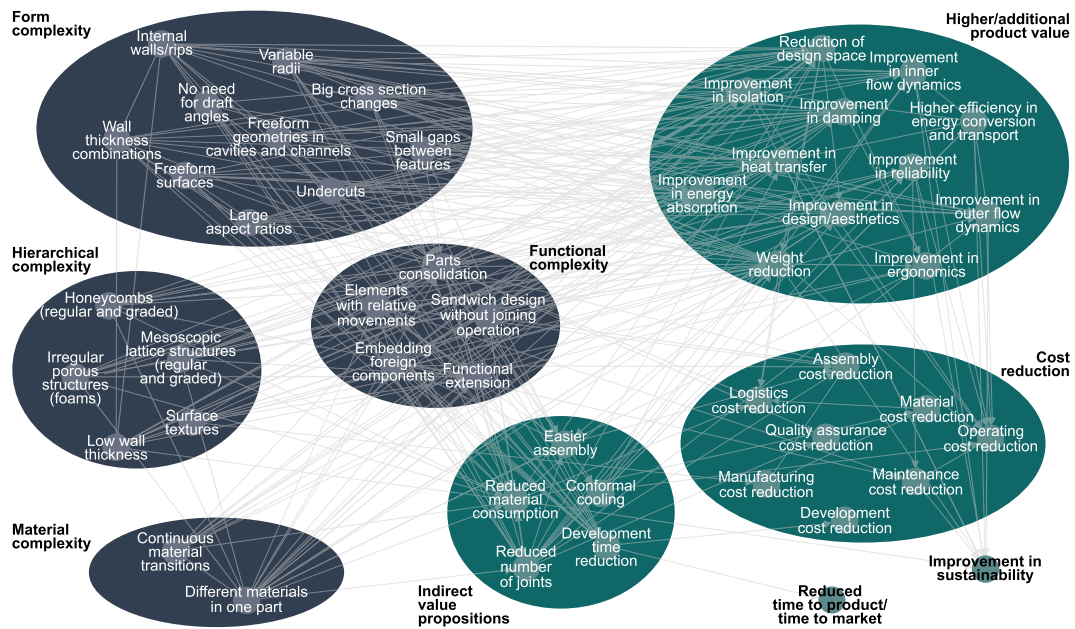


FIG. 1.2 Semantic network of AM design potentials. Different printable features achievable using AM are grouped by type of complexity (green) and linked to various value-creation and cost-saving opportunities (blue) to highlight different routes for the potential advantages of AM solutions (Image after source: [21])

1.2 Problem statement

1.2.1 Complexity of freeform steel and glass façade design and construction

This research project deals with the use of Additive Manufacturing for the construction of freeform steel and glass façades. Freeform steel and glass façades are an increasingly popular application in modern architecture. While freeform geometry is an exciting design possibility, freeform enclosures come with a number of unique challenges related to their design and construction that require close collaboration between project stakeholders in order to develop solutions able to achieve quality façade performance in addition to cost efficiency, design and engineering efficiency, fabrication efficiency, assembly efficiency, and material efficiency.

1.2.2 Geometrical complexity at nodal conditions

Freeform steel and glass façades are often built from layered façade systems consisting of planar glazing units and linear profile elements along edges, similar to the archetypal typical stick-built steel and glass façade systems described in Section 1.1.2. This strategy results in complex intersections (also referred to as nodal conditions) at which each of the layers of the façade system must be resolved in such a way that does not jeopardize façade performance. This comes with a few distinct challenges. First, it is common for nodal conditions in a freeform façade to each have unique geometrical configurations and different functional requirements. For example, each structural node might have unique loading patterns, and different drainage paths will have to be provided across the façade surface depending on its topology. Solutions to address nodal conditions must be able to accommodate a wide range of possibilities.

Additionally, providing continuity of functional layers across nodal conditions is made more challenging by the fact that the incoming branches are at different heights and angles relative to one another. From a structural perspective, the composition of different geometrical configurations across a freeform façade creates relatively unpredictable loading patterns at nodes compared to orthogonal façades that must be accommodated by connections, and potentially creates additional bending

moments in the structural layer due to the misalignment of the central axes of the structural profiles. The different relative heights and angles of structural profiles at node conditions also pose a challenge for gaskets, since the misaligned outer faces of the profiles create an uneven surface across which the integrity of the compressive seal between the glass and structural layer must be maintained. Misalignments vary depending on their angular configuration and relationship to the reference geometry in the digital model (e.g. reference mesh edge represents top of steel centreline, or profile central axis, or other). This is illustrated in Figure 1.3, which highlights the U-Angles (polar angle of the profiles around the node axis), V-Angles (angle of the profiles in plane with the node normal), and W-Angles (twisting of the profile axis relative to the node normal).

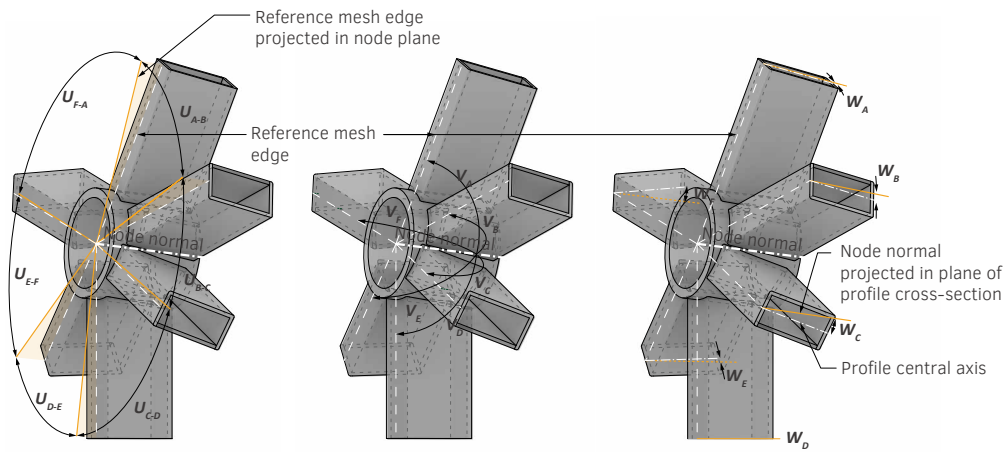


FIG. 1.3 Schematic illustration of U-angles (left), V-angles (middle) and W-angles (right) typical at nodes in freeform construction (Image by author)

1.2.3 Quality façade performance

These irregular geometrical conditions make nodal conditions particularly susceptible to performance issues, especially when it comes to air and water-tightness. Performance relies heavily on workmanship which is prone to human error [22]. This is especially notable since connections in freeform systems are challenging to resolve. The use of full-scale façade mock-up testing is often required to prove the ability of a solution to meet a certain performance standard [23]. Despite this, the speed and standard of workmanship can be drastically different between mock-ups and actual construction, resulting in underperforming façades.

1.2.4 Additive Manufacturing: an opportunity

Additive Manufacturing (AM) presents a unique opportunity to address the challenges outlined above. AM is a form of Computer Aided Manufacturing (CAM), which enables the fabrication of mass-customized parts, responding to the need to address a multitude of geometrical configurations. While other CAM methods have been used to fabricate structural nodes for FFSGF construction for a long time, AM enables an unprecedented level of geometrical flexibility in potential node designs. This in turn creates new possibilities in terms of design freedom and material savings using a single fabrication procedure. In addition to this, AM encompasses a range of different technologies suitable for a wide range of materials, some of which were not compatible with more traditional CAM technology. AM technology has been advancing very rapidly over the past decade in terms of its possibilities, quality, reliability, industrialization, and accessibility. While for a long time, cost was a prohibitive barrier for the adoption of AM by the Architecture, Engineering and Construction (AEC) industry, as the technology continues to steadily advance towards the so-called “plateau of productivity”, now is a good time to explore the potential of AM for solving specific challenges faced by the construction industry.

1.2.5 The AM learning curve

The integration of AM into the construction industry, however, is not without its challenges. Requirements for products for the construction industry are demanding owing to the importance of life-safety and the increasing demands for high-performance sustainable solutions. AM technology is relatively new and thus not yet as well understood or trusted as more traditional tried-and-true fabrication methods. This is exacerbated by the fact that the properties of printed parts are different to those of traditional building products. In addition to this, different AM methods have different strengths and limitations that should be taken into consideration during AM product design. These are important not only because they dictate what is possible with the different printing methods, but also because they will impact the cost and efficiency of the fabrication process, which are key to developing AM products that are viable alternatives to existing products. In order for the AEC industry to be able to take advantages of the potential of additive manufacturing, the implications of working with this type of technology for architectural products need to be better understood, and strategies for the integration of AM into buildings are needed to guided AEC professionals in the development of AM solutions (Figure 1.4).

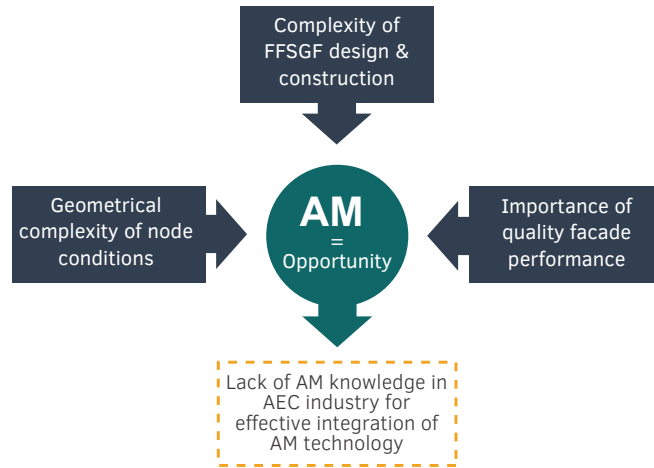


FIG. 1.4 Summary of problem statement for the use of AM in FFSGF construction. (Image by author)

1.3 Research objective and questions

1.3.1 Aim

The aim for this research is to facilitate the integration of AM into the design and construction of freeform steel and glass façade construction in order to improve their design, fabrication, and performance. This research focuses specifically on the design and production of AM node components. This choice is made deliberately in order to apply AM technology sparingly in areas with the highest geometrical complexity and susceptibility to performance issues, acknowledging the high cost and low speed of AM in comparison to mass-manufacturing methods.

The main outcome of this research is the exploration of the integration of AM technology in freeform steel and glass façades to improve on existing node solutions. This is achieved by developing several proof-of-concept AM node products for a freeform steel and glass façade, and by evaluating the key potentials and limitations associated with the proposed products and integration processes.

The recommendations and findings that are obtained from this research should serve to inform AEC professionals about the implications of working with AM technology for façades, and to inform AM industry professionals about the specific requirements and complexities involved in these types of applications, which have a high-potential for the use of AM, effectively bridging the gap between design and execution to facilitate further innovation.

1.3.2 Research questions

This dissertation aims to answer the following research question:

How can additive manufacturing be effectively utilized to develop node solutions that support freeform steel and glass façade construction?

In order to answer this research question, several sub-questions investigating different aspects of the design and development of freeform steel and glass façade construction and additive manufacturing technology must also be answered.

The major sub-questions correspond to the chapter structure. Additional sub-questions are in some cases necessary to arrive at an answer.

Chapter 2

What are the limitations of current FFSGF construction practices that could be improved with the use of AM?

Chapter 3

What is the state-of-the-art in the use of additive manufacturing for freeform façade construction?

Chapter 4

To what extent can the use AM improve the design of structural nodes?

- A What are the available AM methods for the fabrication of structural steel nodes for FFSGF construction?
- B Are the material properties of AM steel suitable for application in the building industry?
- C What are the relevant design guidelines for structural parts using metal AM methods?

Chapter 5

To what extent can AM provide better solutions for node conditions in the interior drainage layer?

- A What are the available AM methods for the development of gasket nodes for FFSGF construction?
- B Are the material properties of AM elastomeric materials suitable for application in the AEC industry?

Chapter 6

How can additive manufacturing be effectively integrated into interdisciplinary workflows for the realization of freeform steel and glass façades?

1.4 Research strategy

1.4.1 Research methods and organization

The exploration of AM as a means of improving freeform steel and glass façade construction is a broad endeavour because it encompasses a wide breadth of different possibilities. First, there are many different design variables and construction typologies for the realization of freeform steel and glass façades that can be explored for potential improvement. In addition, AM encompasses many different printing methods, each with their own strengths, limitations, and design possibilities. These two factors create a remarkably broad range of possibilities to explore.

This dissertation begins with an exploration of freeform steel and glass façade design and construction focusing on the main key barriers and discussing the multiplicity of design choices that can emerge during the process. Subsequently, the focus of this research is narrowed to two specific node applications, and to a subset of relevant AM methods and materials in order to develop proof-of-concept designs for AM system products, and to explore the consequences of specific design choices in the development of such AM products. In addition, the design process for the integration of AM in FFSGF is also demonstrated in a large-scale physical façade assembly prototype. In this way, the dissertation provides both broad and detailed information to support the development of similar products in the future. This dissertation consists of five main chapters, each of which corresponds to one or more of the research sub-questions. Figure 1.5 outlines the specific chapter structure and how these correspond to the sub-questions and project phases.

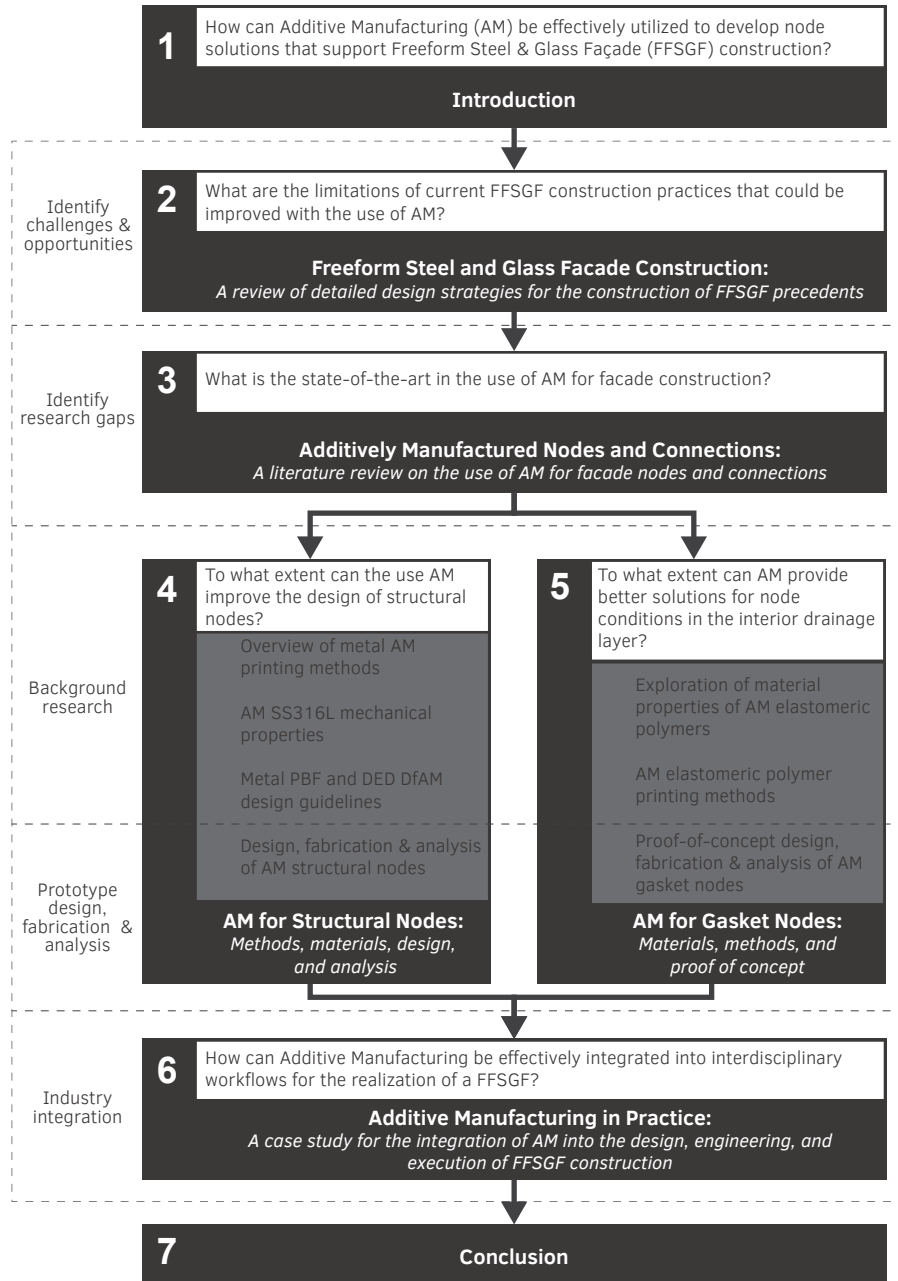


FIG. 1.5 Chapter organization and corresponding sub-questions. (Image by author)

The first two chapters are used to evaluate the state-of-the-art and identify opportunities for AM intervention. Chapter 2 is a state of the state-of-the-art review for FFSGF construction. The chapter starts with an exploration of freeform steel and glass façade construction methods wherein a collection of 40 FFSGF precedents is studied, and the general construction methods are identified and classified into typologies. These typologies are analysed and specific opportunities for AM intervention are identified based on this analysis. Chapter 3 is a short literature review on the use of additive manufacturing for nodes and connections in façades to identify specific research gaps for further exploration.

The next part of this research is divided into two streams, each exploring the development of a high-potential AM part for freeform steel and glass construction: structural nodes and gasket nodes. Each product has its own dedicated chapter in which there is first a background exploration of the available AM methods and an overview of a subset of relevant material properties, after which the product is designed, printed, and the results analysed. Cost is notably excluded from these analyses as it is a very volatile and quickly changing metric.

Chapter 4 explores the design and development of AM structural nodes, and the ability for systemized AM nodes to improve on current building solutions. The chapter begins with an overview of AM methods for metals. Two families of AM printing methods are selected for further exploration: Powder Bed Fusion (PBF) and Directed Energy Deposition (DED). The mechanical properties of PBF and DED materials are reviewed from literature in order to assess the suitability of the mechanical properties based on building industry requirements. Since mechanical properties vary by material and printing method, stainless steel 316L, a common alloy in AM as well as the construction industry, is used as a basis for evaluation. Subsequently, designs are developed for AM nodes using PBF and DED technology. As a first step, the design guidelines for DED and PBF are outlined and used to inform the design of different node iterations. Each of the nodes is dimensioned so that the structural capacity is sufficient for the same minimum structural requirements, and fabricated for the same geometrical configuration. The process for fabricating each of the nodes is described in detail, and the nodes are compared in terms of their design, fabrication efficiency, and material usage. The results are compared to a solid Computer Numerical Control (CNC) milled node. The results are discussed, in particular the extent to which the particular node design and configuration of the benchmark node impact results. The original version of this chapter included only laser-based powder bed fusion (PBF-L) and gas metal arc directed energy deposition (DED-GMA) nodes. It was decided during the course of the structural node study to add an additional node and design using laser-based directed energy deposition (DED-L) fabrication to overcome a major shortcoming of the fabrication process that was identified during the fabrication process. The materials study was updated retroactively.

Chapter 5 explores a slightly different process for the gasket development, since the objective is to develop the first AM gasket for façades, and design flexibility is a much less important component feature. In this case, the material properties are explored first, using a database for commercial AM materials to identify potentially suitable materials. The AM methods corresponding to those materials are subsequently described. Then, a benchmark model is designed with features likely to be incorporated into node gaskets, and a small prototype of the model is printed for each of the identified method/material combinations. A final gasket design is developed to improve on current node gasket solutions and subsequently printed as a proof-of-concept.

Chapter 6 discusses the integration of the product development undertaken in Chapters 4 and 5 in the larger context a construction project. It is a case study outlining the way in which the design, development, and fabrication of the AM products was conducted in the context of an interdisciplinary collaboration between a designer, engineering team, and execution team, for the realization of a full-scale freeform steel and glass façade. This chapter also outlines the digital strategy that was used to facilitate the interdisciplinary collaboration. The dissertation concludes with a reflection on the challenges faced over the course of the exploration, the most prevalent barriers to the integration of AM for architectural products and recommendations for future innovation.

1.5 Research impact

1.5.1 Societal relevance

FFSGF are a relatively common part of modern architecture. Freeform geometry is a powerful tool in the belt of architects that can be leveraged to sculpt dramatic and unique spaces, and give them expressive qualities such as movement, sculpture, or the impression of natural phenomena. It can also be leveraged to achieve structurally efficient forms that enable long spans with minimal supporting structure. Combined with glass as an infill element, freeform enclosures not only fill spaces with natural daylight, but also evoke a sense of lightness and openness. FFSGF are applied primarily in public spaces and cultural institutions. Notably, they have often been used to cover the courtyards of cultural institutions housed in heritage buildings, expanding their program without obtrusive intervention. FFSGF have also been an instrumental component of a number of new iconic architectural projects across the globe.

Despite the inherent complexity in the design and realization of FFSGF, their challenges have not outweighed their design potential and they continue to increase in popularity. Particularly as these enclosures are mostly applied for public buildings and spaces, those responsible for their realization should ensure that enclosure performance is high-quality and durable, and that the ecological footprint is as light as possible. Additive manufacturing presents an opportunity to reduce the vulnerability of these enclosures to air- and water-leakage through more geometrically suitable solutions and simplified assembly, and to reduce material usage for structural nodes and the supporting structure.

1.5.2 Scientific relevance

This dissertation adds to knowledge on the use of AM as a means of designing and producing parts for FFSGF construction. The process undertaken in this research provides a roadmap for the future design and development of FFSGF with systemized AM components. Besides the central aim, this dissertation also makes several specific contributions advancing knowledge in a few key areas. Chapter 4 approaches the design of structural node solutions differently than previous studies, namely as parametrically-driven systemized solutions rather than relying on topological optimization. It also provides practical information on the fabrication process and intensity for structural nodes using different AM methods, which can be used as a basis for designers of future structural node solutions to make informed decisions when it comes to node design and selecting a suitable AM method. Chapter 5 explores the use of AM for a novel application, namely for the production of mass-customized gaskets for façade construction. Chapter 6 outlines a workflow for the design, engineering and fabrication process as an interdisciplinary collaboration involving multiple stakeholders. It defines the specific responsibilities of each party and identifies pivotal areas of structural node design that are of collective interest to these stakeholders. This chapter also specifies the flow of information between stakeholders and across digital platforms.



Mansueto Library under construction (Image courtesy of Quinn Dombrowski)

2 Freeform Steel and Glass Façade Construction

A review of detailed design strategies for the construction of freeform steel and glass façade precedents

Over the last several decades, freeform steel and glass façades have increasingly become a popular option for building enclosures. They have been applied most commonly in commercial and institutional buildings in many countries, and using many different construction methods.

In order to support the aim of this dissertation, which is to improve the design, fabrication, and performance of freeform steel and glass façades through the use of additive manufacturing, this chapter explores the landscape of existing solutions for such constructions in order to identify opportunities for improvement. In order to do this, this chapter explores a wide range of different FFSGF precedents, classifies the different systems into general typologies, analyses the strengths and limitations of the different typologies, and through this analysis identifies opportunities for the use of AM in overcoming these challenges.

2.1 Introduction

The detailed design of any freeform façade should strive to achieve a few key objectives. First, the façade system must provide all the basic functional requirements of a building enclosure in such a way that it has good façade performance despite its geometrical complexity. Second, the façade system should respond to practical requirements related to execution (fabrication, assembly and installation). These factors include: cost [24], time efficiency and project scheduling [25], construction tolerances [26], existing conditions on site [27], the experience and resources of the execution team [28], and many other potential factors. Third, the system should respect the design intent of the architect.

Early examples of freeform façades required the development of bespoke solutions for addressing the unique challenges of freeform steel and glass construction that commercially available façade systems could not address. The development of freeform façade construction over the past several decades saw the emergence of not only an increasing collection of bespoke solutions, but also a catalogue of commercially available system-solutions capable of addressing a wide range of freeform projects. Similar to typical façade construction, systemized freeform façade solutions enable designers to accommodate a range of design variables such as profile geometries, connection methods, dimensions, capture system, etc. providing many unique façade system compositions for design teams to work with. Freeform façade system products differ from typical façade system products most notably in the resolution of complex intersections and the resulting introduction of node products.

This chapter identifies typological strategies applied to the node conditions of the main functional systems of steel and glass façades from a large collection of previous work. The two main functional systems under review are the structural system and the enclosure system. A glazed enclosure typically consists of four principal functional elements: (1) glazing or panel units that form the main enclosing element providing the primary thermal/acoustic/solar/etc. barrier for the envelope; (2) joining elements that provides continuity of the air, water and vapour management systems between panels; (3) a load-bearing structure that supports the enclosure self-weight and against positive and negative pressures; and (4) a capture system (or fixings) that transfer loads to the structural system [17].

The two main functional systems under review in this chapter are the structural system, which refers to the load-bearing structure; and the enclosure system, which refers to primarily the panel and joining elements that effectively separate the indoor from the outdoor environment by providing an air- and water-tight enclosure, a thermal barrier, a sound barrier, etc. It should be noted that the categorization of typologies proposed in this chapter is not the only possible option, but is selected since it provides an overview of the landscape of current construction strategies for freeform steel and glass façades, and a base for analysing opportunities for AM intervention. The typologies are defined primarily by geometrical characteristics, which include shape, orientation, and relationship to other components in the façade. Most obviously, these typologies all have different aesthetic qualities, which is an important part of the system selection. However, these geometrical characteristics are also inextricably linked to the detailed design, function, and construction of a given façade. Information collected for each project includes the size, scope, geometry and panelization of the enclosure, the shape, dimensions, and end conditions of the structural profiles, the structural node typology and fabrication methods, as well as the enclosure system typology and gasket joining strategy. The key information collected for each of these precedents is compiled in Appendix A.

Section 2.2 provides a categorization of structural node typologies and discusses the strengths and limitations of each; their typical fabrication methods; the context in which they were applied; and provides notable examples of such typologies. Structural system typologies are defined based on the geometry of the node, the interface with the structural members, and the fabrication method. Section 2.3 provides a similar categorization, analysis and notable examples for enclosure system solutions. Enclosure system typologies are defined based on their relationship to the structural system, and method of providing continuity of the enclosure system along panel edges. Section 2.4 outlines potential opportunities for improving structural nodes and enclosure systems through the use of additive manufacturing that were identified over the course of the precedents review.

2.1.1 Previous research

There are several key sources that provide an overview of freeform steel and glass façade solutions. Research is largely centred on structural node solutions.

Stahr [29] provided an overview of 6 different proprietary structural nodes, with a brief overview of the design of each of the structural node systems, their fabrication, their structural behaviour and their connecting parts. The author identifies a few

options for enclosure systems with continuous edge supported glazing, but this particular part of the review is brief, and is not a comprehensive overview of the different available options for enclosure systems.

Stephan, Knebel and Alvarez [30] provide an overview of 12 different proprietary structural node systems analysed with an emphasis on the relative ability of the different nodes to transfer internal forces and to accommodate local geometry. Based on these criteria, the authors identify overall geometry classifications to which each node system is most applicable, namely whether they require an underlying grid shell pattern that is structurally optimized and/or geometrically optimized.

Schober [31] provides an overview of steel and glass grid shells, engineered by Schlaich, Bergmann and Partner between 1989 and 2014. The author provides a table of information for different precedent buildings. Documented data includes geometrical information on the overall shape and rationalization of the enclosures, detailed design information about the structural system and glazing build-up, and the inclusion of cables. A brief description of the different structural node systems including in some cases insight into their fabrication, assembly, and structural behaviour is also provided.

Both [30] and [31] present information related the structural system and overall geometry of the enclosure. However, in both of these studies, the selected precedents do not present a comprehensive overview of current buildings methods. Since the publication of [30], several newer node typologies have been developed and applied in built projects. [30] also does not address constructions in which members are connected without an intermediary node component. While lattice-type construction using structural node components is a very popular strategy in FFSGF, many precedents worth including in the study of freeform façades do not make use of structural node components. [31] only addresses such cases where discretization is quadrilateral and members in one direction are continuous. Neither of these studies discuss enclosure systems or their relationship to the underlying structure.

This study categorises a comprehensive collection of freeform façade node systems by geometrical typology rather than commercial affiliation. It also focuses not only on the structural system, but also the enclosure system, which covers a wide and important range of the functional requirements of a façade, and considers how the two systems are applied in relation to one another.

2.1.2 Precedents selection

For this study, a collection of 40 precedents was compiled. An overview of the case studies can be found in Table 2.1. Criteria for the selection of the precedents was as follows; conformance to the definition of a *Single-Layer Freeform Steel and Glass Façade* applied in both building enclosures and watertight canopies; and construction between the year 2000 and the time of writing this chapter in the beginning of 2020. This time frame, starting with the pioneering construction of the British Museum, is marked by a decreased reliance on structurally and geometrically optimal design surfaces, and an increasing boldness in the form, size, and span of freeform steel and glass façade construction.

To identify relevant precedent studies, two strategies were used. First, precedents were collected by searching the portfolios of architectural firms and structural engineering firms with large, diverse portfolios or that habitually work on freeform projects including Studio Fuksas, Coop Himmelb(l)au and Foster and Partners. The portfolios of the following structural/façade engineering firms were also searched: Buro Happold, Arup, Schlaich Bergermann and Partner, knippershelbig and Werner Sobek. In addition to this, projects were uncovered by searching building databases of Arch Daily, Detail Inspiration, and Structurae. To identify relevant projects, keywords such as “freeform”, “façade”, “reticulated”, “lattice”, “grid shell”, “steel and glass” were used. The final precedents selection was narrowed based on the availability of information related to their detailed design.

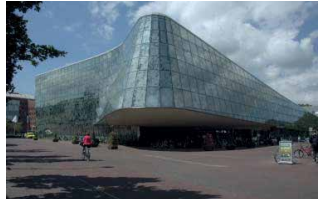



The final collection of precedents includes 40 buildings from 16 countries across Europe, North America, Australia, South America, and Asia. Data collected on these case studies was retrieved from the following sources: websites of the members of the project teams including architects, structural engineers, façade engineers, façade consultants, fabricators, and contractors; articles, conference papers and books identified from company references; databases Structurae, Scopus, and Science Direct; and photographs of active construction sites from online photography databases and construction blogs. Additional information was also collected in personal communication with project team members.

TABLE 2.1 Cases studies for the exploration of structural and enclosure system typologies

#	Project Name	Year	Pl.	Project Team	Data Source	Reference Photo
1	British Museum	2000	UK	Design: Foster and Partners Engineer/ Consultant: Buro Happold Execution: Waagner Biro	[4, 27, 32]	 Image source: [33]
2	Schubert Club Band Shell	2001	US	Design: James Carpenter Design Associates Engineer/ Consultant: Skidmore, Owings & Merrill LLP Execution: Meisinger Construction; TriPyramid Structures; Van Noorden	[34-38]	 Image source: [35]
3	DZ Bank Berlin	2001	DE	Design: Frank O. Gehry & Associates Inc. Engineer/ Consultant: Schlaich Bergermann Partner Execution: Josef Gartner	[31]	 Image source: [31]
4	Bosch Areal	2001	DE	Design: Prof. Ostertag Engineer/ Consultant: Schlaich Bergermann Partner Execution: Mero	[31]	 Image source: [31]
5	German Historical Museum	2002	DE	Design: I. M. Pei Engineer/ Consultant: Schlaich Bergermann Partner Execution: Mero	[31, 39]	 Image source: [31]

>>>

TABLE 2.1 Cases studies for the exploration of structural and enclosure system typologies

#	Project Name	Year	Pl.	Project Team	Data Source	Reference Photo
6	Alphen aan den Rijn	2002	NL	Design: Erick van Egeraat Engineer/ Consultant: Octatube Execution: Octatube	[40, 41]	 Image source: [41]
7	London City Hall	2002	UK	Design: Foster and Partners Engineer/ Consultant: Arup Execution: Westcol Glosford; Seele; Schmidlin AG Fassadentechnologie	[42-44]	 Image source: [42]
8	Uniqa Tower Vienna	2004	AT	Design: Neumann + Partner Engineer/ Consultant: Schlaich Bergermann Partner Execution: Mero	[31]	 Image source: [31]
9	The Sage at Gateshead	2004	UK	Design: Foster and Partners Engineer/ Consultant: Buro Happold Execution: Waagner Biro	[5, 45-47]	 Image source: [48]
10	Hessing Cockpit	2005	NL	Design: ONL Engineer/ Consultant: Faktor Civil Engineering Execution: Meijers Staalbouw	[6, 49, 50]	 Image source: [50]

>>>

TABLE 2.1 Cases studies for the exploration of structural and enclosure system typologies

#	Project Name	Year	Pl.	Project Team	Data Source	Reference Photo
11	New Milano Trade Fare (Logo)	2005	IT	Design: Fukasas Engineer/ Consultant: Schlaich Bergermann Partner Execution: Mero-TKS	[9, 31, 51]	 Image source: [9]
12	New Milano Trade Fare (Vela)	2005	IT	Design: Fukasas Engineer/ Consultant: Schlaich Bergermann Partner Execution: Mero-TSK	[9, 31, 51]	 Image source: [9]
13	Smithsonian Courtyard	2007	US	Design: Foster and Partners Engineer/ Consultant: Buro Happold Execution: Josef Gartner	[13, 52-55]	 Image source: [52]
14	BMW Welt	2007	DE	Design: Coop Himmelb(l)au Engineer/ Consultant: Bollinger and Grohmann; Emmer Pfenninger Partner; R+R Fuchs Execution: Josef Gartner; Maurer Söhne	[47, 56, 57]	 Image source: [56]
15	Cabot Circus	2007	UK	Design: Chapman Taylor Engineer/ Consultant: Schlaich Bergermann Partner Execution: SH Structures	[24, 31, 58]	 Image source: [31]

>>>

TABLE 2.1 Cases studies for the exploration of structural and enclosure system typologies

#	Project Name	Year	PL	Project Team	Data Source	Reference Photo
16	Zlote Tarasy	2007	PL	Design: The Jerde Partnership; Epstein Global Engineer/ Consultant: Arup Execution: Waagner Biro; Zenkner & Handel; Zeman HDF	[11, 59]	 <p>Image source: [33]</p>
17	Westfield Shopping Center	2007	UK	Design: Benoy; Buchanan Group Engineer/ Consultant: Knippershelbig Execution: Seele	[10, 60]	 <p>Image source: [10]</p>
18	MYZeil	2009	DE	Design: Fuksas Engineer/ Consultant: Knippershelbig Execution: Waagner Biro	[28, 61, 62]	 <p>Image source: [28]</p>
19	Salvador Dali Museum	2009	US	Design: HOK Engineer/ Consultant: Walter P Moore & Associates; Novum Structures Execution: Novum Structures	[63-65]	 <p>Image source: [63]</p>
20	Cybele Palace	2009	ES	Design: Arquimatica Engineer/ Consultant: Schlaich Bergermann Partner Execution: Lanik; Hiberlux	[1, 31, 66]	 <p>Image source: [1]</p>

>>>

TABLE 2.1 Cases studies for the exploration of structural and enclosure system typologies

#	Project Name	Year	Pl.	Project Team	Data Source	Reference Photo
21	De Blob	2010	NL	Design: Fuksas Engineer/ Consultant: IMD raadgevende ingenieurs; Knippershelig Execution: Waagner Biro; Heijmans Bouw	[7, 59, 67, 68]	 Image source: [67]
22	Dutch Maritime Museum	2011	NL	Design: Dok Architecten Engineer/ Consultant: Ney + Partners Execution: Anemco; BRS Building Systems	[2, 69-71]	 Image source: [69]
23	Shaw Center	2011	CA	Design: Brisbin Brook Beynon Architects Engineer/ Consultant: Novum Structures Execution: Novum Structures; PCL Constructors	[47, 72]	 Image source:[72]
24	Mansueto Library	2011	US	Design: Murphy/Jahn Architects Engineer/ Consultant: Werner Sobek; Wiss, Janney, Elstner Associates; Engelsmann Peters Execution: Seele	[73-75]	 Image source: [76]
25	Hyatt Capital Gate	2011	AE	Design: RMJM Engineer/ Consultant: Hyder Consulting; RMJM Execution: Waagner Biro; Al Habtoor	[77-79]	 Image source: [79]

>>>

TABLE 2.1 Cases studies for the exploration of structural and enclosure system typologies

#	Project Name	Year	Pl.	Project Team	Data Source	Reference Photo
26	King's Cross	2012		Design: John McAslan + Partners Engineer/ Consultant: Arup Execution: Seele; Taylor Woodrow/Vinci	[47, 80-82]	 <p>Image source: [81]</p>
27	Paunsdorf Center	2012	DE	Design: Lüttgenau Architekten Engineer/ Consultant: Schlaich Bergermann Partner Execution: Roschmann Group	[31]	 <p>Image source: [31]</p>
28	Höfe am Brühl	2012	DE	Design: Grüntuch Ernst Architekten Engineer/ Consultant: Schlaich Bergermann Partner Execution: Roschmann Group	[31]	 <p>Image source: [83]</p>
29	Gardens By The Bay	2012	SG	Design: Wilkinson Eyre Architects Engineer/ Consultant: Atelier One; Arup Execution: YKK AP Façades	[47, 79]	 <p>Image source: [79]</p>
30	Carioca Wave	2013	BR	Design: Nir Sivan Engineer/ Consultant: Knippershelbig Execution: Seele	[12]	 <p>Image source: [12]</p>

>>>

TABLE 2.1 Cases studies for the exploration of structural and enclosure system typologies

#	Project Name	Year	Pl.	Project Team	Data Source	Reference Photo
31	Ex Unione Militare	2013	IT	Design: Fuksas Engineer/ Consultant: Tecnobrevetti srl; Esa Engineering Execution: Stahlbau Pichler	[84-88]	 Image source: [86]
32	Ernst & Young Plaza	2014	LU	Design: Sauerbruch Hutton Engineer/ Consultant: Schlaich Bergermann Partner Execution: Bellapart	[31, 89]	 Image source: [31]
33	Bory Mall	2014	SK	Design: Fuksas Engineer/ Consultant: Knippershelbig Execution: Metal Yapi	[90-92]	 Image source: [92]
34	Musée Des Confluences	2014	FR	Design: Coop Himmelb(l)au Engineer/ Consultant: Bollinger and Grohmann; Coyne et Bellier; VS_A Execution: Josef Gartner; VINCI Construction France	[14, 93, 94]	 Image source: [94]
35	34th Street Canopy	2015	US	Design: Toshiko Mori Architects Engineer/ Consultant: Schlaich Bergermann Partner Execution: Enclos; TrussWorks International; TriPyramid	[95, 96]	 Image source: [95]

>>>

TABLE 2.1 Cases studies for the exploration of structural and enclosure system typologies

#	Project Name	Year	Pl.	Project Team	Data Source	Reference Photo
36	Chadstone Shopping Center	2016	AU	Design: CallisonRTKL Engineer/ Consultant: Atelier One; Bath University Execution: Seele	[3, 97-100]	 <p>Image source: [3]</p>
37	Grand Hotel Dieu	2018	FR	Design: AIA Life Designers; RL&A Engineer/ Consultant: AIA Ingénierie; Arcora Execution: Eiffage Construction; Renaudat Centre Constructions; HEFI	[101, 236]	 <p>Image source: [101]</p>
38	Capital C	2019	NL	Design: ZJA Zwarts & Jansma Architecten Engineer/ Consultant: Octatube Execution: Octatube	[102, 103]	 <p>Image source: [103]</p>
39	Moynihan Train Station	2019	US	Design: Skidmore, Owings & Merrill Engineer/ Consultant: Schlaich Bergermann Partner Execution: Seele	[104-107]	 <p>Image source: [104]</p>
40	Jewel Changi Airport	2019	SG	Design: Safdie Architects Engineer/ Consultant: Buro Happold; RSP Architects Planners & Engineers Execution: Mero-TSK	[26, 108-111]	 <p>Image source: [108]</p>

2.2 Structural node typologies

As part of the structural layer, the structural node has a load-bearing function that is defined predominantly by its shape, materiality, dimensions, and connection method. The shape of the node has a number of practical implications: it affects the interface with the enclosure system, provides the load path for the transfer of forces, affects the manufacturing possibilities of the part, and also affects the aesthetic of the façade. The typologies identified in this study focus on the shape of the node. They are categorized first by the orientation of the node geometry, second by the interface between the structural node and the incoming members, and third by the actual shape of the node. Figure 2.1 illustrates this categorization, which is elaborated on below.

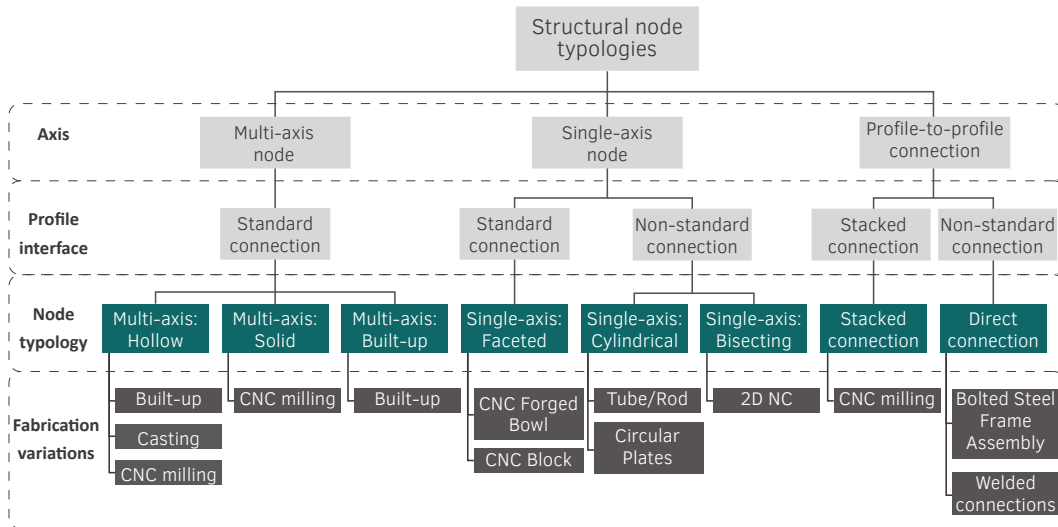


FIG. 2.1 Categorization of structural node typologies (Image by author)

The first tier of the categorization for the structural node typology is the nature of the node axis, which is divided into three families: multi-axis nodes, single-axis nodes, and direct profile-to-profile connections. In a multi-axis node (Figure 2.2a), the node has “arms” equalling the number of incoming members that extend towards them and meets them tangentially at their end-face. In this way, the geometrical complexity of the intersection is resolved in the node while the node arms always

meet the profile member at a standard interface. This is a key advantage of multi-axis node typologies. Multi-axis nodes generally require 3-dimensional fabrication methods, or 3-dimensional assembly of part generated by 2-dimensional fabrication methods. In a single-axis node (Figure 2.2b), there is a single central axis aligned with the node normal. The single-axis node is typically fabricated from one or two main subcomponents. Because of the varying orientations of the incoming members, the inner and outer faces of the node will not align exactly with those of the incoming profiles, and the interfaces will generate “stepped” surfaces that must be accommodated by the interior gaskets. The fabrication of single-axis nodes is relatively simple compared to multi-axis nodes, since they mostly require only 2-dimensional fabrication or simple 3-dimensional fabrication operations. Lastly, members can also be connected directly to one another without the use of a node component at all, which requires the members to be cut and joined at complex angles (Figure 2.2c) or to be continuous.

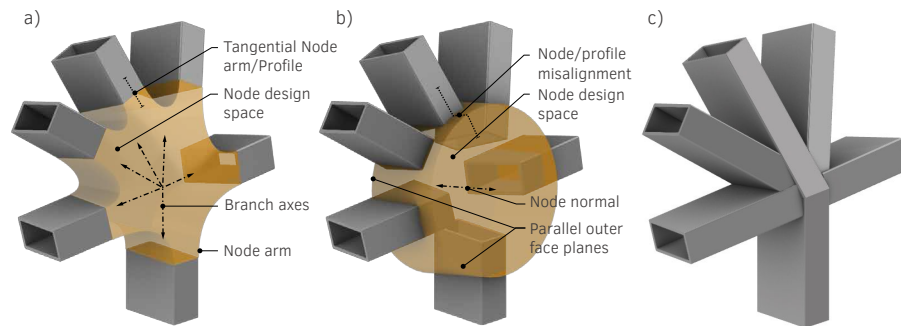


FIG. 2.2 Structural system categorization by axis: a) Multi-axis node; b) Single-axis node; c) No node component (Image by author)

These three families of node solutions are further divided by their interface with connecting profiles. Standard end connections (Figure 2.3a) simplify fabrication of the profiles since the geometrical complexity is contained within nodes, which are both fewer and smaller than profiles. Corresponding members have relatively simple fabrication, which generally includes cutting, notching, and/or adding standard attachments to facilitate strong mechanical connections. Members can also be welded to the node when structurally required, although mechanical fastening is generally preferred [92]. Non-standard end connections (Figure 2.3b) require that profiles be carefully cut at different shapes and/or angles, which can in many cases be quite complex. The majority of non-standard end conditions observed in the precedents used welded connections. The others were mechanically connected either

with end plates, with the use of embedded connection plates, or with CNC machined notching for a splice connection. In a continuous member connection (Figure 2.3c), the members are stacked, and the interface is made along the length of structural members rather than end faces, enabling the members to be continuous.

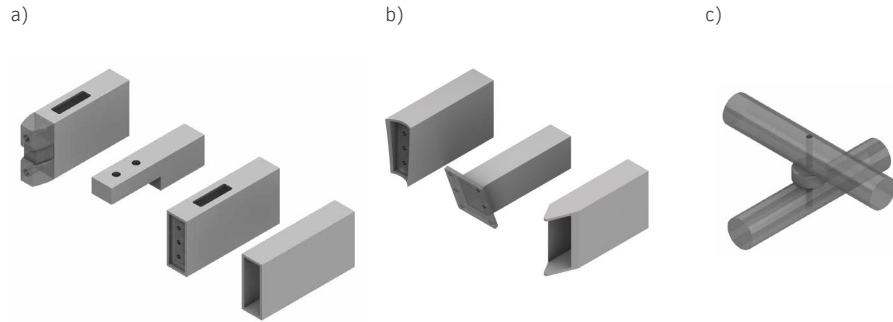


FIG. 2.3 Structural system categorization by profile end condition: a) examples of standard member end conditions; b) examples of non-standard member end conditions; c) example of continuous members. (Image by author)

The final categorization is based on the actual shape of the node, which affects the aesthetic of the system, the interface with the enclosure system, and the suitable fabrication methods for the part. Further categorization of these main typologies can be made by different fabrication methods employed to construct them. The typologies are expanded upon below.

2.2.1 Multi-axis: hollow

In a multi-axis hollow node, the node is a volumetric component whose end conditions correspond to the shape and orientation of incoming profiles. The relative rotation and twisting of the members are resolved in the central part of the node. The size of the node and the reach of its arms towards members varies, however each arm extends at least far enough to meet profiles before adjacent members intersect one another. The interior of the node is hollow, making it potentially significantly more lightweight than a multi-axis solid node of the same dimensions. The actual material efficiency of the node would depend also on minimizing material waste while fabrication sub-components.

Multi-axis hollow nodes can be fabricated in several ways. An early example of this node typology was a built-up assembly of steel plates and CNC-milled end components that form a shelled version of the node volume [60]. In this system, developed by Seele for the Westfield Shopping Center, the nodes had variable plate thicknesses and bolt diameters based on the specific structural requirements of the nodes [10]. In order to get smooth node geometry from planar elements, the upper and lower faces of the node assembly are covered with a synthetic fibre filler that is grinded down to smooth the geometry of the node [60]. This node typology relies on the automation of several NC fabrication processes for efficiency, and eventually the subcomponents (Figure 2.4) are assembled and welded [10].

A total of 4 Precedents used this structural node typology. Within the multi-axis hollow node typology, 2 out of the projects were for true freeform overall geometries and 2 for geometrically optimized overall geometries. 3 out of the 4 projects used bolted end-face connections as the primary connection type. Bolted end-face connections for multi-axis hollow nodes are concealed and are fixed and tensioned through a hole in the incoming profiles, which are cut at 90 degree angles and complete with an end plate (Figure 2.5).

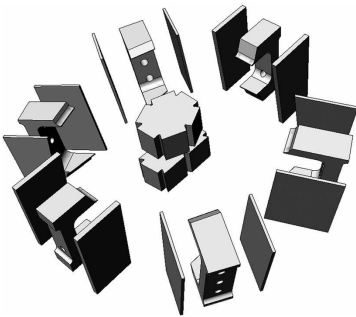


FIG. 2.4 Node sub-component assembly for Westfield Shopping Center roof (Image courtesy of ©Seele)

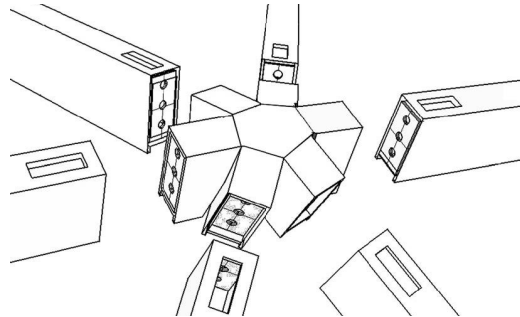


FIG. 2.5 Standard end connection with end plate and opening in profile for access to fix and tension bolts (Image source: [10])

2.2.2 Multi-axis: solid

Similar to the previous typology, the solid multi-axis node (Figures 2.6–2.8) is a volumetric component whose end conditions correspond to the shape and orientation of incoming profiles, resolving the relative rotation and twisting of the members in the central part of the node. The interior of this typology, however, is solid material. This node typology is fabricated using multi-axis CNC-milling as applied in [26, 89, 92]. Compared to the other two multi-axis node typologies, the fabrication of the solid node is relatively simple as it does not require a series of intensive fabrication steps, but rather a single NC process. This simplicity of fabrication, however, comes at the cost of material efficiency: while the other multi-axis nodes' sub-components can be adjusted in thickness (even parametrically) to address specific load conditions, the solid nodes will often be heavier than necessary [112], and can have low utilization percentages.



FIG. 2.6 CNC-machined node with simple geometry from DZ Bank Berlin (Image source: [113])



FIG. 2.7 CNC-machined node with end-face connection from shopping center in Bratislava. (Image source: [92])



FIG. 2.8 CNC-machined node with splice connection from 34th street Canopies. (Image courtesy of TrussWorks Intl)

8 precedents were observed used this structural node typology. Within the multi-axis solid node typology, 4 instances were for true freeform overall geometries and 4 for geometrically optimized overall geometries. Early versions of this node typology consisted of relatively simple geometric forms as can be seen in Figure 2.6, while later applications tend towards more organic forms (Figure 2.7). These more organic forms are similar in appearance to the hollow node typology shown in Figures 2.4 and 2.5, but can more easily incorporate rounded profile edges. 3 out of the 8 precedents used a similar concealed bolted end-face connections as described in the multi-axis hollow node as the primary connection type. This type of connection can be seen in Figure 2.7. Another connection strategy observed in 2 cases is to use

a splice connection which requires a standard notch in solid members such that they can lap over or around the node and be connected with fasteners along the main axis of the profile as shown in Figure 2.8 [31, 95]. In some cases, a combination of welded and bolted connections are used where forces are too high for the bolted connection [30, 92, 113]. In 3 projects using multi-axis solid nodes, welded connections were used the default connection type [28, 31, 89].

2.2.3 Multi-axis: built-up

The multi-axis built-up node is a node typology in which there is a central element aligned to the node axis from which arms reaching out to meet the members in standard end connections are built up from simple sub-components such as plates. While this node requires significant fabrication effort as there are many sub-components to fabricate and assemble, it can result in relatively lightweight nodes. Similar to the multi-axis hollow typology, the actual material efficiency of the node depends on minimizing material waste while extracting the sub-components. This node typology, unlike the two previous multi-axis node typologies, strongly articulates the presence of the node by interrupting the visual continuity of the members.

Only one precedent included in this study used this structural node typology for a true freeform overall geometry. However, this node typology was also used in several other less well-documented projects by ONL [49, 114, 115]. The built-up node (Figure 2.9) uses two connection types: an end-face connection for the circular profiles that can be fastened from the node side without requiring openings in the structural members; and a splice connection that uses a standard end connector on the rectangular profiles. The exposed bolted connections of these nodes contribute to the strong tectonic expression of the node design. A similar node strategy is also sometimes applied in timber grid shell construction [116].



FIG. 2.9 Built-up node with end-face and splice connections from A2 Cockpit in Utrecht. (Image courtesy of ONL)

2.2.4 Single-axis: faceted

The single-axis faceted node typology is characterized by having a single-axis node with facets or small grooves that are planar to the end-face of the incoming members, enabling the node to meet the end-faces of orthogonally-cut members with standard end conditions. The geometry of the single-axis node can vary but is visibly distinct from that of the incoming members. The radius of the node is generally repeated across a project such that standardized billets can be used to CNC mill nodes, and is large enough to enable all of the incoming branches to meet the node without adjacent profiles intersecting one another. This requires a panelization strategy with large enough U-angles to avoid having very large nodes [64]. In order to have a more accommodating U-angle tolerance, tapered profile extensions can be used to avoid intersections between adjacent profiles [47].

This node typology is commonly fabricated by CNC milling of forged steel components [9, 47, 117]. Although they use the same fabrication process as the multi-axis solid node, the fabrication of single-axis faceted nodes is significantly less intensive since the forged blanks are near-net-shape and only require minimal material removal, while the multi-axis nodes require significant material removal as well as surface finishing operations to get an architectural finish. The material efficiency of these nodes is also good in comparison since, even when the node itself is solid, the size of single-axis nodes is generally smaller than multi axis ones.

The design and assembly of this node can vary significantly. The choice of base component for milling gives the designer some freedom in the appearance of the node, and also the access conditions. When hollow steel tubes or discs are used

as a main subcomponent as shown in Figure 2.10, the bolted connections can be exposed from inside the node. This strategy is also structurally efficient as the loads will be effectively distributed around the node by membrane action. This strategy can be applied in either a single-layer or double-layer configuration. In a single-layer configuration (Figure 2.10) there is a single node component that spans the entire depth of the profile, whereas in a double-layer configuration (Figure 2.11) there is one node component aligned with the top flange of the incoming members and another aligned with the bottom. This division provides efficient bending moment capacity as it divides bending moments into compressive and tensile forces [9].

This was the most popular structural node typology having been applied in 11 precedent studies: 7 true freeform and 4 geometrically optimized overall geometry. It was applied with both bolted connections and welded connections.

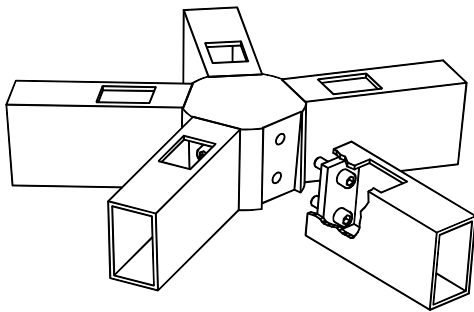


FIG. 2.10 Faceted single-axis node in single-layer configuration (Image source: [30])

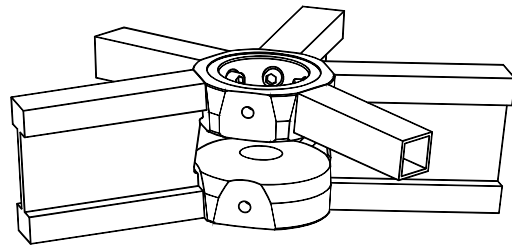


FIG. 2.11 Faceted single-axis node in double-layer configuration (Image source: [30])

2.2.5 Single-axis: cylindrical

The single-axis cylindrical node is a cylinder-shaped component or group of components aligned with the node normal. This node typology has been observed to be fabricated from standard components such as steel rods, tubes, and plates, which are then cut to length and potentially either grinded or machined to the appropriate outer surface relief.

Similar to the faceted node, the radius of the cylinder should enable all of the incoming branches to connect to the node without intersecting one another, and benefits from large U-angles to avoid large nodes. Rules for required depth and radius of cylindrical nodes specifically is discussed in [29]. A notable characteristic

of the cylindrical node is that the U-angle interface between the node and the member is always circular. It is because of the unique V- and W-angles of members that the end conditions are characterised as non-standard, since they must conform to their unique profile orientation. Alternatively, profiles can be oriented in the same direction, eliminating the relative twisting of members (W-angle), enabling the use of discrete cylinders with very small radii, and simpler profile end conditions.

A total of 4 precedents used this structural node typology, all true freeform overall geometry. In 3 of these cases, welded connections were used [71, 101, 118]. In the case of the Unione Militare (Figure 2.12), recessed end plates are used to hold the profiles in place during construction via node-access bolted connections prior to getting welded [118]. In the 4th case of Höfe am Brühl, the cylindrical node is made up of circular plates sandwiching CNC notched profiles for a splice connection [31]. Two precedents studies, namely the courtyard roof of the Grand Hotel Dieu Lyon [101], and the courtyard roof of the Dutch Maritime Museum [71], the nodes and profiles are all oriented vertically. In the former, this enables very slim nodes (Figure 2.13), and in the latter, a normalized orientation for lighting embedded in the nodes.



FIG. 2.12 Cylindrical nodes of Ex Unione Militare by Stahlbau Pichler (Image courtesy of Guido Ranieri Da Re)



FIG. 2.13 Hotel Dieu courtyard roof cylindrical nodes by Roschmann Group (Image source: [101])

2.2.6 Single-axis: bisecting

The single-axis bisecting node has “arms” branching out between adjacent pairs of incoming profiles. These arms extend about as far the surface of intersection of the two adjacent profiles (Figure 2.14). Several of the observed examples of this node typology utilize a façade system patented by Waagner Biro. The node is fabricated using 2-dimensional NC operations such as “electronically controlled combustion,

laser or water jet” [59] to cut a thick steel plate. The plate thickness is such that its outer faces are slightly recessed from the top and bottom faces of the incoming grid members. Incoming members are cut at complex angles to interface with the node arms, and stop at the plane of intersection with the node (Figure 2.14), or have a top flange that extends above the node towards a central mandrel [68]. It was also applied in the structural diagrid of the Capital Gate Abu Dhabi façade [47].

This system allows for minimally visually intrusive nodes with simple node fabrication, only requiring 2D NC cutting. The simplicity of the node fabrication, however, is offset by the complexity of fabricating the member end conditions. This typology requires welded connections and is typically pre-assembled in large prefabricated ladders or lattice frames which are assembled on site [4, 11, 31, 81, 89, 103].

A total of 5 precedents used this structural node typology, all true freeform overall geometry. It was first developed for the British Museum courtyard roof in London [33], a project which, because of its interface with an existing structure that could not bear additional lateral loads, was placed on sliding bearings and thus resulting in nodes subject to high bending moments and shear forces [27]. The fully-welded connections, while intensive in terms of fabrication, provide adequate bending moment resistance for such an application.

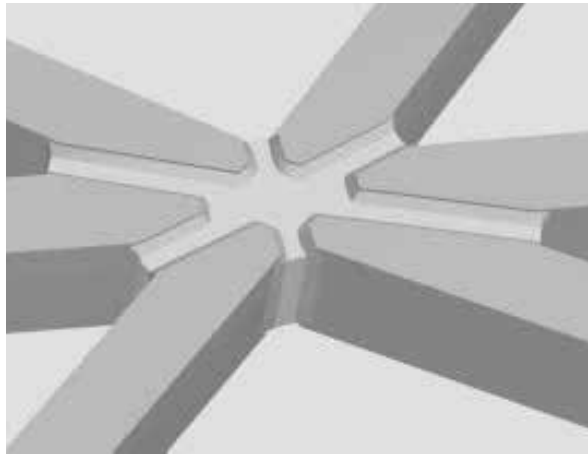


FIG. 2.14 Single-Axis bisecting node from British Museum, London. (Image source: [27])

2.2.7 Stacked connection

In a stacked connection, profile members are made continuous at joints, and joined using a pinned connection. The node is located between two strata of structural profiles and interface with the profiles along their length rather than at their end faces.

Only one precedent was observed to use this typology, namely the Schubert Club Band Shell canopy. The profiles are connected by a post and a through-bolt, around which every other node is fitted with a machined split ring that houses diagonal rods in the interlayer to provide lateral support for the shell (Figure 2.15a). This particular project relies heavily on optimal geometrical conditions. The geometry of the canopy consists of a toroidal surface (Figure 2.15b), which discretizes to Planar Quadrilateral (PQ) glazing, planar beams, torsion-free nodes, and a constant vertex-to-vertex distance between the two layers of structure, enabling the use of the same pin-jointed detail at all intersections [38]. The axis of the posts is defined by the surface normal and passes through the two layers of profiles which cross one another orthogonally. The profiles are curved to create the curvature of the overall geometry rather than faceting at nodes. Despite the advantages of geometrical optimization in this project, this strategy has been applied in true-freeform applications using wood [119-121] suggesting that it could also be executed in steel, although it would require more complex bending of the profiles which are in this case planar and curved at a single radius.

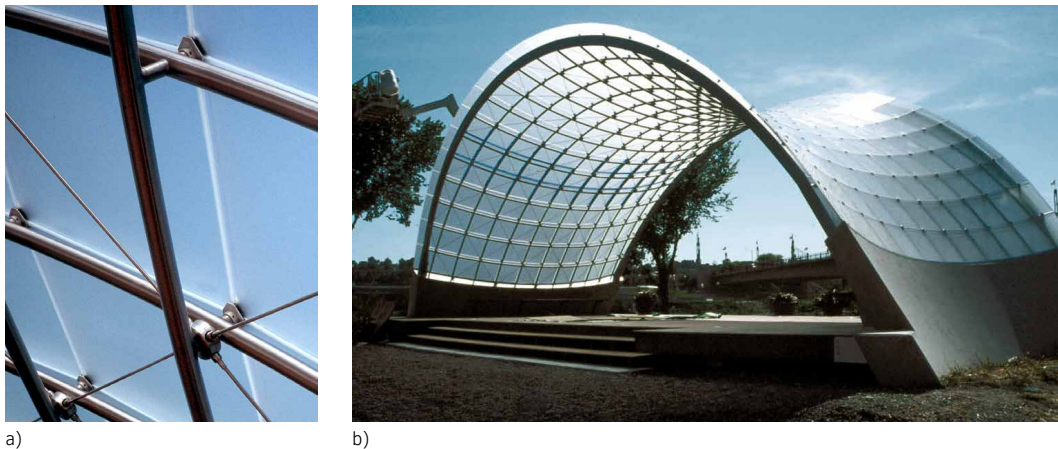


FIG. 2.15 Schubert Club Band Shell: a) detail with and without cable housing unit; and b) overall toroidal geometry. (Image source: [35])

2.2.8 Direct connection

In direct connections, profiles are attached directly to one another without an intermediary node product at the junction. Such systems typically have a visible hierarchy of primary, secondary, and sometimes tertiary members (Figure 2.16) which is visible by the continuity of the members at the joint. The complexity of this strategy can vary depending on the geometry of the façade.

In geometrically optimized scenarios, traditional steel framing methods can reasonably be used to construct the steel frame. The Sage at Gateshead (Figure 2.17), for example, is rationalized into various rotational surfaces [5], which allows all framing members to be planar, and intersections to be orthogonal. This project uses traditional steel framing methods with primarily bolted connections and limited welding [45]. In more geometrically complex applications where careful angular cutting of the profile ends is required, welded connections are used [47, 56, 77, 103]. This options is somewhat limited in terms of geometrical flexibility since, particularly when hollow profiles are used, the flanges of the profiles must align sufficiently such that they have enough overlap for a sufficient transfer of forces through the welded connections. A total of 8 precedents used this structural node typology, 5 of which were for true freeform overall geometries and 3 for geometrically optimized overall geometries.



FIG. 2.16 Directly welded node from BMW Welt façade, a true freeform geometry requiring complex cutting and welding of profiles (Image courtesy of Frank Dinger)



FIG. 2.17 Structural node of the Sage at Gateshead façade – a geometrically optimal surface divided into quad panels) constructed using traditional steel framing methods (Image source: [47])

2.3 Enclosure system typologies

Detailed information on enclosure systems is not as openly documented and published as strategies for structural nodes. As such, the typologies in this section are more general. Figure 2.18 illustrates the categorization, which is described more in detail below.

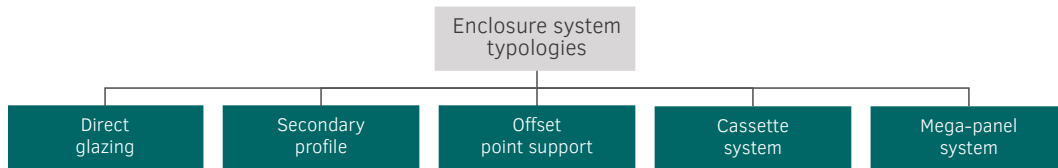


FIG. 2.18 Categorization of enclosure system typologies (Image by author)

2.3.1 Direct glazing

A directly glazed system (Figure 2.19) resembles the typical stick-built steel and glass façade system described in Chapter 1 in that an infill panel is applied to the main structural framing with an extruded gasket compressed between the infill panel and the steel frame. A continuous seal is provided by the compression of the gasket layer between the glazing and structural layer. There are various strategies for joining of the interior drainage layer at nodes which are elaborated on in Section 2.3.6. In all cases where the information was available, this enclosure typology was detailed with a wet-glaze exterior seal.

A variation of this typology includes an aluminium profile with rebates to mechanically secure the gasket along the length of the steel structure. This strategy can be applied to bridge gaps or misalignments in the structural layer and/or to facilitate installation since the aluminium profile secures the gasket in place along its entire length.

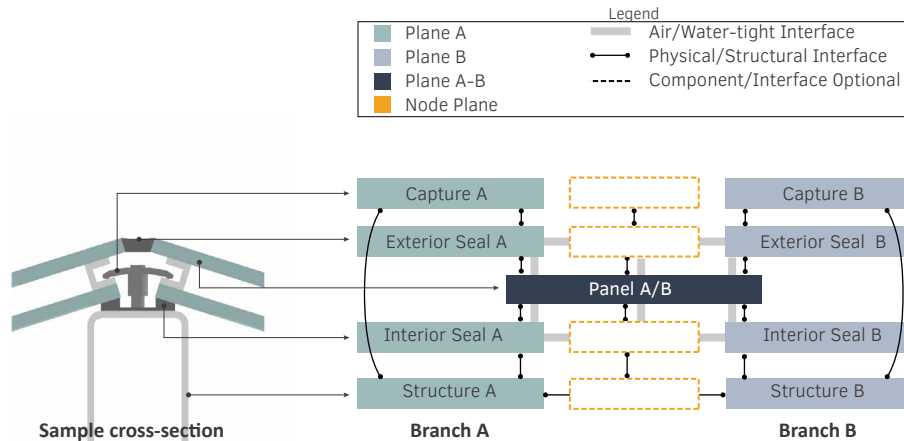


FIG. 2.19 Schematic illustration showing the key elements and interfaces in the direct glazing typology with a sample detail for reference (Image by author)

The direct glazing method can be desirable because of the relative simplicity of the assembly, because it does not require a secondary layer of structure, and because it provides redundancy in the air/water control system. This strategy, however, can be challenging in complex geometries since it relies on the continuous, compressive seal around the entire perimeter of the glazing units for redundancy in the air/water management system as described in Section 1.2.2. This becomes even more challenging when the underlying structure has bulky cross-sections since large profiles magnify misalignments. Another limitation of this enclosure typology is that wide structural profiles in combination with convex glazing units risks collisions between the structural layer and glass.

It is common in this type of application to locate the reference mesh on the outer face of the structure or at the inner glazing joint such that misalignments near the seal are relatively minor. A noteworthy disadvantages of this strategy is that it magnifies misalignments of the bottom flanges, which are visible from the building interior, and that additional bending moments are introduced in the structural layer due to the misalignment of the central axes of incoming profiles [11].

Direct glazing was the most popular enclosure typology, observed in 26 precedent studies. Within the direct glazing typology, 18 instances were for true freeform overall geometries and 8 for geometrically optimized overall geometries. It was observed applied in combination with every structural node typology with the exception of the stacked node connection which is logical since the layers of structure are both circular and at significantly different distances from the glazing.

2.3.2 Secondary profile

In some cases, the glazing unit is supported by a secondary structural layer offset from the main structural layer (Figure 2.20). In this case, the “direct glazing” typology is effectively applied onto the secondary structure which is tied back to a primary steel lattice by intermediate stands or posts. The secondary structural layer can also be of steel [94] but is more often aluminium. As with the direct glazing typology, the interior drainage plane can be joined in various ways which are elaborated on in Section 2.3.6. In all cases where the information was available, this enclosure typology was also detailed with wet glazing for an exterior seal.

In this typology, it is possible to have two layers of reference geometry: an outer mesh near the glazing layer and an inner mesh corresponding to the main structure. In this way, the outer layer can be configured to enable the direct application of glazing, while the main structural layer can be configured in the structurally optimal configuration without physically interfering with the performance of the interior drainage layer. Another advantage of this strategy is that it enables the primary and secondary structural grids to be different densities, creating zones of very high transparency with only the less obtrusive secondary profiles. A limitation of this strategy is that the addition of a secondary layer of structure negatively impacts factors such as cost, material usage, and assembly intensity.

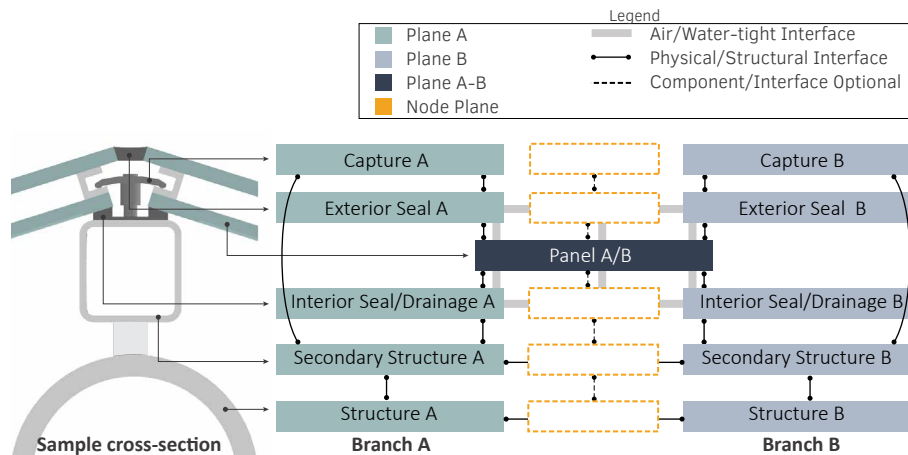


FIG. 2.20 Schematic illustration showing the key elements and interfaces in the secondary profile typology with a sample detail for reference (Image by author)

The secondary profile typology was observed in 5 precedent studies. Within the secondary profile enclosure system typology, 2 instances were for true freeform overall geometries and 3 for geometrically optimized overall geometries. This typology was applied in 4 of the 6 precedent studies where circular or elliptical profiles were used (Figure 2.21) or where combinations of profile geometries were used (Figure 2.22). In such cases, the different profiles can be aligned at their central axis to avoid additional moment forces despite having variables depths since the outer surface of the structural layer does not have to provide a base for a compressive seal.



FIG. 2.21 Offset support of Mansueto Library (Image source: [122] (CC BY-SA 2.0))



FIG. 2.22 Cylindrical node on steel structure of King's Cross Station. (Image courtesy of Barrie Tate)

2.3.3 Offset point-supports

The offset point-supports typology consists of intermittent point supports at edges or corners of the panel (Figure 2.23), with sealant along the panel edges providing the sole layer of air/water/vapour management for the system. Such systems do not include a continuous interior drainage layer. While on one hand this means that there is less redundancy to the enclosure system, on the other hand, the offset point support typology provides a significant amount geometrical freedom, both in the design of the overall structure and the design of the node, as it is not restricted by having to maintain

a dry compressive seal between the structural layer and panels. Similar to the previous typology, this enables the assembly to have two sets of reference geometry: an inner reference mesh defining the structure, and an outer reference mesh defining the glazing joint, such that both systems do not interfere with one another's performance.

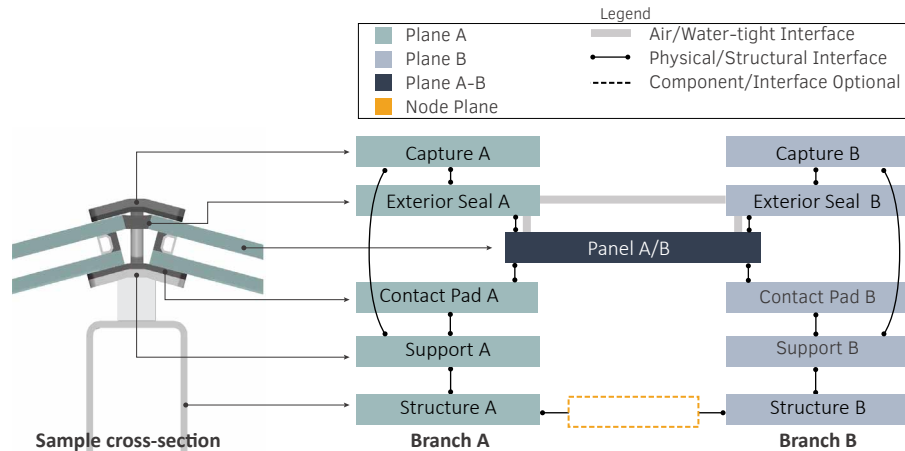


FIG. 2.23 Schematic illustration showing the key elements and interfaces in offset point-support typology with a sample detail for reference (Image by author)

A total of 6 precedents used this enclosure system typology. Within the offset point support enclosure system typology, half were for true freeform overall geometries and the other half for geometrically optimized overall geometries. In the freeform applications, it was applied in 2 instances that have particularly extreme geometry such as the Dali Museum (Figure 2.24). The Dalí Museum in St. Petersburg has a complex envelope with sharp faceting with angles between glazing units ranging from negative angles of more than 40 degrees to positive angles of almost 50 degrees [8]. The freeform system by Novum Structures was used, which enabled the construction of a façade with hurricane-level resistance [123]. This structural resistance is helped by the fact that this system allows the central axes of the profiles to be aligned without limiting the allowable angles due to the internal drainage layer. If direct glazing had been used, for example, the reference geometry would have had to be nearer the glazing joint which would result in additional bending moments at nodes.

This enclosure typology was also observed in applications where the supporting structure is not continuous around panel edges either because it is layered or curved like the previously mentioned Schubert Club Band Shell (Figure 2.15) [34], or unidirectional like Town Hall Alphen aan den Rijn (Figure 2.25) [41].



FIG. 2.24 Salvador Dali Museum Façade by Novum Structures. (Image courtesy of ©Salvador Dali Museum, Inc., St. Petersburg, FL.)

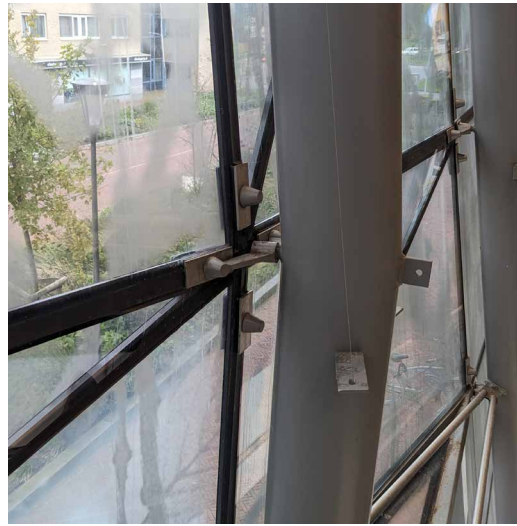


FIG. 2.25 Façade from Town Hall Alphen aan den Rijn which has a unidirectional support structure consisting of columns. (Image by author)

2.3.4 **Cassette system**

Cassette systems are a common strategy also in standard façade construction. A cassette consists of a prefabricated unit of a glazing unit and a secondary frame usually made of aluminium. In cassette systems, a weather seal is provided between the glazing unit and their respective frames, as well as between adjacent cassettes. A secondary drainage layer may also be provided beneath the cassettes.

General advantages of cassette systems include that the frame provides continuous support at the glazing panel edges, which reduces glass deflections and can be leveraged to have larger panels and ultimately a more transparent façade, and that the independent mechanically fastened units can help speed up installation [124]. In freeform fabrication, there is also the advantage that the enclosure system does not rely on the alignment of adjacent glass units, since they are not joined directly (Figure 2.26). As such, Planar Quadrilateral (PQ) glazing units can be used also in non-optimal geometrical configurations, which is generally desired as they are simpler and more cost-effective to produce than triangular or curved quadrilateral Insulated Glazing Units (IGU).

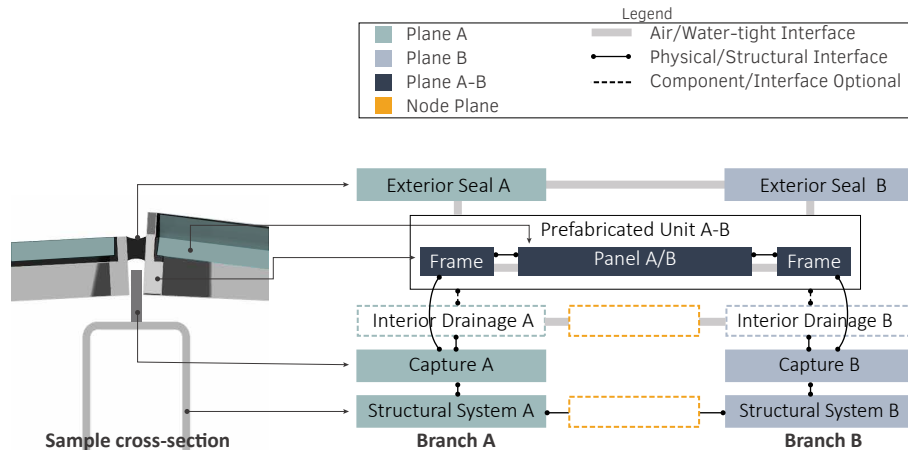


FIG. 2.26 Schematic illustration showing the key elements and interfaces in cassette system typology with a sample detail for reference (Image by author)

The cassette typology was observed in two projects, both of which make use of the cassette as a means of having planar quadrilateral panels in a freeform roof without a PQ reference mesh: the Smithsonian Institute Courtyard and Moynihan Train Hall. The Smithsonian Institute Courtyard by Foster and Partners (Figure 2.27) is a good and well documented example of how this strategy was applied. A planar quadrilateral construction was desired to maximize the overall transparency of the roof, and while affine transformations were explored to generate a planar quadrilateral mesh, the resulting geometry did not fulfil design intent [54]. The discretization of the roof is based on the projection of a diagonal grid onto a freeform design surface [125]. Then, each panel is made planar by maintaining two of the four panel vertices in their location on the design surface, and displacing the other two from the design surface by equal amounts such that all four points are on a single plane [54]. Each resulting 4-point surface is the base for a cassette panel which is mechanically connected to the structural gridshell (Figure 2.28). The structural gridshell incorporates twisted beams oriented normal to the design surface for structural efficiency. Aluminium channels run along the top of the twisted beams along which the cassette units are mechanically fastened.

It is worth noting that at the time of the construction of the Smithsonian museum, this particular detailed design was an innovation that enabled the use of planar quadrilateral panels for true freeform geometry, which was previously only observed in geometrically optimized scenarios. Since then, computational processes such as those developed in [3] and [102] use advanced computational methods to rationalize freeform surfaces into (near)PQ meshes. These computational methods

enable the construction of true freeform façades using minimally cold-bent quadrilateral panels with a direct glazing enclosure typology, which notably doesn't have the added cost and weight of a secondary frame. A significant disadvantage of this strategy, however, is that architects lose their design freedom when it comes to the layout of the structural grid, since it is calculated from the input geometry, resulting in irregularly shaped panels such as those applied in the Chadstone Shopping Center [3]. The cassette strategy applied in the Smithsonian and Moynihan Train Hall conveniently facilitates the application of a structural grid that is orthogonal in plan with PQ IGUs.



FIG. 2.27 Outer appearance of Smithsonian Kogod Courtyard roof (Image source: [48])

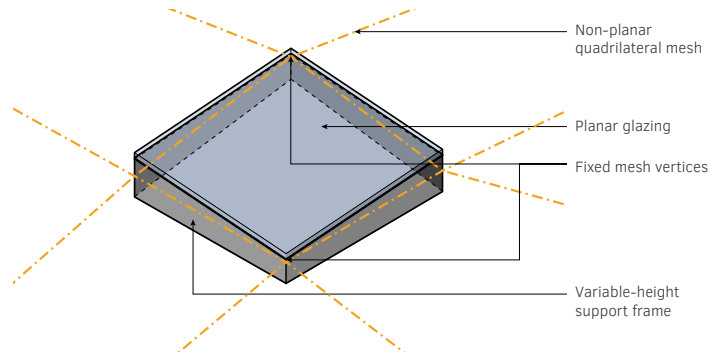


FIG. 2.28 Schematic representation of planar quadrilateral panel relative to non-planar quadrilateral reference geometry (Image by author)

2.3.5 Mega-panel system

The final enclosure system typology observed in the collection of precedents is the mega-frame system. This particular typology is an application in which a large prefabricated frame contains an interior substructure supporting multiple glazing units. This typology is considered a hybrid because the exterior frame is sealed like a cassette system, while the interior portion of the mega-panel uses direct glazing. This type of approach allows a significant amount of prefabrication and expedited on-site assembly.

The hybrid system enclosure typology was observed in two projects: London City Hall and Hyatt Capitol Gate. The latter, located in Abu Dhabi, is the second largest of all of the precedent studies. Each of the 700 unique 8m high diamond-shaped mega-panels

(Figure 2.29) correspond to the layout of the main structural diagrid, and are subdivided into 18 triangular glazing units. The mega-panels are tied back to the main diagrid at its nodes and are relatively concealed from view [44]. Drainage for each mega-panel is compartmentalized [79]. The scale of the project also requires that the seal between mega-panels is not only a weather seal but also acts as an expansion joint [79]

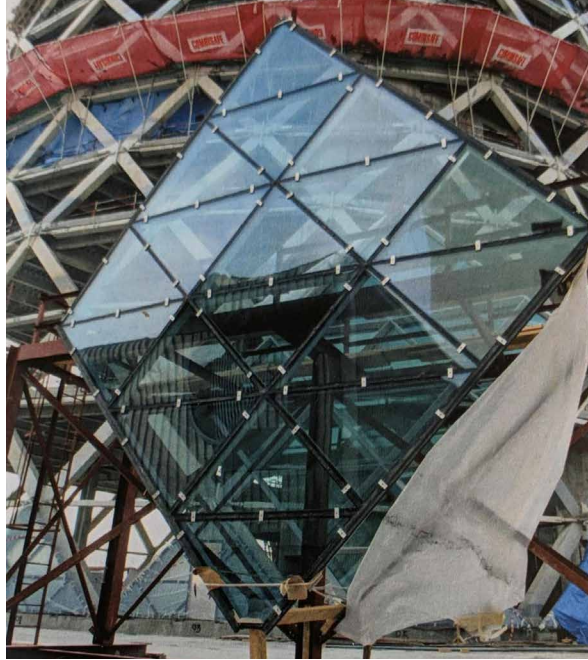


FIG. 2.29 Mega-panel for construction of Hyatt Capital Gate (©Jeff Schofield - Image courtesy of Synthesize Architecture)

2.3.6 Variations in joining methods for the interior drainage layer

For several enclosure system typologies in this study, a primary challenge of the façade system is to provide the continuity of the interior seal at nodes despite the types of misalignments discussed in Section 1.2.2. As a first strategy, it is common in these types of applications for the reference mesh to be located at the outer surface of the structural members [10] or at the glazing joints [11, 61] such that misalignments around the compressed gasket will be minimal. Then, an appropriate approach must be selected to join the incoming branches of the gasket system at the node. There exists a range of possibilities for doing this, although it should be noted that this type of information is seldom published or shared for publication, and therefore was not able to be collected for the majority of precedents under review.

Cut and join

The gasket branches can be manually cut and joined at the node, either as a single-layer system (Figure 2.30), or using a hierarchical drainage system (Figure 2.31). Joining gaskets manually at nodes can be a meticulous and time consuming task, typically requiring either gluing, heat welding, vulcanizing, or moulding joints [23]. When hierarchical drainage is used, care should be taken during façade rationalization that primary drainage lines can be continuous.



FIG. 2.30 Single-layer cut and joined joint Ex-Unione Militare (Image courtesy of Guido Ranieri Da Re)



FIG. 2.31 Multi-layered cut and joined drainage system in Hotel Dieu Courtyard roof (Image courtesy of Pierre Chassagne)

Nodal gasket: circular

Alternatively to directly joining the gasket profiles, a node gasket can be used to provide continuity of the internal seal at nodes. Two types of such node gaskets were observed in the precedents, the first of which is circular gaskets (Figure 2.32). Circular gaskets have the advantage that they can be mass-manufactured. However, similar to cylindrical nodes, circular gaskets are limited in that their radius limits the minimum U-angles allowed between members. Particularly in cases with 6 incoming arms, the U-angles must be almost evenly distributed, as sharp angles between profiles mean that a much larger circular node gasket would be necessary to connect to the incoming gasket profiles. In cases of torsion-free node conditions, gasket profiles connecting to circular gasket nodes have standard 90 degree connections.

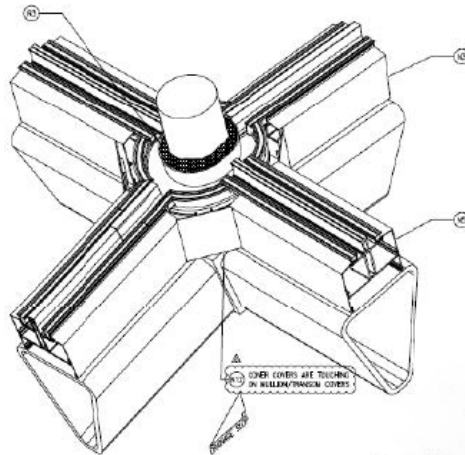


FIG. 2.32 Circular gasket applied on aluminium adaptor profile in Gardens by the Bay (Image courtesy of YKK AP Façades)

Nodal gasket: multi-axis

Another option for node gaskets is to produce specialty multi-axis gaskets using injection moulding. These gaskets have arms similar to multi-axis structural nodes that reach out to meet incoming gasket profiles at an orthogonal interface, enabling a standard connection between the nodal gasket and the profile gasket. The injection moulding process enables the fabrication of nodal gaskets with variable cross-sections across their width such that they can effectively bridge the gap between the structural node and the glass for a continuous compression seal. In addition to this, injection moulded gasket joints are noted as having a higher performance and being more durable than using sealant and glued/vulcanized solutions [23]. They can also be equipped with an interface that connects to a mandrel on the structure helping locate and fix the node in place. The big drawback of this type of solution is that it relies heavily on node congruence in order to be economical, since injection moulding is only really economical in mass-production. This type of gasket was applied in the 34th street canopy, which has high node congruence due to its being a rotational surface with torsion free nodes.

Interior drainage channels

While in most cases, the interior drainage layer is wanted for both air and water tightness, in some cases, this layer is only used for drainage. This strategy was observed in the construction of the Smithsonian Kogod Courtyard Roof in combination with a cassette system (Figure 2.33). In this case, the main air/water/vapour seal is provided by a wet seal between the cassettes, and a back-up drainage layer is provided by channels above the main structural components. This layer is drained through the hollow columns which act as downpipes from the low points of the freeform roof [126]. The channels are joined at nodes using a flexible silicone gasket capable of accommodating different angles.



FIG. 2.33 Smithsonian Kogod Courtyard roof cassette system detail (Image source: [54])

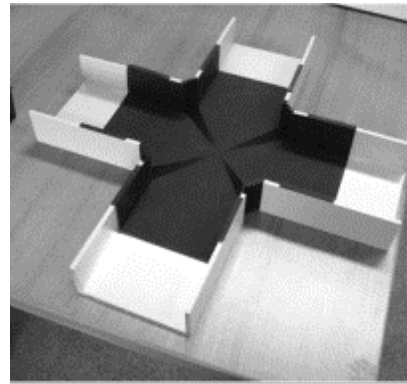


FIG. 2.34 Smithsonian Kogod Courtyard roof internal drainage connection (Image courtesy of Foster + Partners)

2.4 Opportunities for the use of additive manufacturing in freeform steel and glass façade construction

2.4.1 Opportunities for AM structural nodes

The following qualities are identified from the literature of the various case studies as desirable qualities for structural nodes, in addition to their main function, which is to effectively transfer loads across the structural layer:

Fabrication efficiency: The node should make use of numerically controlled fabrication methods in order to maintain controlled tolerances and reduce human labour and error. The number of different fabrication operations and machines should ideally be limited to avoid complicated coordination and time-consuming logistics and set-up between operations. When multiple fabrication operations are required, transfer of information between operations should be coordinated and automated as much as possible.

Assembly efficiency: The assembly of the façade system should be as simple as possible, in particular to reduce the amount of on-site labour required. In general, this is achieved in two ways: in the use of mechanical connections that can swiftly be fastened on site; and/or in the use of large prefabricated welded ladders that are subsequently connected on site, reducing the number of on-site connections.

Material efficiency: The node should use material as necessary such that it does not add superfluous dead-load to the structure, and such that it is overall more sustainable.

Geometrical flexibility: The node should be able to accommodate a suitable range of U, V, and W angles required of the façade geometry without compromising façade performance, or the ability to apply the desired enclosure system typology.

Design efficiency: The node design should consist of a systemized topology, which can be integrated into a parametric workflow and configured to a wide range of geometrical node configurations, and parameters adjusted according to specific design and load requirements. This enables the node modelling, engineering,

and generation of fabrication files to be done through relatively automated digital processes. Ideally, achieving material efficiency through the adjustment of geometrical parameters, for example plate thicknesses, would also be integrated into this workflow.

The different structural node typologies are compared in terms of fabrication efficiency (node fabrication and profile fabrication), material efficiency (direct material efficiency, and indirect material efficiency), and geometrical flexibility (u/v-angle geometrical flexibility, and smooth plane transition). Assembly efficiency is excluded from this analysis since the right assembly strategy varies by project. Design efficiency is also excluded since all of the typologies can reasonably be integrated into parametric workflows. Table 2.2 denotes the structural node typologies ranked according to different facets of fabrication efficiency, material efficiency, and geometrical flexibility. The typologies are ranked from relative best to worst. Further explanation of the rankings is given in Table 2.3, and comparative rankings are illustrated in Figure 2.35.

TABLE 2.2 Relative ranking of structural node typologies

	Node fabrication efficiency	Profile fabrication efficiency	Direct material efficiency (node weight)	Indirect material efficiency (waste)	U/V Geometrical flexibility	Smooth geometrical transition
Multi-Axis Hollow	--	++	-	--	++	++
Multi-Axis Solid	-	++	--	0	++	++
Multi-Axis Built-Up	--	++	-	--	++	0
Single-Axis Faceted	0	++	0	++	0	0
Single-Axis Cylindrical	+	0	+	++	0	0
Single-Axis Bisecting	+	--	+	0	++	0
Stacked Connection	+	--	++	++	--	--
Direct Connection	++	--	++	++	++	-

TABLE 2.3 Rubric explaining relative node rankings

Relative Ranking	Ranking	Explanation
Node Fabrication Efficiency	--	Node has many subcomponents which need to be fabricated and assembled.
	-	Node requires a single 3D subtractive fabrication operation, however blank for milling is not near net-shape.
	o	Node requires a single 3D subtractive fabrication operation, blank for milling is near net-shape.
	+	Node requires a single 2D fabrication operation; or connection between profiles consists only of post, which can be repeated for all connections; or node can reasonably be fabricated manually with simple, traditional fabrication materials and methods.
	++	There is no structural node component.
Profile Fabrication Efficiency	--	End conditions are non-standard and relatively complex, requiring careful cutting of profiles at unique angles; or profiles are curved to be continuous.
	o	End conditions are non-standard, but relatively simple.
	++	End conditions are standard, 90 degree connections.
Direct Material Efficiency (node weight)	--	Node is relatively large, and materially inefficient.
	-	Node is relatively large, but materially efficient.
	o	Node is relatively small, and can be materially efficient, but is also sometimes solid.
	+	Node is relatively small and materially efficient.
	++	Node is very small; Or there is no structural node component.
Indirect Material Efficiency (material waste)	--	Base and stock materials for subcomponent fabrication for nodes with many subcomponents are not near net shape
	o	Stock materials for milling/NC fabrication of nodes with 1-2 subcomponents are not near net shape
	++	Fabrication produces very little material waste, limited to primarily trimming of end conditions of cut-to-length subparts (of nodes and profiles); or base materials for milling/NC fabrication/subcomponent fabrication are near net shape.
U/V Geometrical Flexibility	--	Distribution of incoming arms is limited by continuity and curvature of profiles as it requires continuous lines.
	o	Distribution of incoming profiles is limited by the fact that profiles must reach the node of a set radius/reach without intersecting one another.
	++	Node is not very limited in terms of the distribution of incoming profiles and can accommodate acute and obtuse angles between profiles.
Smooth Geometrical Transition	--	Structural profiles are on different levels such that direct glazing cannot be used.
	-	Structural profiles connect directly with no intermediate node component. Resulting transition may be better or worse (corresponding to either "--" or "o" rating) depending on profile geometries.
	o	Central component aligned to "node axis" is used bridge between flanges of incoming profiles resulting in "stepped"
	++	Misalignments are resolved smoothly/organically in the center of the node

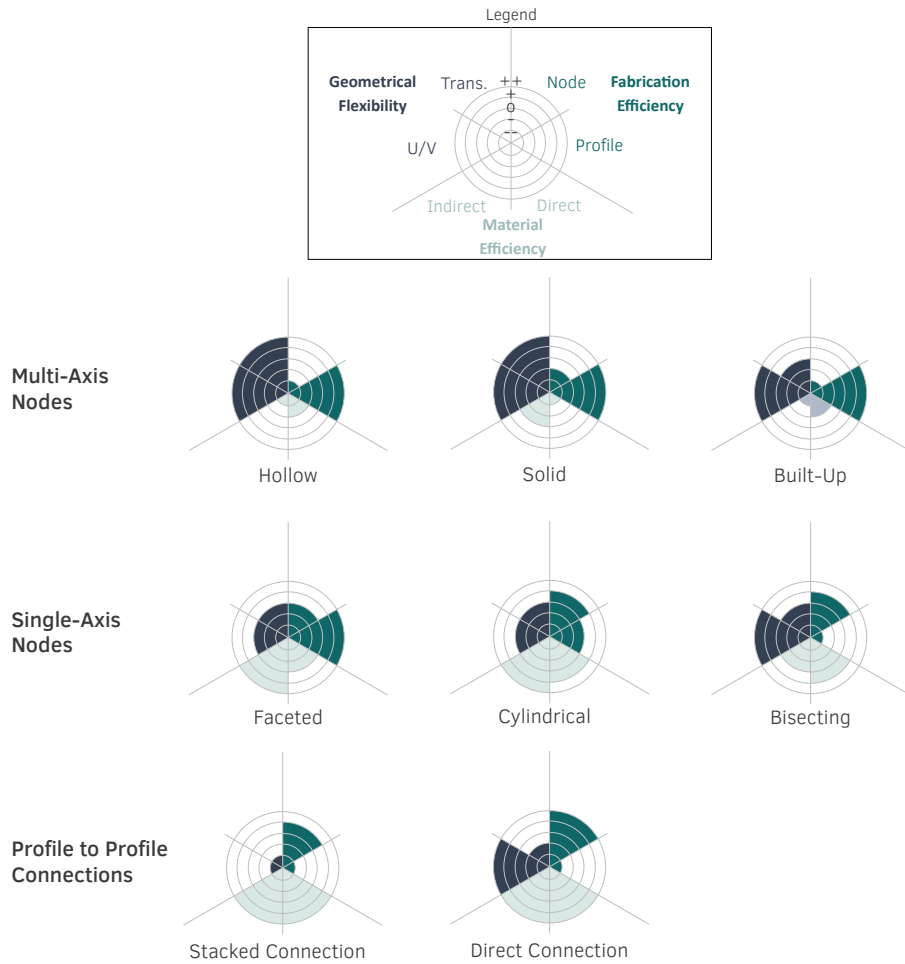


FIG. 2.35 Relative fabrication efficiency, geometrical flexibility, and material efficiency of structural node typologies (Image by author)

Analysis of the structural node typologies according to these qualities reveals a number of compromises in the current structural node system solutions. One of the most evident compromises is that there is often a direct trade-off between material efficiency and fabrication efficiency. For example, in multi-axis node typologies, the solid node is the easiest to fabricate having only a single CNC fabrication operation. These nodes however, as mentioned, can be very materially inefficient, especially in direct material utilization, often having very low utilization percentages and adding considerable dead-load to the structure. Attempts to achieve lighter nodes through the other two multi-axis typologies decreases the fabrication efficiency, requiring the fabrication of multiple subcomponents which then have to be welded together. Single-axis bisecting nodes and node-less solutions respectively drastically improve upon the material use and fabrication effort required for nodes. However, the fabrication effort is simply diverted from the nodes to the cutting and welding of the profiles.

It can also be observed that where fabrication and material efficiency are achieved, geometrical flexibility is compromised. Single-axis faceted and cylindrical nodes are material-efficient and fabrication-efficient solutions, however they are limited in terms of their geometrical flexibility on two fronts, which are illustrated in Figure 2.36. First, the radius of the nodal component poses a restriction on the distribution of the profiles around the node axis. This is because the angles between profiles have to be large enough for the profiles to reach the node without intersecting one another. For any node configuration, there is therefore a minimum possible node radius. Second, single axis nodes inherently result in misalignments at the intersections of the nodes and members. These misalignments increase as the node radius increases and can potentially compromise the integrity of direct glazing. These two limitations are inversely affected: smaller nodes limits the arm distribution while larger nodes create larger misalignments. In cases where other typologies than direct glazing are desired, these misalignments are not problematic. However, the application of enclosure system typologies that require secondary structural systems to achieve more geometrical flexibility also necessarily compromise the material efficiency of the structural node by requiring additional material in the secondary support structure.

There is an opportunity, therefore, to leverage additive manufacturing to improve on the design of nodes by improving the overall balance of fabrication efficiency, material efficiency, and geometrical flexibility, without compromising design efficiency, and assembly efficiency.

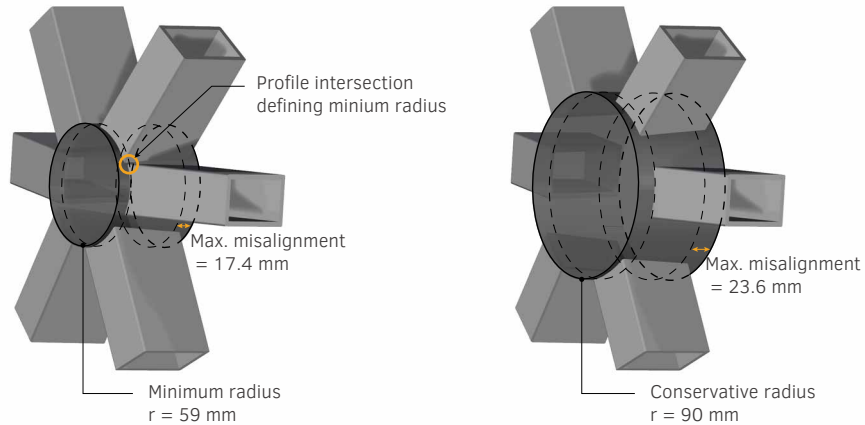


FIG. 2.36 Example illustrating the definition of the minimum node radius and the impact of increasing node radius on misalignments between structural later and outer faces in single-axis nodes. (Image by author)

In addition to the more functional and practical aspects that stand to be improved by the use of additive manufacturing, there is also the fact that structural nodes are exposed and a visible part of the architectural language of the envelope. Often, freeform façades are a formal expression of a particular design intent, yet the node solutions used to construct them typically fall into one of two categories: an attempt to be visually unobtrusive, or a practical, purpose-driven, tectonic approach. There is an opportunity through the formal freedom afforded by additive manufacturing to be more expressive in designing the appearance of nodes to further contribute to the architectural expression of freeform façades. For example, structurally optimized nodes can articulate load paths in complex gridshells, or more organically-shaped node designs can complement aspirations of biomimicry at the larger scale. Ultimately, additive manufacturing can enable designers to approach the design of structural nodes as an integral part of the façade design rather than as a constructional necessity.

2.4.2 Opportunities for AM in the enclosure system

A total of five different enclosure system typologies were defined in this study. Within these typologies, two major opportunities were identified as potentially benefiting of additive manufacturing: in the development of interior gasket nodes as a means of improving façade performance, and in the development of exterior gasket nodes as a means of enabling a high-performance fully dry-sealed freeform façades.

In the overview of solutions for internal drainage solutions at nodes, a number of gasket features are identified that are either commonly integrated into or desirable in internal gasket solutions:

Standard connections: Many freeform steel and glass façades are currently constructed by directly cutting and gluing together the gaskets on-site. This requires a high quality of workmanship as well as a considerable amount of time. Standard connections facilitate on-site assembly and reduce on-site time and labour, which is in line with the overarching trend in the building industry to reduce on-site assembly times [18]. In addition, even in standard curtain-wall construction, junctions and corners are the most susceptible areas for air/water leakage [23]. Gaskets that are cut too short or that have been stretched during installation and creep back are the most common installation error leading to leakage in glass and metal façade [23]. The majority of observed gasket shrinkage occurs due to stretching during installation [23]. Simplifying the connection requiring simpler tools and less hands-on manipulation of the gaskets on site should also reduce the occurrence of this and other installation-related façade failures.

Standard interface with structural node: When a node gasket is used, a standard interface with the structural node that integrates a mechanical hold can be helpful to hold the node gasket in place while the adjoining gasket profiles are cut-to-length and glued in place. This can facilitate installation and precision work and reduce installation-related errors such as cutting gaskets too short which, as previously mentioned, is the cause of a significant amount of façade failures.

Cross-sectional change: Gaskets rely on compression between adjacent layers to create an air- and water-tight seal. This compression is maintained by the elasticity of the gasket material, and in some cases, in the flexibility of the gasket geometry. Both a lack of compression and excessive compression can lead to loss of seal [23]. Along profiles, where the profiles, gaskets and glazing are all running parallel to one another, a relatively constant compression and a high-quality seal is easily achieved. However, at the node condition, the glazing unit remains planar while the structural node changes planes – either gradually or drastically – and it is the responsibility of the interior gasket to maintain the compressive seal in the intermediate space between the glass and steel. This is made particularly difficult by the fact that the exact shape of that intermediate space is often unique for each node and for each glazing unit within each node – a difficult scenario for gaskets of a constant cross-section to address. In cases when gasket profiles are directly connected, bending a gasket extrusion to pass over the structural node will cause its cross-section to distort locally [127]. This can cause susceptible areas in the seal. Thus, the ability

of a gasket to adapt to the shape of this void can help maintain the integrity of the compressive seal, particularly where more extreme angles are concerned.

Water pooling avoidance: Water leakage can occur through many different mechanisms: gravity; air/wind pressure; kinetic energy; surface tension; and capillary action. An important part of the water management system is not only watertightness, but also water management [127], which includes effectively draining water via the internal drainage layer to avoid pooling water which can then penetrate the envelope through any of the aforementioned mechanisms. In order to avoid water pooling, the geometry of the node should allow a smooth path for water to drain with gravity, and the connection method should avoid potentially messy glue that can impede smooth water flow when dry.

Hierarchical drainage: Hierarchical drainage in the internal drainage layer – as opposed to single-layer drainage – is used as a means of controlling water flow in building envelopes. In freeform façades the interior drainage layer can have 2 or even 3 drainage layers to help control water flow.

Geometrical flexibility: A good node solution for freeform applications should have the ability to address a large range of U, V, and W angles such that the various node conditions across a project are effectively addressed without compromising performance, and such that unevenness and misalignments between components at nodes are minimized.

These desirable features of nodal gaskets are present to varying degrees across the observed solutions for nodal conditions for the internal drainage layer. The relative degree to which these features are present is denoted in Table 2.4. The classification is made based on the descriptions provided in Section 2.3.6.

TABLE 2.4 Comparison of node solutions for internal drainage layer

	Direct gasket connection: hierarchical	Direct gasket connection: single-layer	Node: standard circular	Node: multi-axis injection moulded
Standard connection	-	-	0	+
Standard interface with structural node	-	-	+	+
Cross-sectional change	-	-	-	+
Water pooling avoidance	0	0	-	+
Hierarchical drainage	+	-	+	+
Geometrical flexibility	-	0	-	-

+: has feature

0: has feature in limited capacity

-: does not have feature, or has feature in very limited capacity

Perhaps the weakest point of all these solutions is geometrical flexibility, as each of the available node solutions is limited geometrically in a significant way. Hierarchical drainage and circular drainage pose limits on the discretization of the façade, multi-axis gaskets rely on high node congruence due to the use of injection moulding, and both single-layer and hierarchical direct gasket connections necessarily require bending gasket extrusions which compromises the integrity of the gasket cross-section. There is an opportunity with AM to produce a gasket that provides superior geometrical flexibility to the available options, in addition to the other 4 features. This geometrical flexibility can be achieved through mass customization.

While the use of mass-customized CAM fabrication is almost ubiquitous in the design and fabrication of structural nodes for freeform construction, the lack of CAM methods suitable for elastomeric materials has meant that gasket node solutions have relied mostly either on manual intervention or less-than-ideal standard parts. As previously mentioned, it is the role of the gasket to maintain a compressive seal in the void between the glass and steel, and the actual shape of that void varies consistently in freeform applications. The potential to create mass-customized node gaskets would mean that the cross-section of the gasket as well as the distribution of the arms could be parametrically driven to provide a continuous compressive seal for each individual node condition. As an added feature, mass customization could also allow for the embedding of additional information into a part which can be helpful for assembly or disassembly. The use of node identifiers, for example, is common in mass-customized structural nodes as a means of specifying where and in what sequence it should be installed. QR codes for purposes of design for disassembly, for example, can also be embedded directly into the part. The development of a mass-customized node solution that integrates standard connections, standard interfaces with the structural node, hierarchical drainage, cross-sectional changes, and a high level of geometrical flexibility would provide a solution that is not only easy to assemble, but also has a superior, reliable performance.

It was also observed that, where the information was available, every precedent in this study used a wet seal as a means of exterior air/water tightness. This is unlike traditional façade construction, where it is also common to see dry-dry glazing systems [23]. Dry-dry façades create the opportunity for pressure equalized systems, which are helpful in avoiding pressure-driven leakage as well as addressing condensation problems [17]. One can assume that a large part of this difference can be attributed to the complexity of addressing node conditions.

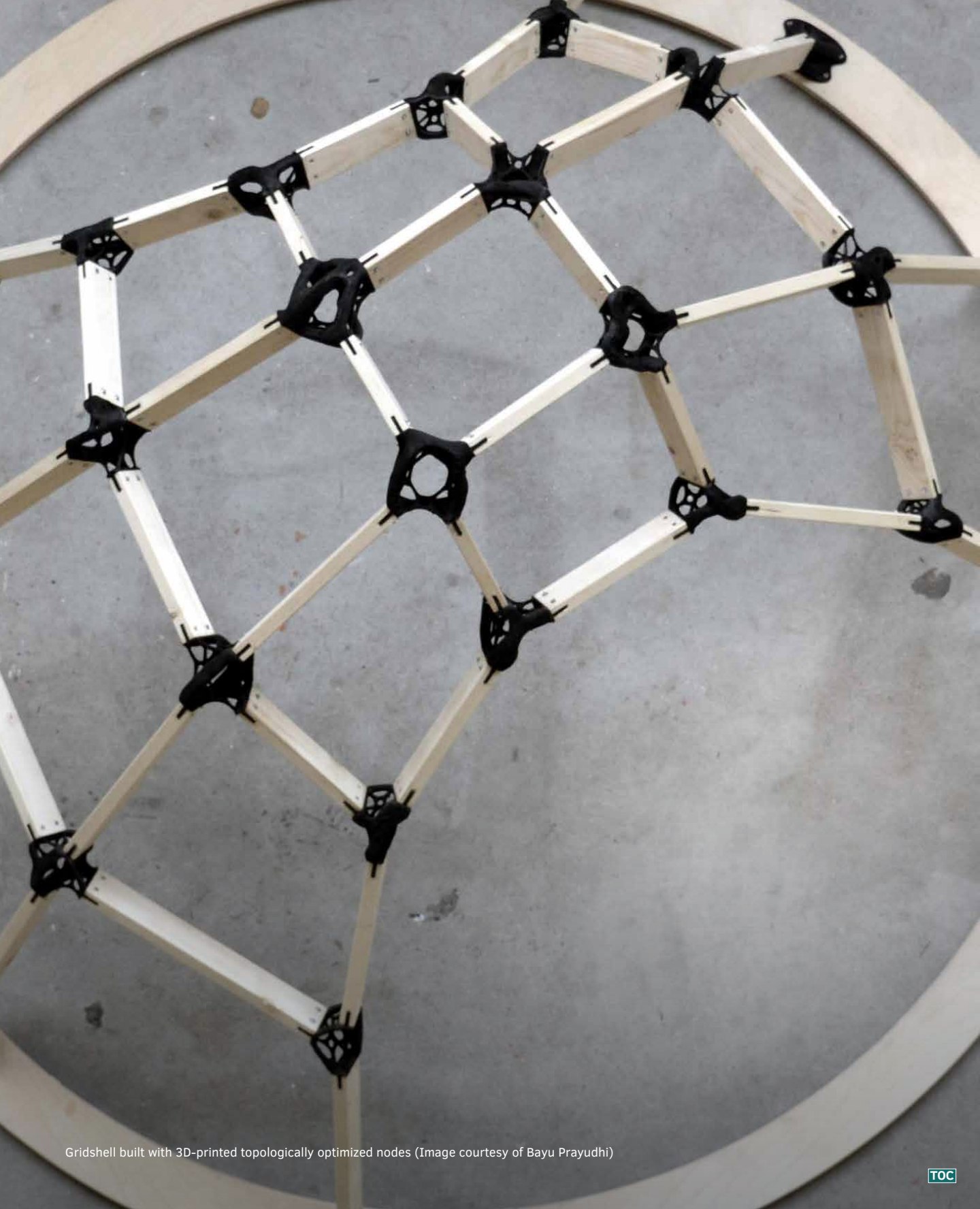
In the wet-dry system, which was observed in all precedents, the exterior wet-applied sealant provides the primary air- and water-tightness for the envelope while the interior gasket layer provides an added layer of protection. In a dry-dry system, the exterior gasket layer is often locally air- and water-permeable to enable ventilation of the rainscreen cavity for pressure equalization, which means that there is a much higher degree of reliance on the internal drainage layer. While the available solutions for gasket nodes may be deemed good enough for a redundant layer of protection, they may not be sufficient as primary defence. In addition, the integrity of compressive seals in a dry-dry system relies on providing continuity of the clamping plate, which would also need to be resolved along with the cover cap. As such, there is room to explore whether mass-customised interior and exterior AM node gaskets can help facilitate freeform dry-dry pressure equalized façade systems.

2.5 Conclusion

In this chapter, information on design and construction was collected for 40 freeform façades constructions worldwide over a 20-year period from 2000 to 2020. This study provides a categorization of system design strategies for two main functional systems of reticulated single-layer freeform steel and glass façade construction, analyses the general strengths and weaknesses of the different defined typologies. Typologies for the structural system and enclosure system are defined and observed in relation to the overall geometry of the building, other relevant aspects of the detailed design, and in relation to their application with one another. Additional insight into the detailed design for several case studies in the different typologies is provided. Based on evidence presented in the results, the following conclusions can be drawn regarding the application of the defined typologies and the potential application of AM for such solutions:

In terms of structural nodes, the application of specific typologies is not observed to be significantly limited by the geometrical design of the envelope. It is desirable for structural nodes to be: fabrication-efficient; material-efficient; design-efficient; and geometrically flexible. Amongst current structural node solutions, there is generally a trade-off somewhere between fabrication efficiency, material efficiency, and geometrical efficiency. Design efficiency through parametric design, automated processes, and CNC fabrication is the norm. In addition to this, there is room to explore the freedom afforded by additive manufacturing to further contribute to the design intent or architectural expression of the façade.

The choice of enclosure system is observed to be influenced by the façade panelization, the geometry of the primary structure profiles, and potentially limited by the sharpness of the angles between panels. The directly glazed façade is the most popular enclosure typology, likely due to its relative simplicity. There is an opportunity through additive manufacturing to introduce the advantages of mass-customized digital fabrication, which is commonly used for the fabrication of structural nodes, also to node gaskets. There is also an opportunity to investigate the plausibility of an AM exterior node gasket as a means of enabling dry-dry freeform steel and glass façades, eliminating reliance on sealant as the only means of providing the exterior seal.



Gridshell built with 3D-printed topologically optimized nodes (Image courtesy of Bayu Prayudhi)

3 Additively Manufactured Nodes and Connections

A literature review on the use of additive manufacturing for façade nodes and connections

In the previous chapter, several opportunities for potential improvement of existing solutions through the use of additive manufacturing were identified. The findings were focused largely on nodal solutions for two layers in the assembly: the structural layer, and the internal drainage layer.

In this chapter, a literature review is conducted to identify the extent to which the existing scientific body of research addresses the challenges and opportunities discussed in the previous chapter. This review surveys two scientific databases for precedents in the use of 3D printing technology in building enclosures, and explores in more depth the use of this technology for nodal components and connections.

3.1 Introduction

Façades are one of the most complex and most technologically advanced parts of buildings. Energy consumption, occupant comfort, durability, and aesthetic amongst other important building qualities are all largely dependent on good façade design. It is unsurprising then that as additive manufacturing technology is becoming of higher quality, more industrialized, and more accessible, building façades have been an area of interest for application of AM in the built environment.

Freeform construction in particular is a potential high-impact area for additive manufacturing for a number of reasons. Building components for freeform construction are of inherently complex geometry relative to regular building systems in order to be able to maintain high performance in non-standard geometrical conditions. They are also often mass-customized as a way to facilitate design and fabrication. Finally, the design, engineering, and fabrication processes for freeform construction are heavily reliant on digital workflows in order to be able to efficiently design, engineer, and fabricate parts via CAM. The purpose of this chapter is to explore existing examples of additive manufacturing in façades, and in particular as a means of fabricating complex nodes and connections.

3.2 Literature selection and overview

In order to identify relevant research gaps in the scope of this research, existing research on the topic of additively manufactured connections for façade construction was reviewed to answer the following questions:

- Which AM processes are being applied and for which materials in façade construction?
- Which building components have been the focus of the application of AM for building façades?
- To what extent has AM been explored for complex joints for freeform façade construction?

Scientific databases Scopus, and CumInCAD were searched in order to identify relevant scientific articles as well as state-of-the-art precedents that could help answer these questions. The databases were searched using search listed in Table 3.1 in the title, abstract, and keyword list.

TABLE 3.1 Search keywords by category

Technology	Object
<div><div>– Additive Manufacturing</div><div>– Rapid Manufacturing</div><div>– 3D Printing</div></div>	<div><div>– Façade</div><div>– Building Enclosure</div><div>– Building Envelope</div><div>– Building Skin</div><div>– Curtain wall</div><div>– Canopy</div><div>– Skylight</div><div>– Gridshell</div></div>

The literature was then narrowed using specific inclusion criteria:

- Type of article: journal articles, conference papers, and academic theses
- Language: English
- Topic relevance with respect to additive manufacturing in the context of façades
- Accessibility: some articles were excluded due to not being accessible through either open-access publications or direct requests to authors.
- Development: Projects which were purely theoretical and had not yet reached any kind of engineering or prototyping phase were excluded

From the abstract and the articles, information pertaining to the AM methods, material, and component was collected. In order to answer the third question, the articles were further narrowed to only those that were specifically focused on nodes or connections for geometrically complex construction. Several additional articles were included based on citations of these specifically relevant articles.

3.3 Literature review findings

3.3.1 Use of AM in façades

A total of 66 articles were found from the general searches excluding duplicates, and 39 remained after narrowing the selection based on the inclusion criteria. Of these sources, 4 main families of components were under investigation.

- panel elements and panel infills
- porous façade elements for either ventilation and/or shading
- structural nodes and connections
- brick elements and solid walls

Figure 3.1 illustrates the distribution of these different elements, their materiality, and whether they are fabricated by Additive Manufacturing (AM) or Rapid Tooling (RT) in the literature. The majority of the literature is focused on panel elements and porous façade elements such as ventilated elements and sun-shading elements. Of the 39 articles included in this study, only 4 were specifically related to nodes and connections for complex façades. While this is a small portion of the total number of articles, these 4 articles make up two-thirds of the relevant literature from these databases exploring metal as a base material.

3.3.2 AM nodes and connections

In addition to the 4 articles from above, an additional 6 articles were identified from citations as being on the topic of AM nodes for freeform façades. These articles were evaluated to identify specific areas in which AM can be further researched in order to facilitate the construction of freeform steel and glass façade construction. Table 3.2 summarizes relevant information in these studies including the material and printing method used, the connection type, and the strategy for the topology of the node.

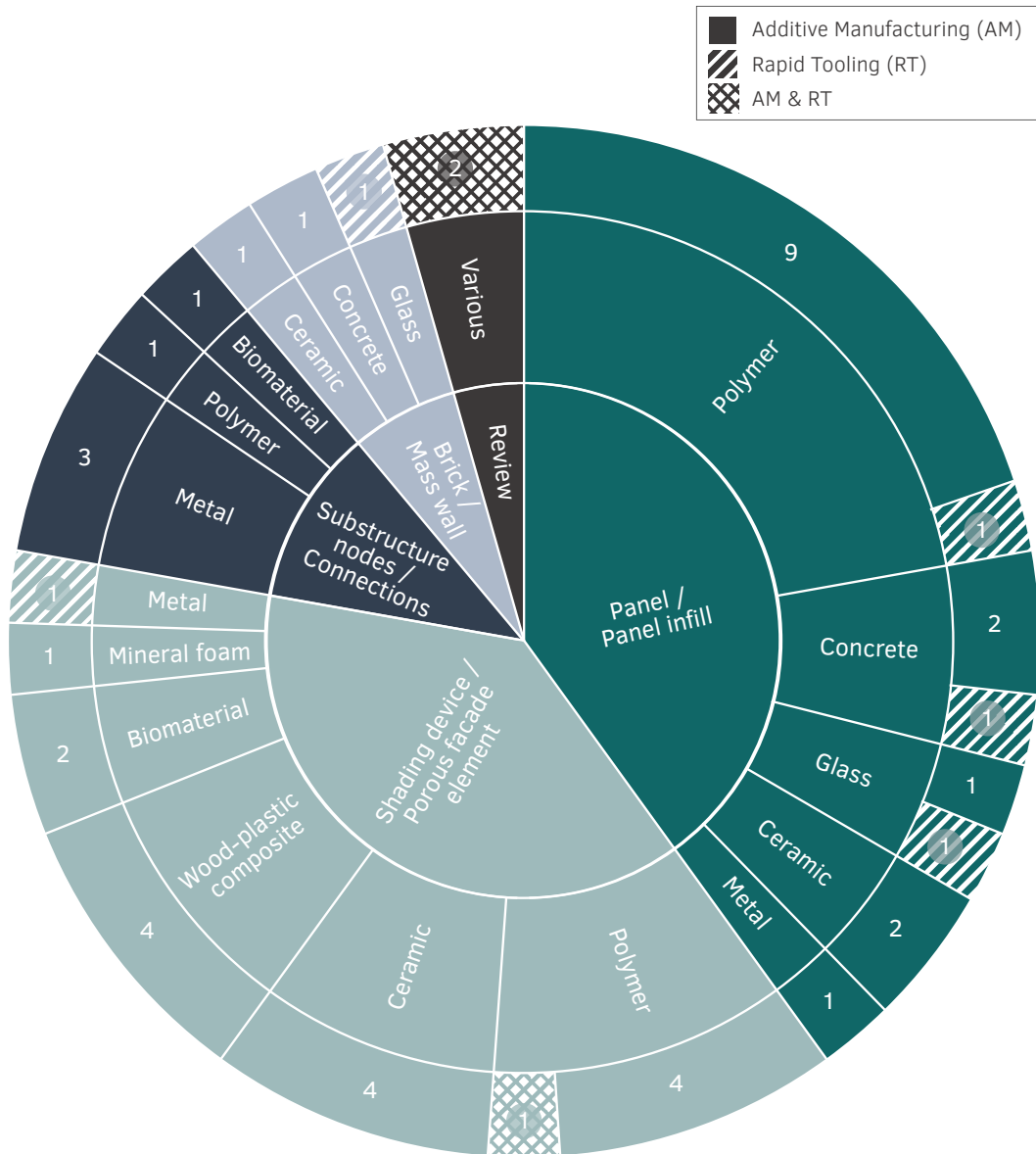


FIG. 3.1 Number of collected articles by AM façade elements, material and 3D printing strategy (Image by author)

TABLE 3.2 Summary of AM structural node precedents

Name	Year	Façade Component and System	Connection Type	Node Topology	Material/ Fabrication Method	Sources
Functionally Graded Façade	2009	Integrated edge and corner connection for functionally graded panel	Snap-fit connection	N/A	PLA/ FDM	[128]
Nematox I and II	2012	Node for aluminium post and beam glazed façade	Sleeve connection	Standard topology	Aluminium/ PBF-L	[129]
SmartNodes Pavilion Iteration 1	2014	Node for timber and fabric canopy	Transverse bolts	Optimized topology	Steel/ PBF-L	[130]
3F3D	2016	Node for steel glass grid-shells	In-plane bolts	Optimized topology	Steel/ BJ	[131]
SmartNodes Pavilion Iteration 2	2017	Node for aluminium tube and fabric canopy construction	Transverse bolts	Systemized topology	ABS/ FDM	[132]
Smooth Transitional Node	2018	Node for steel and glass post and beam canopy construction	In-plane bolts	Systemized topology	unspecified	[133]
BESO Node	2018	Node for steel and glass post and beam canopy construction	unspecified	Optimized topology	unspecified	[133]
N-AM_Li3	2020	Node for aluminium unitized glazed façade	Sliding dovetail connection	Optimized topology	Aluminium/ PBF-L	[134]
Smart node System	2022	Node for steel and glass stick-built façade construction (with pre-assembly)	Welded end-face connection	Standard topology	Steel/ Rapid Tooling: BJ and casting	[112]

Included in Table 3.2 is the node topology. The topology of a structural part refers to the configuration of the material within the design space. There were 3 approaches to topology observed in these precedents: standard topology, systemized topology, and optimized topology. Standard topology in this study refers to cases where the node parameters are only geometrical, and no additional parameters for structural efficiency are taken into consideration. A systemized topology in this study refers to cases where the geometry and material efficiency are achieved parametrically through additional variables related to the structural requirements of each node. This approach is consistent with the approach of designing nodes as “system products”. An optimized topology refers to cases where a topology optimization tool is used to find an optimized distribution of material for each node. The following sections provide a summary of the literature relevant to AM nodes and connections for freeform façade construction.

Functionally graded façade

One paper was found to investigate AM connections integrated as a functional feature directly into panel elements. In 2009, Taseva, Eftekhar et al. [128] developed an AM panel element that leveraged the freedom of additive manufacturing to integrate connections directly into monolithic panels as a means to ease design and fabrication. This strategy is notably different from the other AM connector strategies which consist of structural node components. The panels include distinct vertical edge (Figure 3.2a), horizontal edge (Figure 3.2b), and cross-point detail conditions. The AM panels are printed in PLA using FDM printing technology. The connections integrate snapping features which take advantage the bending properties of the printed materials and must consider the geometrical tolerances of the printing process.

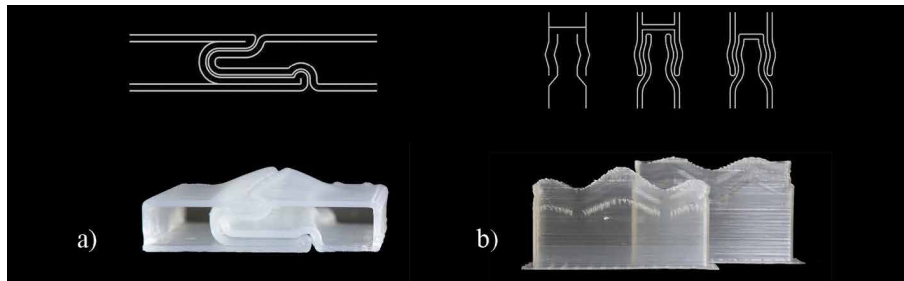


FIG. 3.2 a) Vertical panel edge connection with a tolerance of 1mm. b) Horizontal panel edge connection with a tolerance of 2mm. (Image source: [128])

Nematox I and II

The Nematox nodes (Figures 3.3, 3.4) [129] are the first found previous work exploring AM structural nodes for freeform metal and glass façade construction developed by Holger Strauss in 2013. It was developed as a node solution for a commercial aluminium stick-built glazed façade. The node design merges the post and beam profiles and provides continuity of channels which can help solve critical water drainage issues. Incoming posts and beams require only 90 degree saw cuts, and are slipped onto the arms of the node and fastened in place.

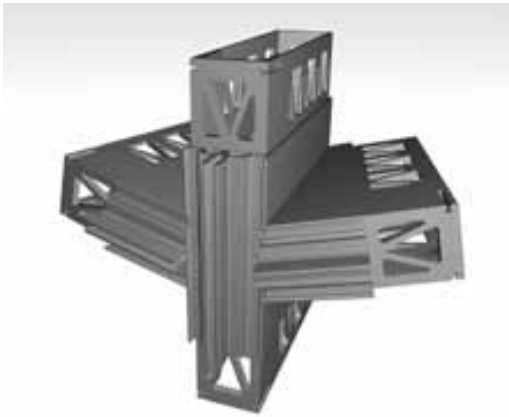


FIG. 3.3 Rendering of Nematox I façade node by Holger Strauss [129]; the first AM structural node for freeform metal and glass construction. Design for stick-built aluminium façade system and equipped with standard connections, and integrated screw channel and gasket rebates. (Image source: [129])

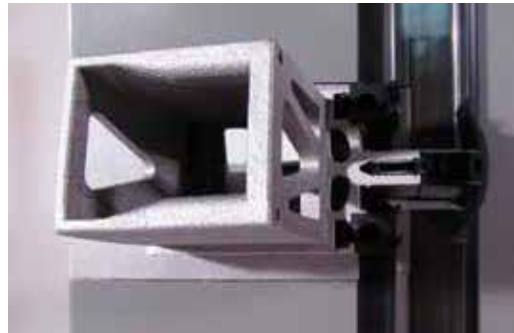


FIG. 3.4 Nematox II, additively manufactured using PBF-L technology and mounted to AA-100 façade system by Alcoa (Image source: [129])

The node configuration explored for this design is not as geometrically ambitious as future studies. The vertical post is continuous and only the transoms deviate from the orthogonal configuration. The author solves the question of seals with non-orthogonal cuts to the gasket components and suggests that a “system-fit execution of all seals” is a potential solution to avoiding construction defects in the ‘critical zone’. The node is printed in aluminium using PBF-L technology. The author also provides some insight into the intensity of the design and modelling process as well as the printing time.

SmartNodes pavilion

The SmartNodes project [130, 132] has developed two node iterations for freeform canopy structures, with the objective of achieving “unique freeform architecture, primarily built from standard available means and requiring limited on-site skill, through the integration of all complexity into individually customised and 3D printed nodes” [132].

The first iteration first published in 2014 [130] (Figure 3.5) consists of a topologically optimised metal connector for a freeform timber canopy structure. The authors use the BESO (Bi-Evolutionary Structural Optimization) technique to get a structurally optimized node design. The connections between the metal nodes and the timber profiles consist of very simple transversal bolted connections. The nodes in this case are purely structural and do not contribute to any additional building enclosure function. They are proposed to be printed in stainless steel using PBF-L technology.

The second iteration of the node, which was published in 2017 [132] (Figure 3.6), is designed for a temporary canopy made of aluminium pipes and a fabric membrane connected by AM nodes. The node design consists of 8 different fixed parametric typologies based on the number of adjoining struts, and the size of the node cross-sections were sized intuitively based on roughly anticipated structural requirements. The node is thickened at the connection points, where flattened rod ends are slotted into the node and fixed in place. Again, these nodes are purely structural and do not require any interface for a drainage system. This iteration was printed in ABS filament using FDM technology, however the authors note that future iterations will be done for a metal version using PBF-L.



FIG. 3.5 3D Printed stainless steel node for timber canopy, prototyped at full-scale using SLM. (Image source: [130])



FIG. 3.6 3D Printed ABS node using FFF for aluminium pipe and lycra canopy. (Image source: [132])

3F3D node

The 3F3D node is a topologically optimized node meant to “optimize the structural performance and [reduce] the amount of structural material in comparison to the existing design and manufacturing process” [131]. The topological optimization was done using Altair Optistruct [135]. The node (as shown in Figure 3.7) is calculated to provide a material reduction of 30% compared to a single-axis bisecting node type as described in Chapter 2. The proposed connections consist of in-place bolted connections. The design space for the optimized node is designed to be housed within an assembly that provides support for glazing (Figure 3.8). The enclosure strategy detail is only developed to a conceptual level is proposed to be a wet-seal between “variable support brackets”. The node was designed and engineered for PBF-L printing but was eventually printed in 420 stainless steel using binder jetting AM technology.



FIG. 3.7 3D Printed stainless steel node for steel and glass canopy, prototyped at 25% scale using BJ. (Image source: [4])

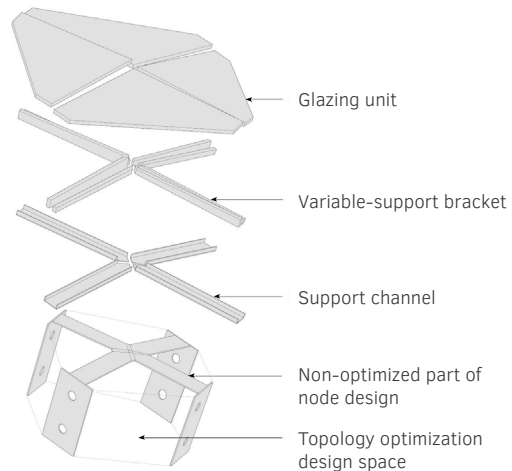


FIG. 3.8 Exploded detail of the proposed glazing connection for 3F3D node. (Image source: [4])

Smoothed transitional & BESO nodes

In 2018, Seifi, Rezaee Javan et al. [133] developed two different AM node designs for steel and glass single-layer façades. The first AM node (Figure 3.9a) is essentially a hollow shell with an interior wall structure that joins each common edge between adjacent profiles to a central axis, and creates freeform surfaces at the inner and outer face of the node that bridge between the members. Laplacian smoothing is then applied to “round the edges and connections, and eliminate the

stress concentrations” [133]. The second AM node (Figure 3.9b) uses topology optimization based on Bi-directional Evolutionary Structural Optimization (BESO) on a generous design domain which results in organic volumes concentrated between the inner and outer flanges of the members. The emphasis of this study is on the relative weight and stiffness of the different structural solutions compared to the Seele node as applied in the Westfield Shopping Centre [133] and the node from the Sun valley project in the 2010 Shanghai Expo. A prototype of each node is printed, but no information is provided on the material, printing method, or the application of principles of Design for Additive Manufacturing (DfAM).

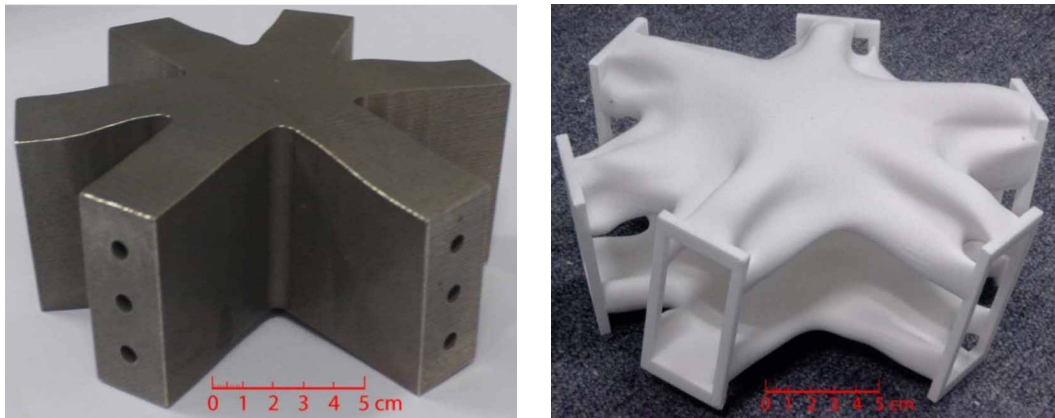


FIG. 3.9 Additively manufactured prototypes of structural nodes: unsmoothed transitional node with the end of each member closed for bolt-connection (left); BESO node (right). (Image source: [133])

Smart node system

The Smart node system by Sangho N, Sungjin Kim, and Sungkon Moon [112] was used in the construction of the Galleria mall in Gwanggyo for which construction was completed in 2020. This node was designed for a single-layer freeform steel and glass construction. The node is a hollow construction with open end faces that are welded to connecting profiles. As is common for welded connections, the profiles and nodes are largely pre-assembled off-site into frame segments and connected only intermediate profiles on-site. This project employs a secondary structural layer enclosure system typology, presumably to allow adequate space and sufficiently slim glazing joints for sharp glazing angles given the width of the structural profiles.

The nodes were produced using Rapid Tooling (RT) rather than AM, meaning that the AM process was applied to a fabrication tool rather than the end product. In this case, sand moulds were fabricated using a binder jetting process and the steel nodes were cast from the 3D-printed moulds. The casted node is similar in appearance to solid CNC nodes but have a hollow core which save considerable amounts of material. The authors outline their method for the fabrication of the AM node casts and nodes (Figure 3.10), provide a comparison to the normal sand-casting process, and describe the process for the fabrication and assembly of the façade. They also provide a brief description of the geometrical challenges of reticulated free-form façade construction, as well as some comparisons to solid CNC node fabrication, noting that to CNC-mill a solid node that is the equivalent to a 15 kg Smart node, 120 kg of steel is required. They also milled a solid node and found that the milling of such a node took 4 days.

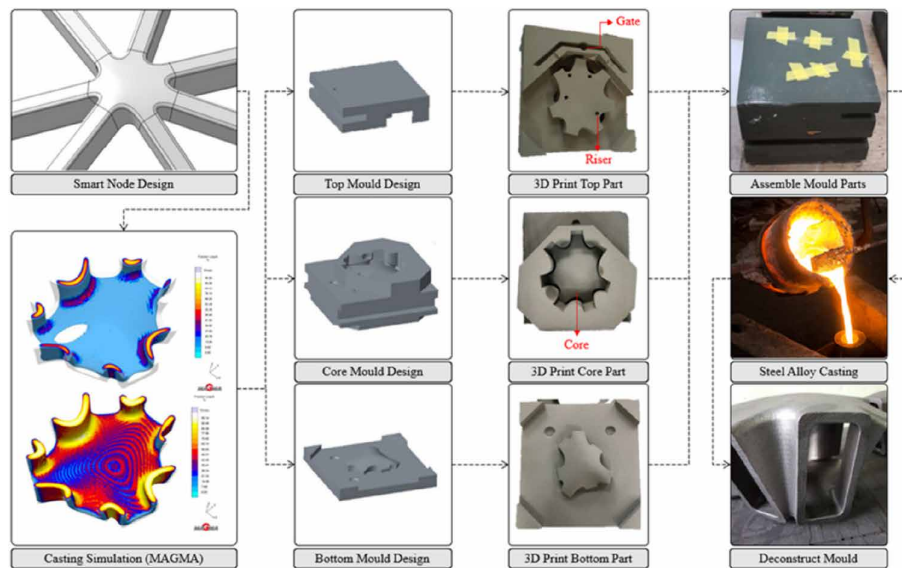


FIG. 3.10 Process used for the manufacturing of the AM sand moulds and cast “Smart nodes” for Galleria mall in Gwanggyo (Image source: [112])

N-AM_Li3

The N-AM_Li3 node system (Figure 3.11) was developed by Mohsen [134] in 2020. This node is designed to be integrated into standard aluminium unitized façade units. The centre and interior face of the node consists of the topologically optimized geometry, while the outer face provides an interface for the enclosure system. The end conditions consist of a mechanical slide-in dovetail connection fixed with two screws at the outer-face for a concealed connection. The node design provides integrated channels so that gasket extrusions for aluminium curtain wall systems can be made continuous at the nodes. The nodes are printed in aluminium using PBF-L technology.

The design and printing of the nodes are part of an overall research aim to develop a provides a methodology for the design, engineering, and manufacturing process of such nodes. This methodology also includes the establishment of tensile properties of PBF-L printed stainless steel 316L and aluminium AlSi10 Mg through testing as well as an analysis of geometrical implications of reticulated freeform façades and their tessellation.

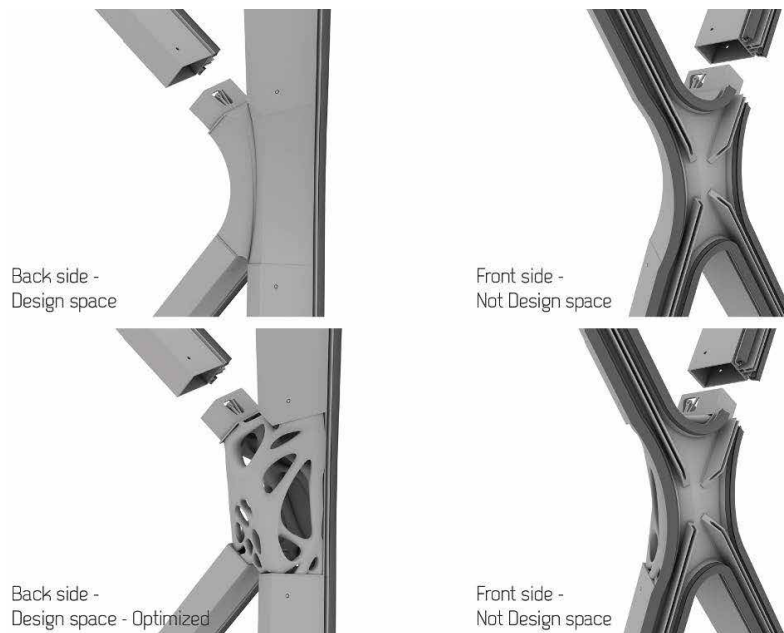


FIG. 3.11 Design for N-AM_Li3 node system for aluminium and glass façade system and connection to commercial system. (Image source: [134])

3.4 Identification of research gaps

The existing body of work touches on a number of different relevant facets of AM structural nodes. These include: the development of topologically optimized node solutions as a means of achieving lighter nodes and saving material [130, 131, 133, 134]; the development of mass-customized AM structural node system products [129, 132, 133]; direct comparisons to existing solutions in terms of material usage [131, 133]; case studies with node prototypes [129-131, 134] and architectural-scale wall prototypes [112, 128, 132]; explanations of the geometrical implications for nodes in freeform metal/glass façade design [112, 128, 131, 133, 134]; mechanical properties of AM materials [131, 134]; and methods for the design, engineering, and manufacturing of topologically optimized AM structural nodes for freeform metal and glass façades [136] and for the design and fabrication of rapid tooling for structural nodes for steel and glass façades [112]. There are, however, still many notable research gaps in this collection of work.

3.4.1 Gasket nodes

While Strauss [129] and Mohsen [134] provide in their designs conscious interfaces to support glazing and provide a drainage plane, both solutions pertain to aluminium systems, which employ fundamentally different drainage strategies compared to steel systems. Aluminium is resistant to moisture-related corrosion and therefore the structural profile is often exposed to moisture and used as an integral part of the drainage system. The interior drainage layer then consists of two individual extruded gaskets, one on either side of the profile fitted into rebates in the aluminium profile, and the profile itself provides an drainage channel (Figure 3.12a).

In steel systems, the susceptibility of steel to corrosion makes this type of solution inapplicable. As such, steel systems with an interior drainage plane are equipped with a gasket that is continuous across the width of the profile (Figure 3.12b). The two different types of drainage strategies require entirely different gasket solutions at nodal conditions.

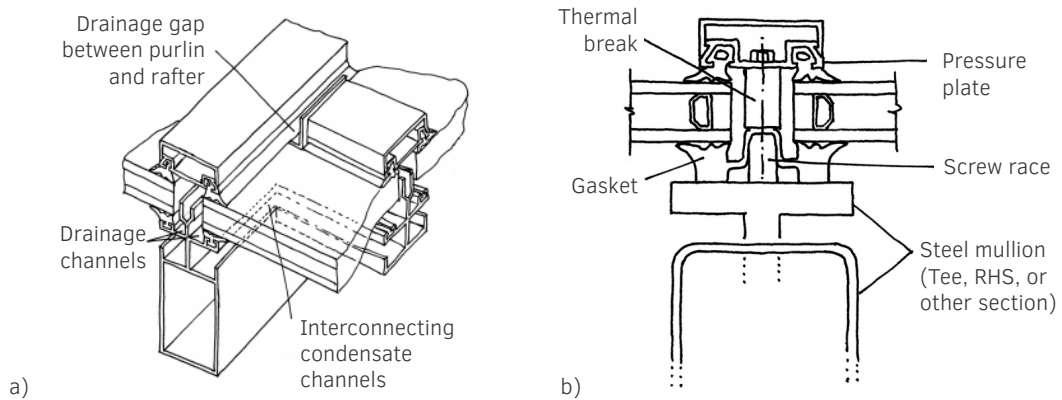


FIG. 3.12 a) Aluminium façade system with exposed profile. b) Steel Façade system with continuous gasket (Images Source: [10])

No article in which AM gaskets were addressed was found. This includes both gaskets for interior drainage, as well as exterior gaskets. This is despite the fact that gasket nodes face many of the same challenges as structural nodes, which have been the subject of many explorations of the potential of AM, namely complex geometry, high performance requirements, and mass customization.

3.4.2 Systemized topology

Topology optimization is a common strategy to reduce node weight in AM structural nodes. While there are many advantages to node weight reduction, the use of topological optimization also has some key disadvantages, for example: it requires that nodes be optimized (often individually) outside of the main parametric modelling platforms; it generates digital models that must subsequently be cleaned into smooth, aesthetic and printable shapes; and it often generates node topologies that require a significant amount of support structure during the printing process which must be removed after fabrication [3]. This additional effort can be significant both in terms of design and fabrication effort, particularly when considering that freeform façade applications have node counts ranging from tens to thousands of individual nodes. In façade applications, depending on the size of the node and the amount of material savings in question, it is possible that the material savings in a materially optimal solution would not justify cost factors including the total material usage, and the labour required to design, engineer, fabricate, and assemble the part.

One solution also had a standard topology fabricated using rapid tooling. Although the topology is standard, the multi-axis hollow node topology achieves a level of material efficiency comparable to other node typologies. The process of rapid tooling, however, which involves producing the casting moulds and subsequently casting each individual node, is a time-consuming and high-effort process [112].

The concept of a node design with systemized topology allows for an entirely parametrically-driven node geometry and, if well-designed, a level of material efficiency. This can potentially be integrated within a workflow that is fully parametric from design to fabrication without having to deal with each node on a case-by-case basis. The Nematox I and II and SmartNode Pavilion Iteration 2, which use systemized topology, are not directly relevant as they are for aluminium systems and membrane systems, respectively. The smoothed transitional node is a steel node with systemized topology, however, this node is not developed for any specific AM method, and further, is not particularly well-suited to fabrication using metal AM printing methods according to principles of DfAM. There is therefore an opportunity to explore the extent to which a steel node using systemized topology can be comparable in terms of material efficiency, fabrication efficiency, and design efficiency (through parametrically-driven systemized topology), to the current standard of node production.

3.4.3 Metal printing technologies

The existing bodies of research largely focused on design specifically for PBF-L printing methods. Other metal additive manufacturing methods including Fused Filament Fabrication (FFF), Binder Jetting (BJ), and Directed Energy Deposition (DED), for example, have not been explored for the design of structural nodes for freeform façade construction. It is known that quality DfAM includes consideration for the specific printing method in question. New AM methods for this type of application means different design opportunities which have yet to be explored.

It is also notable that there is a wide range, particularly in metal printing technology, in terms of the speed of the printing process. The existing articles each focus on one design using one printing method. There is little quantitative information available on fabrication intensity of AM nodes. The relative fabrication effort that is required between different fabrication methods and how this compares directly to more traditional methods of fabrication has also not been explored.

3.4.4 AM in the AEC industry

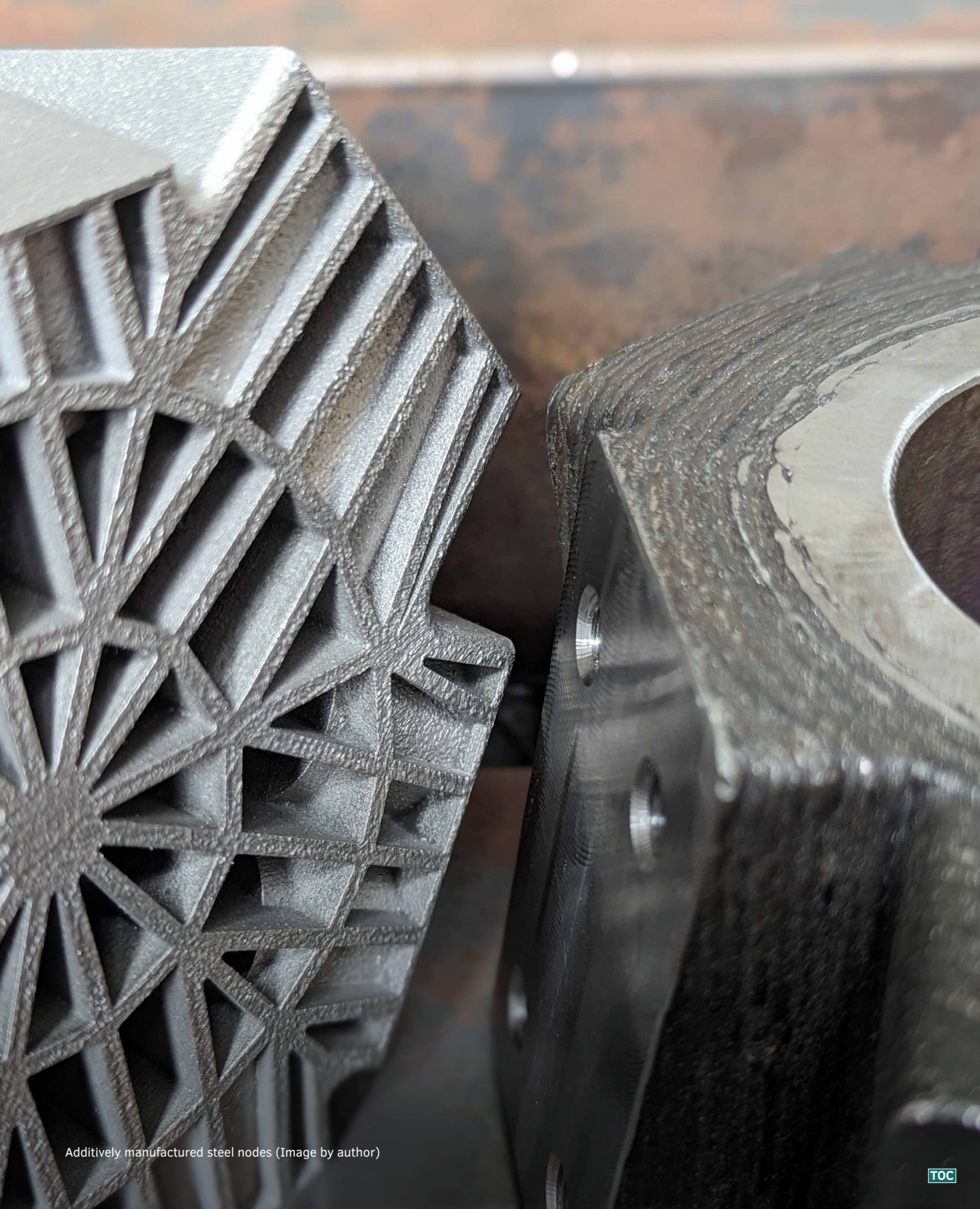
The literature for AM nodes and connections focus primarily on the development of node products and solutions. Only two studies provide methods that can be used for the development of future projects: Na, Kim & Moon [112] provide a method for the manufacturing of casted nodes using 3D-printed sand moulds; and Alamir Mohsen [134] provides a method for the realization of complex façades using standard mullion-transom façade systems (in steel or aluminium) in combination specifically with the “Li3” node. The former relates to rapid tooling which does not directly relate to this dissertation’s focus on additive manufacturing, and the latter is limited in scope to the use of a specific node product. Two key aspects are notably missing from these methods.

The first aspect is the integration of AM into a typical freeform steel and glass façade project with consideration for the roles of the different stakeholders. The realization of freeform steel and glass façade construction even without the use of AM is an inherently multidisciplinary effort that requires close collaboration between the design team, the engineering team, and the execution team in order to achieve high-performance, cost-effective solutions [4, 12, 45, 54, 92]. The introduction of additive manufacturing adds a significant amount of complexity to this already complicated collaboration, and as the use of AM in the building industry is an emerging topic, the extent to which the roles and responsibilities of different stakeholders need to evolve to accommodate the use of AM is unclear. A method incorporating the roles of different stakeholders would be helpful not only in providing instruction on “how” to integrate AM into a project, but also in outlining the flows of information that need to be communicated between collaborators.

The second aspect is the integration of node design into the overall freeform façade design and realization. One of the advantages of AM is the possibility for more creativity and flexibility in node design. However, this design flexibility can be difficult to navigate as the shape, tolerances, structural behaviour, and fabrication efficiency of AM parts are inextricably linked. A method incorporating the design development of nodes into the overall façade design would help project teams navigate this process.

3.5 Conclusion

This chapter provided an overview of studies on the use of additive manufacturing in façades, and a more detailed overview of articles pertaining specifically to AM connections and nodes. From this overview, several key research gaps are identified: the design and manufacturing of AM node gaskets in order to be able to better address geometrical complexity at nodes and introduce mass-customized solutions at interior and exterior seals; the design and development of structural nodes as system products specifically for freeform steel and glass façades; the design and development of structural node solutions that are designed for and printed by a range of metal AM fabrication methods; quantitative information on the fabrication intensity of AM structural nodes and how it compares to more traditional node solutions; and lastly, methods for the integration of AM into an interdisciplinary collaboration towards the design, engineering, and construction of freeform façades with AM node components.



Additively manufactured steel nodes (Image by author)

4 Additive Manufacturing for Structural Nodes

Methods, materials, design, and analysis

In the previous chapter, research gaps pertaining to additively manufactured structural nodes were identified, including a broader exploration of different metal AM methods and more detailed information on the fabrication intensity of additive manufacturing as a solution for the construction industry when compared to existing solutions.

This chapter undertakes the development, analysis, and comparison of three AM node prototypes using three different metal AM methods: Powder Bed Fusion, Laser-based Directed Energy Deposition, and Gas Metal Arc Directed Energy Deposition. This begins with preliminary research on the material properties of AM metals and their adherence to building industry requirements. Subsequently, three node solutions are designed and fabricated. A combination of recorded data and simulations are used to provide a comparison of the fabrication times and material usage of the different solutions, which are presented in comparison to a solid CNC-milled node, and subsequently discussed.

4.1 Introduction

Structural nodes are specialty components that address non-standard configurations and benefit from mass-customizable design and fabrication. As such, they are prime candidates for the exploration of Additive Manufacturing (AM). That being said, the adoption of AM by the construction industry is dependent on the ability of AM parts to adhere to strict standards for safety and building performance, and to be a competitive alternative to the current solutions in terms of design efficiency, fabrication efficiency, and cost. The objective of this chapter is to explore the potential of AM as means of improving freeform steel/glass construction. In this chapter, we explore the following research sub-question:

"To what extent can the use AM improve the design of structural nodes?"

This question will be answered through the design, fabrication, and analysis of 3d printed nodes. In order to arrive at this step, the following questions must also be answered:

"What are the available AM methods for the fabrication of structural steel nodes for FFSGF construction?"

"Are the material properties of AM steel suitable for application in the building industry?"

"What are the relevant design guidelines for structural parts using metal AM methods?"

Since there are several AM methods, each of them with specific advantages and disadvantages, this chapter will explore two principal families of metal AM: Powder Bed Fusion (PBF) and Directed Energy Deposition (DED). The research will focus on stainless steel grade 316L (SS316L) as a baseline material. SS316L is selected for several reasons: first, it is a commonly used alloy in steel construction [137]; second, SS316L is also a commonly used alloy for AM and so there is information available on its material properties, and many supplier and fabricator possibilities for prototype printing; and third, the use of stainless steel as opposed to steel avoids the necessity for additional surface protection such as painting which is outside of the scope of this research. The particularly excellent corrosion resistance of SS316L is due to the inclusion of a small percentage of molybdenum in its chemical composition [138,139].

This chapter is structured as follows. Section 4.2 provides an overview of the different steel AM methods. Section 4.3 outlines the material requirements for structural steel per relevant Eurocode norms and standards, and compares the material properties collected from literature of AM printed SS316L against these requirements and benchmark values of equivalent materials traditionally used in node construction. Section 4.4 outlines the most relevant design considerations for two different families of AM methods: PBF and DED, which were considered during the development of structural node designs. Section 4.5 describes the design and fabrication process of three different AM node designs. Finally, Section 4.6 compares the material efficiency, fabrication efficiency and surface quality of each proposed design and printing method, provides a comparative analysis of the fabrication of these nodes to a solid CNC node, and reflects the strengths and limitations of the proposed node designs and fabrication strategies.

4.2 Metal additive manufacturing methods

4.2.1 Overview of metal additive manufacturing methods

AM is a term that encompasses a wide range of technologies. Even in metal printing, there are various printing methods available. Figure 4.1 shows an overview of the main families of Metal AM and most common subcategories thereof. These are expanded upon below.

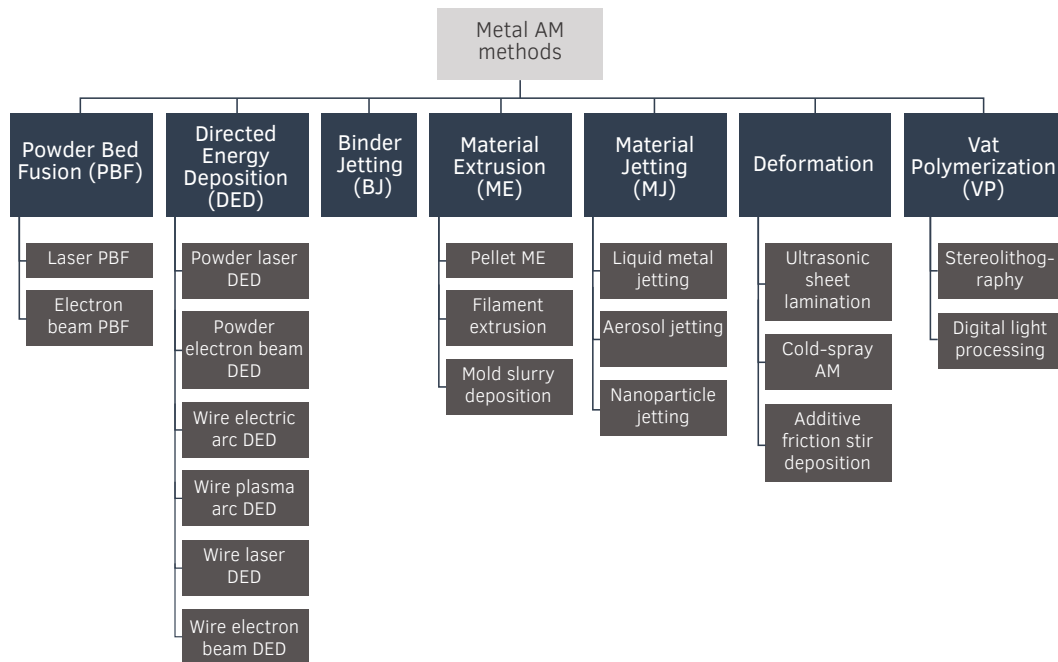


FIG. 4.1 Range of metal AM printing methods. AM methods can be broadly organized into families, which can be further subdivided by the nature of the base material, heat source/binder, machine operations, etc. (Image by author)

Powder bed fusion

Powder Bed Fusion (PBF) is a category of AM processes in which thermal energy selectively fuses regions of a powder bed [20]. The layers are built incrementally to form three-dimensional objects. PBF printing methods are further categorized by the type of heat source that is used to melt the metal powder, most often a laser or electron beam. PBF printing is notable for its ability to produce parts with complex geometry and high levels of detail [140]. Notable limitations of the technology include limitations in part size, equipment and operational costs, and slow fabrication speed [140]. PBF is a printing process that relies significantly on trying to minimize the amount of printed material and post-processing for cost-effectiveness [141]. PBF printing technology can be further subdivided by the heat source used to melt the metal powder. The two most common subcategories of PBF printing use a laser or an electron beam, namely PBF-L and PBF-EB, respectively. PBF-L is also commonly known as selective laser melting (SLM) or Direct Metal Laser Sintering (DMLS).

Directed energy deposition

Directed Energy Deposition (DED) is a family of printing methods in which focused thermal energy is used to fuse materials by melting as they are being deposited [20]. In DED, the substrate and/or the print-head are connected to multi-axis CNC machines that deposit the material in the correct location and orientation to build up three-dimensional parts. The printing process has multiple degrees of freedom to create the desired geometry which vary depending on the type of machinery that is used. DED technology is notable for its high printing speed relative to PBF printing methods. Path planning is particularly important to consider in DED printing. Good path planning should enable printing the required geometry with a few simple operations whilst avoiding conditions such as tight spaces that might result in collisions or printing defects such as splatter [142], as well as allowing for balanced heat dissipation to avoid significant part deformation [143]. DED printing methods are sub-categorized by the type of heat source and base material that are used.

Gas and Metal Arc Directed Energy Deposition (DED-GMA) is a subcategory of DED technology in which a welding wire is fused layer by layer by a welding arc to build up the part. This type of technology is also commonly known as Wire and Arc Additive Manufacturing (WAAM). DED-GMA is particularly notable for several key qualities. First, it has the ability to print very large-scale objects since it does not need to occur in an enclosed environment. The 3D-printed bridge in Amsterdam [144], for example, is printed using this technology. Second DED-GMA has a high material deposition speed [140], which is significantly faster than both PBF and also other variations of DED technology. Third, DED-GMA uses wire feedstock which is an accessible and cost-effective base material compared to metal powder. The main disadvantage of printing with DED-GMA is that the surface quality is rougher and the geometrical tolerances are larger than those of PBF-L and DED-L.

In laser-based Directed Energy Deposition (DED-L), metal powder is blown onto the part and fused with a laser. DED-L requires a contained environment since it uses metal powder, which limits part sizes but is beneficial in terms of quality control. DED-L falls in between PBF-L and DED-GMA in terms of surface finish, economical part-size and material deposition speed.

Binder jetting

Binder Jetting (BJ) is defined as “an additive manufacturing process in which a liquid bonding agent is selectively deposited to join powder materials” [20]. This process resembles powder bed fusion in that it is built up layer by layer of powder, except in the case of BJ, the powder is fused with a binder instead of being melted or sintered. The as-printed parts for metal BJ printing are called “green parts”. Once the green parts are printed, they generally undergo some post-processing to achieve good mechanical properties. Parts can be cured to harden, debinded to remove binding agent, sintered to fuse metal particles together, burn away the remaining binder and reduce part porosity, infiltrated to fill in the voids inherent to the printing process, and finished to improve surface quality. As the binder jetting process is based on principles of metal injection moulding, it yields AM products with comparable properties.

Material extrusion

Material Extrusion (ME) is defined as “an additive manufacturing process in which material is selectively dispensed through a nozzle or orifice” [20]. It is a common family of printing methods also for other materials. ME also encompasses a few sub-categories, including pellet ME, filament ME, and mold slurry deposition. The printed material consists of a matrix of metal powder and binder, and similar to binder jetting, ME processes print “green parts” which are subsequently debinded and sintered to achieve metal material characteristics. ME also produces parts with properties comparable to metal injection moulding.

Material jetting

Material Jetting (MJ) is defined as “an additive manufacturing process in which droplets of build material are selectively deposited” [20]. There exist several subcategories of metal MJ. Liquid Metal Jetting deposits small droplets of molten metal. In Nanoparticle Jetting (NPJ) nano-sized particles are suspended in a liquid formula, which is loaded in cartridges and subsequently jetted in layers simultaneously with support material to build up the part. High temperatures in the build chamber evaporate the liquid formula and allow the metal particles to partially fuse. Once supports are removed the green part is sintered to achieve metal material characteristics similar to metal injection moulded parts.

Deformation-based AM

Deformation-based AM methods make use of deformation bonding to achieve layer adhesion [145]. There are several subcategories of deformation-based AM. Sheet lamination is “an additive manufacturing process in which sheets of material are bonded to form an object” [20] typically using ultrasonic vibration. In additive friction stir deposition, a rod is rapidly rotated and is delivered through a tool head, which starts to generate frictional heat as it contacts the substrate, yields, and fills in the volume between the substrate and print head [145]. In cold spray AM, metal powder particles are jetted at high velocity, fusing to the substrate or previous layer through particle impact.

Vat polymerization

Vat Polymerization (VP) is defined as “an additive manufacturing process in which liquid photopolymer in a vat is selectively cured by light-activated polymerization” [20]. VP printing methods can be broadly categorised by the type and characteristics of the UV source. Stereolithography (SL) consists of a single concentrated beam of UV light; Digital Light Projection (DLP) projects a series of pixelated images. Each of these subcategories can also be further sub-categorized by whether they are top-down or bottom-up printing methods. In metal VP, metal powder is mixed in with the photopolymer. Similar to ME, green parts are subsequently debinded and sintered to achieve metal material characteristics.

4.2.2 Preliminary comparison of metal AM methods

Figures 4.2 and 4.3 illustrate the range of machine build volumes (i.e. range of part size that can be produced by AM technology) and machine costs (retail price of AM machine in USD excluding ancillary equipment, add-ons, and upgrades) based on data collected from the Senvol database [146] for various steel AM machines. The Senvol database is a large database for industrial additive manufacturing machines and materials. It is used here only as a basis for the preliminary exploration of AM methods. In terms of build volume, each printing method is capable of printing in the range of scale for this type of application. Depending on the required size of nodes of a given project, build volumes for VP and ME may be prohibitively small. It is also worth noting that while this graph indicates that these printing methods are capable of printing objects at the target scale, it may not be a cost-effective solution.

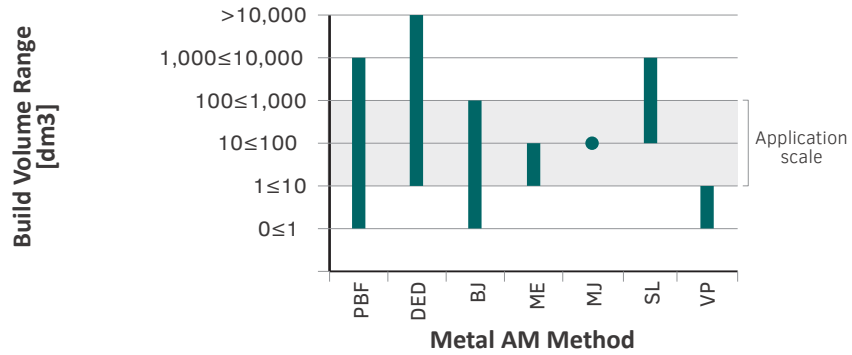


FIG. 4.2 Comparison of range of build volumes for different metal AM methods. (Data source:[146], image by author)

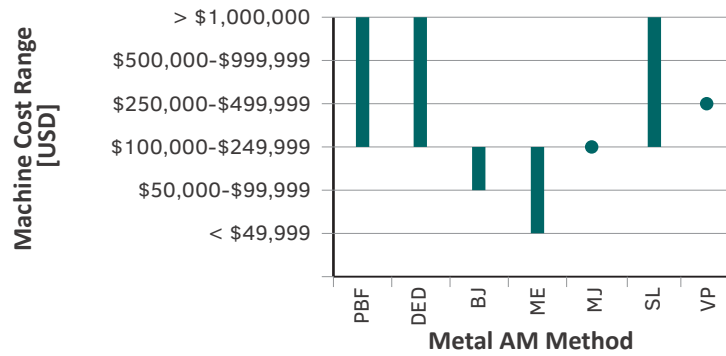


FIG. 4.3 Comparison of range machine costs for different metal AM methods. (Data source:[146], image by author)

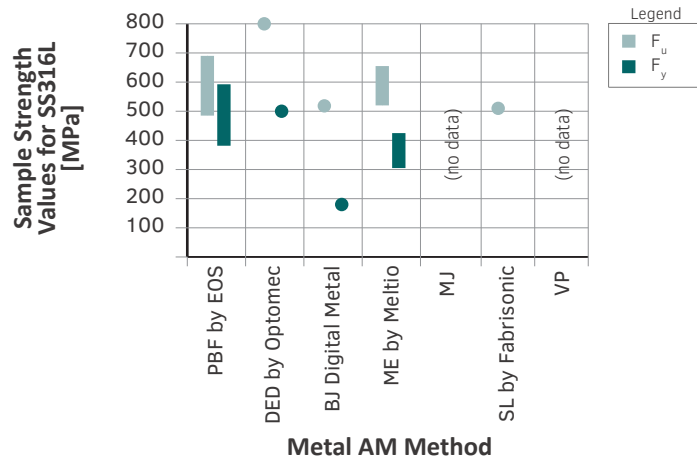


FIG. 4.4 Sample strength values for AM SS316L for different metal AM methods. (Data source: [146], image by author)

Figure 4.4 illustrates the yield and ultimate tensile strength values from technical datasheets for SS316L for the various printing methods without post processing. There is a notable difference in particular between the yield strength values of the different printing methods.

4.2.3 Selection of metal AM methods

The rough comparison provided thus far is not comprehensive, since, as discussed, each family of printing methods encompasses a number of variations, each of which will have their own respective associated costs, size limitations and mechanical properties. The goal of this chapter is to first establish whether AM materials are suitable for use in the construction industry, and subsequently to explore the extent to which AM technology can be leveraged to improve structural node designs. Since to explore each of the AM methods individually is an endeavour too large for the scope of this research, a small selection of printing methods is selected to move forward in the remainder of this chapter. The process followed in this chapter can be used as a roadmap to do a similar investigation for other AM methods down the road.

Three printing methods are further explored for the design and manufacturing of AM structural Nodes: PBF-L, DED-L, and DED-GMA (Figure 4.5). These printing methods are selected because they demonstrate excellent material properties, they are suitable for this scale of application, and because the two families of AM (PBF and DED) provide a variation in design possibilities for exploration.

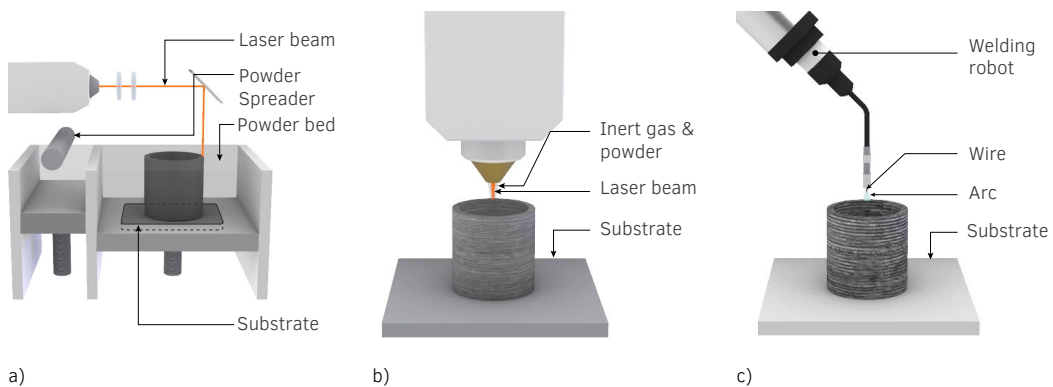


FIG. 4.5 Schematic illustration of a) PBF-L; b) DED-L; c) DED-GMA printing processes (Image by author)

4.3 Material properties of stainless steel 316L fabricated using PBF-L, DED-L, and DED-GMA

This section explores whether the material properties of AM austenitic stainless steel 316L (EN numeric designation stainless steel 1.4404) is suitable for use in the façade construction industry. First, a summary of material requirements for structural steel is compiled from Eurocode 3 (EC3) and EN 1090-2 [147]. Benchmark values for SS316L are also outlined as reference. Based on the material requirements, mechanical properties for SS316L produced by PBF-L, DED-L and DED-GMA are collected from literature and compared to the requirements. Additional data on design values is also collected from the literature and compared to benchmark values.

4.3.1 Summary of requirements for steel structures per Eurocode standards

Table 4.1 outlines the most relevant Eurocode standards for the material requirements of steel and stainless steel structural nodes. Table 4.2 provides a list of the relevant material properties and requirements outlined in Eurocode 3. In addition to this, materials used in buildings which are not constituent products listed in Eurocode standards must, according to EN 1090-2, specify a number of properties. The properties which must be specified are also included in the table. Material properties as they relate to fire safety from EN 1993-1-2 are not included in the scope of this study. As the material in question is a stainless steel, EN 1993-1-4 [149] is referred to for material requirements. EN 1993-1-4 refers directly to EN 1993-1-1 [148] for material requirements for ductility, fracture toughness, and fatigue.

TABLE 4.1 Most relevant Eurocode standards for the design of structural nodes

Standard	Name	Relevance
EN 1993-1-1	Eurocode 3: Design of Steel Structures - Part 1-1: General rules and rules for buildings	Provides ductility and fracture toughness requirements
EN 1993-1-2	Eurocode 3: Design of Steel Structures - Part 1-2: General rules - Structural fire design	Provides fire-safety requirements
EN 1993-1-4	Eurocode 3: Design of Steel Structures - Part 1-4: General rules - Supplementary rules for stainless steels	Provides material requirements and properties specific to stainless steel
EN 1993-1-9	Eurocode 3: Design of Steel Structures - Part 1-4: General rules - Supplementary rules for stainless steels	Provides fatigue requirements
EN 1993-1-10	Eurocode 3: Design of steel structures - Part 1-10: Material toughness and through-thickness properties	Provides toughness requirements
EN 1090-2	Execution of steel structures and aluminium structures - Part 2: Technical requirements for steel structures	Provides requirements for execution of structural steelwork as structures or as manufactured components
EN 1990	Eurocode: Basis of Structural Design	Provides methods for the determination of material characteristic and design values. Also provides tolerance requirements.

TABLE 4.2 Material requirements for steel structures

Property	Requirement per EC3	Specification requirement per EN1090-2
Ductility: f_u / f_y	$\geq 1,10^*$ [148, 149]	No
Ductility: elongation at failure	Not less than 15%* [148, 149]	Yes
Ductility: ultimate strain	$\epsilon_u \geq 15\epsilon_y$, where $\epsilon_y = f_y / E$ * [148, 149]	No
Ductility: Stress reduction of area (STRA)	No Requirement	as req'd
Fracture toughness	Varies*. Is evaluated in terms of temperature. Requirement is $T_{Ed} < T_{Rd}$, where T_{Rd} is the temperature at which a safe level of fracture toughness can be relied upon under the conditions being evaluated. [148, 149]	as req'd
Yield strength / 0,2% proof strength	No Requirement: Design Value Only	yes
Tensile strength	No Requirement: Design Value Only	yes
Modulus of elasticity	No Requirement: Design Value Only	no
Poisson's ratio	No Requirement: Design Value Only	no
Fatigue strength	Varies: Requires acceptable level of reliability that structure will perform satisfactorily for its design life [149, 150]	no
Durability	"The effects of deterioration of material, corrosion or fatigue where relevant should be taken into account by appropriate choice of material" [149, 150]	no

*: denotes value that is recommended in Eurocode but may be defined differently in National Annexes.

4.3.2 Mechanical properties of AM SS316L

The final mechanical properties of AM materials are not only dependent on the material and type of printing technology used, but also on a number of fabrication variables. Such variables include printing parameters, post-processing strategies, and path planning. Many studies explore the effects of different printing parameters and post-processing strategies on the mechanical properties of printed parts.

Literature for this study was found searching Scopus for journal articles in which ductility, fracture toughness, and fatigue strength (properties for which Eurocodes outline requirements) are investigated. Journal papers written in the last 5 years were prioritized. Tables 4.3, 4.4, and 4.5 summarize the mechanical properties collected from literature for PBF-L, DED-L and DED-GMA, and takes note of testing variables, printing parameters, and relevant fabrication data. The results from the literature are subsequently discussed.

TABLE 4.3 Properties and printing variables from literature for PBF-L samples

Source		(Afkhani, Dabiri et al. 2021)	(Braun, Mayer et al. 2021)		(Cacace, Pagani et al. 2022)	(Cegan, Pagac et al. 2020)	
Fabrication Method		PBF-L	PBF-L		PBF-L	PBF-L	
Variables Under Investigation		Orientation & Post Processing	Orientation	Post-Processing	Printing Parameters	Post Processing; Printing Parameters	
Post Processing		Varies: AB; HM; LM; HMFI	AB	Varies: AB; HT; M & HT	AB	Varies: AB; HIP & HT	
Ductility: f_u / f_y	min	1,19					
	max	1,37					
Ductility: elongation	min	22	32.5		25.3±15	30,4±4	
	max	48	42.2		50.4±6	50,1±0.6	
Ductility: ϵ_u	min						
	max						
Fracture Toughness	min	K_{Ic} @ RT= 145					
	max	K_{Ic} @ RT= 150					
Yield Strength (0,2%)	min	439	510		417±39.4	276±1	
	max	471	666		495±10	573±2	
Tensile Strength	min	553	619		532±17.5	549±43	
	max	647	778		623±6.59	662±2	
Modulus of elasticity	min	147	157			154±52	
	max	193	167			245±37	
Fatigue Strength	min			177			
	max			389.9			
	R			R=0			
	runout			2000000			
Surface Roughness	min	6		6,295±0,041			
	max	12,5		41,929±0,065			
Printing Parameters	Printing Orientation	Horizontal; Vertical	zx, yz, xy	-	Vertical	Vertical	
	Layer Thickness	-	40 μ m	40 μ m	-	-	
	Scan Speed	-	-	-	-	400 - 12--mm/s	
	Exposure Time	-	-	-	75 - 280 μ s	38 - 148 μ s	
	Powder Size	-	-	-	15 - 45 μ m	-	
	Laser Spot Size	-	-	-	70 μ m	-	
	Laser Power	-	100–180W	100–180W	150-200W	200 - 350 W	
	Protective Gas	-	-	-	-	-	
	Scan Strategy	-	Meander	Meander	Meander	Meander ; Chessboard	
	Hatch Spacing	-	-	-	75 - 124 μ m	110 μ m	

Post Pocessing: AB: As-Built; G: Grinding; P: Polishing; M: Machined; HM: Heavily Machined; LM: Lightly Machined; HT: Heat Treatment; HIP: Hot isostatic Pressing; HMFI: High Frequency Mechanical Impact Treatment; E: Extraction; EDM: EDM Extraction;

	(Großwendt, Becker et al. 2021)	(Hatami, Ma et al. 2020)	(Kumar, Jhavar et al. 2021)	(Li, Yi et al. 2021)	(Morozova, Kehm et al. 2022)	(Obeidi, Uí Mhurchadha et al. 2021)	(Pauzon, Hryha et al. 2019)	(Zhong, Liu et al. 2016)
	PBF-L	PBF-L	PBF-L	PBF-L	PBF-L	PBF-L	PBF-L	PBF-L
	Material Composition	Layer thickness; Post Processing	-	Orientation	Post Processing	PBF-L Printer; Printing Parameters	Gas Supply; Oxygen Threshold	-
	P	Varies: AB; M & P	E; G; P	E	Varies: AB; Various HT	M	AB	M
				1,18*	1,37*			
				1,28*	1,95*			
	30±0.3		94±2	45,21	34	4	32	42
	51,3±0.5		-	62,57	50,8	44	33	54
			J _q = 203				K _v @ RT = 115	K _v @ RT = 103±4
			-				K _v @ RT = 141	
	481,8±20.4		346±17	513	283		532	487±3
	593,3±20.0		-	588	464		570	
	594,4±22.2		639±4	623	552	200	655	594±4
	758,3±19.1		-	708	683	720	674	
						52		
						214		
		202,5						
		R=-1						
		2000000						
		13,1± 0.8						
		152,0						
	37 degree	Vertical	Vertical	0; 15; 30; 45; 60; 75	Vertical	Horizontal	-	Vertical
	30 µm	30µm; 50µm	50 µm	50µm	50µm	30µm; 60µm	20µm	50µm
	-	700 mm/s	700 mm/s	-	1000 mm/s	800mm/s; 1200mm/s	-	1000 mm/s
	-	-	-	100 µs	-	-	-	-
	20–63µm	30 - 65µm	-	20–50µm	15 - 45µm	average 30µm	20 - 53µm	10 - 45mm
	50 µm	65µm	-	70µm	30µm	70µm	-	75µm
	150 W	-	275 W	185 W	150 W	160 W; 190 W	-	200 W
	Argon	Argon	-	Argon	Argon	Argon; Nitrogen	Argon; Nitrogen	-
	Stripes	Contour - Infill	-	Stripes: 67° rotation	Chessboard: 27° rotation	Stripes: 67° rotation	-	Stripes
	80µm	-	120µm	120µm	80µm	90µm	-	100µm

TABLE 4.4 Properties and printing variables from literature for DED-L samples

Source		(Aversa, Marchese et al. 2021)	(Blinn, Lion et al. 2021)	(Bertolini, Perini et al. 2022)	(Das, Roy et al. 2022)	
Fabrication Method		DED-L	DED-L	DED-L	DED-L	
Sample Variables		Laser Power; Scan Speed	-	Orientation; Post Processing	-	
Post Processing		M	M & P	Varies: E & AB/ M/ Various HT	EDM	
Ductility: f_u / f_y	min					
	max					
Ductility: elongation	min	35±1			20	
	max	36±1			30	
Ductility: ϵ_u	min					
	max					
Fracture Toughness	min					
	max					
Yield Strength (0,2%)	min	434±6			530	
	max	474±9			590	
Tensile Strength	min	615±6			750	
	max	636±12			770	
Modulus of elasticity	min					
	max					
Fatigue Strength	min		225	80		
	max		225	190		
	R		R = -1	R = -1		
	run		2000000	1000000		
Surface Roughness	min			17±5.5		
	max			17±5.5		
Printing Parameters	Printing Orientation	-	-	Vertical; Horizontal	Vertical	
	Layer Thickness	0.3 mm	0.9 mm	0.85 mm	0.45 mm	
	Scan Speed	-	17 mm/s	1000 mm/min	4 mm/s	
	Exposure Time	-	-	-	-	
	Powder Size	50 µm - 110 µm	45-104 µm	50 µm - 105 µm	40-100 µm	
	Laser Spot Size	1.3mm	-	3000 µm	-	
	Laser Power	1500 W; 1800 W	1400 W	1100W -2000W	350 W	
	Powder Feed Rate	-	0.20 g/s	0.20 g/s	1.05 g/s	
	Protective Gas	Nitrogen	Nitrogen	Argon	Argon	
	Scan Strategy	Contour - 0/90°	-	Meander: 67° rotation	-	
	Hatch Spacing	-	1.6mm	1.5mm	-	

Post Processing: AB: As-Built; G: Grinding; P: Polishing; M: Machined; HM: Heavily Machined; LM: Lightly Machined; HT: Heat Treatment;
HIP: Hot isostatic Pressing; HMFI: High Frequency Mechanical Impact Treatment; E: Extraction; EDM: EDM Extraction;

	(Kono, Maruhashi et al. 2018)	(Kumaran, Sathies et al. 2022)	(Pacheco, Meura et al. 2022)	(Qu and Gong 2021)	(Saboori, Aversa et al. 2019)	(Saboori, Piscopo et al. 2020)
	DED-L	DED-L	DED-L	DED-L w/ interlayer CNC milling	DED-L	DED-L
	Cladding Path; Temperature History	Post-Processing	Orientation; Post Processing	Heat Treatment	Powder cycling: Fresh, Recycled	Deposition Pattern
	EDM	Varies: E & AB/ Various HT	Varies: E & AB/ Various HT	M	M	M
		1,3*				
		1,7*				
		62	34,67±3.29	43,3	16,2 ±2.1	17±3
		81	40,34±1.49	62,4	31,2±2.2	23±3
	K _v @ RT = 72		K _v @ RT = 103.87±3.91			
	K _v @ RT = 96		K _v @ RT = 143.18±27.93			
		300	310±4.54	242,5	458,4±29.9	469±10
		425	473,33±4.1	421,1	469±3.4	469±10
		500	665±5.71	497,3	628,2±6.6	624±10
		552	566,67±2.62	596,6	651,6±43.9	649±10
					177,2±6.9	
					200,3±3.3	
	Vertical; Horizontal	Horizontal	Vertical; Horizontal	Horizontal	Vertical	-
	0.46mm	-	-	0.5mm	-	-
	1000 mm/min	500 mm/min	835 mm/min	360 mm/min	-	15 mm/s
	-	-	-	-	-	-
	-	avg 80 µm	60 - 200 µm	10 - 130 µm	50 - 150 µm	44-106 µm
	3mm	-	2 mm	-	-	7.5 mm
	2kW	600 W	540 W	1000 W	< 3kW	900 W
	13.1g/min	4g/min	8g/min	1g/min	-	-
	Argon	-	Argon	-	Nitrogen	Argon
	Varies: Scan & Layer Strategy	-	meander @ 45° rotation	90° rotation	-	Varies: 90°; 67°rotation
	-	-	-	-	-	-

TABLE 4.5 Properties and printing variables from literature for DED-GMA samples

Source		(Gowthaman, Jeyakumar et al. 2022)	(Kumar, Jhavar et al. 2021)	(Joosten 2015)	
Printing Method		DED-GMA	DED-GMA	DED-GMA	
Testing Variables		Orientation; Various Printing Parameters	Printing Method	Orientation	
Post Processing		E	E	AB	
Ductility: f_u / f_y	min			1.41	
	max			2.09	
Ductility: elongation	min	4.26	52±3		
	max	36.6	-		
Ductility: ϵ_u	min			0,16	
	max			0,25	
Fracture Toughness	min		$J_q = 170$		
	max		-		
Yield Strength (0,2%)	min	225	373±20	290	
	max	417	373.99	350	
Tensile Strength	min	269	630±30	560	
	max	606	630.99	690	
Modulus of elasticity	min			110	
	max			180	
Fatigue Strength	min				
	max				
	R				
	runout				
Surface Roughness	min				
	max				
Printing Parameters	Printing Orientation	Vertical, Horizontal	Vertical	Vertical; 30; 60	
	Layer Thickness	-	-	-	
	Wire diameter	1.2 mm	0.8 mm	1mm	
	Wire Feed Rate	6 -8 m/min	1000 mm/s	-	
	Scan/Torch Speed	5.1 - 6.7 m/min	200 mm/s	-	
	Current (A)	100 - 120 A	-	-	
	Voltage (V)	19.9 - 20.7 V	-	-	
	Power	-	800 W	-	
	Dwell Time	-	-	-	
	Scan Strategy	Line on Line	-	Point on Point	
	CMT	CMT	-	-	

Post Pocessing: AB: As-Built; G: Grinding; P: Polishing; M: Machined; HM: Heavily Machined; LM: Lightly Machined; HT: Heat Treatment; HIP: Hot isostatic Pressing; HMF: High Frequency Mechanical Impact Treatment; E: Extraction; EDM: EDM Extraction;

	(Wang, Liu et al. 2020)	(Wang, Zhu et al. 2022)	(Wu, Xue et al. 2019)
	DED-GMA CMT	DED-GMA CMT	DED-GMA
	Orientation	Orientation; Heat Treatment	Welding Current Processes
	E	Varies: E & AB/Various HT	C; G; P; E
	28.42	26.51	
	46.24	58.56	
	346.5	206.1	345,3±16.31
	400.6	395.2	354,57±15.23
	526.9	481.3	578,76±30.5
	586.9	612.7	607,2±44.9
	Vx; Vy; Vz; Hx; Hy; Hz	Vertical, Horizontal	Vertical, Horizontal
	-	-	-
	1mm	1mm	0.8 mm
	11 m/ min	11 m/ min	3.9 - 8.5 m/min
	0.7 m/min	0.7 m/min	0.3 m/min
	150 A	150 A	60 - 100 A
	14.1 V	14.1 V	15.7 - 20.2 V
	-	-	-
	20s	20s	10s
	Meander: no rotation	Meander: no rotation	Line on Line
	CMT	CMT	-

4.3.2.1 Ductility

Ductility in EC3 is measured using three different metrics: elongation at fracture, the ratio of the specified minimum ultimate tensile strength f_u to the specified minimum yield strength f_y (f_u/f_y ratio), and ultimate strain. EN 1993-1-1 [148] provides recommended values for these ductility metrics, however they are officially to be dictated by national annexes. For example, the Dutch national annex [151] uses the recommended values, with the exception of requiring a higher minimum f_u/f_y ratio ductility of 1.20 when using nominal values instead of actual values. Figures 4.6 and 4.7 show the range of ductility values collected from literature in terms of elongation at fracture and f_u/f_y ratio, respectively, compared to the minimum Eurocode requirements, as well as benchmark values for SS316L from EN 1993-1-4 [149]. The range of benchmark values incorporates SS316L in form of cold rolled strip, hot rolled strip, hot rolled plate, and “Bars, rods and sections” up to thicknesses of 8mm, 13,5mm, 75mm, and 250mm, respectively. Too little information was available from literature on ductility in terms of ultimate strain to make an assessment.

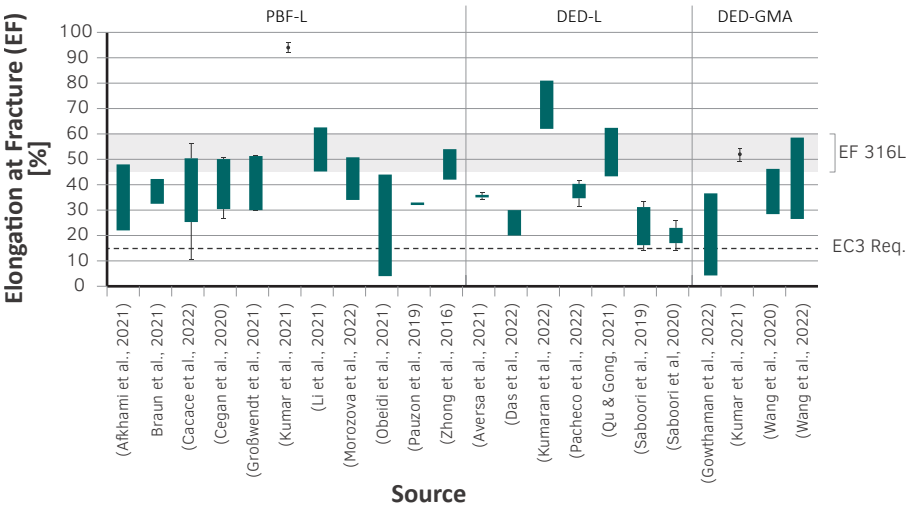


FIG. 4.6 Ductility by elongation at fracture (EF) values from literature relative to benchmark values and EC3 requirements (Image by author)

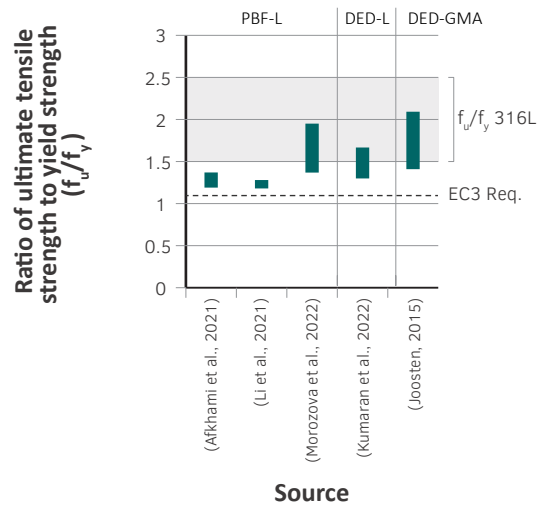


FIG. 4.7 Ductility by ratio of ultimate tensile strength (f_u) to yield strength (f_y) values calculated from literature compared to EC3 requirement and benchmark f_u/f_y ratio calculated from 0.2% proof strength and f_u values from [138] (Image by author)

As can be seen in the graphs, there is a wide spread of reported values for the ductility of AM SS316L, even within the different AM methods. Ductility is generally reported in the range of or lower than the benchmark SS316L values, nonetheless higher than the EC3 requirements. There are, however, several exceptions where elongation at fracture falls below the EC3 requirements. These exceptions are included below.

For PBF-L, ductility values are notably anisotropic with horizontal printed samples (printed perpendicular to the build orientation) having a ductility ranging between approximately 70-80% that of vertical-printed samples [152-154]. The majority of recorded elongation data was well above the EC3 requirement of 15%. However, Obeidi et al. [155] measured elongations values as low as 4%. In [155], the authors explored the differences in tensile properties across different machines for identical sets of printing parameters with varied layer thickness, scanning speed, and laser power. Lower elongation values in general were recorded for parameter settings with a combination of simultaneously higher layer thickness, scan speed and laser power. A wide range of ductility values was also reported using identical printing parameters but different PBF-L printers. The elongation of test samples printed using the same set of printing parameters were reported at 7% and 41% for the Concept Laser M1 and EOS M280, respectively. The authors attribute these differences in general to machine infrastructure such as build chamber size, inert gas inlet/outlet design and

gas flow-rate settings. Cacace et al. [156] also reported some ductility values below EC3 requirements in an exploration of the effect of energy density and power input on tensile properties.

For DED-L, reported ductility values are also anisotropic. Bertolini, Perini et al. [157] reported a higher ductility in vertical samples in a similar range to the PBF-L values, while Pacheco et al. [158] reported marginally higher ductility in vertical samples in the as-built condition, and approximately 15% higher ductility in vertical samples in the heat-treated condition. Saboori et al. [159] recorded minimum ductility values just below the EC3 requirements when recycled powders were used, notably 50% lower than samples produced with fresh powder. Saboori et al. [160] also reported minimum values just below EC3 requirements in an exploration of the effect of deposition pattern.

For DED-GMA, reported ductility values are also anisotropic. Wang et al. [161] reported a ductility in vertical samples approximately 10-30% higher than in horizontal samples. Gowthaman et al. [162] explored different heat inputs and build directions and found that the anisotropic ductile behaviour of DED-GMA SS316L varies with heat input. Samples with high heat input had slightly (~5%) higher ductility the vertical orientation, while samples with low heat input was severely anisotropic. The authors reported minimum elongation values for vertically oriented samples falling significantly below the 15% EC3 threshold. This severe anisotropic behaviour is attributed by the authors to the formation of columnar grain crystals growing in the deposition direction.

Ultimately, sufficient ductility according to Eurocode recommendations is achievable in terms of elongation at fracture and f_u/f_y ratio using all three AM methods. However, while it is possible to achieve sufficient ductility, and in fact most recorded data is above the required threshold, the reported range of ductility values is wide for all three printing methods, and some values were recorded below the threshold elongation requirement. This stresses the importance of selecting suitable printing parameters and post-processing to achieve the desired ductility. Currently, too little information is available from literature on ductility in terms of ultimate strain to assess whether ductility in terms of ultimate strain is also sufficient. Further research is required on this topic.

4.3.2.2 Fracture toughness

Requirements per EC3 demand an “sufficient fracture toughness to avoid brittle fracture of tension elements at the lowest service temperature expected to occur within the intended design life of the structure” [148] where the lowest service temperature can be dictated in the national annex. For example, the lowest service temperatures in the Dutch national annex [151] are as follows:

- $T_{Ed} = -20\text{ °C}$ for structures in direct contact with outside air, soil or water;
- $T_{Ed} = -10\text{ °C}$ for structures not covered by a) but located inside the outer façades and roofs of the building, wherein no facility for heating is present (an unheated space);
- $T_{Ed} = 0\text{ °C}$ for structures not covered by a) but located inside the outer façades and roofs of the building, wherein a facility for heating is present, which heats the space to at least 0 °C .

The toughness of a material is affected by several factors including temperature, material thickness, and the type of applied stress. In order to simplify toughness calculations, Eurocode designates steel grades which specify the required minimum impact energy value and test temperature. The design approach per [163] is to verify that the steel thickness does not exceed a maximum value based on the steel grade and toughness designation for a reference temperature and design stress level. According to [163], toughness may be expressed in terms of 4 different types of values: CTOD values, J-integral values, K_{IC} values, or K_V values. Since the toughness requirement is project-specific there is no threshold requirement for the toughness value. As such, a comparison to the fracture toughness properties of wrought SS316L is used to assess suitability. In Table 4.6, the results from literature are compared to benchmark values from wrought steel samples and generic values for SS316L.

TABLE 4.6 Summary of toughness values from literature

Type SS316L	Reported by	Toughness Metric	Process Variables	Fracture Toughness
Benchmark	[164]	J_q @ RT	-	156 N/mm ²
Benchmark	[165]	K_V @ 30°C	-	103 J
PBF-L	[164]	J_q @ RT	-	203 N/mm ²
PBF-L	[152]	K_V @ RT	Orientation	145-150 J
PBF-L	[166]	K_V @ RT	Gas supply	115-141 J
PBF-L	[167]	K_V @ RT	-	130 J
DED-L	[158]	K_V @ RT	Build direction, heat treatment	104 – 143 J
DED-L	[168]	K_V @ RT	Printing path	72 – 96 J
DED-GMA	[169]	K_V @ RT	Orientation	83 – 94 J
DED-GMA	[164]	J_q @ RT	-	170 N/mm ²

J_q : elastic plastic fracture toughness value (J-integral value) in N/mm determined as a line or surface integral that encloses the crack front from one crack surface to the other

K_V : impact energy in Joules [J] required to fracture a Charpy V-notch specimen at a given test temperature T

RT: Room Temperature

The available literature for the evaluation of additively manufactured SS316L only included fracture toughness at room temperature - toughness at cooler temperatures was not explored. Since the structural layer may be exposed to much colder temperatures than room temperature, for example when applied in canopies or applications such as railway stations which have less stringent heating requirements, the toughness at lower temperatures must be better investigated. It is worth noting that austenitic stainless steels in general have “excellent ductility, formability, and toughness, even at cryogenic temperatures” [139]. This is because the amount of nickel and manganese allows them to depress the temperature at which the transformation of austenite to martensite begins, which enables them to maintain their crystallographic structure upon cooling [139] and thus maintain good toughness. As cryogenic temperatures are considered below 150°C, SS316L, which is classified as a cryogenic steel, should have sufficient toughness even at the coldest service temperatures to be expected from urban outdoor environments, even when additively manufactured.

For PBF-L, the fracture toughness of PBF-L samples according to several authors [152, 164, 166, 167] is in a similar range or higher than benchmark values. Both [166] and [167] measured 10-45% higher K_{Ic} toughness in PBF-L samples than the benchmark value. Results from [164] showed a 30% higher toughness based on J-integral calculation of a three-point bending test. The higher fracture toughness of PBF-L SS316L is attributed to its microstructure, whose presence of twins avoid the nucleation of micro-cracks and hinders crack propagation [164]. [152] reported minimal (<5%) difference in toughness between vertical and horizontal samples.

For DED-L, the K_{Ic} fracture toughness values by [158] of machined samples were between 104 J and 143 J, namely equal to or superior to the benchmark value. This study finds that fracture toughness increased significantly with the applied heat treatment, however this increased the anisotropy. Absorbed energy for vertical samples was approximately 12% higher than horizontal samples in the as-built conditions, and approximately 20% higher in with the applied heat-treatment. [168] measured a K_{Ic} fracture toughness that is below the benchmark value by a range of 7-31%. This study explored the effects of path planning on the fracture toughness of DED-L samples and found that a scanning pattern that alternates direction in adjacent layers has a toughness roughly 20% better than one-directional path planning, which enhances crack propagation.

For DED-GMA, annealed samples were found by [169] to have a K_{Ic} fracture toughness about 5-10% lower than the benchmark value depending on the orientation of the sample relative to the printing orientation. J-integral fracture toughness of DED-GMA samples was found by [164] to be higher than wrought samples by approximately 10%. The lower fracture toughness of DED-GMA relative to PBF-L is attributed to DED-GMA samples having crack formation as result of stress build-up at the phase boundaries. Neither study the impact of printing orientation on fracture toughness.

To conclude, toughness values for AM SS316L produced by PBF-L, DED-L, and DED-GMA measured in terms of K_{Ic} and J-integral values ranged from slightly below to slightly above benchmark values at room temperature. Toughness is closely related to the microstructure of the printed part, and as such, varies based on a number of variables such as printing parameters, path planning and orientation. While these results are encouraging for the use of AM in façades, additional study of the behaviour of these materials at colder temperatures is needed for a conclusive assessment of the suitability of the material for architectural applications.

4.3.2.3 Fatigue strength

Fatigue requirements per EC3 demand an “acceptable level of reliability that structure will perform satisfactorily for its design life”, represented corresponding to $N_C = 2 \times 10^6$ cycles [148]. The requirement is project-specific and does not require a threshold fatigue strength value. As such, a comparison to the fatigue properties of wrought SS316L is used to assess suitability. Table 4.7 outlines the fatigue strengths for PBF-L and DED-L from literature.

TABLE 4.7 Summary of fatigue strength values from literature

Fabrication Method	Source	Runout	Stress Ratio	Sample Condition	Fatigue Strength [MPa]
Wrought (Benchmark)	[153]	2×10^6	R=-1	-	436.7
			R=0	-	348.4
PBF-L	[153]	2×10^6	R=-1	As-built	165.0
			R=0	As-built	177.0
				Heat treated	208.0
				Heat treated & machined	389.9
PBF-L	[170]	2×10^6	R=0.1	As-printed, 30 μ m Layer Thickness	< 112.5
				Machined, 30 μ m layer thickness	< 202.5
				Machined, 50 μ m layer thickness	< 180
DED-L	[171]	2×10^6	R=-1	Machined & polished	≈ 225
DED-L	[157]	1×10^6	R=-1	As-built	< 80; < 120
				Machined	180;190

For PBF-L, Figure 4.8 from Braun et al. [153] illustrates the measured S-N curves for high-cycle fatigue of PBF-L samples in the as-built, heat treated, and heat treated/ machined conditions compared to wrought samples. In this study, PBF-L samples in the as-built condition were shown to have a fatigue strength approximately half that of wrought samples. A 17.5% increase in fatigue strength was achieved with heat treatment, and an additional 87% increase was achieved with machining, achieving values slightly above wrought samples [153]. Another study by Hatami et al. [170] similarly achieved an improvement of 55% in high-cycle fatigue strength with machining. The improvement in fatigue strength with heat treatment is attributed to the reduction of residual stresses and the improvement of crack initiation behaviour due to grain coarsening and homogenization[153]. The improvement in fatigue strength with machining is attributed primarily to the removal of surface defects, and also to a lower surface roughness and the inducement of residual compressive stresses at the surface [170].

Two studies explored the high cycle fatigue strength of DED-L samples using a stress ratio of $R = -1$. Both studies showed high cycle fatigue strength significantly lower than the roughly 350 MPa wrought SS316L benchmark. Bertolini, Perini et al., [157] tested high cycle fatigue strength for only 1 million cycles and found that as-printed samples had a runout fatigue strength between 80 and 120 MPa. Fatigue strength increased significantly with surface machining. Vertically printed machined samples reached a fatigue strength of 180 MPa while horizontally printed machined samples reached 190 MPa. The authors attribute this significant change in fatigue strength with machining largely to the surface condition, for which it is noted that valleys in rough surfaces act as stress risers which are prone to the nucleation of fatigue cracks. The difference in fatigue strength between vertical and horizontal samples, which was only measured for machined samples, was marginal. The authors note that while the main factor of tensile properties is the build direction, the main factor for fatigue strength is the surface finish [157].

Blinn et al. [171] tested high cycle fatigue strength for 2 million cycles for DED-L machined samples only and found a runout as high as about 225 MPa for machined samples (Figure 4.9), even higher than found by Bertolini, Perini et al. [157] despite using the same printing technology and similar printing parameters.

No relevant studies were found which produced relevant fatigue strength values for SS316L DED-GMA printed parts.

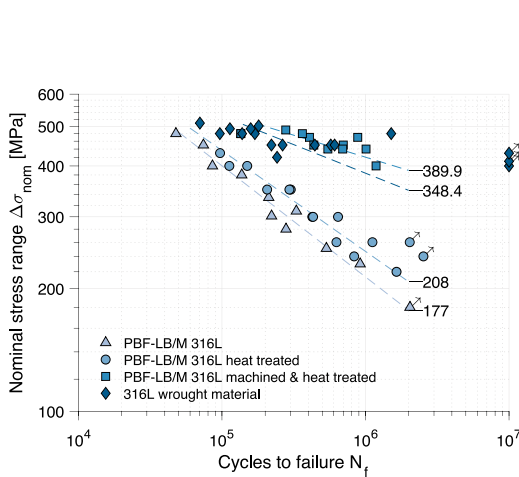


FIG. 4.8 Comparison of S-N curves for different PBF-L production routes with wrought material at stress ratio $R = 0$ (Image Source: [153])

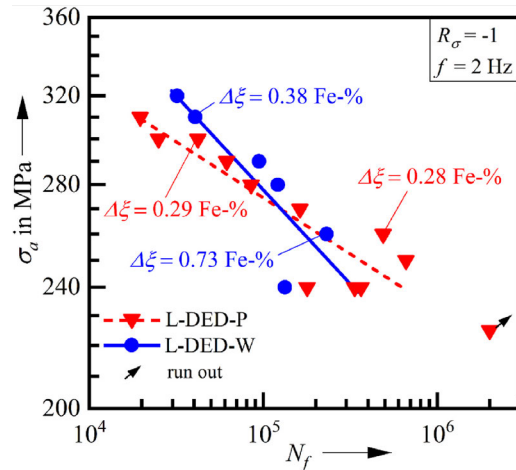


FIG. 4.9 Comparison of S-N curves of DED-L (Powder) and DED-L (Wire) at stress ratio $R = -1$ (Image Source: [171])

To conclude, the suitability of the use of AM parts in terms of fatigue strength depends on the fatigue requirements of the specific application. When compared to the fatigue strength of wrought SS316L, DED-L and PBF-L samples in the as-built condition measured significantly lower fatigue strength than the values for wrought samples. In both printing methods, fatigue performance is significantly improved with surface machining by the smoothing of the surface finish and elimination of surface defects which mitigates fatigue crack nucleation, and by inducing surface compressive stresses which are beneficial for fatigue performance. If higher fatigue requirements are necessary based on specific fatigue loads, heat treatment and/or post machining can be used to improve fatigue strength. Fatigue strength of PBF-L SS316L parts even superior to that of wrought SS316L were recorded when using both surface machining and heat treatment. No study explored this combination for DED-L. Further research is required to investigate the fatigue performance of DED-GMA parts.

4.3.2.4 Ultimate tensile strength, yield strength/0.2% proof strength, and elastic modulus

While there is no explicit requirement for the strength and stiffness values of steel to be used in construction, these mechanical properties are of obvious importance to structural design, since reliable and predictable values for these properties, which are outlined in tables for the common construction alloys in their various formats, form the basis for much of the engineering procedures outlined in Eurocodes. As a stainless steel, SS316L falls under the scope of EN 1993-1-4, which enables the engineering design to use either nominal values or stress-strain curves, since stainless steels exhibit typically non-linear stress-strain behaviour. Because this section serves to establish the preliminary potential of AM SS316L for structural applications, only a few design values are explored, namely ultimate tensile strength, yield strength (or 0.2% proof strength), and the elastic modulus. More in depth analysis and engineering, however, should consider the actual stress-strain curves of the printed material. Figure 4.10 outlines the range of ultimate tensile strength, yield strength/0.2% proof strength, and elastic modulus reported in the collected literature in comparison to benchmark values SS316L in the following product forms: annealed sheet, strip, plate and bar, according to [165].

It can be observed that the ultimate tensile strength and yield strength are generally similar or superior to the benchmark values, while the elastic modulus is generally similar or inferior to the benchmark values. It can also be observed that there is a large range of recorded values. Such large discrepancies in reported values are

largely due to the use of different printing properties, as well as different post-processing and surface finishing strategies. Notably, the tensile behaviour of AM SS316L is anisotropic. Reported values for ultimate tensile strength and yield strength are generally reported higher for horizontal samples than vertical samples [152-154, 157, 158, 161, 162].

Many studies explored different variables in order to understand their effect on mechanical properties. Obeidi et al. [155], for example, explored different PBF-L printers and combinations of printing parameters. Cegan et al. [172] explored the effect of Hot Isostatic Pressing (HIP) and heat treatment. Gowthaman et al. [162] explored the effect of different heat inputs on DED-GMA printed samples by altering welding current, wire feed speed, and travel speed. These explorations highlight the wide range of possibilities when it comes to the mechanical properties of AM parts, and the importance the selection of suitable printing parameters for the specific technology.

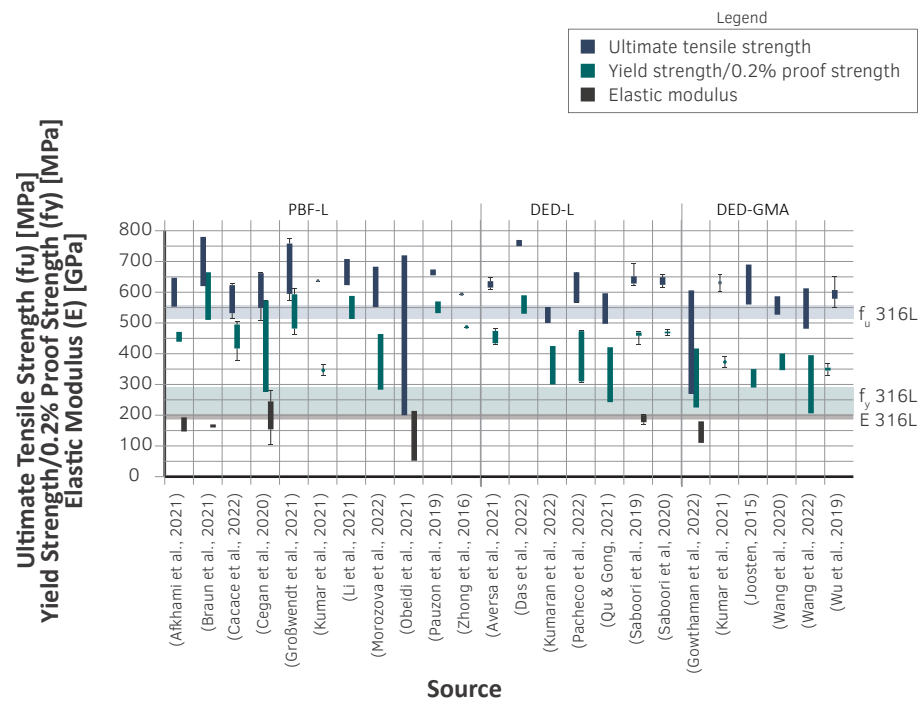


FIG. 4.10 Ultimate tensile strength, yield strength, and elastic modulus values from literature (Image by author)

To conclude, based on the literature, there is an overarching trend that YS and UTS are higher than that of the wrought material while the elastic modulus is generally lower. As with ductility, there is a large range of reported values, some of which are exceptions to the aforementioned trend. The design values for AM SS316L are typically anisotropic based on the printing orientation for all printing methods. The large range of reported values stresses the importance of proper fabrication design and the selection of suitable printing parameters, path planning, and post-processing to achieve desirable mechanical properties.

4.3.3 Discussion on the mechanical properties of AM SS316L

In this section, the evaluation of the mechanical properties of AM SS316L stainless steel was used as a basis to validate its potential use in architectural applications. EC3 explicitly outlines three minimum material requirements: ductility, fracture toughness, and fatigue strength. Ductility requires minimum ductility expressed in three terms: elongation at fracture; the ratio of ultimate tensile strength to yield strength; and ultimate strain. Fracture toughness and fatigue strength are application specific. In addition to this, the design properties of AM SS316L, namely yield strength, ultimate tensile strength, and elastic modulus, are also compared to benchmark values.

The literature reveals that AM SS316L produced by PBF-L, DED-L and DED-GMA demonstrate promising material characteristics which are in many cases able to meet or exceed EC3 requirements and/or benchmark values for wrought SS316L. However, there are notably some instances where the mechanical properties are significantly inferior to benchmark values and even below the EC3 requirements. Crucially, there was also a large spread of reported values for mechanical properties between, and also within the three different AM methods under investigation. The literature that evaluated mechanical properties often correlates them to either physical properties observed in the samples, and/or to fabrication variables which were explored in the experiments. The following definitions are provided for clarity:

Mechanical properties: Mechanical properties describe how a material reacts to external forces like pushing, pulling or twisting. These are the properties explored in the previous section such as ductility, toughness, yield strength, etc.

Physical properties: Physical properties refer to observable characteristics of a material. Examples of physical properties include its density, microstructure, grain morphology, and defects such as porosity and residual stresses.

Fabrication variables: Fabrication variables refer to the collection of choices made during fabrication such as the selection of printing parameters, part orientation, printing path, choice of printing machine, type and quality of base material, surface finishing operations etc.

Ultimately, mechanical properties are dependent on physical properties of the sample, which are effectively determined by fabrication variables. The literature investigated in this section highlights the complex network of interdependencies between various fabrication variables, physical properties, and mechanical properties. Aiming at AM becoming a standard fabrication option for the production of structural parts for architectural applications, these interdependencies should be well understood such that AM parts can be fabricated with a balance of fabrication speed and good mechanical properties. Further, this complex network of interdependencies makes yet another case for the systemization of AM components, since the systemization of final part geometry and its corresponding process variables would facilitate the fabrication of mass-customized parts with reliable and reproducible physical and mechanical properties.

Despite the promising results of this study, in which AM SS316L was reported to meet all Eurocode requirements and benchmark values for which studies were available, it does not provide a definitive answer on the suitability of AM SS316L for the fabrication of structural parts for the construction industry. This is because each study investigated only select mechanical properties for samples produced with a specific set of process variables. As such, while the properties reported are in many cases suitable for architectural applications, or even exceeding the performance of the wrought equivalent material, these properties are significantly affected by fabrication variables which are notably inconsistent across studies. A more comprehensive experiment testing ductility, toughness, and fatigue strength using controlled sets of fabrication variables is necessary in order to definitively ascertain whether AM parts can meet all material benchmarks to be deemed suitable for use in architectural applications. Additionally, the suitability of AM SS316L for the construction industry will necessarily depend on the selection of suitable and compatible fabrication variables for the chosen printing method.

4.4 Design guidelines for metal DED and PBF additive manufacturing

In this study, two families of metal AM are under exploration: PBF and DED. For each of these methods, there are several resources available that provide guidelines for designing with the technology in question in order to design quality parts, with minimal defects, and a level of fabrication efficiency. Table 4.8 outlines the most relevant strengths and limitations of DED and PBF technology. Table 4.9 outlines the most relevant design guidelines for the respective AM methods.

TABLE 4.8 Key strengths and limitations of DED and PBF additive manufacturing

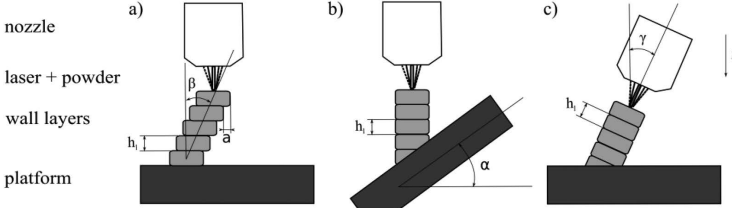
	DED	PBF
Process strengths	<ul style="list-style-type: none">• Higher material deposition rates [140]• Possibility to print on various types of substrates and integrate them into the part [140]• Can be integrated as part of hybrid additive/subtractive fabrication process [140]• Suitable for large objects [140]• Lower material cost than PBF both in wire and powder form [140]	<ul style="list-style-type: none">• Suitable for complex design with integrated functions [140, 173]• Suitable for parts with internal structures or channels [173]• Suitable for features with undercuts or structures that cannot be realized by casting, forging or metal cutting processes [173]
Process limitations	<ul style="list-style-type: none">• May be limited by medium-to-large scale features [140]• Limited part complexity [140]• More complex NC software and programming due to tool path planning [140]• Less accurate than PBF [140]	<ul style="list-style-type: none">• May be limited by availability of the required materials [140, 173]• Part size limited by build chamber [140, 173]• High production costs [173]• Low material deposition rates [140]• High material cost of metal powders [140]

TABLE 4.9 Relevant design guidelines for DED and PBF additive manufacturing

Feature	AM	Guideline
Build size	DED	Depending on specific DED technology, build size varies from medium to large scale. Powder-based DED takes place in a build chamber so part size is limited, but DED-GMA for example may be produced in an open environment and extremely large parts are possible [140].
	PBF	Part height has a significant impact on build times/cost consideration [173]. Part orientation to minimize build height should be taken into account. Likewise, printing multiple parts using up the available area in the build plate is an effective way of improving the fabrication efficiency of the individual parts [173].
Corners and edges	DED	Corners and edges should have a minimum radius of the layer width – smaller radii requires post-processing and are prone to stress concentrations [143, 174]
	PBF	Sharp corners should be avoided to avoid cracking due to residual stresses [173].
Holes, channels and cavities	DED	Enclosed features are possible by using multi-axis build techniques or strategic deposition paths which allow unsupported regions to be deposited without support structures [143].
	PBF	Unsupported integral channels are possible [175]. Holes counter to z-axis with diameter smaller than 8mm typically do not require support material [173]. It may be preferable to drill straight holes rather than print them [173]. Cavities are possible, and can be a good measure for minimizing warpage, as well as reducing build time and material consumption. Cavities will contain un-fused powder after printing. This powder can be removed by providing openings, or left in place [173].
Machining	DED	Depending on the machine, DED parts may be machined during or after the print process [143]. Machining during printing requires a hybrid additive/subtractive machine.
	PBF	Machining can be used for PBF parts to remove support structures, or achieve final tolerances [173]. Hybrid additive/subtractive machine incorporating milling into PBF printing to achieve high accuracy also exist [140], although it is less common than with DED machines.
Orientation	DED	Build orientation in DED printing is closely tied to build time, surface finish and manufacturing cost [143] A methodology for the selection of part orientation for DED fabrication is available in [143].
	PBF	Part(s) should be oriented in build chamber to take account of the direction of the spreading device so as to minimize contact length and avoid bending critical geometries [173]. Part orientation in the build chamber will also have a significant effect on the required amount of support structures [173]. Part orientation will also affect the mechanical properties of the part, since they are anisotropic [173]

>>>

TABLE 4.9 Relevant design guidelines for DED and PBF additive manufacturing

Feature	AM	Guideline
Overhangs	DED	<p>There are several ways of achieving overhangs in DED printing without support material as shown in graphic below by Ewald and Schlattmann [174]: a) by printing materials in a stepped configuration in a single printing plane; b) by rotating the substrate; and c) by rotating the orientation of the print-head. The use of stepped overhangs in a printing plane results in reduced effective wall thickness, increased residual stresses and an increased potential of printing defects [174]. On the other hand, rotating the substrate and the print-head should be done with careful consideration since additional time has to be allocated for machine movement and interlayer cooling [142, 174].</p> 
	PBF	<p>A rule of thumb for PBF is not to go below a 45 degree downskin angle in order to avoid support structures. Lower angles are possible but there is a decrease in surface quality [173, 175]. Typical minimum downskin angle is between 30-45 degrees [173]. Overhangs lower than these thresholds are achievable through the use of support structures. See "Support Structures" for additional information.</p>
Path planning	DED	<p>Path-planning should consider size, orientation, and position of the print-head relative to the printed part [176]. For example, print-head clearance may dictate the positional orientation of the build or limit the part geometry [140]. Another important aspects of DED planning is symmetry to reduce part deformations [143].</p>
	PBF	None specified
Substrate integration	DED	<p>It is possible with DED technology, to integrate the substrate into the printed product[177]. This can be a good strategy for saving on cost and printing time [140, 174, 178].</p>
	PBF	<p>Substrate integration in PBF can only be achieved to the extent that it consists of the integration of the base plate, as it cannot interfere with the powder spreader.</p>
Support structures	DED	<p>Support structures are not typical in DED printing. Rather, low overhangs are achieved though path planning.</p>
	PBF	<p>Support structures are necessary for overhang angles below the prescribed limit. Support structures are also necessary as a heat sync, to improve surface roughness, and avoid part deformation [179]; as well as to provide provisional support for pieces under construction [173]. Supports should however be applied only as necessary since superfluous supports mean superfluous material usage and printing time, and can also lead to build failure [173]. Part shape and orientation have a significant influence on how many support structures are required [173]. Support structures should also be designed with consideration for how they will be removed [173]– in particular, allowances such as access should be made if the supports are to be removed manually. Parts orientation in the build volume plays a significant role in the amount of necessary support structures [173]. Well-designed support structure design should strike a balance between "support structures, efficiency, process stability and part quality" [173].</p>

>>>

TABLE 4.9 Relevant design guidelines for DED and PBF additive manufacturing

Feature	AM	Guideline
Symmetry	DED	DED parts are prone to distortion due to high heat input and cooling rates. Depositing material symmetrically around the substrate can help reduce residual stresses and distortion [143].
	PBF	None specified
Tolerances	DED	Actual tolerances vary by specific printing method, material, and printing parameters, but are in general larger than for PBF [140]. Additional material should be provided for a machining allowance to overcome surface roughness and dimensional tolerances [143].
	PBF	Typical geometrical tolerances for PBF printing methods are around $\pm 0,2\%$ with minimal 0,2mm [173]. Functional surfaces should be designed with allowances for surface roughness and deformations [175]. Rounded corners are also recommended to curb distortion [177]. Large flat sections and thin sections are susceptible to warping and may require ribs or other support structures [140]. Large surfaces should also not be oriented such that they are fused in a single path in order to avoid curl effect [173].
Wall curvature	DED	Curved walls are possible, but straight walls facilitate programming effort [174].
	PBF	None specified
Wall thickness	DED	Walls may be produced by single-bead widths or multiple-bead widths. In cases where multiple bead-widths is used, rows should overlap to fuse effectively [174].
	PBF	Minimum wall thickness depends on size of melt pool [173]. Thin walls should also take into consideration the part orientation in relation to the coating direction since this may cause deformation [173].

Additional guidelines for DED-L specifically are available in [140], [174] and [178]. Additional design guidelines for DED-GMA specifically are available in [143] and [180]. Additional PBF-L guidelines are available in [179], [173], and [140]. The information in these tables was used to inform the node designs developed for Section 4.5.

4.5 Design, fabrication, and analysis of AM structural nodes

In this section, three metal AM nodes are designed and fabricated as a basis for comparison, and compared to solid CNC-milled nodes as a benchmark of current node solutions. This enables a comparison of different AM methods and an exploration of the extent to which AM nodes can improve on current building methods. The quality of design is defined in key terms: design efficiency, material efficiency, fabrication efficiency, assembly efficiency, and geometrical flexibility.

Design efficiency, assembly efficiency, and geometrical flexibility are assumed through the development of system products, which is further explained in Section 4.5.1. Since fabrication efficiency in the design of AM depends largely on compatibility of the design with the AM method being used, one node design specific to each of three selected AM technologies (DED-GMA, DED-L, and PBF-L) is developed. The different AM method/node design are then compared in terms of their respective fabrication time, material usage, and surface quality.

The design and prototyping of the structural nodes for this analysis were part of a larger project discussed in Chapter 6, for which the objective was to eventually build a full-scale freeform façade using AM nodes. This larger project included an exploratory phase to develop structural nodes using different AM methods, the results of which are compared in this chapter. The design process for the structural nodes began with schematic designs informed by the guidelines outlined in Section 4.4, as well as feedback from structural engineers to improve the structural efficiency of the node topologies, and feedback from AM fabricators to improve fabricability.

In this section, specific boundary conditions that influenced node design are explained, the resulting designs and some of their key iterations are illustrated, the fabrication process and material usage for each node design are explained, and finally the different node designs and the experience of working with the different technologies are discussed.

4.5.1 Design boundary conditions

In order to provide a basis for comparison, the node designs conform to a set of boundary conditions: First, they are designed as “system products” such that they can achieve design efficiency, geometrical flexibility, and assembly efficiency through systemization. Each node is designed with systemized connections and interfaces such that they are interchangeable in a façade assembly. The node models are also generated using a parametric definition in Rhino/Grasshopper that outputs multiple node configurations. Using this definition, a version of each node in the same configuration is outputted and engineered to a base level of structural capacity in order to provide a good basis for comparison of material efficiency and fabrication efficiency.

Structural nodes as system products

The term “system products” refers to the development of series’ of parts within a façade system that can be interchanged and/or adjusted based on the specific requirements of a given project without modifying the technical core of the system. This approach allows façade system providers to provide architects and engineers with a wide range of design possibilities for their buildings with a high level of engineering and manufacturing efficiency, since specific product capacities can be pre-engineered and the appropriate elements from the kit-of-parts can then be selected with ease once design requirements are established. The development of system products also is a means to achieve the production of products with consistent quality, and is thus helpful for the acquisition of certifications and approvals such as CE markings.

In façade construction, the systemized approach means developing a range of system products, for example different profile shapes and dimensions, panel types and thicknesses, and gasket profile geometries. The interfaces between the different layers of the façade system as well as between elements within the same layer remain the same regardless of which specific system product is included in the façade assembly, such that they remain interchangeable.

The development of structural nodes as “system products” is a key requirement for the development of the AM parts for this study with the idea that the structural node solutions developed in the context of this research could become an integrated part of a systemized façade that can eventually be adapted to other real-life applications. In order to design the structural nodes as system products, they require 2 key features: standard connections, and a systemized node topology.

For this particular exploration, a standard connection is defined which consists of a flat end face at all node arms with a smooth surface finish and four 17mm deep M8 threaded holes. In this connection, compression forces are introduced through contact, while tension forces are introduced via the four bolts anchored via the threaded blind hole. The exact nature of the connection could be changed in future projects, but its core components (a flat end face and threaded holes) are common features for mechanical connections in freeform façades [31, 92], and thus serve their purpose as a basis for the comparison of the different AM nodes.

The second key feature for the design of structural nodes as system products is a systemized topology. A systemized node topology refers to a parametrically-defined form that can be reconfigured to be applied to a wide range of geometrical configurations, and that has defined variable parameters that can be prescribed different dimensions based on the specific structural requirements of the node condition.

For each metal AM method and corresponding node, a different topology and different variables are defined based on the strengths, limitations, and DfAM guidelines of the technology. This excludes a design integrating topological optimization, a process in which material is removed from a design space based on specific applied loads, and that tends to generate unique, organic shapes. The purpose of this requirement is bearing in mind the eventual mass-customised design and production of the object - while topological optimization is an effective strategy to reduce material usage in structural parts, it comes with a significant amount of effort required for optimization and print-ready modelling that would likely be problematic in projects with hundreds or thousands of individual nodes.

In addition to the aforementioned advantages of system products, the design of structural nodes as system products comes with a number of additional advantages: the fabrication operations and path planning can remain consistent; printing parameters, which can take significant effort to fine-tune for high-quality prints and reduced failed prints, can quite reasonably be standardized; and the engineering process can be made more efficient.

Structural node dimensioning

In order to provide a basis for comparison, the nodes are generated for the same geometrical configuration and dimensioned to withstand the same minimum loading conditions. The DED-L node is more conservatively dimensioned than the DED-GMA and PBF-L nodes since it was influenced by available pipe size and prioritized printing path efficiency over material efficiency. In order to validate the capacity of the nodes, a simplified (planar) version of each node was engineered to withstand the same 4 load cases covering crucial load configurations and type of dominant load outlined in Table 4.10. Force distributions for the two different load configurations are as shown in Figure 4.11. These force values as applied, correspond to a percentage of the profiles' design capacity for a S235 50 x 80 x 2mm profile with 2mm radii at edges, which were used to construct the mock-up.

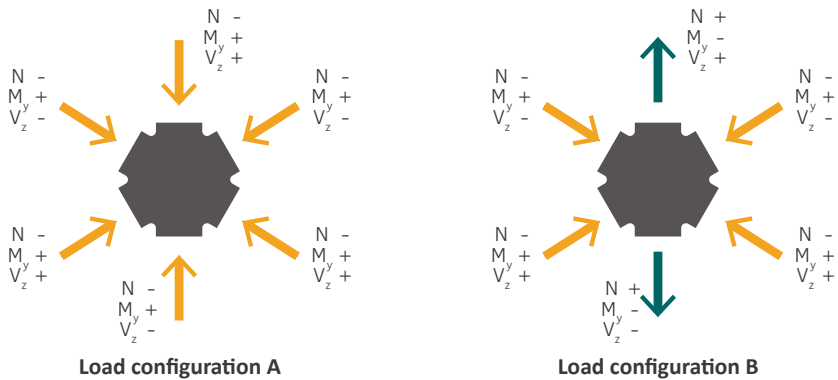


FIG. 4.11 Schematic load configurations A and B applied to nodes for FEA validation (Image by author)

TABLE 4.10 Applied load cases for structural node verification

	Normal force dominant		Moment force dominant	
	LC 1	LC 2	LC 3	LC 4
N = 117.3 kN	0.55 N	0.55 N	0.25 N	0.25 N
My = 3.15 kNm	0.25 My	0.25 My	0.55 My	0.55 My
Vz = 41.7 kN	0.05 Vz	0.05 Vz	0.05 Vz	0.05 Vz
Load configuration	A	B	A	B

4.5.2 Structural node designs

This section gives an overview of the design of the different structural nodes, explaining the specific design decisions that were made based on a combination of AM guidelines from the previous section, feedback from the AM fabricators, and experience from having printed preliminary prototypes.

4.5.2.1 Design of benchmark CNC-milled node

The CNC benchmark node is based on a common structural node strategy, which is simply a solid CNC-milled node with threaded holes (Figure 4.12). It consists of a solid volume of steel with filleted edges, a radius of 5mm between arms, and threaded holes per the standard connection defined for this comparison exercise.

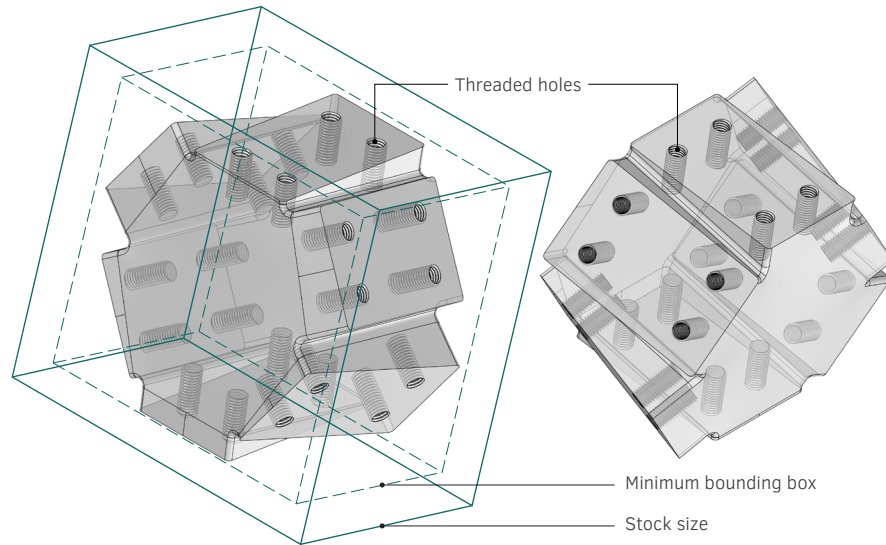


FIG. 4.12 Benchmark CNC node design (Image by author)

4.5.2.2 Design of DED-GMA node

The print sequence and overhang implications of DED-GMA have a significant impact on the design of the DED-GMA node (Figure 4.13). The node consists of a primary arm that runs through the centre along the main load bearing artery of the node, and secondary and tertiary arms that connect to that one. The hierarchy of arms corresponds to both the hierarchy of forces acting on the node and the sequence in which they are printed. The path planning strategy is explained in more detail in Section 4.5.3.2.

Each arm consists of exterior plates at the inside and outside faces of the node, and interior plates running at around 45 degrees from the edges of the outer plates and joining at the centre of the node, gradually decreasing in width to meet at the center of the node. For the end conditions, the plates gradually increase in thickness merging together to form volumetric components with flat end faces that allow the standard end-face detail. This strategy allows the end faces to be achieved with relatively simple path planning. The end faces and threaded holes are subsequently CNC-milled to overcome the tolerances of the DED-GMA printing process.

The structural logic behind the node geometry is that continuous exterior plates allow a smooth transfer of in-plane forces from bending and axial forces across the node, while the webs connected at the centre and the gradually increasing end volumes transfer shear forces. The arm hierarchy is clearly visible in the surface pattern of the printed node. Depending on the specific loads conditions at the node, the thickness plates can be adjusted parametrically.

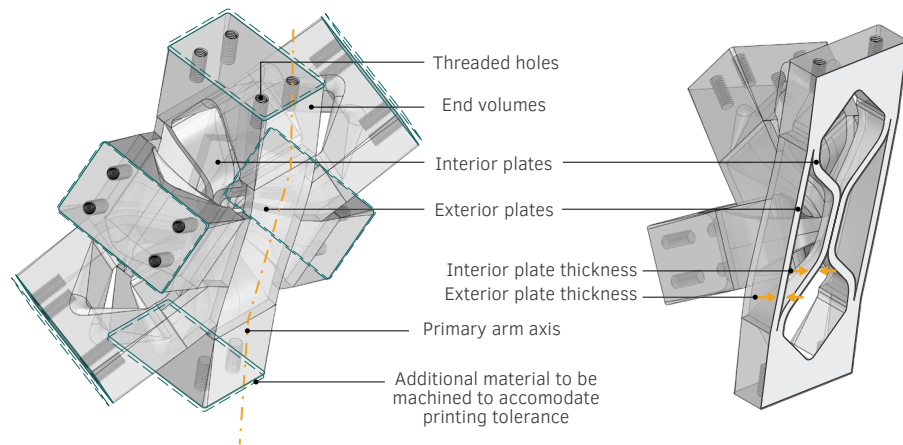


FIG. 4.13 DED-GMA node design (Image by author)

4.5.2.3 Design of DED-L node

The DED-L node (Figure 4.14) is printed radially around a substrate consisting of a pipe with a cap welded at the end. The material is deposited in a solid volume so there are little to no overhang considerations. The path planning strategy is explained in more detail in Section 4.5.3.3. The end faces and threaded holes are subsequently milled to achieve the required tolerances.

A solid structural ring is formed by the steel pipe and AM material, which redistributes forces primarily by membrane action. This strategy allows for a relatively lower material usage than a solid milled node, as the overall node boundary is the same, but material in the center of the node where stresses are at their lowest is removed. Depending on the specific load conditions at the node, the pipe dimensions and minimum thickness of the structural ring can be adjusted parametrically.

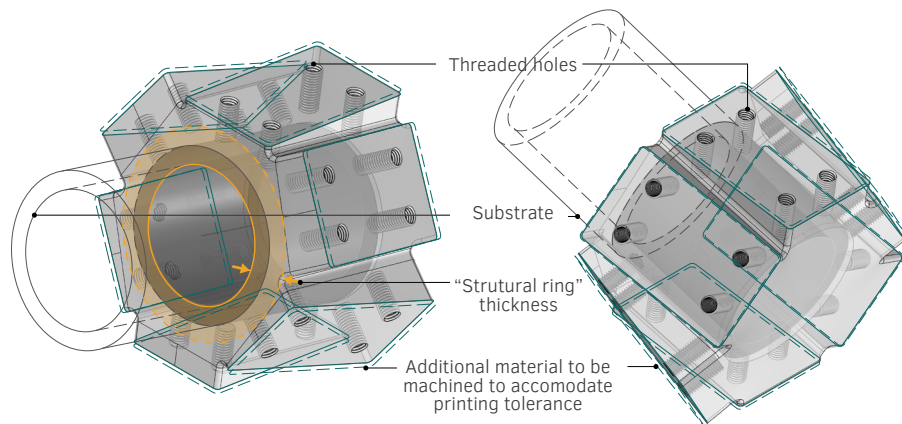


FIG. 4.14 DED-L node design (Image by author)

4.5.2.4 Design of PBF-L node

The design for the main geometry of the PBF-L node (Figure 4.15) consists of a network of walls aligned roughly with the z-axis of the printer. As such, most of the walls are oriented so their overhangs are well within the printing limitations. End faces and side walls define the volumetric boundary of the node, while an interior structure of concentric cylindrical walls with varying radii are at the centre, and plates running from each end face along the normal force direction of each arm connect the network of walls creating a structural lattice. Additionally, volumes of solid steel are printed around the threaded holes with a parametrically-driven thickness that corresponds to a factor of the diameter of the bolts as defined in EC 1993-1-8. As the joining of the wall structures and volumes create enclosed cavities, openings are made on the end face for powder removal. The outer face of the node also has a thin plate at the outer face of the node to support the gasket, and a small triangular inset to provide an interface with the gasket.

The thus created radially oriented webs of the node arms provide a direct load path for the normal and shear forces as well as bending moments onto the cylinder at the centre of the node. The central cylinder efficiently redistributes these loads predominantly via membrane action through the curved walls to the neighbouring arms and back into the adjacent structural profiles. Depending on the specific loads conditions at the node, the thickness and density of the walls can be adjusted parametrically.

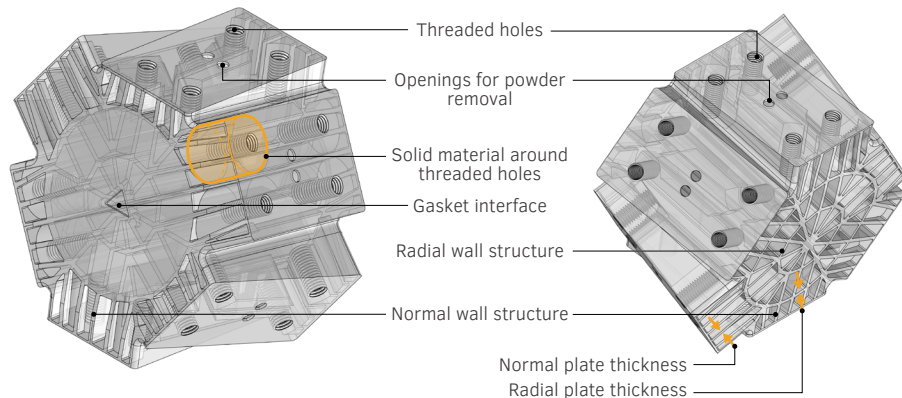


FIG. 4.15 PBF-L node design (Image by author)

4.5.3 Node fabrication

A sample of each AM node described in Section 4.5.2 was generated using a parametric model for the same geometrical configuration, validated using FEA to withstand the same base loading conditions, and was fabricated for comparison. In the following sections, the process for the manufacturing of each node is outlined, and fabrication times for the major fabrication steps is provided based on the experience of the fabricators and fabrication simulations. A CNC simulation of a solid node is used as a benchmark to compare the designs and processes. The direct and indirect material usage of the nodes is also documented. Comparison and analysis of results is provided in Section 4.6.

4.5.3.1 Benchmark CNC node fabrication simulation

The fabrication data collected for the CNC node is based on CNC milling simulation.

CAM modelling

The CNC-milling node fabrication is simulated in Fusion 360 for a generic 5-axis CNC mill. The CAM modelling for this node took approximately an hour and a half.

Stock preparation and machine setup

The assumed stock material has a dimension of 145mm x 161mm x 100mm which is a 10mm-13mm tolerance from the minimum bounding box of the actual finished node on every face (Figure 4.12).

Milling operations

Table 4.11 outlines the main milling operations, parameters, and fabrication times for the fabrication of the CNC-milled node based on the Fusion 360 simulation. The total simulation time for CNC milling excluding tool changes is about 12 hours and 40 minutes.

TABLE 4.11 Parameters and simulated fabrication time for CNC milled node

Process Parameters							Duration		
Operation		Mill type	Specific operation	Stepdown / Packing [mm]	Stepover [mm]	Feedrate [mm/ min]	[h]	[m]	[s]
Roughing	Main volume	Bullnose Ø25 R1.5	Adaptive clearing	0.10 - 80	10 (optimal)	5000-6000	0	37	48
	Arm cavities	Flat End Ø5	Pocket clearing	1 - 10	< 3	300-500	1	40	59
Surface finishing	End faces	Bullnose Ø16 R4	Flat	0,2-0,5	8-10	500-1000	0	7	36
	Arm cavities	Ball Ø5	Ramp	0,2-0,5	0,2-0,5	200-400	3	7	15
	Outer faces	Ball Ø5	Scallop	0,2-0,5	0,2-0,5	200-400	6	36	41
Holes	Centring	Centre Ø5	Centring	-	-	10-50	0	4	33
	Drilling	Drill Ø6.8	Drill - chip breaking	0,5-1,0	-	10-50	0	21	9
	Threading	Thread M8	Thread	-	-	100-200	0	4	18
Total							12	40	19

Material usage

The material usage, which is calculated from the volumes of the billet and node, equals 6.8 kg for the node, and 11.8 kg of recyclable waste from the milling process.

4.5.3.2 DED-GMA node fabrication process

CAM modelling

The main steps in the CAM modelling include subdividing the model based on the print sequence, and applying the welding program, orientation, scan strategy, and operation sequence to the model. While plates had a linear scanning strategy, a contour strategy was applied to end conditions to have a better surface finish quality. The CAM modelling took approximately an hour and a half per node.

Substrate preparation

The substrate for the DED-GMA node consisted of a 100x100x10mm plate clamped onto the machine. Prior to printing, the oxide layer is grinded from the substrate.

Additive operations

The DED-GMA node was printed in 308LSi Stainless Steel. Table 4.12 outlines the fabrication settings. The print sequence is outlined in Figure 4.16. The first printing operation was the bottom end condition on the substrate followed by the rest of the primary arm. The secondary arm plates were printed next, followed by the tertiary arm plates. Once the plates were complete (Figure 4.17), the end volumes were printed in tandem such that the interlayer cooling time was used to print the other volumes. End volumes were printed with an additional 2mm of material to be milled off to reach the required tolerances for the structural profile interfaces. The total printing time for the node was not recorded during fabrication. The fabrication times provided are based on a combination of simulation and best recollection from the AM fabricators. Total active printing time for this part is approximately 9 hours with an additional 40% added for machine movement and cooling.

TABLE 4.12 Process parameters for DED-GMA node additive manufacturing

Setting	Value
Wire diameter	1 mm
Wire feed rate	4.5 m/min
Voltage	11.3 V
Current	85 A
Layer thickness (t)	1.6 – 2.4mm
Gas flow rate	10-20 L/min

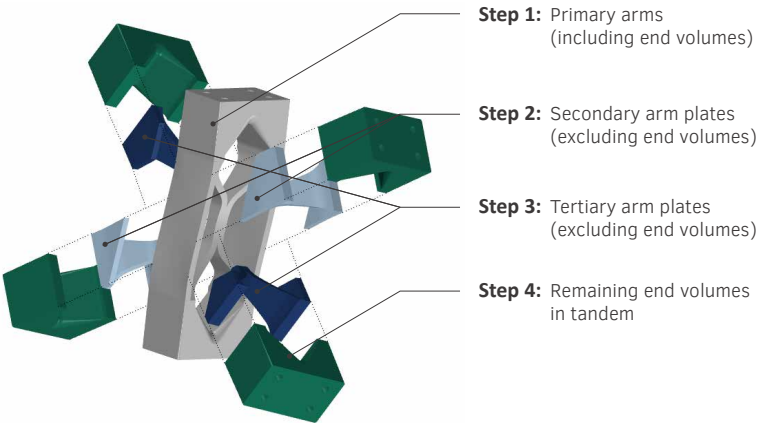


FIG. 4.16 Order of additive operations for AM process of DED-GMA node (Image by author)

Surface finishing

After printing, the part was sandblasted to improve the surface finish (Figure 4.18).

Milling operations

The tolerances for DED-GMA printing are not sufficient for the connection details. As such, additional milling is necessary. It is assumed for this comparative study that the surface finishing of the end faces and the drilling operations for the threaded holes would take the same amount of time as was recorded in the DED-L node fabrication.

Material usage

The final weight of the DED-GMA node is 10.6 kg, approximately 80% of which is located in the end conditions. A weight of 0.8 kg is calculated to have been removed during the milling of the end faces and threaded holes. The baseplate can be refinished and reused for another print. Process waste for DED-GMA consists primarily of splatter and is prescribed a value of 1% of the node weight.



FIG. 4.17 DED-GMA node during printing process (Image courtesy of Mx3D)



FIG. 4.18 Final DED-GMA node after surface finishing (Image courtesy of Jansen AG)

4.5.3.3 DED-L node fabrication process

CAM modelling

Both the additive and subtractive processes are modelled in the CAM software Siemens NX [182], which is a process that took approximately 45 minutes per node.

Print preparation and machine setup

The substrate for the DED-L node consists of a CHS with a 3mm plate welded to the end to provide a solid base on which to print the outer node face. The substrate is then welded to a standard mount (an approximately 100 x 100 x 60mm steel block) and subsequently fixed into the hybrid machine. The fabrication of the substrate takes approximately half an hour per node. During this time, the powder is also preheated for 2 hours prior to printing.

Additive operations

The nodes were fabricated using a hybrid DED-L/CNC milling machine. Table 4.13 outlines the main process parameters for the fabrication of the DED-L Node.

TABLE 4.13 Process parameters for DED-L node additive manufacturing

Setting	Value
Powder size	40 – 150 μm
Powder flow rate (g/min)	24g/min
Laser power (P)	1800 W
Hatch spacing	1,5mm
Scan speed (v)	1000 mm/min
Layer thickness (t)	1,6mm

The path planning for this node consists of two major movements: the substrate rotating around its own axis, and the print head perched vertically above the substrate moving in the x and y axes. The printing process is illustrated in Figure 4.19. The substrate is first oriented vertically, and material is deposited on the end cap to the correct thickness. The substrate is subsequently rotated to be

horizontal, and again rotates around its own axis to print the arms while the print-head moves along the x and y axes. This path-planning gives the node a visible radial texture. Because of the tolerances of DED-L printing, the node is printed with an additional 2mm of material in the end faces to be milled off in order to reach the tight tolerance required for a good interface with the adjoining structural profiles and the threaded hole connection detail. Total printing time for the node was approximately 6.5 hours.

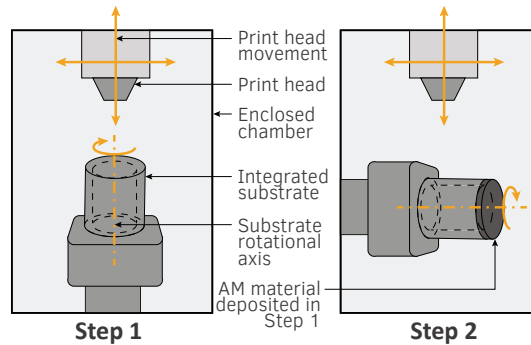


FIG. 4.19 Main additive operations and movements axes for DED-L node. (Image by author)

Milling operations

Once the solid geometry is printed, the end conditions are milled to the required tolerances. Table 4.14 outlines the main subtractive operations, parameters, and fabrication time. The total CNC milling time for the end faces and threaded holes is approximately an hour.

TABLE 4.14 Process parameters for DED-L node subtractive operations

Operation		Bit type	Specific operation	Stepdown / packing [mm]	Stepover [mm]	Feedrate [mm/ min]
Surface finishing	End faces	Facing cutter	Face milling	2-5	20	250-500
Holes	Centering	Center $\varnothing 12$	Centering	-	-	50-100
	Drilling	Drill $\varnothing 6.8$	Drill	0,5-1,0	-	250-500
	Threading	Thread M8	Thread	-	-	250-500

Substrate removal and surface finishing

As a last step, the part has to be removed from the substrate. The majority of the substrate is removed using a band-saw. The remaining protruding material is subsequently grinded off until smooth. Rough edges from the milling process are also smoothed (Figure 4.20). Lastly, the node surface is polished using a grinding brush and the node is washed for a nice surface finish. The combined substrate removal and surface finishing for the part take less than an hour per node.

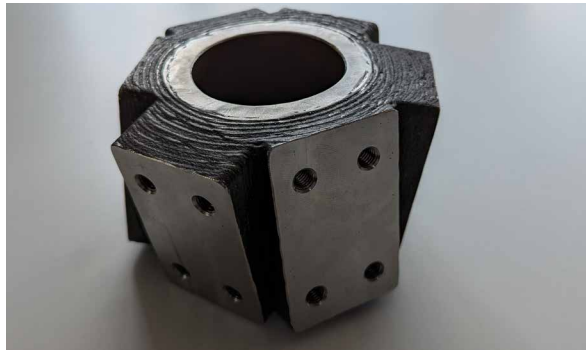


FIG. 4.20 DED-L node after substrate removal, before polishing (Image by author)

Material usage

The final weight for the DED-L node was 5,2 kg, 4,9 kg of which is calculated to be AM steel and the remainder the integrated substrate. The rest of the 130mm long cylindrical substrate can be recycled and the base plate is reusable. Unused powder is calculated from values provided in [183, 184]. Unused powder is calculated based on a powder supply efficiency of 60% powder utilization (range in [183] was 50%-66%), of which 95% is deemed reusable per [184], and the remaining 5% waste.

4.5.3.4 PBF-L node fabrication process

CAM modelling

For CAM modelling, RDesigner [185] was used for orientation and support design and CELOS [186] was used for the path planning and the printing parameters. The main steps in the CAM modelling consist of verifying the model, orienting the part, and defining the support structure. Supports can be generated automatically, but

can also be altered manually suit specific purposes. In this case, supports were placed beneath the node, inside interior cavities, and inside the connection holes. The CAM programming process took approximately 1 hour.

Substrate and printing preparation

The substrate consists of a standard plate that is placed into the machine before starting the printing process. Prior to printing, the machine is flushed with argon to protect the material from oxidation, the powder supply is replenished, the lenses are cleaned, the building plate is wiped with the re-coater, the printing environment is preheated, and the machine is calibrated. This preparation takes less than an hour.

Additive Operations

The PBF-L node was printed in SS316L. Table 4.15 outlines the main printer settings.

TABLE 4.15 Process parameters for PBF-L node additive manufacturing	
Setting	Value
Build volume dimensions	300 × 300 × 300 mm
Powder size	10 – 45 µm
Laser power (P)	Contour: 140 W; Hatch: 254 W; Support: 176 W
Hatch spacing	0.1mm
Scan speed (v)	Contour: 0.3m/s; Hatch: 1 m/s; Support: 0.5 m/s
Layer thickness (t)	50 µm
Scan strategy	Contour path and alternating adjacent layers 63,6°
Re-coater speed	150-250 mm/s
Oxygen target value	0.2%

The node is printed with an additional 0.5mm of material added in the end faces to be milled off in order to reach the tight tolerance required for a good interface with the adjoining structural profiles. This is less material than was added to the other two nodes since the geometrical fidelity of PBF-L is much better than that of the DED printing methods. The printing time was 45,25 hours. Based on the printing software, approximately 8% of this total printing time corresponds to machine movements and re-coating and 10% is printing of support structures.

Substrate and support structure removal

The part is removed from the substrate (Figure 4.21) using Electrical Discharge Machining (EDM) (Figures 4.22, 4.23). This is common practice for the removal of PBF-L parts. EDM technology uses a thin strand of metal wire and de-ionised water to cut through metal by the use of heat from electrical sparks. The EDM cutting of this part took approximately 2 hours, with the wire moving at an average speed of 1.4mm/minute across the part. Once the part is removed from the substrate, the top surface of the substrate is machined so that it can be re-used for the next application.

The design and removal of supports proved a challenging aspect of this design which resulted in the printing of several prototypes. The first prototype was printed using the “very strong” setting for supports, which were very challenging to remove manually using tweezers, a hammer, chisel, and pliers (Figure 4.24). As this proved difficult, support removal was then attempted using CNC milling, however milling the recessed areas where the support structure was nested required long, narrow end mills to be able to fit in the small recesses and also reach the required depths. The mills repeatedly broke while trying to remove the supports since they were slender, causing them to bend and eventually break. Since the support removal in this location was not critical and would be concealed by a gasket, the support removal process via milling was abandoned and leftover supports left in place (Figure 4.25).

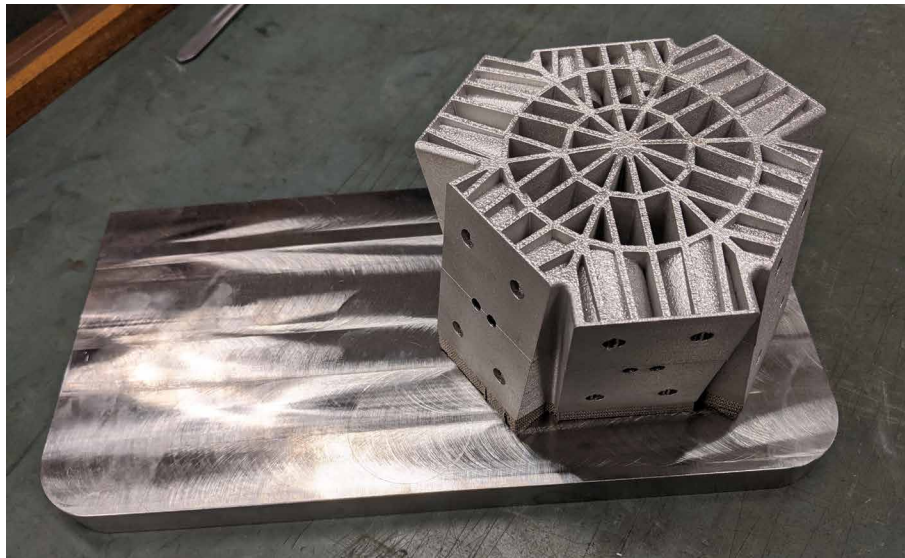


FIG. 4.21 PBF-L node on substrate (Image by author)



FIG. 4.22 EDM process on PBF-L node (Image by author)

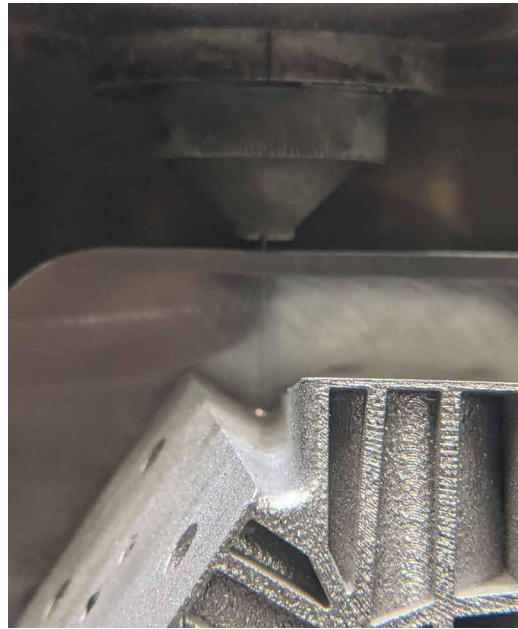


FIG. 4.23 Close-up of EDM process (Image by author)



FIG. 4.24 PBF-L node with difficult to remove support structure (Image by author)



FIG. 4.25 Leftover support structures after removal effort with CNC milling (Image by author)

Surface finishing

The surface finishing for the PBF-L node consisted of sandblasting, a process that takes less than 15 minutes per node.

End condition fabrication

The prototype was printed with integrated 6.8 mm boring holes. It is assumed for this comparative study that the surface finishing of the end faces and the drilling of the threaded holes would take the same amount of time as recorded in the DED-L node fabrication.

Material usage

The final PBF-L node weighs 4.3 kg. The additional 0.2 kg of support material can be recycled, and the substrate, a 6.9kg base plate, can be reused. Because the boring holes are provided for the threading of holes, milling waste is negligible. Unused powder for the PBF-L is node calculated from value provided in [187], and corresponds to 1% material loss due to AM equipment filtration, 2% material loss during component and machine clean-out process, and 3% material loss during sieving of the powder. The base material weight from which the percentages are calculated corresponds to a 300 x 300 x 100mm volume of powder with a density of 3.75 kg/dm³ per the material data sheet.

--- 4.6 Results and discussion

This chapter evaluates the design and fabrication of the different nodes. When interpreting the results of the fabrication time and material usage comparison, certain key aspects should be taken into consideration, some of which are outlined in Table 4.16. The size of the nodes, for example, varied. The DED-GMA node, more specifically, had twice the average arm length as the other nodes due to the design of the end conditions.

Surface roughness also varied between nodes. Figure 4.26 shows the relative surface roughness of the different nodes. The photographs show the nodes aligned with a ruler for scale running parallel to the printing orientation.

TABLE 4.16 Comparison of AM node size and surface roughness

Node	CNC	PBF-L	DED-L	DED-GMA
Node average arm length	58 mm	58 mm	58 mm	115 mm
Surface roughness	++	+	0	-



FIG. 4.26 Relative surface roughness of PBF-L node (left); DED-L node (middle); and DED-GMA node (right). (Image by author)

Additionally, while the node designs were informed by common boundary conditions and method-specific guidelines, the design process was in many instances not systematic as it was influenced by subjective preferences. This was particularly the case with the DED-GMA node, whose design was guided by the goal of having an organically-shaped, flowing aesthetic. The results of the following section, particularly the fabrication times, should therefore not be considered conclusive assessments of the relative efficiency of the AM processes, but rather as a tool for the discussion to follow.

4.6.1 Fabrication times and material usage

The final values for fabrication times and material usage for the different nodes in comparison to the CNC benchmark are summarized in Figures 4.27 and 4.28, respectively.

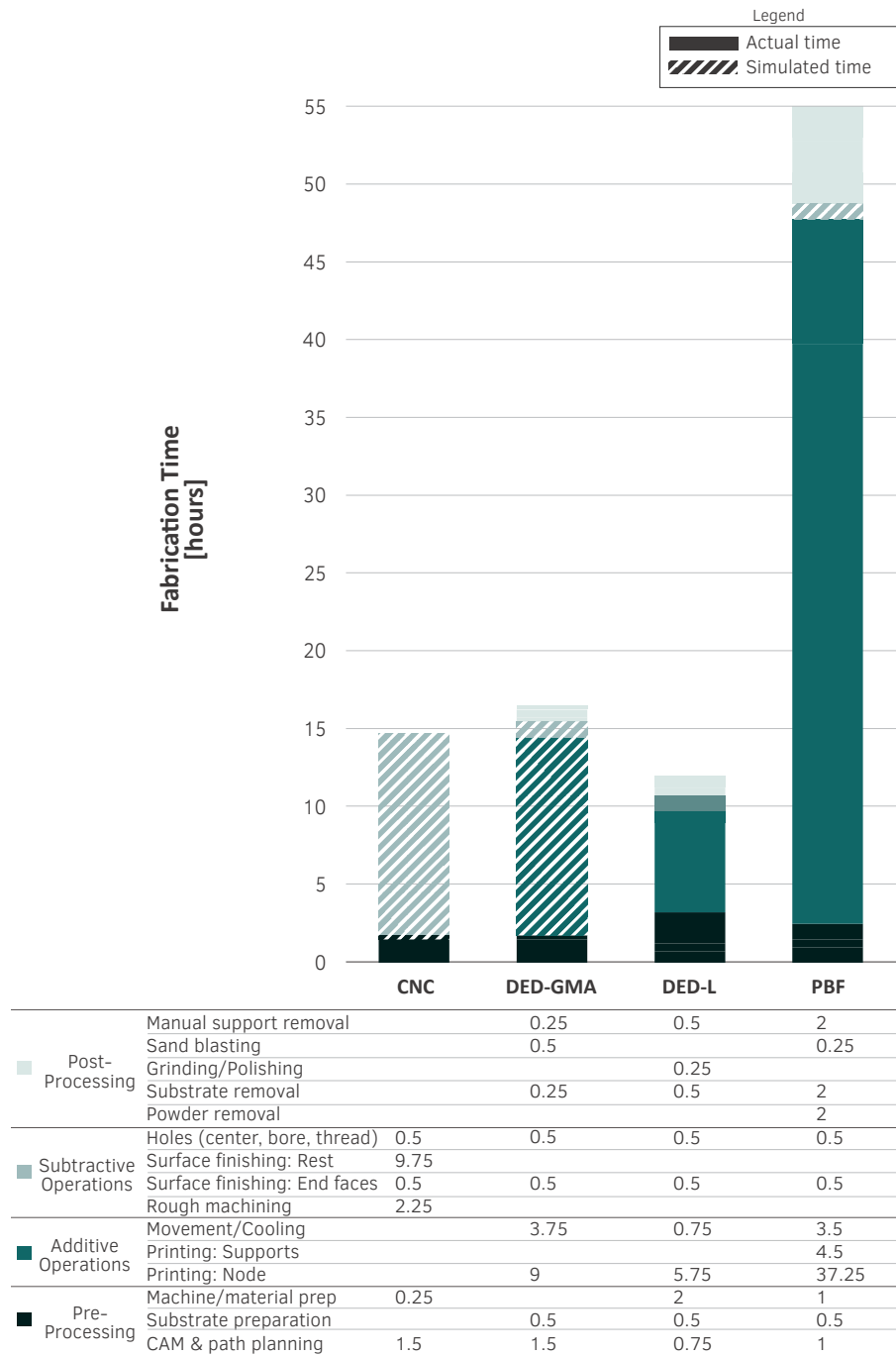


FIG. 4.27 Fabrication time comparison for different nodes (Image by author)

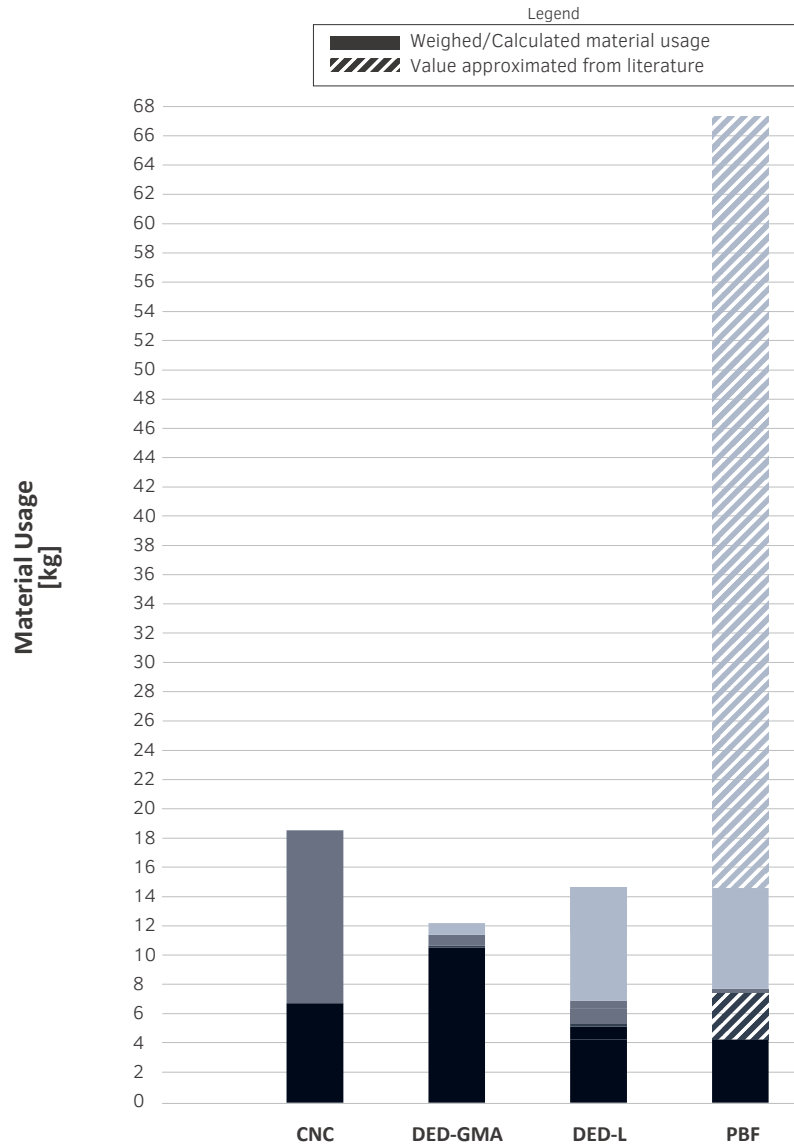


FIG. 4.28 Material usage comparison for different nodes (Image by author)

4.6.2 Reflection on the design and fabrication of nodes

The extent to which the use of AM as a fabrication method is capable of improving on the design of current construction methods is, in the context of this dissertation, measured according to 5 main metrics as outlined in Chapter 2: geometrical flexibility, design efficiency, material efficiency, fabrication efficiency, and assembly efficiency.

This section will discuss the relative material efficiency and fabrication efficiency by reflecting on the following for each of the AM nodes/methods: the strengths and limitations of the node designs in reference to their respective AM methods, according to their impact on the results, and based on experience during the design and fabrication process; the strengths and limitations of the broader fabrication methods (PBF and DED) based on the results; the identification of variables in the fabrication process that would impact the results; and the identification of system variables (profile dimensions, node configuration, etc.) that would considerably impact the results. Based on the experience as a whole, namely designing and fabricating different node using different AM technologies, a few general observation are also made, and recommendations for design of future AM structural nodes.

4.6.2.1 Reflection on the design and fabrication of the CNC node

Strengths and limitations of the proposed CNC node design

The solid CNC node is a design that, aesthetically, provides visual continuity of the profiles at intersections, resolving the geometry of the incoming profiles organically in the exposed face, resulting in a homogeneous-looking structural layer. The nodes have a smooth architectural surface to match profiles.

Its most significant limitation is that it is solid, with no options to adjust to specific parameters to the required structural loads. The size and corresponding weight of the nodes is therefore dictated mostly by overall profile dimensions, and, depending on the structure, there will be many cases where the solid nodes will be severely underutilized. The extra weight of the nodes could have significant negative ramifications on the rest of the structure, requiring reinforcement to support the unnecessary weight in the nodes.

Strengths and limitations of the CNC milling fabrication process

While the CNC node was not fabricated, a few general strengths and limitations of the CNC milling process are worth mentioning. One strength of CNC milling nodes is that the mechanical properties are predictable as they correspond to those of commercial steel products such as plates and billets.

Another advantage is the speed of the fabrication method. The CNC node/fabrication was the second fastest calculated of the fabrication processes, slightly slower than the DED-L node, and faster than the DED-GMA. However, the 9.75 hours calculated for the surface finishing of the exposed faces of the node account for approximately 75% of the total CNC milling process. This surface finishing operation is what gives a node a smooth architectural finish. If that same time to smooth the surface of the node using CNC milling would be added to the other nodes, the CNC node would have a lower relative fabrication time. As such, if a smooth architectural surface finish is required for a structural node, it is very difficult to compete with the solid milled node in terms of fabrication efficiency.

A key limitation of the use of CNC milling for structural nodes is that it is limited in terms of what it can achieve geometrically. This contributes significantly to the unnecessary weight of the nodes, as it can be difficult or impossible to remove excess material to make the node lighter. This is also limiting in terms of design, as features such as the interior structure of the DED-GMA node would not be feasible with CNC milling due to accessibility constraints.

Another notable limitation of the fabrication process is the amount of waste material that it produces. While the material can still be recycled, the environmental impact of recycling is far greater than re-use and especially than just reducing material usage altogether. There is also notably cost associated with the unused material.

Key CNC milling process variables

The relative size of the stock material is a process variable that would impact the fabrication and material efficiency of the node. In the node analysis, the dimensions of the stock material used in the simulation were actually quite conservative, with only an extra 10-13mm on each side of the nodes minimum bounding box. The resulting Buy-To-Fly (BTF) ratio was roughly 2.75, a number that rises quickly as the stock dimensions become less conservative. In a project with many nodes, a few standard billet sizes might be selected based on fitting a large number of nodes, or the stock cut from thick plates with comfortable spacing between nodes. In such cases, the

BTF ratio quickly gets significantly worse. For example, by adding only 5cm to the length and width (not the height) of the stock for the CNC node in this analysis would increase the BTF ratio to over 6.5. A high buy-to fly ratio has negative fabrication implications as it increases the intensity of roughing operations, and material implications as it produces more steel for recycling. Process variables such as changes to path planning, tools, and parameter selection for the milling operations could also have a significant impact on the efficiency of the milling process.

Key geometrical metrics and system variables for CNC milled node

The volume and the surface area of the node are two important geometrical metrics to take into consideration for the fabrication and material efficiency of the node. The size, proportions, and configuration of the profiles will impact the volume of node, which when solid nodes are concerned, defines its weight. The surface area is also important as it is directly related to the amount of surface-finishing necessary which is time-consuming. This is particularly relevant for surfaces other than end-faces which are relatively quick to finish as they are flat. The distribution of the node arms will have a significant impact on total surface area, since nodes with more evenly distributed arms will be more compact. Less evenly distributed arms will result in larger surface area of the inner and outer faces which are mostly doubly-curved, as well as of the side faces which are generally a combination of both straight and curved. To illustrate the impact these system variables can have, Figure 4.29 provides a comparison of the calculated surface area and volume of the minimum nodes for three different profile dimensions in two configurations. This comparison highlights how small changes in system variables can have a significant impact on volume and surface area.

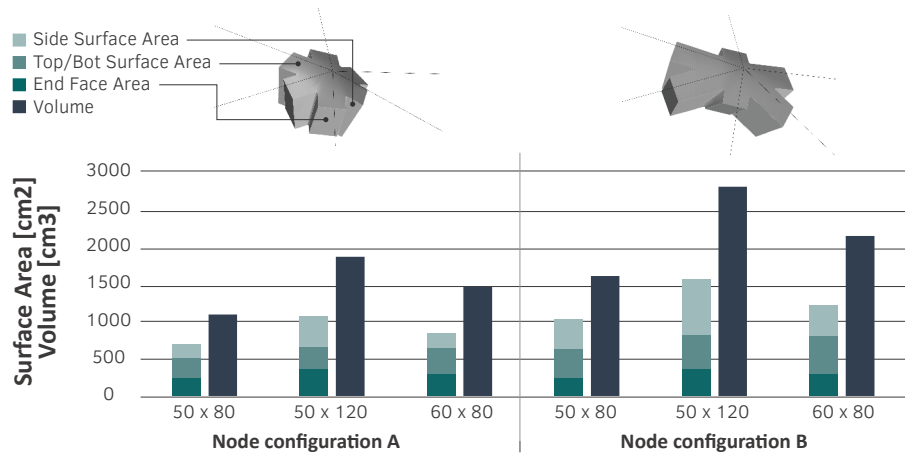


FIG. 4.29 Comparison of node surface area and volume based on different profile dimensions and node configurations showing the impact these variables can have on the weight of solid nodes and fabrication metrics related to surface area and volume (Image by author)

4.6.2.2 Reflection on the design and fabrication of DED nodes

In this study, two different DED nodes were designed using different approaches. Both designs were given the same connection detail, strove in their topology to be structurally efficient, and respected the design guidelines for DED fabrication, however the design approaches were drastically different. In the first iteration, namely the DED-GMA node, the design team strove for a more organic, flowing node design with curved plates and a more intricate topology, in a design process that was often directed by subjective design choices. In the second iteration for the DED-L node, the design approach was much more pragmatic, prioritizing ease of fabrication and path planning over other factors.

It should be noted that the main reason for the switch from DED-GMA over to DED-L between designs was to improve the transition from additive to subtractive manufacturing via a hybrid machine, a process which proved time- and cost-intensive during the first round of prototypes. While hybrid DED-GMA machines also exist, the AM fabricator that collaborated in this project for the second iteration was only equipped to fabricate nodes using DED-L, and therefore a different type of DED technology was used for the second node iteration. Ultimately, fabrication logistics and cost were significantly improved by the hybridization of additive/subtractive processes and by the simplification of the node design - not by the difference in DED technology.

Strengths and limitations of the proposed DED-GMA node design

The design for the first iteration DED node (the DED-GMA node) is the most architecturally ambitious of the four designs. It has an intricate interior structure of curved connecting plates, and the reach of the node arms is twice that of the other designs in order to expose it. Upon reflection, two major design decisions had significant negative ramifications: the end conditions and the interior structure.

The end conditions of the node were designed as gradually increasing volumes so that they could be fabricated with unidirectional path-planning to contain fabrication costs. However, as a result, a significant portion of the total weight of the node – approximately 75% – is located in the end volumes. This ultimately resulted in a node that is even heavier than a compact solid node. These end conditions also require relatively high inter-layer cooling time because of the surface area of each printed layer. This is mitigated by printing the end conditions in tandem, moving to print on the next arm as the first one cools.

An alternative end condition was explored via small prototypes, namely a flat end without the gradual increase in thickness. It is realized by depositing a layer perpendicular to the outer plates, and resuming printing along the arm direction above. This would have resulted in an overall lighter solution, but would have had a negative impact on printing time and cost. The reason for this is because the 90 degree end face would have lower cooling rates, and reachability constraints would require more complex tool path planning and execution (Figure 4.30) [188].



FIG. 4.30 End connection alternatives explored during the development of DED-GMA node: increasing thickness with simple path planning (left) and flat end face with multiple steps and orientations (right). (Image by author w/ photo courtesy of Mx3D)

The interior structure was designed to have a node that can effectively transfer all the required loads, and also to have an organic-looking form with curved features. The relative small size of the sample node, which is largely driven by profile dimensions, in combination with the intricate node topology creates particularly tight printing conditions. Such tight conditions had a number of drawbacks – intricate path planning and refined printing parameters were necessary to avoid clashes and printing defects; adjacent walls were sometimes marked with residual welding wire or welding splatter which had to be removed during post processing; and specialized tools were needed to fit and manoeuvre in such tight spaces. The size of the regular print head relative to the size of the node can be seen in Figure 4.31.

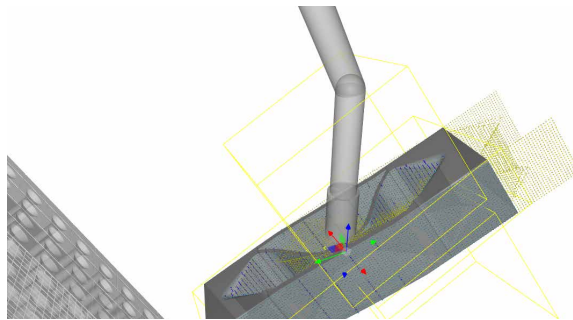


FIG. 4.31 Relative size of node arms and DED-GMA torch (Image courtesy of Mx3D)

Another limitation of the DED-GMA node design is that, since the interior structure is made of plates, the plates would need to twist to accommodate more extreme angles and geometrical configurations, thereby impeding the load-bearing capacity of the node.

Strengths and limitations of the proposed DED-L node design

By comparison, the design for the second iteration DED node (the DED-L node) is much less demanding in terms of fabrication complexity, albeit less architecturally ambitious. Upon reflection, the anatomy of nodes is quite compatible with radial printing, as the node arms effectively radiate out from the node axis.

The strategy to integrate a cylindrical substrate in the centre has a few key advantages: first, the integration of the substrate into the node reduced the amount of necessary printing time; second, the cylindrical shape of the substrate is structurally efficient as it can distribute forces across the node through membrane-action; and third, the material is concentrated towards the meeting points of adjacent arms where peak stress concentrations are, and the node is void in the centre where stresses would be lowest.

The DED-L node has 25% lower weight compared to the solid node, with further room for optimization. For example, hollowing out arms while leaving a 9mm wall thickness and 9mm distance from the bolts (which would still be conservatively dimensioned for profiles used in this study), would increase that weight reduction to 40%. A different end condition requirement could improve this number even further.

The requirement for flat end faces for the DED-L node, as with the DED-GMA node, is the root cause of material inefficiency in the node design, since the end face is more or less orthogonal to the build direction, and needs to be somehow supported during the build process. If end faces were not required for the connection, for example if the connections were to be welded, and the arms could be printed as open tubular elements, perhaps with some internal reinforcements, the material efficiency of this strategy could be excellent. At the scale of this application, even a high-percentage weight reduction in node is not significant. However, at a much larger scale this type of material efficiency could have important ramifications such as reducing the dead-load of the structure, and have the additional benefit of requiring smaller or thinner profiles.

The potential weight reduction would, of course, depend on the forces acting on the nodes, and the necessary structural dimensions. Consider as an example, a long-span freeform roof with deep hollow profiles. Such a project would necessarily have deep nodes and high bending moments, with high stress concentrations at the top and bottom flanges where compression and tension are at their highest. A solid node in this case, would likely be severely underutilized, and since the node is relatively large, the material savings that could be achieved through a node like this one would be significant, and the dead-load significantly reduced, especially in a project with a very high number of nodes.

Strengths and limitations of the DED printing process

An advantage of the DED process is that it is relatively efficient in terms of material usage as it produces limited recyclable waste, almost negligible material loss, is conducive to metal powder reuse in powder-based printing, and conducive to substrate re-use and integration when adequately considered.

Another notable strength of the DED process is its high deposition speed, which enabled fabrication times in the same range as the CNC milled node when path planning efficiency was prioritized in the node design. This deposition speed, however, when compared to the PBF node, comes at the cost of surface roughness and part tolerances. This, in turn made the use of CNC milling for the connection detail a necessity, not only to make the threaded holes, but also to ensure that the node

boundaries (i.e. the end faces) respected the tight construction tolerances typical of complex façade substructures to avoid expensive misalignments during assembly.

While it is not documented in Figure 4.27, the additional effort, logistical and otherwise, of switching machines between additive and subtractive manufacturing can be considerable if not taken into account from the beginning. This effort can be mitigated for example by having a compatible substrate for both processes and/or the same fabricator, but still requires effectively double the effort in machine preparation and calibration. The use of a hybrid machine, however, bypasses much of the additional effort, and has the added benefit that milling can also be leveraged intermittently throughout the progress of the print.

Key DED process variables

There are several variables in the DED printing process that, if modified, can have a notable impact on the results. For example, the printing parameters could be adjusted to improve surface quality, although this would come at the cost of some additional fabrication time. Similarly, the choice of a specific DED method over another would have a similar impact. It would be a worthwhile exercise to print the second node design also using DED-GMA to get a clearer picture of the relative impact of the different DED methods.

Also, as mentioned in the discussion on the CNC nodes, if the DED nodes need to have a smooth surface finish, this will require a significant increase in fabrication time. For the DED-L node, this would almost double the total fabrication time.

There is, in addition to the above, a particular aspect of DED printing that was observed as a key factor in deciding the fabrication efficiency of a structural node design: path planning. The additional degrees of freedom afforded by DED fabrication, in addition to the gamut of printing parameters, creates a network of interactions impacting mechanical properties, printing time, geometrical possibilities, etc. that are challenging to navigate while also striving for fabrication efficiency. The extent to which the complexity of path planning impacts fabrication efficiency can be seen in the relative proportions of printing time and machine movement/cooling time of the two DED node designs.

A few key facets of path planning that can have a noticeable impact on results were not mentioned in the explored literature. First is the active use of inter-layer cooling time. Necessary cooling times between layers vary based on printing parameters and also the part geometry. Good path-planning design should be mindful of the required cooling time between layers, and be configured to be operating productively as much

as possible. The geometry of the part, for example whether you are printing a single-bead wall or solid volume, will affect the cooling rate and this also needs to be considered. Fabrication efficiency can be improved by either printing multiple nodes per build, or by alternating depositing material at different areas of the node. The printing sequence should try to achieve efficient machine movements, whilst being mindful of a balanced material deposition so as to not exacerbate part deformations. DED-GMA experts at MX3D have suggested that the DED-GMA node could, at an optimal with some path planning improvement, print up to 4 or 5 nodes in tandem in only marginally more time than it takes to print a single node.

Key geometrical metrics and system variables for DED-GMA node

The design of the first DED node has a few key geometrical variables. The first is the size of the node. The scale of the nodes in this comparison, which are based on 50 x 80mm profiles, are at the lower limit of the appropriate part size for the use of DED-GMA. As previously mentioned, the node topology, in particular its intricate interior structure, resulted in a significant path planning effort to deposit the material in such a tight space. An increase in the node size, particularly its depth (via the profile depth), would create more spacious node interior, and consequently a much less restricted environment that would alleviate the complexity of manoeuvring the print head to avoid collisions.

On the other hand, the increase in profile depth would also come with two main drawbacks. The first is that, if keeping the same end condition strategy, the volume of the end conditions would drastically increase, since additional distance between the outer flanges means a proportional increase in the length of the gradually increasing end volume required to bridge the gap between them.

The second consideration is that the walls of the DED-GMA node are printed using a single-bead multi-layer strategy, and a 6mm bead width. It is likely that an increase in profile dimensions is driven by an increase in structural loads, and in any case the increase in size without a proportional increase in wall thickness would decrease the buckling capacity of the plates. In order to increase the wall thickness, there are two possible routes: the first is to increase the bead width which comes with an increase in surface roughness; the second is to change over to a multi-bead strategy, which would have a negative impact on printing time, although if paired with a decrease in bead width could improve surface quality.

Key geometrical metrics and system variables for DED-L node

The print speed and material efficiency of the DED-L node design depends heavily on the overall volume of the node, and the volume ratio between the printed material, the pipe material, and the void in the centre of the node. The structural principle of this node is that a cylindrical structural ring of solid steel of a minimum thickness is provided around the node core. In general, a reduction in the volume of printed material reduces printing time. An increase in the proportion of the pipe material in the structural ring reduces the amount of steel that needs to be printed. An increase in the proportion of the void in the node volume also reduces the weight of the node and improves its material efficiency relative to a solid node. An optimal pipe size has a diameter that takes up the majority of the node core, and a pipe thickness that consists of the majority of the structural ring. This increases the proportion of the void, and reduced the amount of material that needs to be printed.

The distribution of the node arms will impact whether the node is compact or spread out. A node whose arms distribution is relatively uneven will have a larger total volume, with a smaller core that fits a smaller pipe. A compact node on the other hand will have a smaller total volume, and also a larger core capable of fitting a larger pipe further reducing the necessary amount of printing. This is illustrated in Figure 4.32 in which two nodes with the same systemized design, due to their geometrical configuration, have drastically different volumes of printed material, and have a different maximum allowable pipe size. The difference in the amount of printing required is particularly relevant when the node arms are printed as solid volumes.

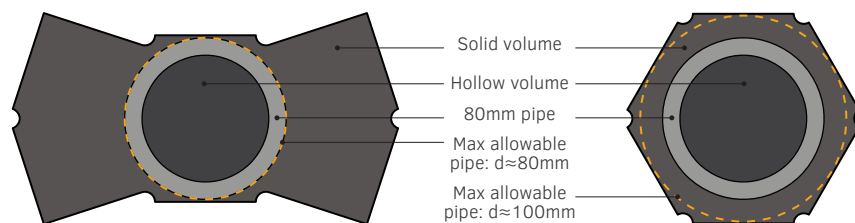


FIG. 4.32 Relative amount of solid (printing) volume vs hollow for DED-L nodes in different configurations: uneven arm distribution (left) and compact (right). (Image by author)

Strengths and limitations of the proposed PBF-L node design

The design for the PBF-L node is compatible with the printing orientation and requires few support structures. The main walls of the node, which consist of end faces, side walls, and interior reinforcements, are oriented to strike a balance between load transfer and avoiding unnecessary supports. While this configuration was sufficient for the applied loads for this analysis, this node topology is not optimal for transfer of strong-axis bending moments, for which material concentrated along inner and outer faces of the node is more effective compared to along the interior walls due to a greater moment of inertia. This could prove to be a limiting factor in the application of this particular node design in higher load scenarios. Another limitation of the PBF-L node design is that, similar to the DED-GMA node, the internal wall structure would twist as the façade angles become more extreme, thereby impeding their load-bearing capacity. Additionally, the interior wall structure has a high surface to volume ratio which means an increase in areas vulnerable to tensile and fatigue failure.

There are also a few aspects of the design that negatively impacted the fabrication process. The first was the small recesses from which support structures were challenging to remove. The design attempts to prioritize material reduction, and in doing so created a tricky situation for support removal. Future development of this node should give greater consideration to the removal of support structures. Additionally, the high surface to volume ratio also impacts fabrication because the scan speed of contour scanning is less than a third of hatch scanning, thus negatively affecting printing time. Contour scanning is used to provide a good surface finish, which is also associated with better fatigue behaviour [152, 153, 189], but is time-consuming.

Strengths and limitations of the PBF printing process

PBF-L printing has excellent surface finish compared to DED printing without requiring extensive post-processing. It is also capable of printing more intricate geometry, which would enable a PBF-L node with a different connection design to potentially not require CNC milling to meet construction tolerances. This is important since hybrid PBF-L machines are less accessible, and less capable than hybrid DED machines, hence the transfer from one fabrication setup to another should be considered in the fabrication design to minimize inconvenience. It's biggest

drawback in terms of productivity is that its build rate is much lower than DED, although significant steps are being made in the industry to improve build speeds and the industrialization of PBF printing.

Key PBF process variables

The printing time for the PBF-L node is significantly higher than all of the other fabrication options despite having only a slightly lower weight. This was expected, since PBF-L is an inherently time-intensive process. However, it should be noted that there are several process variables that have the potential to improve the fabrication time and material efficiency. Build rate is commonly attributed to specific factors including layer thickness [170, 190-192]; scan speed [190]; hatch spacing [190]; and build volume utilization [190, 191].

The modification of scan speed and layer thickness on the mechanical properties of PBF-L parts were briefly discussed in Section 4.3. [193] studied the effects of increasing the scanning speeds on the mechanical properties of SS316L and found that part density increased with scanning speed increases from 350 mm/s to 950 mm/s and then drastically reduced at 1250 mm/s (Figure 4.33). The authors note that increasing the scan speed too much does not allow for enough inter-layer fusion which drastically reduces yield strength, and that both too-high and too-low scan speeds cause internal defects such as pores, holes, and unmelted powder particles [193].

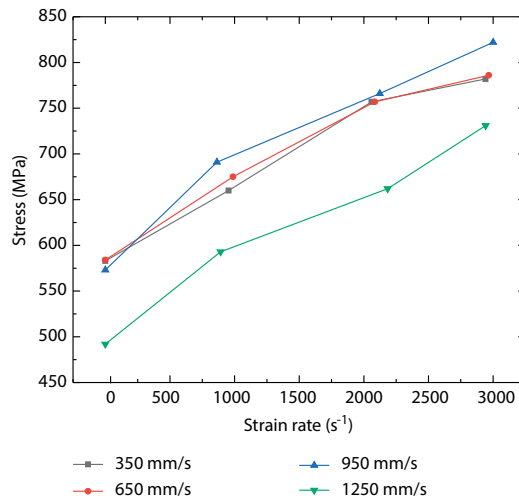


FIG. 4.33 Peak yield strength of four scanning speed specimens under different loading strain rates. (Image Source: [193])

In [170], a layer thickness increase from 30 to 50 μm reduced printing time by 58%, however it also resulted in an approximately 15% increase in surface roughness, and a roughly 270% increase in porosity which is related to the yield strength [172], tensile strength [155, 172], ductility [152, 155, 172, 192], toughness [152], and fatigue strength [153] of PBF-L parts. Increasing layer thickness was also reported to decrease ductility [155, 192]. This is particularly significant because of the minimum requirement for ductility outlined by Eurocodes, and an increase in layer thickness can result in ductility values below the minimum threshold [155]. It is worth noting that the adverse effects on the mechanical properties of the as-built part in favour of improved productivity via increase layer height or scan speed could potentially be overcome in post-processing, for example through the use of HIP [172].

The build area utilization also plays a significant role in printing productivity [173], reducing the printing time per part/volume of printed material by effectively dividing all of the inactive printing time, machine prep and maintenance amongst all of the parts in a batch. Machine preparation includes for example gas flush and preheating. Inactive printing time includes for example lowering the build plate to avoid collision between the re-coater and part, movement of the re-coater, lowering of the build platform, raising of the dispenser system, and re-coating [190]. In a study by [191] in which the fabrication time was recorded for printing 1 and 21 similar but mass-customized parts, the average printing time per node in the batch print was about 26% of the print time of the individually printed node. Batch printing also notably improves the cost-effectiveness of PBF printing, which, although not the focus of this study, is an important factor. Part height is also an impactful factor on build time, particularly for the printing of single parts [173].

Lastly, there is much development in the AM industry towards the industrialization of AM fabrication technology. Industrial PBF-L printers have a few notable qualities to improve productivity: bigger chamber sizes that can print larger parts and compound advantages of batch printing; higher powered lasers that enable increased layer thicknesses; and multiple lasers (typically 2 or 4, sometimes more) that drastically increase build rate [194]. These heavy industrial machines, according to [194], “can compete with DED systems to produce faster and bigger parts”. The PBF-L printer used for this study is considered a medium-sized machine – not an industrial one. Even so, the newest generation of the same printer is equipped with two lasers, which is quoted by the manufacturer to improve productivity by 80% up to 90 cm^3 [195]. The jump from 2 to 4 lasers in the SLM solutions product range increased (manufacturer-quoted) build rate from < 88 cm^3 to < 171 cm^3 , namely a 51% increase [194]. There is also development in other productivity increasing measures related to maintenance, machine setup, powder management, and the re-coating process [194].

All of the above considered, while the results of this study paint a very unfavourable picture of the PBF-L process, the gap in fabrication time per-node between these printing methods could be reduced significantly with batch production and more industrialized technology.

Key geometrical metrics and system variables for PBF-L node

Minimizing the node size in general can help reduce print load and maximize batch-printing potential. Smaller profile dimensions and arm distribution are important factors in keeping nodes compact. In addition to this, the support structures in this node account for roughly 10% of the total printing time. A key metric to consider to minimize support structures for PBF-L node designs in general is the footprint of the bottom face relative to the printing orientation (which for this node is aligned to the node axis). A key design variable for this metric is profile width. For nodes that are oriented with the node axis perpendicular to the build orientation, node distribution and profile depth will have a more significant impact. The decision as to how the node will be oriented in the print bed should be decided with consideration not only for the resulting support structure directly below the node, but also the resulting support structures elsewhere in the node to address overhangs, material properties, and build height, particularly in cases with low build volume utilization. The surface-to-volume ratio of the node should also be taken into consideration in order to avoid unnecessarily high fabrication times due to contour scanning.

4.6.2.4 General reflection

Comparison to the benchmark CNC-milled node

The potential for node weight reduction and the extent to which weight reduction at nodes would positively impact the structure is an important point to consider when considering the benefits of a solid CNC node versus and AM one. Where solid nodes are large and underutilized, AM nodes (and in particular DED), are more likely to be in a similar range or maybe even better than solid nodes in terms of fabrication efficiency, and are therefore a more viable alternative fabrication strategy. However, if the forces acting on the nodes are so high that the node walls and minimum thicknesses have to be increased to the point that the node density becomes too high, the resulting increase in printing load will take away the competitive edge of AM nodes. There is therefore a tipping point at which the structural parameters

of the node are sufficiently small that building a node additively is quicker than subtractively. That tipping point will depend on the node topology, fabrication parameters, and AM method.

There is also the point to consider that reducing the weight of nodes also has other benefits. Lightening the node will lighten the dead weight across the entire façades, which may, as a residual benefit, enable additional material savings by requiring smaller or thinner profiles. It could also be, depending on the size of the node, that the weight of solid CNC nodes and the weight of a lighter AM nodes are on either side of the maximum threshold weight above which workers are not allowed to lift manually. Such a weight reduction could therefore also have implication on the efficiency of assembly. These residual benefits of lighter nodes may, depending on the project, make AM a better choice, even if the fabrication is longer than the CNC node.

While this study focuses on the value of structural nodes as functional objects, it is also a necessary part of the discussion to consider structural nodes as a key part of the architectural language of the façade. In freeform steel and glass façade construction, the overall design of the envelope is generally quite expressive, and the structural nodes are exposed and visible from the inside of the building. Their design should, ideally, conform or contribute to the design intent of the overall façade.

Design intent therefore plays an important role in the assessment of whether or not the use of AM is a better choice over solid milled nodes. For example, if the design intent is to have a highly transparent, seemingly monolithic structural gridshell, and the structural nodes should therefore be rounded, compact, and have a smooth surface finish, it will be difficult for an AM node to compete with the solid CNC milled node in terms of fabrication efficiency. On the other hand, where the node design should be more expressive, and its topology more intricate, it could be the case that CNC milling as a fabrication route would be either impossible, or much less efficient.

The design of structural nodes

At the beginning of this exploration, a hypothesis was held that design efficiency could largely be maintained through the design of systemized node topologies that could be generated and eventually engineered and sized as part of parametric workflows. The design of AM nodes, however, is more involved than existing alternatives as it requires closer collaboration between node designers, engineers, and fabricators to develop a fabricable solution and explore printing parameters to achieve the right combination of mechanical properties and printing efficiency. Also, especially where maximal material/structural efficiency are required to minimize

printing time, it may be beneficial to use less conservative but more intensive engineering methods, for example using detailed FEA modelling with accurate anisotropic material properties based on comprehensive material testing, in favour of reducing printing times. This in effect increases the overall design effort despite the use of parametric design and modelling. In such cases, design efficiency can only really be achieved in future projects using pre-existing systemized node solution, since the effort required to develop and fine-tune the solution up-front is so significant.

During the node development of the structural nodes for this study, the task of the node designer was to propose a node topology based on relevant DfAM guidelines, and to refine that topology by implementing feedback from structural engineers, the façade system provider, and the AM fabricators. The nodes were developed iteratively with several rounds of feedback. During the course of the node development, there was a notable difference between the design effort for PBF and DED. PBF design guidelines are more straightforward to implement, since it is much easier as a designer to conceptualize the efficacy of a process in which both the part and the machine are always in a single orientation, building in a single direction. The fine tuning of the process parameters is then largely left to the AM fabricator. The design process for DED nodes, on the other hand, is more complicated to navigate, particularly when intricate geometry is attempted. This is because one is not only designing the node, but also simultaneously planning the printing operations and movements of the machine as well as their sequence and timing. Crucially, the node design and machine operations must be harmonized in terms of movement, orientation, spatiality, and chronological progress, in order to achieve a level of fabrication efficiency. Path planning in DED not only impacts fabrication efficiency, but also the very visible texture of the printed part.

As an additional note, when it comes to the design of nodes, it was observed over the course of this study that the anatomy of nodes is such that only certain parts of the node topology can be in an optimal orientation for printing. The favourable orientation of the node axis, end faces, top/bottom flanges, and side walls of branches can not all be printed in favourable orientation. The prioritization of one/some over the other(s) in selecting part orientation for PBF printing will dictate support structures, build proportions and mechanical properties. In DED it will require careful consideration of how the faces in the unfavoured orientation will be realized: either by gradual increments respecting overhang limitations (generally at the cost of material efficiency), printing solid volumes, or addressed with careful path planning. In PBF, it will impact the need for support structures.

4.6.3 Recommendations

Based on the results and the discussion, the following are offered as recommendations for the design of structural nodes in the future

General recommendations

- Requirements for connections should be carefully considered in the selection of an AM method, as it will influence whether and the extent to which machining will be necessary in post-processing.
- The size of structural nodes (as it relates to both the dimensions of the base profiles and their geometrical configuration) should be taken into consideration in the selection of a fabrication method and the design of the node topology in order to maximise fabrication efficiency.
- The connection design and the primary structural actions acting on nodes for a given project, should be taken into consideration when defining which parts of the node anatomy will be prioritized for favourable printing orientation.
- The design of systemized nodes should consider closely the structural behaviour of node topologies at different geometrical configurations, including the effectiveness of load transfer in more extreme geometrical conditions.

Recommendations for the design and fabrication of DED nodes

- DED fabricators should be involved early in the design process of structural nodes, particularly when more complex geometry is desired.
- The integration of hybrid and subtractive additive manufacturing goes a long way in improving overall fabrication efficiency.
- The anatomy of nodes is well suited to a radial printing strategy for DED AM methods, particularly if no end faces are needed.
- Considerable fabrication time can be saved by utilizing inter-layer cooling time for active printing elsewhere. The fabrication strategy should consider printing multiple objects, or multiple facets of a single object, in tandem to reduce total fabrication time.
- Path planning with clean, simple, machine movements that avoids impediments such as tight spaces should be seen as a driving force, integral to the design of the DED node topology rather than an elective advantage.

Recommendations for the design and fabrication of PBF nodes

- In order for PBF printing to be competitive in terms of fabrication efficiency, the following facets of production should be considered:
 - PBF technology suited for industrial production should be used, and it should be leveraged to print structural nodes in batches.
 - Printing parameters (primarily layer thickness, scan speed, and hatch spacing) should be selected to maximize build rate while still achieving the required level of mechanical properties.
 - The design of the node should minimize material usage as best as possible, including support structures.

4.7 Conclusion

This chapter aimed to explore the extent to which AM could be leveraged to improve structural node solutions compared to current fabrication methods. A solid CNC node is used as a benchmark for comparison. The quality of design is defined in five terms: design efficiency, geometrical flexibility, fabrication efficiency, assembly efficiency, and material efficiency. “Improvement” in this context is defined as the following: maintaining design efficiency through the systemization of the node design, maintaining geometrical flexibility through the design of a node topology which can be adapted to a range of configurations; improving fabrication efficiency through a reduction of overall fabrication time; maintaining assembly efficiency through the integration of standardized mechanical connections; and improving material efficiency through a reduction in materials usage in the end node, and as by-products of the fabrication process.

In order to this, some background information was first provided. This included an overview of the 7 main families of metal AM methods, including variations within the families of methods. A subset of 3 different metal AM methods (DED-GMA, DED-L and PBF-L) were selected for more in depth analysis. Subsequently, an overview of the mechanical properties of AM SS316L printed using DED-GMA, DED-L and PBF-L was provided and compared to Eurocode requirements and benchmark material values as a means of establishing the extent to which AM materials are suitable for construction. Ultimately, SS316L was able to meet all material requirements for which studies were available, however the reported values varied significantly both across and within the different AM methods stressing the importance of printing parameters and post-processing operations in the design of structural parts. Finally, an overview of key AM guidelines which informed the design of the structural nodes in the second half of the chapter was provided.

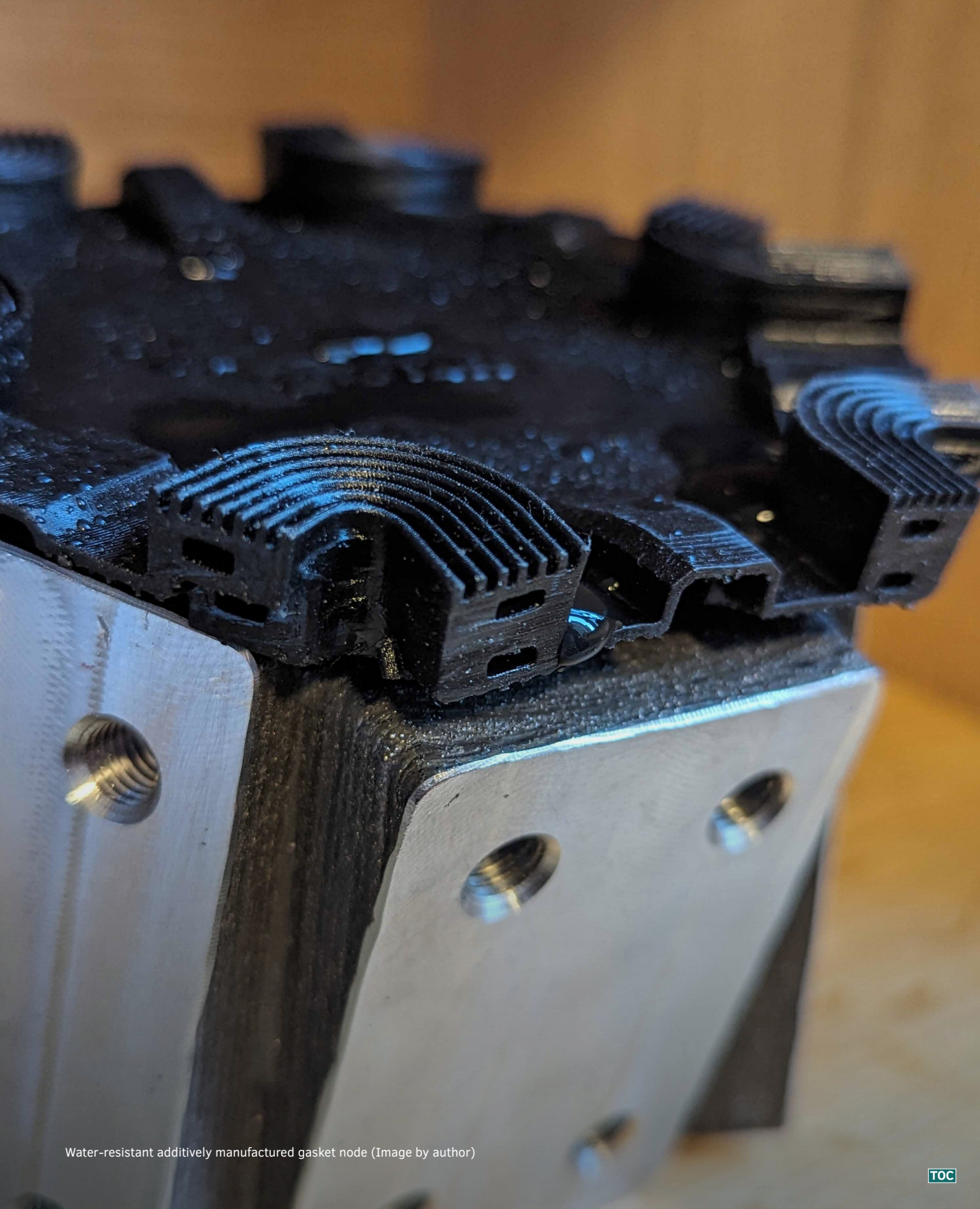
The second half of the chapter focused on the design, fabrication, and analysis of AM structural nodes. 3 different AM nodes based on each of the three printing methods were designed, fabricated, and their material efficiency and fabrication efficiency analysed. Each of the designed nodes had notable strengths and weaknesses which were reflected upon in the discussion. Strengths and limitations of the fabrication process and strategy were also discussed, and the key geometric characteristics that would impact results were identified. Another round of design and printing process refinement would likely improve the results, which already show that AM nodes have the potential to be a good alternative to the solid node under the right set of circumstances. Recommendations for the design of future AM nodes are also provided. Ultimately, whether or not and the extent to which AM is a more appropriate choice than other, more traditional structural node solutions, was found to depend on several key factors.

The efficacy of additive manufacturing can only be as good as the design of the nodes it is used to fabricate. Structural nodes should be designed mindfully to their specific AM method using DfAM guidelines and feedback from AM fabricators. This chapter provides some recommendations for AM structural node design. In addition to compatibility with the AM method, the node design should also be compatible with specific aspects of the project, since material usage and fabrication efficiency will likely be impacted by geometric characteristics such as the size and compactness of the node, which are in turn impacted by specific aspects of the overall façade design such as the type of rationalization, the profile geometry, and dimensions.

The potential for node weight reduction in structural nodes is an important aspect to consider when AM nodes are being considered as an alternative to solid CNC nodes. AM, and in particular DED, can provide an option to improve on fabrication times, particularly where nodes are large and underutilized. Node weight reduction may also enable lighter profiles, and have a positive impact on assembly, benefits which may perhaps outweigh the importance fabrication times. When using AM, node volume reduction is a key factor in mitigating printing times, but care needs to be taken that reducing the volume of printed material by defining more structurally optimal topologies is not negated by an increase in fabrication time due to increased complexity of path planning, support structure removal, or other facets of fabrication.

The design intent of the node is another aspect of node design that plays a part in the suitability of AM as the best route for structural node fabrication. Although this particular study focused more on the practical aspects of structural nodes, the value of design expression and the specific design intent of a project should not be overlooked.

Developing AM structural nodes that are consistent with the design intent of the architect and efficient in terms of structural behaviour, material use, and fabrication intensity, requires close collaboration between the designer, structural engineer, and AM fabricator. Ultimately, the extent to which AM nodes can improve on the fabrication and material efficiency of CNC-milled nodes depends on the suitability of the node design for the geometrical and structural requirements of the project as well as the selected AM method and the corresponding fabrication strategy. Because of this, the design process for AM structural nodes can be quite intensive.



Water-resistant additively manufactured gasket node (Image by author)

5 Additive Manufacturing for Gasket Nodes

Materials, methods, and proof of concept

In Chapter 2, it was identified that current construction strategies consistently leverage digital fabrication methods for structural nodes but not for gasket nodes. It was also identified that current gasket node solutions are limited by their ability to integrate specific functional features. In Chapter 3, it was highlighted that there is no evidence of a precedent for additively manufactured gaskets for façades in the existing body of scientific research.

This chapter undertakes the design and prototyping of an additively manufactured gasket node. First, AM materials databases are explored in order to identify potentially suitable AM materials based on standards for gasket components. Following this, two rounds of prototyping are conducted, the first exploring several different potential AM methods and their ability to integrate geometrical features likely to be present in node gaskets, and the second integrating all of the functional features identified in Chapter 2.

5.1 Introduction

The interior gasket layer is a crucial component for steel façade systems. This layer has several key functions: it allows relative movement of the façade assembly; distributes and absorbs loads; accommodates geometrical and building tolerances; prevents contact between the metal back-up structure and glazing unit to prevent glass breakage; provides continuity of the thermal barrier; and provides a back-up drainage plane. In most dry glazed systems, while the exterior gasket provides a reasonably water-tight seal, the interior gasket drains the water that permeates the exterior seal as well as any condensation that builds up within the assembly. It also maintains the air-tight seal around panel units. In most wet-glazed systems, the interior drainage layer is optional, however it is highly recommended as it provides redundancy for the air- and water-control system of the façade.

As discussed in Chapter 2, current practices for addressing node conditions for the interior drainage layer are generally either labour-intensive on-site, geometrically inadequate to provide a proper seal in geometrically complex and/or unique conditions, or a combination thereof.

The use of AM node gaskets as a means for providing a high-performance, mass-customizable, easy-to-assemble solution for freeform construction is either extremely uncommon, or entirely innovative. The use of AM for interior drainage could allow a number of key advantages. Similar to the structural nodes, connections can be standardized to reduce the need for complex on-site labour. While this is also possible using multi-axis injection moulded gaskets, these require the production of repetitive gaskets to be time- and cost-effective. Such repetition of geometrical conditions is typically rare in freeform applications, and mostly suited to geometrically optimal scenarios.

This chapter aims to explore the suitability of AM for mass-customized gasket nodes. In Section 5.2, benchmark material requirements are identified from standards. Then, material data is collected from commercial AM materials relevant to gasket applications and compared to benchmark values. Potentially suitable materials are identified by searching the Senvol Material Database [146] as well as the technical data sheets available online from a number of major AM service providers including: Materialise; Proto Labs; Shapeways; Sculpteo; Spectroplast; and xometry [196–201]. Material selection is narrowed based on: the proximity of the available material data to the requirements outlined in standard ASTM C864-05; the suitability of the material for architectural gaskets; and on having a range of materials utilizing

different AM technologies. For the final selection of four materials, the printing properties are outlined, and the material properties tabulated for comparison with benchmark values. In Section 5.3, the printing methods relevant to these materials are outlined and expanded upon.

In Section 5.4, two rounds of AM prototypes are produced. In the first prototyping round, a sample gasket is printed in each of the four materials and methods outlined in the previous sections in order to compare the quality of the different printing technologies. The benchmark gasket model incorporates a number of geometrical features that are helpful for nodal gaskets. In the second prototyping round, a gasket design that incorporates all of the functional features identified in the precedents review from Chapter 2 is designed and printed. The resulting gasket node is compared to existing solutions.

5.2 Materials for AM gaskets

5.2.1 Performance requirements for gaskets

Requirements per EN 13830: Curtain walling – Product standard

Eurocode requirements related to façade gaskets are based primarily on the classification of functional properties of the façade assembly, and specific requirements for individual components. The main standard for curtain wall construction is EN 13830 [202], which outlines the different functional characteristics of curtain-wall constructions, and includes a systematic framework of requirements, test methods and compliance criteria. For requirements related to gaskets and weatherstrippings specifically, this document refers to standards EN 12365-1 and 12365-4 for the durability of watertightness. The following assembly-related characteristics are also noted as being affected (or possibly affected) by changes to the number, material, and shape of gaskets [202]:

- Fire resistance
- Fire propagation (to upper levels)
- Watertightness
- Direct airborne sound insulation
- Flanking sound transmission
- Thermal transmittance
- Air permeability
- Durability of watertightness
- Durability of thermal transmittance
- Durability of air permeability

Requirements per EN 12365-1: Building hardware - Gasket and weatherstripping for doors, windows, shutters and curtain walling - Part 1: Performance requirements and classification

EN 12365-1 [203] outlines the main performance and classification requirements for gaskets and weatherstripping. This standard is applicable for gaskets and weatherstripping of doors, windows, as well as curtain-walls. Table 5.1 is a summary of the classification requirements for gaskets per EN 12365-1. In addition to the classification, the standard outlines the following requirements:

- “Gaskets and weatherstripping shall complement the tolerances of the construction materials and the products in which they are to be used, e.g. timber, PVC-U, metal, etc, and the manufacturing process and any variations in gaps caused by loads on the product.” [203]
- “The materials shall be physically and chemically compatible with the contact surfaces of the product and be completely suited to the climatic and environmental conditions of use.” [203]
- “Gaskets and weatherstripping shall sustain the mechanical stress induced in normal use, as considered in the design, e.g. tilt, turn or slide. Consideration should also be given to the frequency of use in such an application.” [203]
- “Gaskets and weatherstripping shall not impair the designed operation of the products, e.g. weatherstripping shall not produce excessive operating forces and gaskets shall not allow infillings to vibrate. During operation they shall reduce the effects of slamming or other undue strains.” [203]

TABLE 5.1 Classification requirements for gaskets per EN 12365-1 [203]

Category	Description	Grades	Standard
Category of use		type G: gasket; type W: weatherstripping.	-
Working range	Distance through which a gasket or weatherstripping can be compressed or deflected when used in an assembly	$\leq 1 \text{ mm}$; $> 1 \text{ mm} \leq 2 \text{ mm}$; $> 2 \text{ mm} \leq 4 \text{ mm}$; $> 4 \text{ mm} \leq 6 \text{ mm}$; $> 6 \text{ mm} \leq 8 \text{ mm}$; $> 8 \text{ mm} \leq 10 \text{ mm}$; $> 10 \text{ mm} \leq 15 \text{ mm}$; $> 15 \text{ mm} \leq 30 \text{ mm}$; $> 30 \text{ mm}$.	-
Linear compression force	Force needed to deflect a specimen to its maximum working range, at a temperature of $23^\circ\text{C} \pm 2^\circ\text{C}$	$\leq 10 \text{ N/m}$; $> 10 \text{ N/m} \leq 20 \text{ N/m}$; $> 20 \text{ N/m} \leq 50 \text{ N/m}$; $> 50 \text{ N/m} \leq 100 \text{ N/m}$; $> 100 \text{ N/m} \leq 200 \text{ N/m}$; $> 200 \text{ N/m} \leq 500 \text{ N/m}$; $> 500 \text{ N/m} \leq 700 \text{ N/m}$; $> 700 \text{ N/m} \leq 1\,000 \text{ N/m}$; $> 1\,000 \text{ N/m}$.	EN 12365-2
Working temperature range	Condition range within which the gasket or weatherstripping is considered to be capable of performing	0°C to $+45^\circ\text{C}$; -10°C to $+55^\circ\text{C}$; -20°C to $+85^\circ\text{C}$; -25°C to $+100^\circ\text{C}$; -40°C to $+70^\circ\text{C}$; 0°C to $+200^\circ\text{C}$.	-
Deflection recovery	Ability of a gasket or weatherstripping to recover its free height after being compressed or deflected	no performance requirement; $> 30\%$ to 40% ; $> 40\%$ to 50% ; $> 50\%$ to 60% ; $> 60\%$ to 70% ; $> 70\%$ to 80% ; $> 80\%$ to 90% ; $> 90\%$.	EN 12365-3
Recovery after aging	Long-term material performance for gaskets and weatherstrippings	no performance requirement; $> 30\%$ to 40% ; $> 40\%$ to 50% ; $> 50\%$ to 60% ; $> 60\%$ to 70% ; $> 70\%$ to 80% ; $> 80\%$ to 90% ; $> 90\%$.	EN 12365-4

Requirements per ASTM C864-05

The assembly-based requirements in the Eurocode standards are not particularly suitable metrics for a preliminary exploration of potentially suitable AM materials for gasket applications. In order to identify benchmark material requirements for the preliminary assessment of potential gasket materials, standard ASTM C864-05 Standard Specification for Dense Elastomeric Compression Seal Gaskets, Setting Blocks, and Spacers [204] is used. Requirements for elastomeric compression seal gaskets from this standard are summarized in Table 5.2 and based on shore hardness of the material.

TABLE 5.2 Elastomeric compression seal gaskets and accessories physical requirements per ASTM C864-05 [204]

Properties	Requirements						ASTM Test Method
Hardness, nominal Shore A durometer± 5, as specified by the purchaser	40	50	60	70	80	90	D2240
Compression set, 22 h @ 100°C, max [%]	35	30	30	30	35	40	D395
Ozone resistance, 100 mPa, 100 h @ 40°C, 20 % elongation	← no cracks →						D1149 (Specimen A)
Tensile strength, min [MPa]	10.3	10.3	11.0	12.4	12.4	12.4	D412, Die C
Elongation at rupture, min [%]	400	300	250	200	175	125	D412, Die C
Heat aging, 70 h, 100°C:							D573
Hardness increase, max durometer points	10	10	10	10	10	10	
Change in tensile strength, max [%]	15	15	15	15	15	15	
Change in elongation, max [%]	40	40	40	40	40	40	
Tear strength, min [kN/m]	26.3	26.3	26.3	17.5	17.5	13.1	D624, Die C
Brittleness temperature, max [°C]	−40	−40	−40	−40	−40	−40	D746
Nonstaining	← no migratory stain →						D925
Flame propagation							C1166
Option I	← 100 mm (4 in.) max. →						
Option II	← no limit						

5.2.2 AM elastomeric materials

Several potentially suitable materials were uncovered during the materials search. Table 5.3 outlines the printing-related data for four such materials. Table 5.4 outlines the mechanical properties of these materials reported in supplier technical data sheets.

TABLE 5.3 Summary of selection of AM elastomeric materials

	Material 1	Material 2	Material 3	Material 4
Material family	Silicone	Silicone	Elastomeric Polyurethane (EPU)	Thermoplastic Polyurethane (TPU)
Material commercial name	TrueSil A60	ACEO Silicone GP Shore A 60	EPU 40/41	TPU-70A
Material provider	Spectroplast	Wacker Chemie	Carbon 3D	Prodways
AM method family	Vat Polymerization	Material Jetting	Vat Polymerization	Powder Bed Fusion
Specific AM technology	Silicone Additive Manufacturing	Drop on Demand	Digital Light Synthesis	Selective Laser Sintering
Prototype printing service provider	Spectroplast	ACEO Imagine	Sculpteo	Protolabs
Build platform dimensions	75 x 130 x 130mm	480 x 480 x 300mm	141 x 79 x 326 mm - 400 x 250 x 460 mm	269 x 304 x 406mm
Minimum wall thickness	0.3 - 0.5mm	1 mm	2.5 mm	0.762 mm
Applications	"Industrial application, e.g. sealing elements, dampers, gaskets, etc"	"automotive, aerospace, medical and many other applications"	"gaskets, grommets, and flexible watertight seals"	"seals, gaskets, grips, hoses, or any other application where excellent resistance under dynamic loading is required"
References	[205, 206]	[207-209]	[210-213]	[214-216]

TABLE 5.4 Material properties of AM elastomeric materials

	Material 1: Spectroplast TrueSil A60	Material 2: ACEO Silicone GP Shore A 60	Material 3: Carbon DLS EPU 40/41	Material 4: Prodways TPU-70A
Shore A Hardness	60 (ISO 7619-1)	60 (ISO 7619-1)	72 / 72 (D2240)	70 (standard not specified)
Compression set [%]	< 20 (DIN ISO 815- 1 Type B)	< 20 (DIN ISO 815- 1 Type B)	~ 55 / 65 (D395-B, 72 h @ 70°C)	not available
Ozone resistance	not available	not available	not available	not available
Tensile strength [MPa]	9.1 (ISO 37 Type 4)	7 (ISO 37 Type 1)	19/ 15 (ASTM D412-C)	6 - 12 (DIN 53504)
Elongation at rupture [%]	270 (ISO 37 Type 4)	200 (ISO 37 Type 1)	400/ 300 (ASTM D412-C)	<300 (DIN 53504)
Heat aging: Hardness increase	not available	not available	not available	not available
Heat aging: Change in tensile strength	not available	not available	not available	not available
Heat aging: Change in elongation	not available	not available	not available	not available
Tear strength	13.5 MPa (ASTM D624 C)	> 15 MPa / > 5 MPa (ASTM D624 C/DIN ISO 34-1-A)	25 kN/m / 20 kN/m (ASTM D624 C)	not available
Brittleness temperature	Service temp: - 30 °C to 180 °C	Service temp: - 55 °C to 180 °C	not available	not available
Nonstaining	not available	not available	not available	not available
Flame propagation: Opt I	not available	not available	not available	not available
Flame propagation: Opt II	not available	not available	not available	not available
Precision Tolerance	± 0.2 mm (DIN ISO 2768-1 m, 6-30mm)	± 1.0 mm (DIN ISO 2768-1 v, 6-30mm)	±75 µm + 10 µm/ mm	±0.25mm plus 0.1% of nominal length
Color	unspecified, black possible	various colors incl. black	black	white
References	[205, 206]	[207-209]	[210-213]	[214-216]

5.3 Printing methods for AM gasket nodes

The materials presented in Tables 5.3 and 5.4 are produced using four different AM printing methods. This section provides an overview of these methods.

Vat polymerization

Vat polymerization (VP) is a family of additive manufacturing processes “in which liquid photopolymer in a vat is selectively cured by light-activated polymerization” [20]. This family of AM methods encompasses different technologies. Amongst these variations, VP technologies can either be top-down or bottom-up production. Two different versions of VP were tried for this exploration and expanded upon below, namely Silicone Additive Manufacturing (SAM) by Spectroplast, and Digital Light Synthesis (DLS) by Carbon 3D.

SAM is the proprietary form of polymerization by Spectroplast which is used for one of the selected materials, namely Spectroplast TrueSil A60. In SAM, a thin layer of photopolymer is spread on the print-bed (Figure 5.1), and the substrate operated from above the print-bed is lowered onto the layer of photopolymer. A projector below the print bed selectively cures the photopolymer. The substrate is lifted, and the process repeated layer-by-layer.



FIG. 5.1 Silicone additive manufacturing technology by Spectroplast. (Image Source:[217])

Digital Light Synthesis is a proprietary AM process by Carbon 3D that is based on a Continuous Liquid Interface Production (CLIP) process, which was used to print EPU 40/41. The CLIP process projects light through an oxygen-permeable window into a photopolymer-filled vat (Figure 5.2). Compared to other vat polymerization printing methods which build one layer at a time, in this process, the movement of the build platform, the projection of a smooth sequence of UV images, and the solidification of the photopolymer take place concurrently [218]. The result of this continuous printing technology is parts with exceptionally smooth surface finish, instead of the stepped surface finish inherent to many other printing methods. The surface resolution is dependent on the pixelation of the projection.

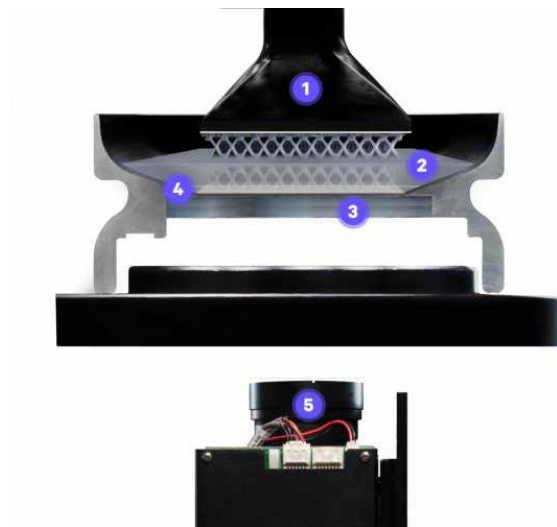


FIG. 5.2 Digital light synthesis printing technology by Carbon 3D.(Image Source:[219])

Material jetting

Material Jetting (MJ) is an AM process “in which droplets of build material are selectively deposited” [20]. In this process, similar to the VP processes, MJ printing deposits a photopolymer which is subsequently cured with UV radiation. Drop on Demand printing by ACEO (Figure 5.3) is a proprietary version of MJ printing technology that was used to print ACEO Silicone GP Shore A 60. This technology allows one to potentially print multi-material parts and relies on soluble support material to print overhangs [220].

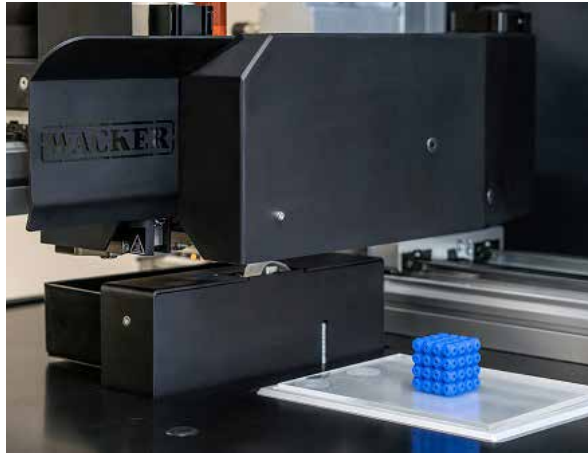


FIG. 5.3 Drop on demand technology by ACEO. (Image Source:[221])

Powder bed fusion

Power Bed Fusion (PBF) is a process in which “an additive manufacturing process in which thermal energy selectively fuses regions of a powder bed” [20]. This process, which was also employed in Chapter 4 for the printing of metal parts, can also be used for printing gaskets. In this case, the powder is nylon-based Thermoplastic Polyurethane (TPU). Unlike metal-based PBF printing, support structures for small overhangs may not be necessary as the powder provides some support, and the non-metal parts do not require a heat-sink. Once printed, the parts are broken from the printing bed substrate, brushed to remove powder, and bead blasted [222].

5.4 Design, fabrication and analysis of gasket nodes

5.4.1 Preliminary prototypes

In order to validate the ability of the printing methods to print node gasket geometry and do a preliminary check on part quality, a small benchmark gasket prototype for a 4-armed node was printed in each of the AM elastomeric materials/methods. The sample gasket model integrates a number of features helpful for the production of node gaskets in general, which are outlined in Table 5.5. In addition to the mechanical properties of the gasket material, these geometrical properties are helpful to ensure the proper functioning of the gasket:

TABLE 5.5 Benchmark features for design and fabrication of AM gaskets

Overhanging lips	Gaskets are generally outfitted with either overhanging lips or rows of small blades. These incorporated features are what prevent water infiltration [17].
Gasket base with thin, low overhangs	Thin, low overhangs are required to print the base of the gasket to conform to the outer face of the structural node.
Cross-sectional changes	Cross-sectional changes in the crown of the gasket allows the gaskets to adapt to the space between the glass and structural node.
Continuous channels	Continuous channels in the crown help to maintain a compressive seal through deformation of the cross-section.
Recessed cap	The recessed cap in the center of the node is helpful to locate and fix the node in place relative to the structural node to help facilitate installation.
Fine features	Fine features in the gasket node such as filleted edges with small radii and sharp edges allow the node gasket to match the shape of the incoming gasket profiles.

The prototypes were printed in the materials, using the methods and AM service providers outlined in Table 5.3. Each of the printed samples (Figures 5.4 - 5.7) was able to achieve these features to a satisfactory degree, “free of porosity, surface defects, and dimensional irregularities that may affect serviceability” according to the outlined requirements.



FIG. 5.4 Gasket prototype printed in EPU 40 by Sculpteo using digital light synthesis printing technology. (Image by author)

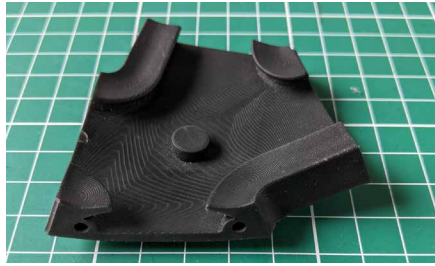
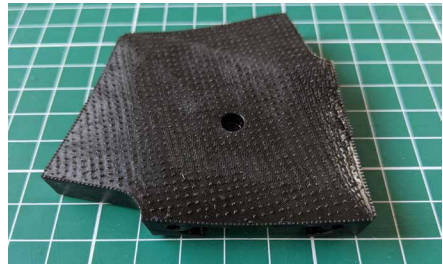


FIG. 5.5 Gasket prototype printed in True Silicone A60 by Spectroplast using silicone additive manufacturing technology. (Image by author)

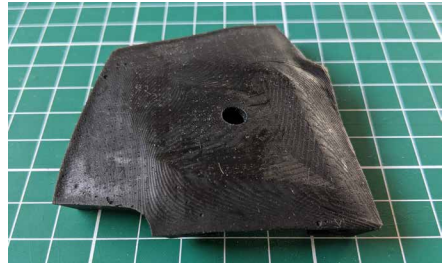


FIG. 5.6 Gasket prototype printed in Silicone GP Shore A 60 by ACEO using drop on demand printing technology. (Image by author)

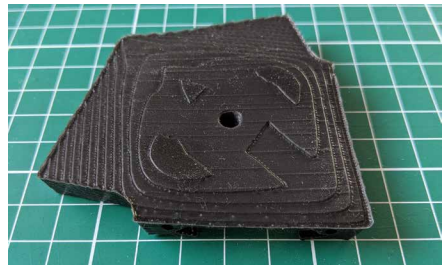


FIG. 5.7 Gasket prototype printed in TPU-70A by Protolabs using powder bed fusion printing technology. (Image by author)

5.4.2 Final gasket node prototype

A version of the gasket prototype from the previous section was printed and mounted in a preliminary mock-up (Figure 5.8). After this initial mock-up, a few other features were integrated into the node design (Figure 5.9). First, the end conditions of the gasket node were partially extended to have a lapped connection with the incoming gasket profiles, improving the interface between the gasket node and incoming profiles. Second, a node identifier was integrated directly into the node gasket to identify to which structural node it corresponds. Third, a triangular protrusion was also integrated to fix the gasket in place and identify its correct orientation since this can be unclear, and if installed incorrectly, would negatively impact performance. Lastly, the base gasket profiles for the parametric generation of the gasket node were changed to a hierarchical profile system.



FIG. 5.8 First gasket design installed in a mock-up (Image courtesy of Jansen AG)



FIG. 5.9 Final node gasket prototype design (Image by author)

A driving force behind the use of AM for gasket nodes is the ability to fabricate them as mass-customized parts compatible with the mass-customized structural nodes. As such, the modelling of node gaskets was integrated into the same digital workflow as the structural nodes and the rest of the mass-customized components. This digital workflow is described in Chapter 6. The following is a brief description of the logic for the parametric generation of the gasket models.

In order to minimize the amount of printing necessary for both the structural node and the gasket node, the minimum arm length is calculated for each component. The gasket node arms may be shorter or longer than the structural node arms depending on the geometrical configuration of the node and whether it is convex or concave. Figure 5.10 depicts the minimum arm lengths of a sample structural and gasket node. This also affects the design of the structural nodes, since where the gasket node arm is shorter, the structural node arm must maintain a planar surface beneath the extruded gasket profiles. The bottom surface of the node gasket is congruent with the outer face of the structural node. The gasket base is a 2mm thick offset from the node surface. The crown of the gasket is configured in such a way that the outer face is aligned with the glazing plane, and the depth of the crown varies to bridge the gap between the glazing plane and the structural node (Figure 5.11). This completes the base geometry of the node. After this, the triangular protrusion and node identifier are integrated based on the corresponding structural node identifier and orientation. The standard end-conditions are then added to the node end faces based on the hierarchical incoming profiles. A final node prototype integrating functional features as outlined in Figure 5.12 was printed (Figures 5.13-5.15) for final validation.

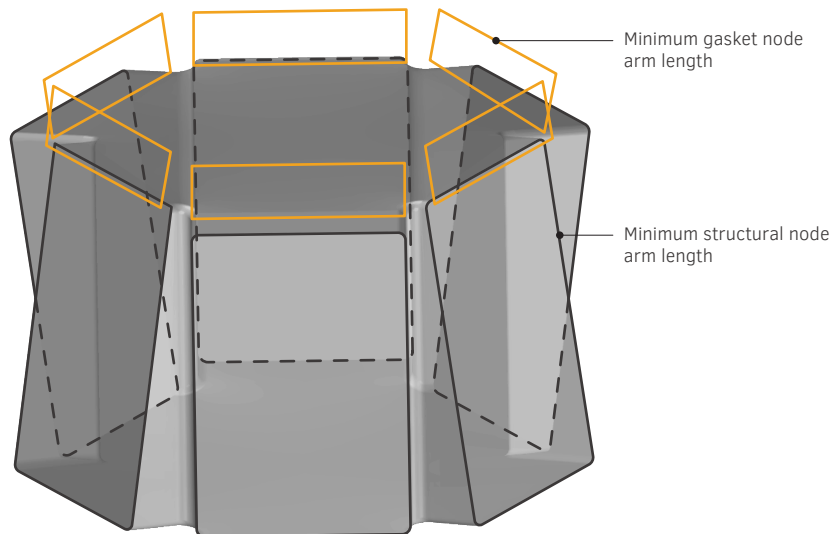


FIG. 5.10 Base geometry for gasket node modelling. (Image by author)

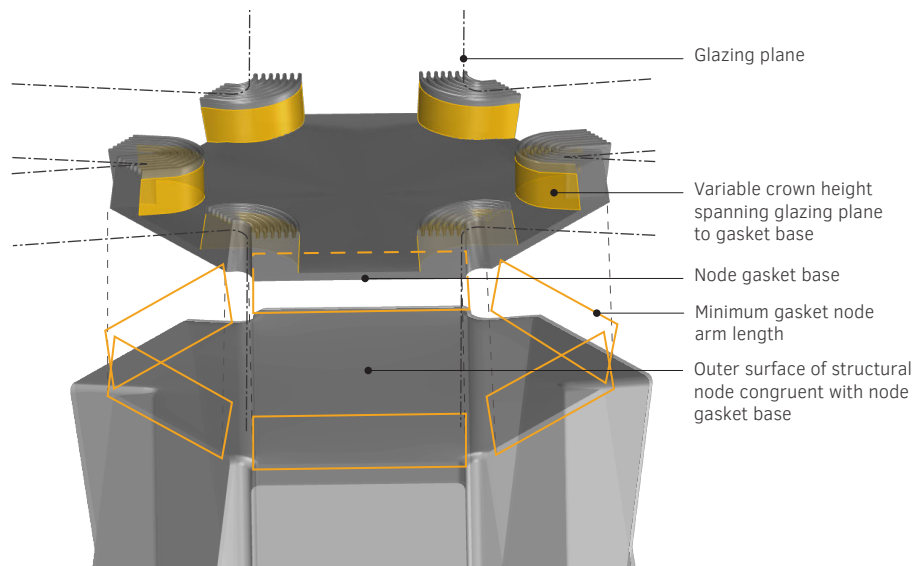


FIG. 5.11 Modelling of gasket crown with variable cross-section spanning space between base and glazing plane. (Image by author)

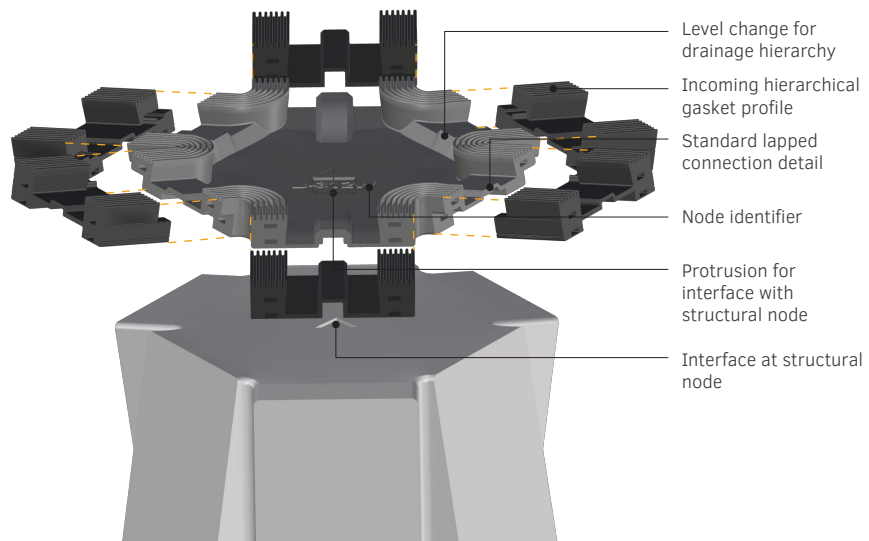


FIG. 5.12 Proposed gasket node design and functional features showing interfaces with structural node and incoming gasket profiles (Image by author)



FIG. 5.13 Top view of printed AM gasket node prototype (Image by author)

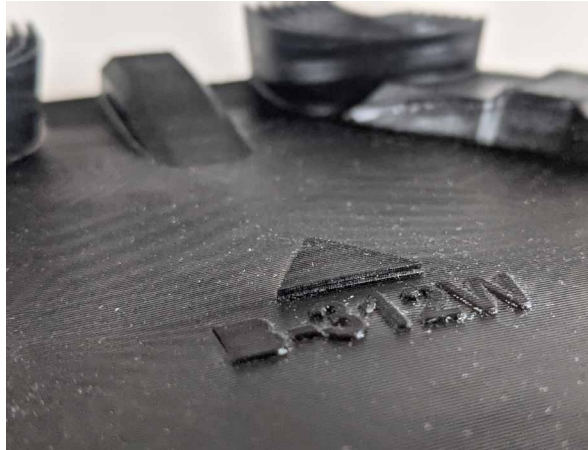


FIG. 5.14 Detailed view of node identifier and triangular protrusion for interface with structural node (Image by author)



FIG. 5.15 Detailed view of connection detail in AM gasket node prototype (Image by author)

5.4.3 Evaluation of AM gasket node solution

The collection of mechanical properties of AM elastomeric materials is meant to be a preliminary exploration for a first proof-of-concept in the development of AM gasket nodes. The information provided from the technical data sheets does not present a definitive answer as to whether or not these materials are suitable, since the available data is incomplete, and the testing standards from the technical data sheets are often different than those outlined in ASTM C864-05. There was also little to no information available from the technical data sheets on the heat aging properties, staining properties, flame propagation, ozone resistance, and brittleness temperature, all of which need to be better understood for an end-use component in this application. Other important material properties such as chemical compatibility with structural sealant and other system materials as well as the hydrophobicity are not included in standard ASTM C864-05. Further, as discussed in Section 5.2, the standard used for evaluation in this chapter is only suitable as a benchmark, since Eurocode standards and requirements for façades are primarily based on the performance of the whole façade-system rather than the material properties of individual components.

It is also worth noting that there is not a single "correct" set of material properties for a gasket. The industry currently uses a range of materials, which have different properties based on several different factors including cost, environmental requirements, fire requirements, gasket geometry etc. [23]. Gasket performance, an obviously important metric in evaluating a gasket product, is impacted by both its shape and materiality, and crucially, the compatibility of both of these aspects with one another. As different projects or system conditions will have different performance requirements, the selection of a suitable gasket material and the development of a suitable gasket design should be influenced by the requirements of a specified context.

Each printing method successfully printed the required geometry, which integrated complex features including: sharp edges; fine features; undercuts; low overhangs; thin overhangs; thin walls; cross-sectional changes; and continuous channels. The surfaces of the PBF, DLP and DLS samples were practically smooth while the MJ sample had a clearly visible stepped surface finish. The surface quality of the MJ sample could be improved in theory by reducing the layer height, however this would increase printing time.

Table 5.6 shows the comparison with the other archetypal solutions for this type of construction that were presented in Chapter 2. The AM node is the only one that is able to provide all of the outlined features, and also allows for mass customization.

TABLE 5.6 Comparison of features of AM node gasket to current construction methods

	Direct gasket connection: Hierarchical	Direct gasket connection: Single-layer	Node: Standard circular	Node: Multi-axis injection moulded	AM Node
Standard connection	-	-	0	+	+
Standard interface with structural node	-	-	+	+	+
Cross-sectional change	-	-	-	+	+
Water pooling avoidance	0	0	-	+	+
Hierarchical drainage	+	-	+	+	+
Geometrical flexibility	-	0	-	-	+
Design and modelling intensity	+	+	+	+	-
Node fabrication intensity	+	+	0	-	-

+: has feature

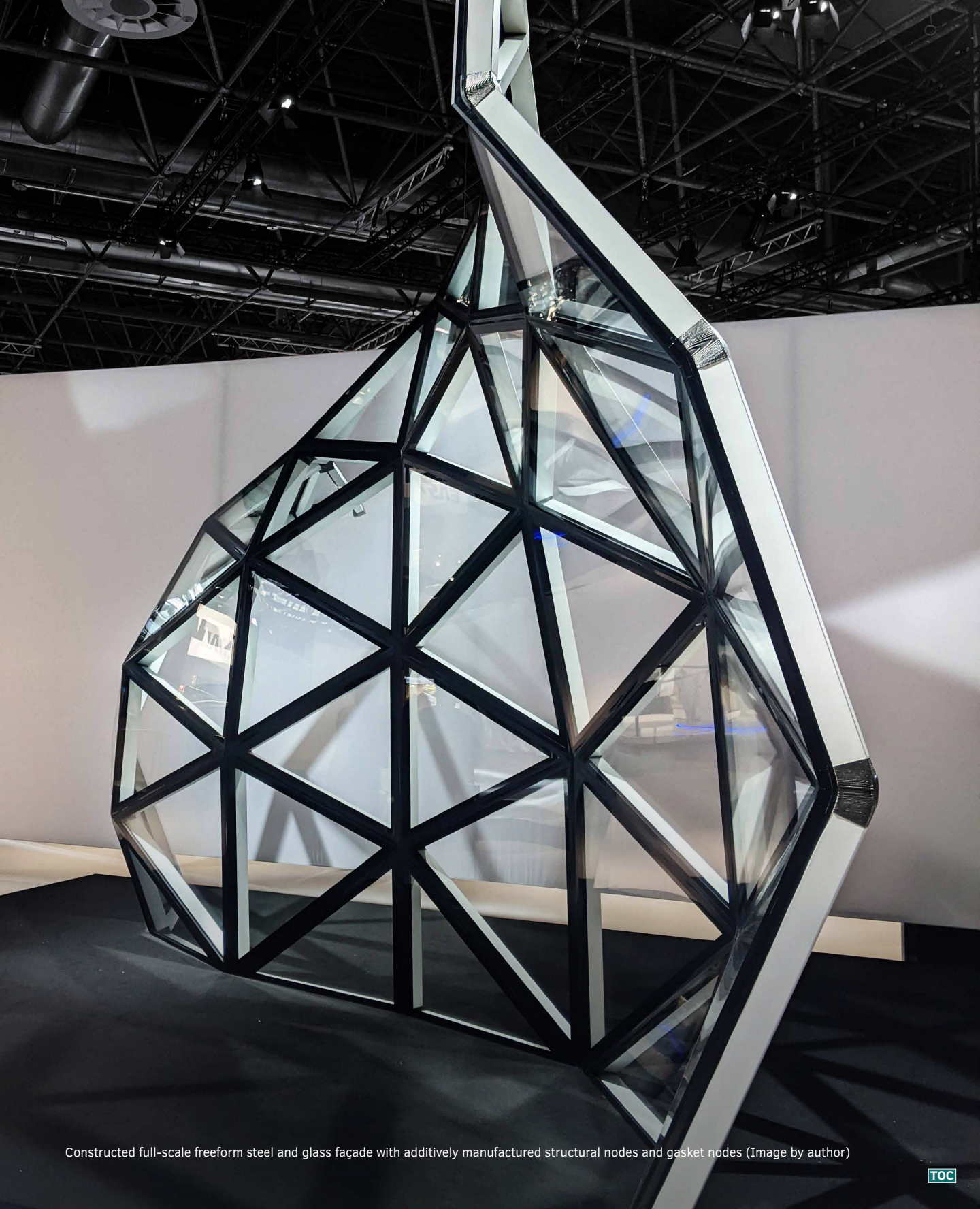
o: has feature in limited capacity

-: does not have feature, or has feature in very limited capacity

The integration of all of the functional features in addition to achieving geometrical freedom through mass customization qualitatively makes the AM gasket the superior choice in terms of performance and assembly – excluding consideration of the increase in design intensity, fabrication intensity, and likely cost. These, however, and the latter in particular, are considerable exclusions. While the node design is defined in a parametric environment and made to be as small as possible, it is still considerably more effort to design, model, and fabricate than the other solutions. Whether and the extent to which the added geometrical flexibility of the AM gaskets facilitates on-site assembly and improves façade performance through avoiding workmanship-related vulnerabilities, improving spatial compatibility with structural nodes in geometrically complex conditions, and reducing pooling potential needs to be better understood before one can begin to ascertain whether the AM gasket is an objective improvement on current solutions.

5.5 Conclusion

In this chapter, material databases were explored in order to identify different materials and printing methods that could potentially be applied to develop AM gasket nodes. Four potential materials were identified and a sample printed of each in order to visually evaluate the surface finish and geometrical fidelity of the printed parts, as well as to confirm the ability of the printing method to print geometrical features that AM gaskets might integrate. A final gasket design combining several existing and additional functional features for freeform steel and glass façade gasket nodes was developed and printed. The design is compared to existing industry solutions. The proposed design integrates all of the functional features through the use of AM. This chapter validates additive manufacturing as a potential avenue for the fabrication of mass-customized gasket nodes.



Constructed full-scale freeform steel and glass façade with additively manufactured structural nodes and gasket nodes (Image by author)

6 Additive Manufacturing in Practice

A case study for the integration of AM into the design, engineering, and execution of freeform steel and glass façade construction

The design and construction of freeform steel and glass façades is an inherently multidisciplinary effort that requires close collaboration between designers, engineers, and contractors. This is particularly true for the development of the substructure, which has heavy implications on the aesthetic, safety, structural efficiency, constructibility, and cost of freeform façades.

In Chapters 4 and 5, additively manufactured structural nodes and additively manufactured gasket nodes were designed and AM prototypes were produced. Chapter 6 is a case study outlining the way in which the design, development, and fabrication of the AM products was undertaken in the context of an interdisciplinary collaboration between a designer, engineering team, and execution team, for the realization of a full-scale FFSGF, as well as the digital strategy that was used to facilitate this interdisciplinary collaboration.

6.1 Introduction

The construction of freeform steel and glass construction is, even without the use of AM, is a multidisciplinary undertaking that requires close collaboration. Any given construction project will include a collection of different stakeholders, each with their respective responsibilities. The following are a few key stakeholders for the realization of freeform steel and glass façades:

Design team: The design is generally lead by the architect, who may be supported by design consultants such as sustainability consultants, façade consultants, etc. Key responsibilities related to freeform façade development include the definition and communication of the design intent.

Structural engineer: The key responsibilities of the structural engineer in freeform façade design include ensuring the structural safety of the construction and its compliance with all of the relevant codes and standards. The structural engineer should also ensure that the design is structurally efficient to minimize cost, improve sustainability, and reduce loads on existing infrastructure when relevant.

Execution team: The execution team is generally lead by a contractor and also includes suppliers, fabricators, subcontractors and installers. Execution team may also include specialty consultants such as construction management consultants, especially in large projects. Key responsibilities include the management and execution of the construction.

The hierarchy of these stakeholder varies based on the specific type of Project Delivery Method (PDM), which varies across different projects. For example, in a design-build project, these three teams could be part of the same entity. In a design-bid-build project, it is not uncommon for the design team and the execution team to each have their own respective structural consultants. In a project using an Integrated Project Delivery method, these three stakeholders might report equally to the owner.

Regardless of the PDM, however, the three teams have many entwined interests. During the course of a project, there are a number of design choices that stakeholders have to make that impact the interests of other project stakeholders. Figure 6.1, shows a number of these choices and responsibilities as they relate to three main aforementioned stakeholders. The decisions that lie at the intersection of these roles represent potentially conflicting interests and/or decisions that benefit

from the expertise of several fields. In order to provide support for endeavours that affect multiple disciplines, relatively new fields such as façade consultancies and digital modelling consultancies have emerged over the past couple of decades and become an indispensable part of the realization of complex projects.

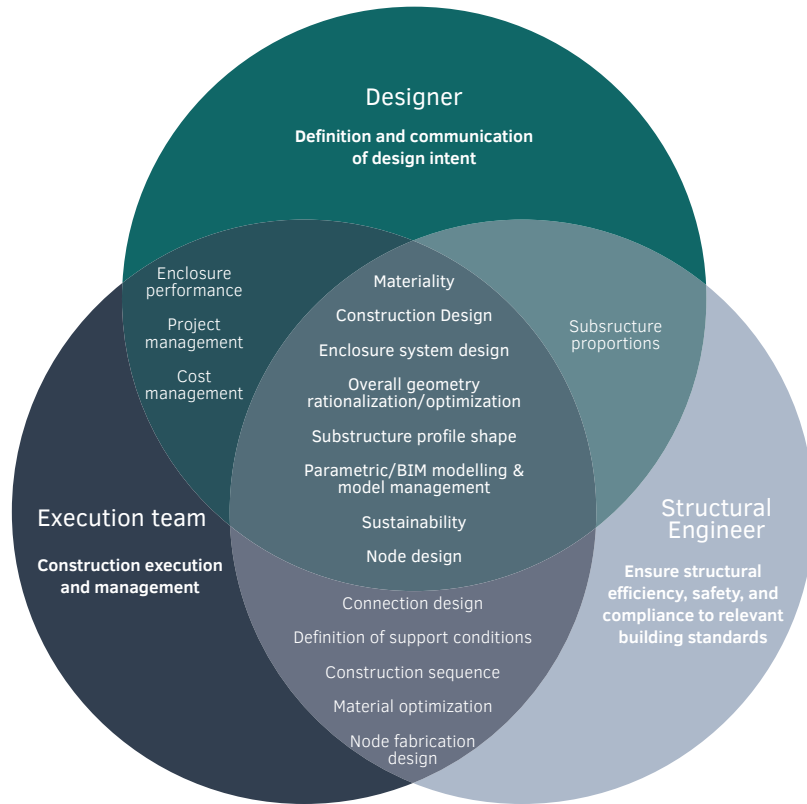


FIG. 6.1 Interdisciplinary responsibilities in freeform steel and glass façade construction (Image by author)

The introduction of additive manufacturing into this framework complicates this already complex collaboration. This additional complexity is largely related to two factors: first, the additional geometrical flexibility afforded by AM gives the design team an unprecedented amount of design freedom to articulate the design intent of the project in the design of the node; and second, the geometry of the node, its material properties, and its fabrication are all very closely entwined and therefore even seemingly minor decisions in the design development process can have considerable implications on the roles and responsibilities of other stakeholders.

In current node fabrication strategies, the material properties of parts are predictable and reliable as they are constructed from standard materials (plates, billets, etc) or tried-and-true methods such as casting. This allows designers to conceptualize node designs using familiar construction methods and materials, and engineers to confidently validate their structural performance. On the other hand, as discussed in Chapter 4, in metal AM the design, material properties and fabricability of the part are dependent on a range of variables in the design and fabrication process including the choice of AM method; part geometry; part orientation; surface finish; part dimensions; tolerances; printing parameters; and path planning. This creates a few specific challenges: first, the general lack of knowledge about how to design parts for AM versus traditional fabrication methods by industry professionals makes it difficult to arrive at quality solutions; second, there is no formal normative basis in building codes for the structural design of AM parts, which can require a more involved engineering process; and third, this creates an even more complex network of entwined and competing interest between project stakeholders increasing the need for close collaboration to develop successful projects.

In this chapter, the design, engineering and construction process of a freeform steel and glass façade project is presented to demonstrate how AM nodes can be integrated in conventional façade workflows. The case study of the freeform façade developed and exhibited at the 2022 Glasstec Fair is used for this purpose. From this experience, a workflow is presented for the design and fabrication of systemized AM structural and gasket nodes for freeform steel and glass façades. The workflow outlines the respective responsibilities of the design, engineering and execution teams, and is supported by a digital workflow in which each of the main stakeholders maintains ownership of their respective models, some of which are parametric to allow for the iterative and collaborative nature of the overall process.

Section 6.2 provides an introduction to the project and the main stakeholders. Section 6.3 describes the collaborative process from design to fabrication of the systemized structural nodes and the roles of the key stakeholders, and outlines the most important competing interests faced during the design and development of structural nodes for the Glasstec project. Section 6.4 describes the collaborative process from design to fabrication of the systemized gasket nodes and discusses the roles of the key stakeholders. Section 6.5 describes the parametric workflow that was used to facilitate the collaboration. Finally, Section 6.6 reflects on different aspects of the workflow based on the Glasstec project experience and provides recommendations for future similar projects.

6.2 The case study

The façade designed and built for the 2022 Glasstec Fair (Figures 6.2–6.5) consists of a roughly 25 m² double-curved free-standing façade. The execution of this project from design to completion brought to light the practical ramifications of working with AM in such a project. From this experience, a workflow for the integration of additive manufacturing into the design, engineering and execution of freeform steel and glass façades was developed.

The project had three main collaboration partners, namely TU Delft, Jansen AG, and knippershelbig GmbH. The project was structured as a design-build PDM where the execution team was also the owner, and the design and structural validation were subcontracted. The owner/execution team was Jansen AG, a steel façade system manufacturer based in Switzerland. The structural validation was done by knippershelbig, a structural engineering firm based in Germany. The role of designer was undertaken by the author, who was the main representative for TU Delft. Several AM fabricators were also subcontracted for the execution team, who were responsible for the CAM modelling of digital node models, AM fabrication, and post-processing of the AM parts.

In addition to the role of designer, the author supported Jansen AG in their responsibilities, undertaking the following tasks: developing and refining the various node designs with feedback from all stakeholders; all parametric design, analysis and modelling in the Rhino/grasshopper environment; the production of parametrically generated fabrication data for glazing units, toggles, and profile lengths; and the production of fabrication files for the AM structural nodes and gasket nodes. The author also supported various engineering and execution tasks, in particular those related to digital modelling.



FIG. 6.2 Exterior view of freeform façade for Glasstec 2022 (Image courtesy of Jansen AG)

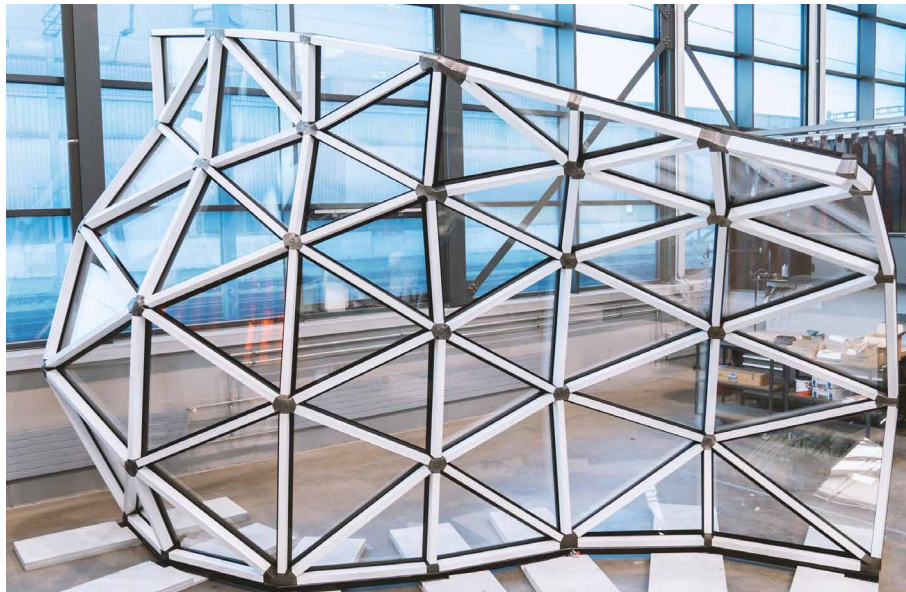


FIG. 6.3 Interior view of freeform façade for Glasstec 2022 (Image courtesy of Jansen AG)



FIG. 6.4 Detail view of additively manufactured structural node in freeform façade for Glasstec 2022 (Image courtesy of Jansen AG)

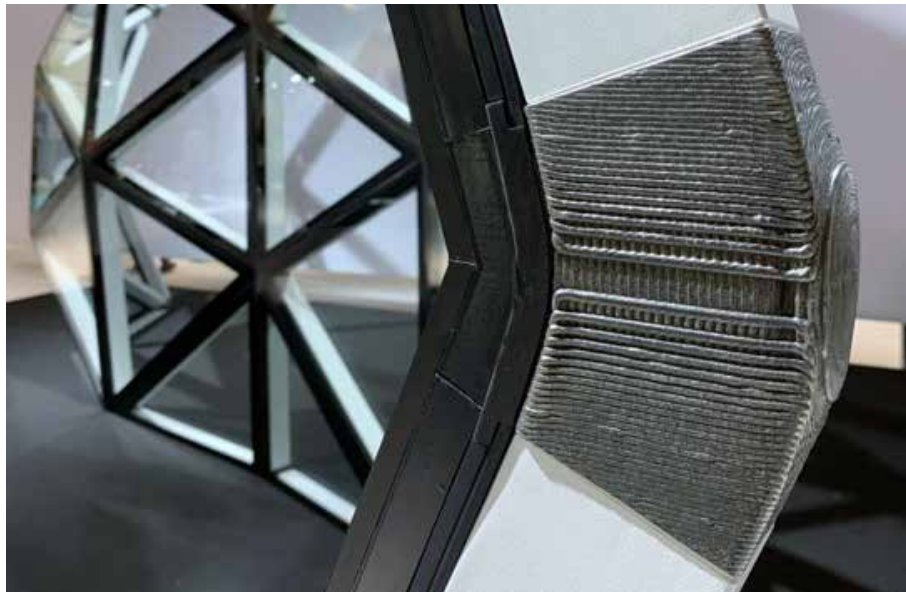


FIG. 6.5 Detail view of additively manufactured structural node and gasket node in freeform façade (Image by author)

The primary object of the project from which the workflow is derived was the development of systemized AM node solutions that would enable the use of a commercial façade system in freeform applications. The emphasis on systemization of the solution is mostly driven by the fact that the design-build project was led by a façade system manufacturer. The systemization of AM nodes is consistent with the normal practice of façade manufacturers to systemize solutions as a means of responding to quick project deadlines, achieve cost-effectiveness, and achieve efficiency in design, engineering, fabrication, and assembly. The systemization of AM products in particular, as mentioned in previous chapters, is also helpful when devising the fabrication strategy. The systemization of nodes also has the quality that the consistent topology creates a coherent architectural language across the envelope which may or may not be desirable depending on the design intent.

6.3 Interdisciplinary collaboration for the design and development of structural nodes

This section and the following outline the roles and responsibilities of the primary stakeholders over the course of the project. The overall process is divided into three main workflows, which are illustrated in workflow diagrams: the design and development of the overall façade design (Figure 6.6); the design, development, and fabrication of AM structural nodes (Figure 6.8); and the design, development, and fabrication of AM gasket nodes (Figure 6.28). It is important to note that the process outlined in these workflow diagrams is in fact very iterative. Typical upstream steps are highlighted in orange. The dotted lines roughly delineate the project phases belonging to parts of the digital workflow explained in Section 6.5.

6.3.1 Overall façade design

Figure 6.6 outlines the main responsibilities for the overall design and development of FFSGF until the start of the node development. This sequence is common also for freeform steel and glass façade projects without AM nodes, since the design decisions made during the overall design of the project will define some the requirements for the design of nodes, or the selection of existing node solutions.

During the preliminary design phase, the designer leads the development of the overall design including the design of the overall geometry, its rationalization, and the architectural design of the underlying structure. The engineering and execution teams provide feedback on the design to help improve cost and efficiency. As such, the overall design phase is an iterative process with several rounds of feedback from the structural design and execution teams.

For the Glasstec project, the design of the façade (Figure 6.7) is a doubly curved surface that creates two “sheltered” zones, one on each side of the façade. The design intent of the façade is a geometry that is reminiscent of a flame. The façade was built from rectangular profiles using the Jansen VISS system [223], which is a proprietary façade system of Jansen AG, as a base for design and construction. The rationalization of the surface was optimized to not exceed the angle limitations of the base façade system and to minimize the size of the nodes such that the 3D-printing load is minimized while maintaining maximum fidelity to the original design surface.

Based on structural analysis, overall dimensions of 50x80mm were specified for the structural profiles. As a next step, the relationship of the façade system to the reference geometry is defined. This simple decision has significant ramifications on the design and performance of the envelope, which were discussed in Chapter 2. Since the structural actions on this particular façade were relatively minor, it was deemed acceptable to locate the reference geometry at the interior glazing joint. The parametric model was updated to incorporate design variables including the location of the reference geometry and the profile dimensions. Once the design was approved, the project progressed to detailed design.

The first step in the detailed design of the envelope was the development of the connection detail, since the standard pinned connections from the base façade system were not suited to effectively transfer the forces of a freeform façade. As such, the structural design and execution teams worked together to develop a connection strategy that was easy to install, and compatible with the base system and fabrication capabilities of the system house.

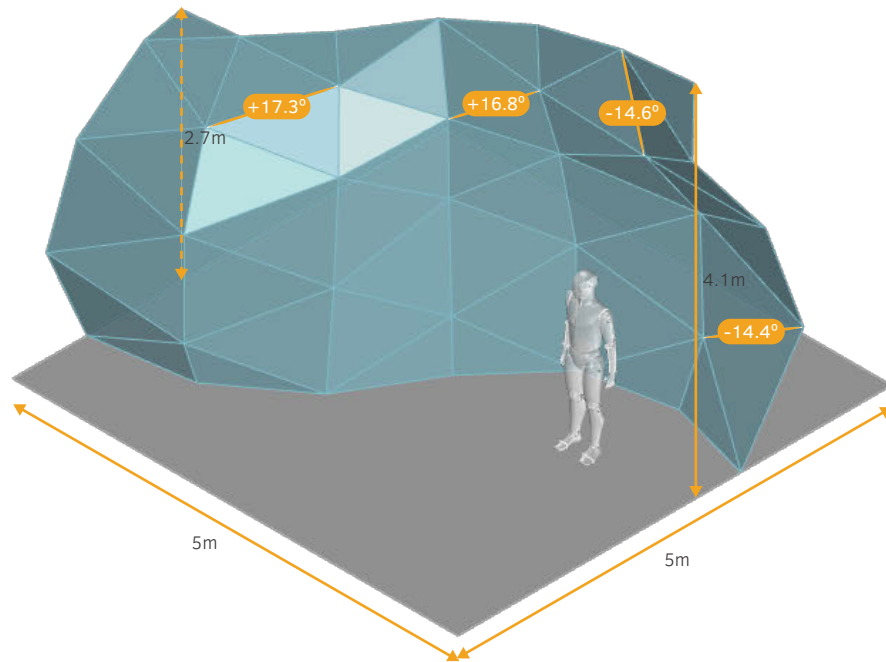


FIG. 6.7 Façade schematic design and rationalization showing overall dimensions and positive and negative critical panel angles (Image by author)

At this phase in a project, it is generally too early to know the exact forces acting at the connections points since these will be based on factors that have not been finalized such as the weight of the nodes. The connection system was therefore designed to withstand a percentage of the profile capacity, and the total capacity of the connection was calculated. Then, once the final structural actions were defined at a later stage, it would be simple to verify whether the system connections were sufficient.

With connections sufficiently defined, the project team moves forward to the node design process. In the overall design, the use of AM did not yet play a significant role in the decision-making, other than optimizing for generally smaller nodes. In transitioning from overall design to node design, several design requirements for the structural node are identified: the approximate dimensions of the nodes which are based on the profile size and their configuration at node conditions; structural requirements based on the preliminary structural analysis; and connections requirements.

6.3.2 Structural node design

Figure 6.8 outlines the main responsibilities for the design and development of AM structural nodes. The process in this figure is presented as a continuation of the process illustrated in Figure 6.6, in which the last outlined task is the collection of the node requirements. This workflow begins with the communication of those requirements to the AM fabricators. It is notable that most of the tasks outlined in the first three columns, namely those of the design team, engineering team, and execution team, are, when broadly defined, also generally typical of non-AM projects. The actual execution of these tasks however varies significantly. The following sections elaborate in more detail the tasks involved in the development of AM structural nodes.

Selection of a fabrication method

Based on design requirements identified during the overall design, a suitable AM method is selected to move forward with node design. As discussed in Chapter 4, there are a number of different factors that may influence the choice of fabrication method. The size, arm distribution, structural requirements, and connection details, for example, play a role in establishing whether AM nodes are potentially a better alternative than other node fabrication methods, and influence which AM methods are potentially suitable. Additional design requirements for the structural nodes based on design intent by the design team may also influence the decision. For AM, a specific AM method needs to be selected since different metal AM methods have drastically different strengths, limitations, and possibilities. The outlined requirements will therefore likely affect the suitability of different AM methods and technologies, and perhaps limit viable options. The selection of an AM method is notably the starting point for the iterative structural node design development process. This enables the node to be designed specifically for the AM method from its initial conception to increase fabrication efficiency.

For the Glasstec project, the design requirements were communicated to various AM fabricators by the execution team to evaluate the suitability of the different AM methods. The design requirements for this projects were not very limiting. The design was driven mostly by practical requirements such as the transfer of structural forces, interface with the gasket node, and integration of the prescribed connection detail. There were no explicit aesthetic requirements, the size of the nodes was within the range of both DED and PBF printing, and the connection detail would require machining regardless of the selected AM method because of the threaded holes.

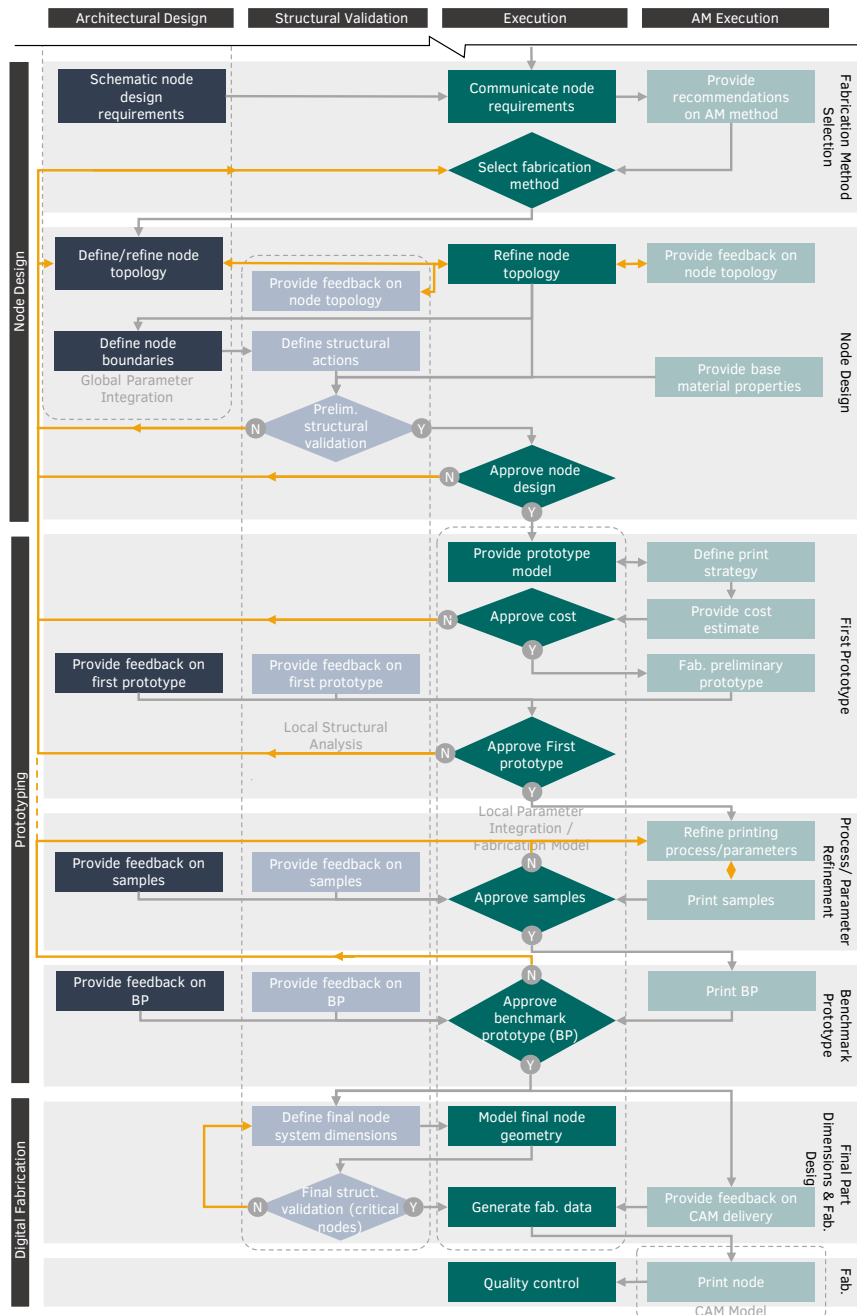


FIG. 6.8 Workflow for the design and fabrication of AM structural nodes for freeform steel and glass façades, a continuation of the workflow diagram in Figure 6.6 (Image by author)

Because this project was part of exploratory research, several AM technologies were explored for this project. The following steps for the node design and development were repeated several times exploring different AM methods and different nodes designs.

Node design

In the methodology presented, the iterative process for node development and prototyping always begins with the selection of an AM fabrication method, and then moves on to iterative node design. For this project, structural node designs were developed for two families of AM: Directed Energy Deposition (DED) and Powder Bed Fusion (PBF). For each printing method, multiple node designs were explored and discussed and several selected for further development and prototyping.

The design team proposes a schematic node topology design that is subsequently refined based on feedback from all stakeholders. Since the objective is to achieve a systemized solution, the topology consists of a parametrically-defined form that can be reconfigured and applied to a wide range of geometrical configurations. Also, the structural node topology has a number of defined variable parameters that can be prescribed variable dimensions based on the specific structural requirements of the application or node condition. This design should, as best as possible, reflect principles of Design for Additive Manufacturing (DfAM) for the selected AM method.

Because of the structure of the Glasstec project, the execution team lead the refinement of the node design. Refinement of the node topology on behalf of the execution team was based primarily on constructibility, compatibility with the rest of the façade system, and integration of the connection detail. The structural team provides feedback on the structural efficiency of the proposed topology and its ability to effectively transfer the primary loads for the project. AM fabricators meanwhile provide feedback on the printability and printing efficiency of the design.

Many node design iteration were explored for this project. Figures 6.9 to 6.12 illustrate the development of the DED-GMA node based on the feedback from the various participants. Figure 6.9 shows several early schematic design possibilities, which include proposals for path planning strategies. Figure 6.10 shows an example of a qualitative improvement proposed by knippershelbig for a preliminary DED node design to enable the effective transfer of bending moments. Figure 6.11 shows a further revision of this node design based on feedback from Mx3D on the printability of the end conditions and the interior reinforcements. The interior reinforcements were then further adjusted to facilitate printability, into the final design shown in

Figure 6.12. Throughout this process, the suitability of the proposed design for compatibility with the base façade system was prioritized. In the end, the final design combines some of the qualities of the four initial design proposals. The design sought to uphold a light and ephemeral quality in accordance with the overarching façade design intent. The extent to which this objective was achieved is open to interpretation.

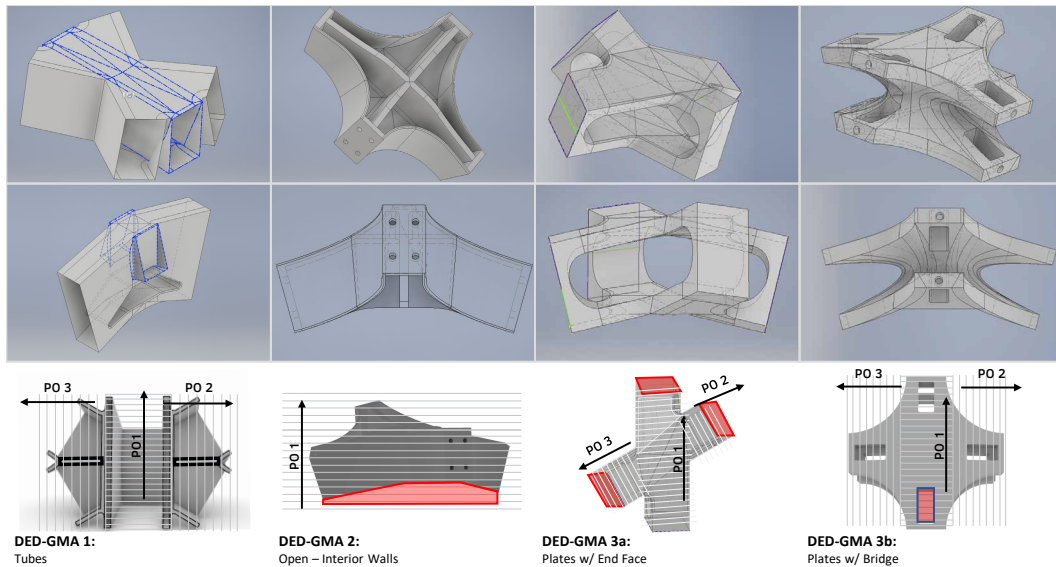


FIG. 6.9 Initial schematic design options for DED-GMA node including proposed printing sequence and Printing Orientation (PO) (Image by author)

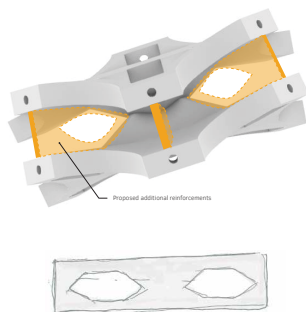


FIG. 6.10 Proposed qualitative structural improvements to initial schematic DED-GMA node design (Image Source: knippershelbig GmbH)

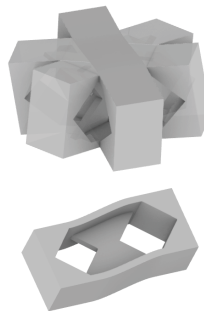


FIG. 6.11 DED-GMA node design iteration following feedback on manufacturability from AM fabricator (Image by author)

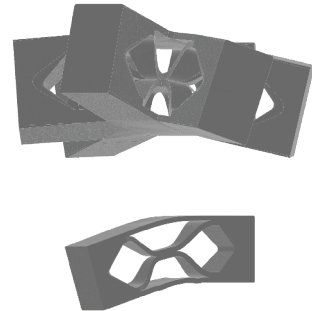


FIG. 6.12 Final iteration of DED-GMA node which was printed and installed in the mock-up wall (Image by author)

Once a node is developed, this first phase has two final checkpoints: the preliminary structural validation of the node topology using FEA, and the final validation of the node schematic design. Figure 6.13 shows the FEA model for a template node for preliminary structural validation for the DED-GMA node. Figures 6.14, 6.15 and 6.16 show the evolution of the of the PBF-L node design. The initial node design was revised several times based on qualitative feedback, and three designs were eventually compared using cursory FEA models. During this iterative design process, the prototyping phase can already begin.

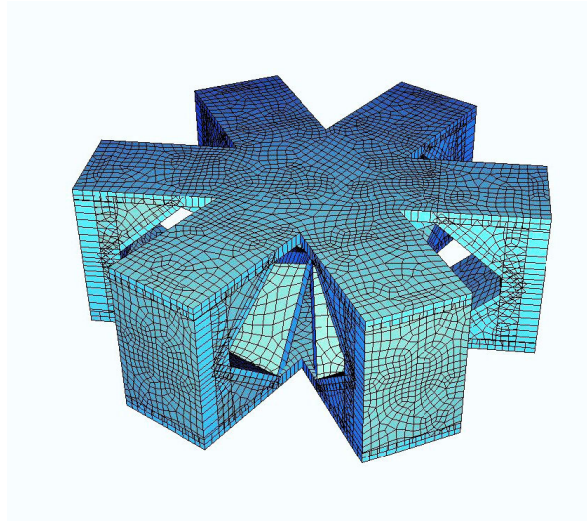


FIG. 6.13 FEA model of template node for preliminary structural validation of DED-GMA node (Image courtesy of knippershelbig GmbH)

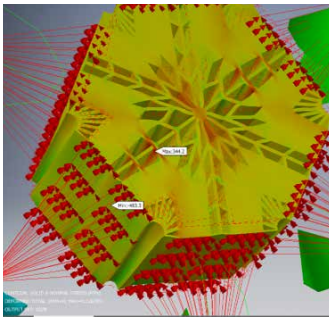


FIG. 6.14 FEA model of first iteration of PBF-L node installed in the first full-scale mock-up (Image by author)

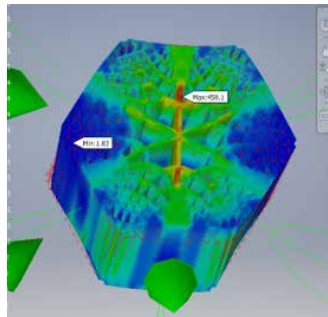


FIG. 6.15 FEA model of second iteration of PBF-L node (Image by author)

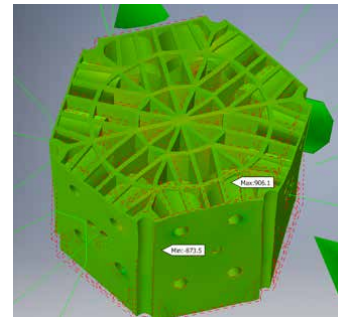


FIG. 6.16 FEA model of third iteration of PBF-L node (Image by author)

First prototype

The first checkpoint in the prototyping phase is approval of costs based on a quote from the AM fabricator. Once approved, a preliminary prototype is printed. The prototype allows the team to establish whether the proposed node topology is promising, and to identify unexpected bottlenecks in the fabrication process. The preliminary prototyping phase may begin with a full node or with a section of the node to establish local feasibility of challenging features and do some small-scale exploration of process and parameter refinement before committing to printing a full node. That being said, the partial prototype should incorporate key areas of the node that may cause challenges or bottlenecks down the road, which may be difficult to predict.

It is worth noting that each of the printed preliminary prototypes brought to light some unexpected challenges. For example, an early iteration of a DED-GMA node (Figure 6.17) warped to an unacceptable tolerance during printing, which is a challenge in the DED-GMA printing of large asymmetrical parts [143]. A preliminary DED-L prototype (which was the first iteration of the node eventually used in the Glasstec façade) had an surface texture at the centre of the node on the exposed side that was not aesthetically acceptable (Figure 6.18). A preliminary PBF-L had support structures that were excessively difficult to remove (Figure 6.19). Another notable bottleneck faced during the preliminary prototyping of the Glasstec project was the significant inconvenience and cost associated with using a different tool and machine setup for the subtractive fabrication operations required for achieving installation tolerances on the node end-faces and connection details.



FIG. 6.17 Preliminary prototype for DED-GMA node with excessive warping (Image courtesy of Mx3D)

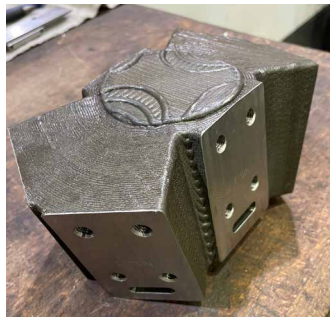


FIG. 6.18 Preliminary prototype for DED-L node with undesirable surface texture (Image by author)

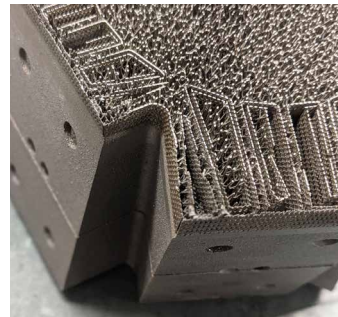


FIG. 6.19 Preliminary prototype for PBF-L node with difficult to remove support structures (Image by author)

The printing of the first prototype may be an iterative process if the prints fail. The next step is to refine the printing process and parameters. Otherwise, the design is refined or another iteration is developed starting at the selection of the AM method. Because the structural node is a key component in the aesthetic, structural performance, system performance, and constructibility of the façade, all main stakeholders are involved in the approval of the prototype.

Printing parameter refinement

In the preliminary prototype, the feasibility of the print is established, and key aspects are identified for improvement of the design and/or fabrication. The next step is to refine the printing process and its parameters in order to improve on the preliminary prototype. Local samples of specific geometrical conditions may be used to improve print quality and efficiency, without committing to full-scale prints. In addition to this, material samples are printed to establish accurate mechanical properties, which prior to this stage were approximate values provided by the AM fabricator or raw material provider.

The following is a good example of the type of printing process refinement that was done during the Glasstec project. The first iteration of node design using DED-GMA the team wanted to explore the possibility of having a relatively hollow node centre with an organic-looking interior structure. The connection which was defined for the project required a flat end face. The AM fabricator for the DED-GMA node printed several iterations for the end conditions. The first prototype was exploratory and a first attempt at achieving the required geometry (Figure 6.20). After that, several local prototypes of the end conditions were fabricated to improve the surface quality (Figure 6.21). A drastic improvement in quality was achieved between the first and last local prototype for this type of end condition by refining the printing parameters and changing the path-planning to integrate a contour path at the perimeter. The possibility of printing a 90 degree end condition to reduce material usage was also explored (Figure 6.22). This material reduction came at the cost of more complex path planning which would ultimately take longer to print than the original end-condition.



FIG. 6.20 First prototype using DED-GMA (Image courtesy of Jansen AG)



FIG. 6.21 End-condition iterations to improve surface quality by integrating contour paths, printing solid end conditions without integrated boring holes, and subdividing the path planning for the solid infill (Image courtesy of Jansen AG)



FIG. 6.22 Sample iteration of end condition using less material but more complex path planning that requires several changes of printing orientation which are visible in the surface texture (Image courtesy of Mx3D)

In the end, a final prototype is printed for approval. This benchmark prototype should be the archetypal node for the development of the rest of the façade nodes. Because of the importance of the structural node in the interest of all stakeholders, everyone is again involved in the approval of the local samples and the benchmark prototype. The evaluation of the benchmark prototype is based on both its quality and fabrication. Quality metrics include its surface finish, general aesthetic, geometrical tolerances, and depending on the project requirements, destructive testing may also be required to validate the quality of the structural strategy. Fabrication metrics consider the intensity of the fabrication preparation, fabrication operations, necessity and intensity of post-processing, and the logistical requirements between operations. Upon approval, the benchmark prototype is also used as a contractual benchmark to establish the minimum tolerances and quality control metrics for the end-use nodes.

As part of the evaluation of nodes for the Glasstec project, a 1.5m x 3m mock-up façade with three nodes, one for each fabrication methods explored (PBF-L, DED-L, and DED-GMA) (Figures 6.23-6.25) was fabricated and assembled (Figure 6.26). The evaluation of the nodes is included in Chapter 4. After the mock-up construction, the decision was made to produce the structural nodes for Glasstec using the nodes developed for hybrid additive/subtractive DED-L.



FIG. 6.23 DED-GMA node in first full-scale mock-up assembly (Image courtesy of Jansen AG)

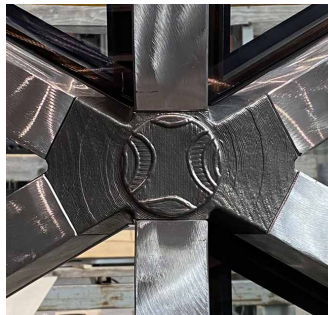


FIG. 6.24 DED-L node in first full-scale mock-up assembly (Image courtesy of Jansen AG)



FIG. 6.25 PBF-L node in first full-scale mock-up assembly (Image courtesy of Jansen AG)



FIG. 6.26 Full-scale mock-up with 3 metal AM nodes fabricated using DED-GMA (top), PBF-L (middle), and DED- (bottom) (Image courtesy of Jansen AG)

6.3.3 Digital fabrication design

With the approval of the benchmark node, there is at this point a systemized node solution. A node topology with integrated connections has been defined and the appropriate printing strategy and parameters selected. The next steps consist of defining the final geometry of the nodes, and preparing the digital output required to fabricate the nodes and the rest of the façade. In this workflow, the execution team is responsible for the modelling of the final nodes.

The systemized node consists of a prescribed topology that can be parametrically generated according to specified geometrical configurations, and pre-defined dimensional variables can be adjusted based on specified structural conditions. It is then the responsibility of the structural design team to size the nodes, namely prescribe values for the dimensional parameters, based on the results of material testing, the loads calculated from global structural analysis, and the proposed node designs and configurations. The necessary parameter values are communicated to the owner of the parametric model.

The Glasstec project was constructed using the DED-L node design described in Chapter 4. The structural engineer defined several critical minimum dimensions that had to be respected for all node configurations. To facilitate fabrication and reduce cost for a small façade, only three pipe sizes with different radii and thicknesses were selected as a basis. The parametric definition defines the volumetric boundary of the node, selects the maximum profile size which fits in the node and lengthens the arms as necessary to respect the minimum dimensions outlined by the structural engineers. Following this, critical nodes in the façade are selected and verified by the structural engineer using FEA to ensure that the worst-case scenarios are within the system capabilities.

The last step prior to final fabrication consists of the generating the digital fabrication data. For the structural node, the AM fabricator provides feedback to improve the Computer Aided Manufacturing (CAM) setup, based on the digital models provided during the prototyping phase. Depending on the AM fabricator and their workflow, this process may be more or less involved. For example, there is an opportunity particularly for DED to integrate the majority of the CAM modelling directly into the parametric workflow using tools such as the Kuka/PRC plug-in for Rhino/Grasshopper. For this project, it was decided that the effort required to generate tool paths parametrically was not worthwhile given the small number of nodes, and the incompatibility of the parametric modelling and CAM software. Rather, the model output consisted of additive phase solids and subtractive phase solids for each the AM material and the substrate subcomponents. Furthermore,

vector-friendly text was provided to engrave assembly information in the node faces. With this digital data as a starting point, further CAM modelling for final fabrication took the AM fabricator approximately 45 minutes per node. The models used for digital fabrication design are discussed in more depth in Section 6.5.

6.3.4 **Entwined interests of project stakeholders**

The development process of AM structural nodes (Figure 6.27) took a top-down design approach: the node requirements are outlined based on the overall design; these requirements influence the selection of the AM method and node design; the fabrication process is then refined to realize the design with a quality/aesthetic finish, good material properties; and high-level of fabrication efficiency.

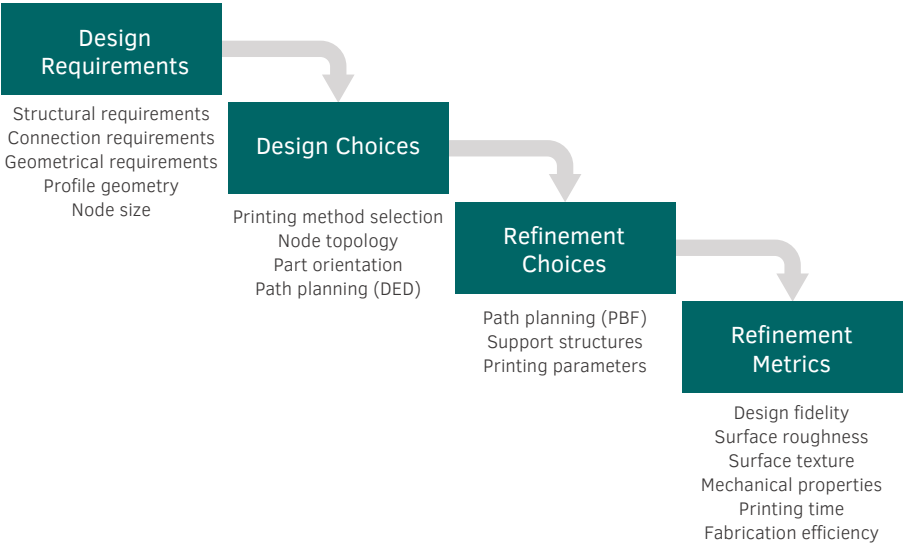


FIG. 6.27 Top-down decision-making approach for structural node design (Image by author)

In the two methodology graphs (Figures 6.6 and 6.8), design decisions are assigned to a single stakeholder. However, in reality, most design decisions have consequences for the tasks and responsibilities of the other stakeholders. During the development of the Glasstec project, many instances of conflicting interests between stakeholders during decision making were encountered. Table 6.1 outlines the most significant of these conflicting interests.

TABLE 6.1 AM-related entwined interests of project stakeholders for the development of AM structural nodes

	Stakeholder	Interest
Choice of AM method	Designer	Different AM methods have different strengths and limitations regarding what is possible/suitable in terms of the geometry of the final product, which impacts design possibilities and also the design approach. Final products will have different tolerances and textures.
	Structural engineer	Samples produced with different AM methods have different mechanical properties. They also generally have different standard deviations of mechanical testing results [164] which will impact safety factors. The difference in mechanical properties is largely due to the effect of different base materials, different heat input, and different environmental conditions on the microstructure of the part.
	Execution team	Choice of different AM method requires different printing technologies and different technical expertise to employ them effectively. They also have different implications on design possibilities, tolerances, printing time and cost.
Node size	Designer	Size and proportions of the node affect the degree of visual intrusion.
	Structural engineer	Mechanical properties of the part may vary along the axis of the printing orientation because of the difference in thermal history, which results in different microstructures at different levels [162]. This is more relevant in DED printing, which does not occur in a heated/controlled environment, since the difference in cooling rates will be more significant. This can be addressed in the printing settings by varying the heat input by adjusting the wire feed speed and torch speed along the height of the print [162].
	Execution team	Since printing methods are typically suited to a particular range of part size, the execution team must select an appropriate AM method and fabrication partner. Outside of this range, printing becomes inefficient and less cost-effective. Also, larger nodes (which are often correspondingly heavier nodes) may complicate assembly.
	AM node fabricator	In printing methods with enclosed environments, part size may be a limiting factor in the selection of printing equipment. In DED printing in particular, the scale of the object must allow space for the print head without clashing with the part. Since larger nodes typically require more printing time, it may be desirable to adjust printing parameters, for example increasing layer height, to improve printing speed.
Surface finish	Designer	Surface finish will affect the appearance of the node and whether it is consistent with or noticeably different than the rest of the structure. Overhanging surface features in PBF printing will have rougher surface finish on the down-skin regions (i.e. the downward-facing surfaces of overhanging parts).
	Structural engineer	Surface finish has significant ramifications on the mechanical properties of the printed parts and in particular ductility and fatigue strength [152, 153, 157, 170].
	Execution team	Since printing methods typically achieve a particular range of surface quality, the execution team must select an appropriate AM method and fabrication partner. Surface quality will also impact the node interface with other system components. There is typically a trade-off between printing time and surface quality.
	AM node fabricator	Parameter selection for good surface finish will likely negatively impact printing time. If the surface finish of printed parts is not suitable, or if the mechanical properties of raw printed parts are not sufficient, additional machining may be required.

>>>

TABLE 6.1 AM-related entwined interests of project stakeholders for the development of AM structural nodes

	Stakeholder	Interest
Tolerances	Designer	Tolerances affect the achievable level of detail, feature integration, the precision of joints and interfaces, and may dictate geometrical features such as minimum radii.
	Structural engineer	Rough tolerances result in smaller effective dimensions of the structural parts. Rough tolerances in structural interfaces and connections result in more allowable movement in the structure which has to be taken into consideration in structural analysis. Connection tolerances are also an important part of structural analysis.
	Execution team	Node tolerances affect interfaces with the rest of system components, and must be taken into consideration in the development of the connection detail. Assembly tolerances must also be considered and accounted for. Since printing methods are typically suited to a particular range of tolerances, the execution team must select an appropriate AM method and fabrication partner.
	AM node fabricator	Care must be taken in the selection of printing parameters to find a balance of meeting required tolerances and minimizing printing time. If tolerances are not suitable, additional machining may be required.
Profile geometry	Designer	Profile geometry is a key component of a façade's aesthetic.
	Structural engineer	Different profile geometries have different resistance to bending, torsion, shear etc.
	Execution team	The base profile geometry will affect the node size, its relative proportions, and the severity of its overhangs. These factors may affect the suitability of different AM methods and printing time. The profile geometry also affects the buy-to-fly ratio, thus the relative efficiency of AM vs. CNC fabrication. In addition, the execution team may have a specific range of available profiles.
	AM node fabricator	Profile geometry will likely influence the node topology. In PBF this impacts the surfaces that require support structures. In DED this impacts path planning and printing parameters, for example adjustments for corner conditions.
Node topology	Designer	Node topology is a key element of a node's aesthetic.
	Structural engineer	The node topology should provide efficient structural load paths within the node to address the structural requirements of the project. The node topology will also impact the formation of residual stresses in the printed part, which need to be taken into account by the structural engineer. Mechanical properties are also impacted by node topology since it defines the relative amount of surface area of the node, and impacts the alignment of node features with the printing orientation.
	Execution team	Node topology may impact suitability of various AM methods. The execution team must therefore select an appropriate AM method and fabrication partner.
	AM node fabricator	Node topology affects printability of the part, whether the AM method is suitable, necessary supports and/or path planning, and potentially limits orientation during printing. The configuration and dimensions of features in the node topology will impact the heat accumulation and dissipation in the part as it is being printed. As such, care must be taken to ensure that the desired topology can be achieved without resulting in problematic deformations and residual stresses.

>>>

TABLE 6.1 AM-related entwined interests of project stakeholders for the development of AM structural nodes

	Stakeholder	Interest
Part orientation during printing	Designer	Part orientation during printing will affect the surface roughness and thus the visible texture of the printed part [153, 154].
	Structural engineer	Mechanical properties (especially without heat treatment) are anisotropic. The orientation of the part relative to the print orientation will directly affect its mechanical properties [152-154, 157, 158, 162, 224]. Part orientation may also impact the effective dimensions of structural features.
	Execution team	Part orientation will affect the surface roughness of the printed part, which will impact tolerances at interfaces with other system components.
	AM node fabricator	The cost- and time-effectiveness of printing in both PBF and DED is largely affected by part orientation. Overhang limitations in both technologies are relative to the part orientation during printing. In PBF printing, the orientation of parts will dictate the required supports [173]. It will also dictate the overall height of the print, which, if minimized, reduces printing time and cost especially for one-off parts [173]. In DED, the part should be oriented such that the desired geometry is feasible and efficient to fabricate. Geometric possibilities are limited by degrees of freedom of the printing equipment that is used. A compromise may have to be found between printing efficiency and the desired geometry.
Path planning	Designer	Path planning, particularly in DED printing, will be visible in the texture of the printed part. In both DED and PBF printing, path planning will impact surface roughness.
	Structural engineer	Path planning affects mechanical properties of the part as it impacts porosity [172], microstructure [157, 160], and surface roughness [157]. In PBF printing, ductility in particular is affected by the selected scan strategy [160]. Path planning can negatively impact residual stresses [143, 160, 225], which should be taken into consideration during engineering.
	Execution team	Path planning will play a significant role in the printing time and cost of the printed part. Path planning can also cause/worsen undesirable part deformations [143, 225] and as such should be defined with care so as to not negatively impact system tolerances.
	AM node fabricator	Path planning strategies varies by technology. In PBF, good path planning should enable the printing of the required geometry with minimal support structures. In DED, good path planning avoids tight spaces and potential collisions with the part, minimizes superfluous machine movements, and finds a complimentary balance between active printing and cooling times while meeting aesthetic and structural requirements.
Support structures	Designer	Support structures may leave behind a different surface finish once removed.
	Structural engineer	Support structures in PBF printing are necessary as a heat sink to mitigate residual stresses in printed part which impact mechanical properties. Support structures can also be integrated as structural reinforcement.
	Execution team	Support structures are sometimes required to minimize part deformation which will impact system tolerances. Excessive support structures negatively impact printing time and cost.
	AM node fabricator	Care must be taken by the AM fabricator to design support structures that provide a sufficient heat sink without adding too much additional printing time to meet the requirements of the other stakeholders. Support structure design can be a time-consuming effort. Support structures also often require removal and must therefore be designed for accessibility and easy removal.

>>>

TABLE 6.1 AM-related entwined interests of project stakeholders for the development of AM structural nodes

	Stakeholder	Interest
Printing parameters	Designer	Printing parameters will affect the visible surface quality of the part.
	Structural engineer	Printing parameters significantly affect the mechanical properties of the part.
	Execution team	Printing parameters significantly affect the printing speed and efficacy, as well as the surface quality of the printed part which may impact the node interface with other system components.
	AM node fabricator	Care must be taken by the AM fabricator to select printing parameters that address the needs of the other stakeholders, namely a balance of shape fidelity, surface finish, good mechanical properties, and printing efficacy. Fine-tuning parameters for this balance can be time-consuming and require iterative prototyping and testing.

The table highlights some of the many aspects of the node design development that affect the interest and responsibilities of the other stakeholders. The “design” of the AM fabrication process (including selecting an AM method, defining a path planning strategy, selecting printing parameters, and support structure design) is integral to the function of the node as it relates to the architecture, the structural safety, and construction of the enclosure. This entwining of interests requires good communication between the different stakeholders, and particularly with the AM fabricator. As such, the node design development process benefits from the designer, structural engineer, and façade execution team being familiar with the strengths and limitations of AM technology and principles of DfAM. Further, the clear communication of specific requirements and priorities to the AM fabricator is crucial for the fabrication of an AM part that balances the demands of the other stakeholders.

6.4 Design and development of node gaskets

The process for the development of AM gasket nodes (Figure 6.28) is in many ways similar to that of structural nodes, however the biggest difference is that the design and structural teams are not involved in the gasket node development. The entire process is led by the execution team, and supported by AM execution partners.

In the development of the gasket node, the initial validation of the material properties takes place prior to the design of the node topology since there is a wide range of possible gasket materials which may influence their design. For example, material properties might influence whether the material is better suited to providing

a compressive seal via the compression of bulk material or via the deflection of a cantilever arm or tubular volume. There are a number of material properties outlined in Chapter 5 that provide a basis for the initial validation of gasket materials. In addition to having good mechanical properties, the selected material should be compatible with those of the base façade system with which it will be interfacing, and which was defined in an earlier phase of the project development. The execution team takes on the preliminary validation of material properties – a responsibility that for the structural node belongs to the structural engineer.

Once a material is selected, the node topology is defined per the design guidelines of the corresponding AM technology. The execution team takes on the responsibility of designing the nodal component, which for the structural node was the task of the designer. The topology of the gasket node will reflect base façade system as it needs to connect to the gasket profiles and provide a seamless continuity of the compressive seal. For the Glasstec project, the gasket node was based on one of standard gasket profiles that are part of the Jansen VISS façade system. The design of the gasket node should also be compatible with the design of the structural node.

Another key difference in the development of the gasket node is that the final functional validation of the structural nodes and gasket nodes belong to different stakeholders. The structural node is an integral part of the façade's aesthetic, structural system, and façade system performance. As such, approval of the structural node is shared by all stakeholders. Metrics for the gasket node performance are related to façade performance such as air- and water-tightness, which is the responsibility of the façade system supplier i.e. the execution team. This final approval should entail full-scale façade testing according to EN 13830 [202].

For the Glasstec project, gaskets were printed and installed in the mock-up façade, but performance testing was not performed. As such, there was no need for process/parameter refinement steps (denoted in dotted lines). The logical next step in this project is to perform façade testing, and to refine the printing parameters and/or the gasket node design until satisfactory façade performance is achieved.

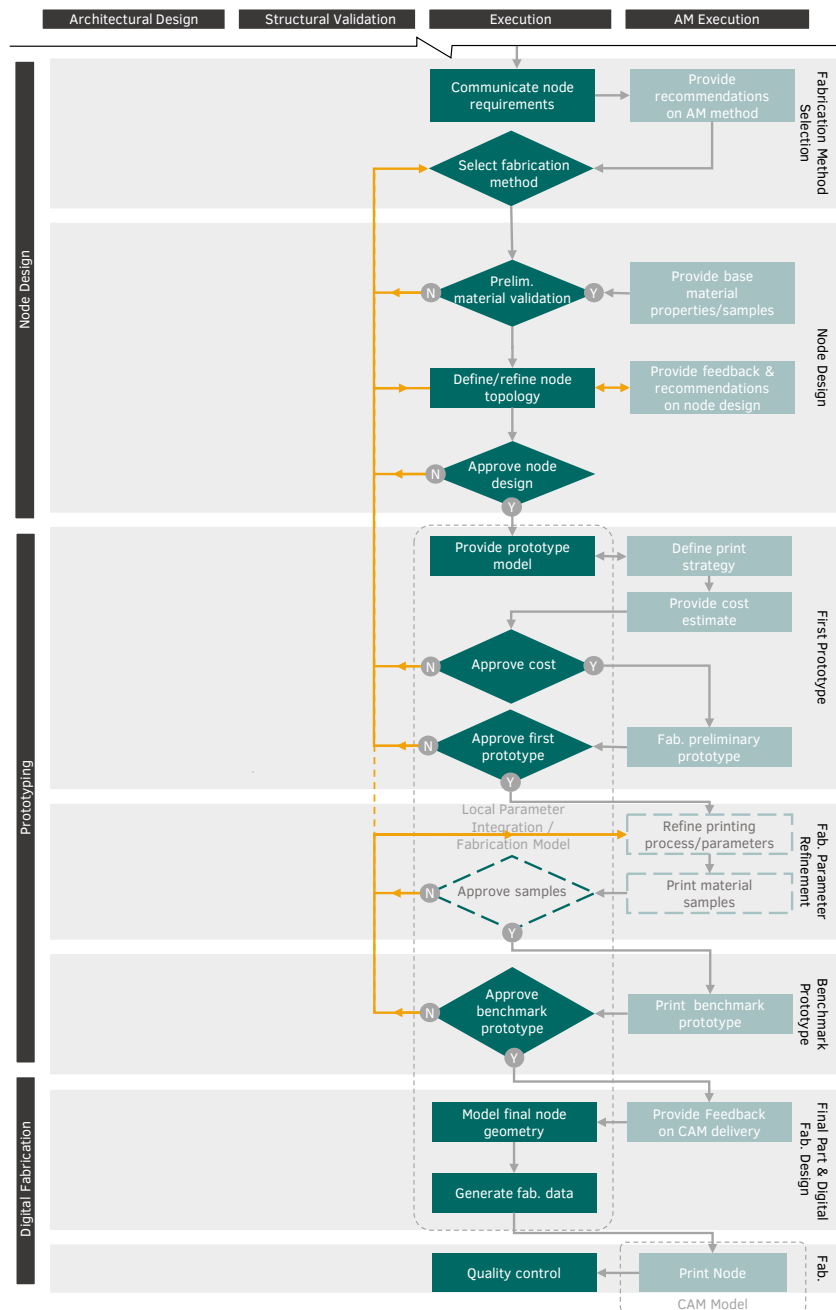


FIG. 6.28 Workflow for the design and fabrication of AM gasket nodes for freeform steel and glass façades, a continuation of the workflow diagram in Figure 6.6 (Image by author)

6.5 Interdisciplinary digital workflows in AM FFSGF

The entire process as described in Sections 6.1-6.4 relies on close communication, creative design and engineering, and parametric modelling – aspects that can prove challenging when working in multidisciplinary projects. In order to facilitate the collaborative, flexible, and iterative nature of the project, the process is rooted in a digital workflow that spans from the design of the overall geometry to the generation of the CAM models. The digital workflow described in this section, which was developed for and used in the Glasstec façade, is subdivided into 6 phases summarised in Figure 6.29:

- 1 Architectural Design & Rationalization (AD&R)
- 2 Global Parameter Integration (GPI)
- 3 Overall Structural Analysis (OSA)
- 4 Local Structural Analysis (LSA)
- 5 Local Parameter Integration & Fabrication (LPIF)
- 6 Computer Aided Manufacturing (CAM)

The division of models is defined by the ownership of different tasks and responsibilities of the stakeholders as outlined in the previous sections and by the level of detail of the model. The ownership of different tasks also generally corresponds to the use of different digital platforms. In the case study, the author was responsible for the design, development and management of models attributed to the design team and execution team, namely the AD&R, GPI and LPIF models. Structural analysis models were the responsibility of knippershelbig. The different AM fabricators undertook CAM modelling from the provided geometry.

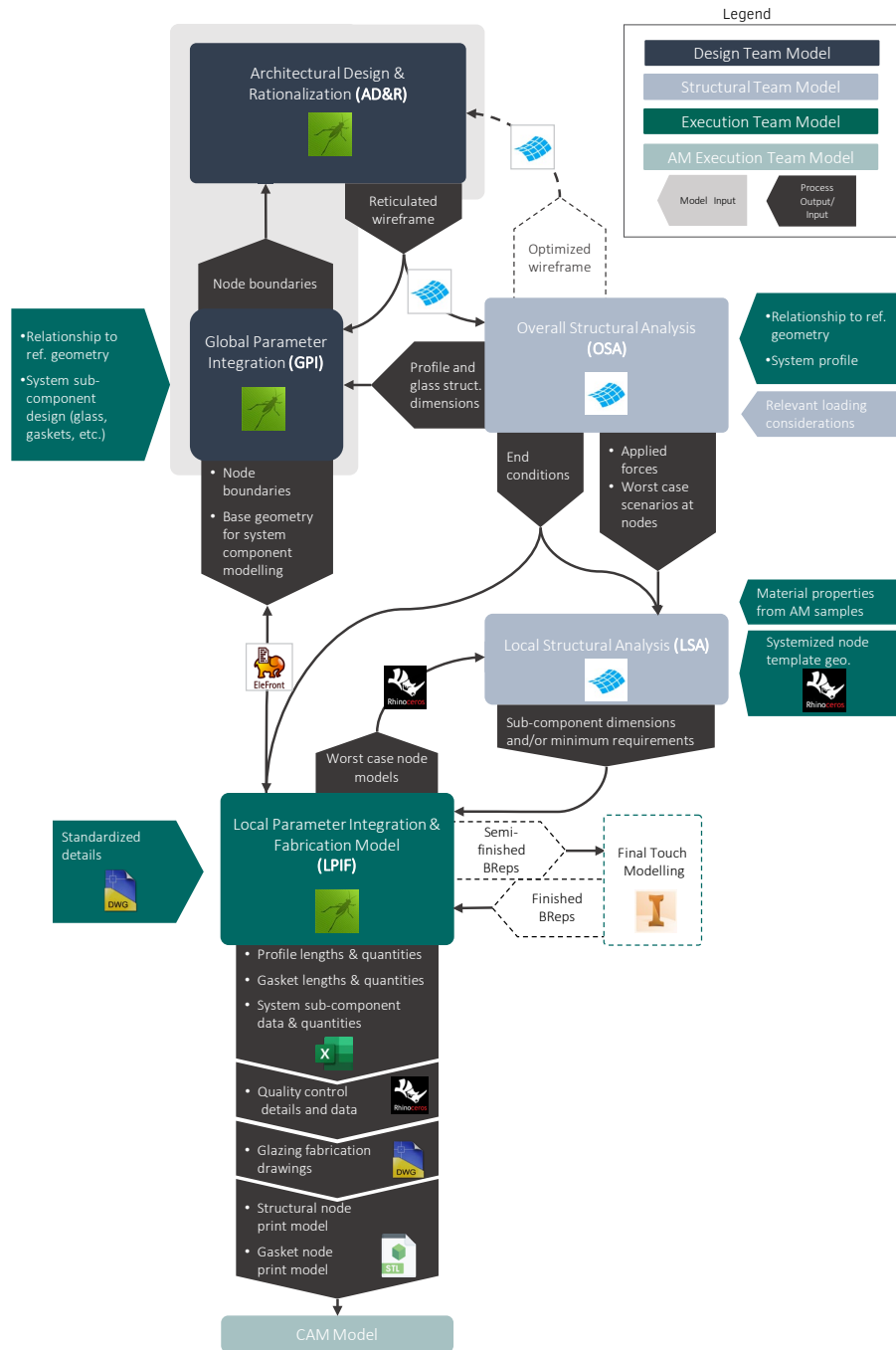


FIG. 6.29 Digital workflow for interdisciplinary collaboration for the design and construction during the development of the Glasstec project. (Image by author)

The first phase of the digital workflow is Architectural Design and Rationalization (AD&R). The starting point for the architectural design is the definition of a doubly-curved surface by the design team. In order to construct the freeform surface using planar (glass) and linear (profiles) elements, the freeform surface is reinterpreted as a polygonal mesh. The faces and edges of the mesh become the reference geometry from which the layers of the façade system are set out.

The AD&R of the design surface is an integral part of FFSGF design as it impacts the structural efficiency, constructibility, and cost of the façade. The early development of the project requires iterative refinement of the geometry and the rationalization to suit several sometime contradictory objectives. It is thus common for this phase to be integrated with one or both of the next two phases which provide a basis for the optimization of the base surface and/or its rationalization. The phases can either be combined directly, or an interoperable strategy leveraged for file and data transfer. The main optimization priority in the design of AM structural nodes in this project was to minimize the size of the printed intervention in order to reduce printing time and cost. Minimum node size (while maintaining a flat end-face connection) is dependent on a number of system variables including: the shape and dimensions of the incoming profiles; the relationship to the reference geometry; and the minimum radius required between arms. As such, the AD&R model was integrated with the Global Parameter Integration (GPI), which defined the approximate minimum node size, and used it as a fitness value for the optimization of the surface rationalization (Figure 6.30). The geometrical limitations of the base façade system, namely a maximum deviation of 35 degrees from flat adjacent panels, and shape fidelity to the original surface were also integrated into the optimization algorithm.

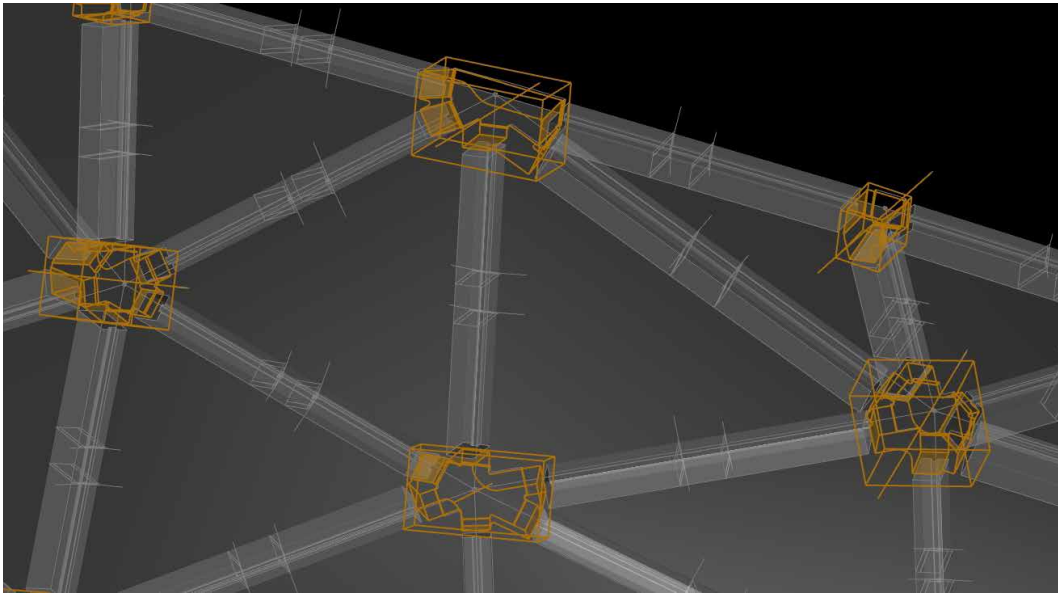


FIG. 6.30 Screenshot of digital data from GPI model fed back to AD&R model for node size optimization. (Image by author)

The integration of minimum node size as a fitness value in the optimization algorithm requires an iterative loop between the AD&R, GPI, and Overall Structural Analysis (OSA) models:

- 1 The AD&R model (owned by the designer) defines and optimizes the rationalized surface .
- 2 The OSA model (owned by the structural engineer) defines the required profile dimensions.
- 3 The GPI model (owned by the designer) calculates the minimum node sizes based on the profile dimensions.
- 4 The AD&R model then optimizes the surface/rationalization based on node size.
- 5 The OSA model is updated to integrate the node sizes to account for the location of the connections in the applied forces to be used in the validation of individual nodes.

This iterative loop is facilitated in the Glasstec project by the integration of the AD&R and GPI phases into a single parametric model, as well as by the use of the SOFiSTiK AG Rhino/Grasshopper Interface tool to facilitate data transfer between the design team and the structural team.

6.5.2 Global parameter integration

The Global Parameter Integration (GPI) model takes as input the reference geometry provided from the AD&R model and the defined profile geometry/dimensions from the preliminary structural analysis. Parametric input variables in this model include the relationship of the façade system to the reference geometry and the main dimensions for the rest of the façade system components in order to properly set out the “digital building blocks” for each of the façade system layers and components. These digital building blocks are the main output of the GPI model. They consist of predetermined geometrical data that is eventually used as a basis for the precise parametric modelling of the different nodes and other system components. The GPI model is also a useful tool for exploring different input parameters and visualizing the design and proportions of the proposed façade (Figure 6.31)

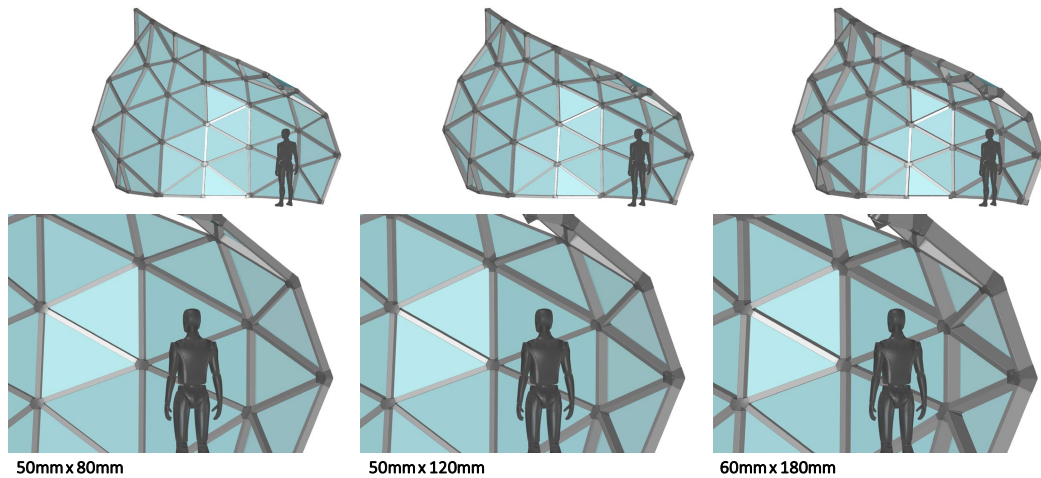


FIG. 6.31 Screenshots of GPI model for quick visualization of project with different profile dimensions. (Image by author)

For the Glasstec project, the GPI model, as previously mentioned, was integrated with the AD&R model. The GPI phase was used to define the minimum length of each node arm required to enable a 90 degree end face. A minimum bounding box was built around the node boundary geometry to quickly calculate the overall node sizes. This information was fed back to the rationalization phase as a fitness value for rationalization optimization.

6.5.3 Overall structural analysis

Overall Structural Analysis (OSA) validates the structural stability of the overall structure and calculates the internal forces in the façade system. The output wireframe from the AD&R model is imported into the OSA model, and can be embedded with additional information to facilitate the analysis model setup using the SOFiSTiK AG Rhino/Grasshopper Interface tool [226]. In the first iteration(s) of OSA, the connection type is defined, and the connections modelled at arbitrary locations. The analysis is used to define the profile dimensions. The profile dimensions are fed back to the GPI model, as they are a critical dimension for the setting out of the digital building blocks, and also for establishing the minimum node size. There is an opportunity for the overall structural analysis phase to optimize the wireframe for structural efficiency, but this was not done for this project.

Once the rationalization is finalized and the node size is firmly defined, the reticulated wireframe is updated in the AF&R model to indicate the correct location of the node-to-profile connections and re-output the model for OSA. The OSA model can then run a final round of analysis and calculate the precise loading conditions at connection points, which will be applied to the nodes in the local structural analysis phase.

6.5.4 Local structural analysis

Local Structural Analysis (LSA) is an iterative phase that exchanges data with the Local Parameter Integration and Fabrication (LPIF) model. During the first iteration, the execution team provides a sample or template node, and communicates the variable parameters for the systemized node design. Based on the results of FEA analysis, which takes into consideration the mechanical properties of the printed material, the structural team validates the node design and provides minimum values for the variable parameters based on the structural requirements for the nodes. The minimum values can either be blanket minimum dimensions for all nodes, or unique values for each node depending on its specific geometrical configuration and applied loads. These values are then used as input variables for the LPIF model, which can generate the final node geometry based on the requirements outlined by the engineers.

For the Glasstec project, it was decided to define blanket minimum dimensions for all nodes in order to save time and meet a rapidly approaching project deadline. The engineering team defined a minimum cylinder thickness of 9mm of solid steel required around the hollow core of each node.

The second round of LSA consists of the verification of critical nodes. The critical nodes are generally nodes with extreme geometrical configurations and/or high loads. They are identified by the structural team. The LPIF model owner (in this case the execution team) provides the structural team with accurate geometrical models of the critical nodes, and the structural team validates the nodes through FEA.

6.5.5 Local parameter integration and fabrication

The Local Parameter Integration & Fabrication (LPIF) model translates the geometric building blocks from the GPI model and dimensional requirements from the structural engineer into parametrically generated mass-customized façade component models and supporting fabrication data for a given application. The models and data generated from this parametric definition are used by structural engineers to do FEA of critical nodes and also by various fabricators to fabricate the façade components. The LPIF model has three streams of input:

- The base geometry for system components modelling outputted from the GPI model. These digital building blocks consist of lines and curves delimiting the main system components boundaries and key geometrical information such as structural/gasket profile edges, radii between profiles, node/profile axes, etc. (Figure 6.32)
- Dimensional requirements based on the results of LSA
- Standardized details in the form of CAD drawings or models

For the Glasstec project, these inputs were translated into a comprehensive set of outputs that included:

- Quantity, dimension, and volume data to inform early fabrication quotes
- Structural node fabrication models (Figure 6.33)
- Gasket node models (Figure 5.12)
- An overall model containing the key components in the assembly (Figure 6.34)
- Tabulated datasheets containing the lengths of all the different structural and gasket profiles
- 2D CAD drawings for the fabrication of the insulated glazing units which included the individual panel dimensions and the relative set-out of the interior and exterior panes (Figure 6.35)
- Quality control data including full system cross-sections taken at each profile to do quality-assurance on the model from which the glazing drawings were generated, and data output of critical angles and dimensions to do quality control on node sizing and adherence to system tolerances

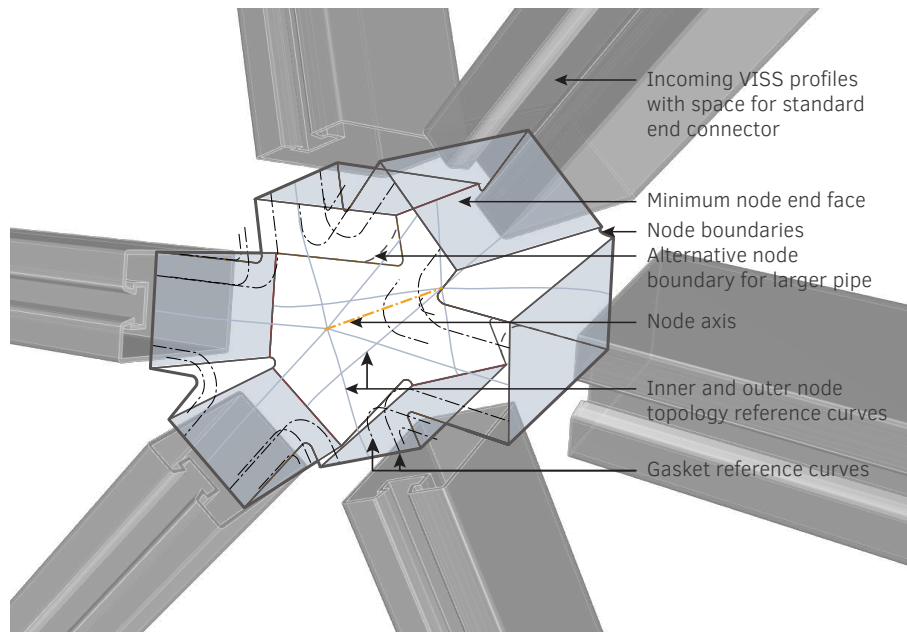


FIG. 6.32 Geometric node “building blocks” that are output from GPI model and input for LPIF model (Image by author)

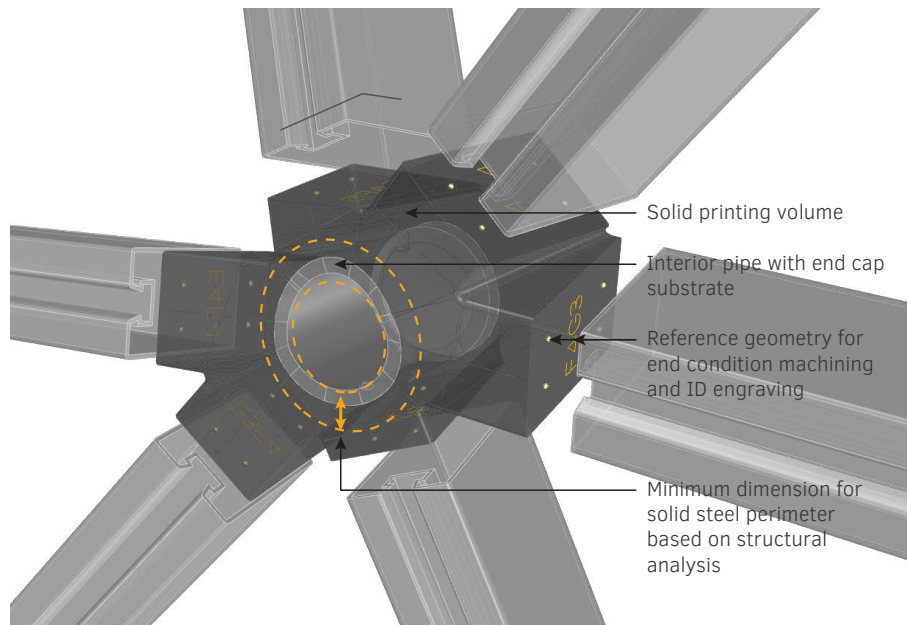


FIG. 6.33 Geometric node data that is output from LSA model and used FEA validation and CAM fabrication (Image by author)

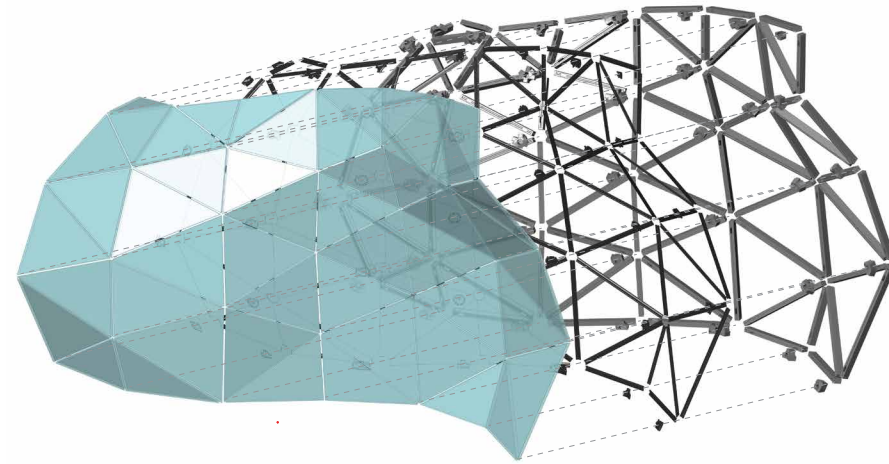


FIG. 6.34 Exploded view of simplified LPIF model (Image by author)

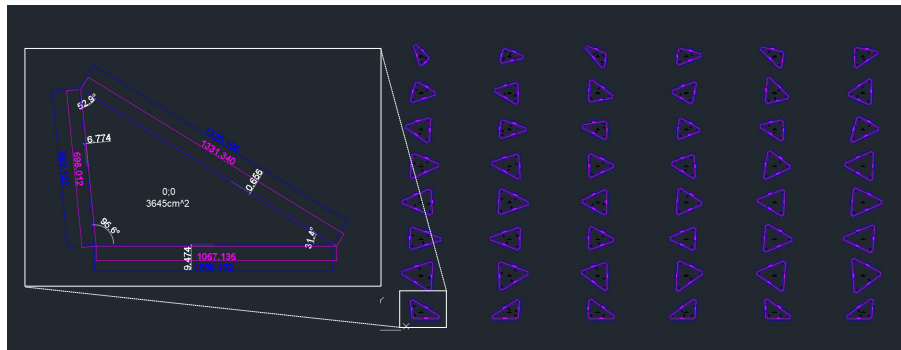


FIG. 6.35 2D CAD output from LPIF model for the fabrication of the insulated glazing showing the individual panel dimensions and the relative set-out of the interior and exterior panes (Image by author)

6.5.6 CAM modelling

CAM modelling is an integral part of AM. For the AM structural node and gasket node explorations, the CAM modelling was undertaken by the respective AM fabricators. The geometry provided for PBF-L and DED-L structural nodes as well as the gasket nodes consisted of solid BRep geometry. For the DED-GMA structural node, a combination of solid BRep geometry and centreline surfaces was provided. The task of CAM modelling varies depending on the AM technology, the CAM software used, and the node design.

6.6 Reflection and discussion

This chapter outlined three design development workflows: one for the initial overall design of the project which informs the AM parts; one for systemized AM structural nodes; and one for systemized AM gasket nodes. It also outlines a digital workflow that facilitates this process and its data exchanges. This section reflects on the strengths and limitations of the approach outlined in the previous sections and offers recommendations based on experience gained during the implementation of the Glasstec project.

6.6.1 Reflection on the proposed project workflows

The realization of the Glasstec project and the workflow outlined in this chapter were structured as best as possible to reflect a plausible project delivery using AM. That being said, the impact of the stakeholder hierarchy inevitably impacts this workflow. Upon reflection, the tasks of the designer and structural engineer seem fairly well represented, although larger projects would benefit from the input of a façade consultant to bridge the gap and between façade design and engineering and facilitate well-rounded façade development.

The outlined role of the execution team, however, could potentially be much more intricate in the context of a different project. In this project, Jansen AG is both the owner, and the majority of the execution team, assuming almost all of the responsibilities of the execution team in the project, including lead contractor, system supplier, steel fabricator, and installer. This is logical for a project in which the objective is to design a system solution for a system house. However, a project whose aim is to develop an object-solution for a one-off construction project would likely integrate a few additional key players such as installers, fabricators, and suppliers, adding additional data transfers and feedback loops.

6.6.1.1 Overall design and connection design

In the workflow described in Figures 6.6 and 6.8, the overall design and connection design are presented as early phases in the project before the development of AM nodes. During these phases, requirements are collected to inform a choice of AM method and subsequently a node design, which are downstream in the workflow. In this configuration, the overall design and connection design create a set of

requirements that the design and fabrication process will have to accommodate. In other projects, it is possible for the development of the structural node to start earlier in the overall design process, for example if there is a very clear design intent for the nodes that would dictate the use of one AM method over another. In such a case, the choice of AM method and the AM node design would influence tasks that are presented upstream in the provided workflow, such as the connection design or the rationalization.

In the Glasstec project, the development of the connections was a high-priority item that had to be resolved before the node designs were developed beyond schematically. Also, since the process was part of an exploration in which several AM methods were going to be investigated, a single connection principle was designed that could be applied regardless of which AM method was used to fabricate the node. In the end, the designed connections required the use of CNC milling. However, development of the connections as an integral part of the node design phase instead of as a preliminary step could potentially avoid the need for subsequent CNC milling. This is mostly relevant for AM fabrication methods such as PBF that are capable of printing parts with high geometrical fidelity and tight tolerances, which are needed for connections. The integration of more intricate connection details would likely entail more complex path planning and/or support structures to enable their fabrication.

6.6.1.2 Structural node design and refinement

Structural node design and refinement accounts for a significant portion of the node development effort. In the proposed workflows, while the overall design and rationalization of the façade is mainly led by the designer, the connection design and the structural node design and refinement are led by the execution team. This is largely due to the organization of the project, which was led by Jansen AG, with the purpose of developing a node that is a complementary system-product to one of their existing system solutions. In essence, the execution team was also the main client and therefore at the center of all important decisions. The execution team is generally well-suited to take the lead for the refinement of the node design since they are familiar with specific façade system requirements, and would in any case be the logical point of contact with the AM fabricators whose feedback is invaluable. In a designer-led project, where the goal is an object solution rather than a system solution, many of the final decisions and approvals in the workflow would be instead the responsibility of the design team.

In the scheme for the Glasstec project, the author undertook the task of refining the node typology in close collaboration with the execution team – namely distilling the recommendations of the structural team and AM fabricators and adapting the node designs to reflect the feedback. This was a challenging task that required multiple rounds of feedback. It is helpful in this phase for the team to be familiar with the principles of DfAM for the selected AM method. Then, the execution team can focus on improving the efficiency of the fabrication process, rather than course-correcting big design decisions.

At the beginning of the node development, the main stakeholders familiarized themselves with the general the principles of DfAM and what is possible to achieve with the different AM technologies. Despite this, during design discussions, there was limited understanding in the room of the intricacies of what is more efficient in terms of path planning, part orientation, geometrical features, etc. The iterative process, in which the execution team bounced back and forth between the design/ structural teams and the AM fabricators, resulted in a node development that was time-consuming and progressed slowly. In the end, despite having completed multiple rounds of feedback, the current node designs still have significant room for improvement to arrive at more optimal solutions both in terms of material usage and fabrication efficiency.

A big part of the challenge in the design and development of AM structural nodes is the degree to which simple decisions affect the tasks and responsibilities of the other stakeholders. Table 6.1, which outlines specific aspects of the design decision-making process and their ramifications on the roles and responsibilities of the designer, structural engineer, and execution team, can serve as a tool to help stakeholders navigate the node design refinement process with a better understanding of the ramifications of their design decisions.

Two core changes to the project structure could help improve the efficiency of the node design refinement process. One option is a more integrated project delivery method. A process, for example, with design workshops where all the different stakeholders are present and develop the node together would drastically speed up the design process. First, it would avoid having to plan and coordinate with the stakeholders individually which is time-consuming and logistically tedious. Second, it would also enable the different experts to step in and cut-off impractical ideas quickly, rather than spending time and effort developing them only to be cut off at the next meeting. And third, speeding up design development would allow the team to delve into a level of detail that would enable the design to be more optimal. It should be noted that a design workshop that includes the 3 main stakeholder and the AM fabricator is only practicable after the AM printing method has been selected.

Another possibility to improve this step is to involve an AM consultant in the design development discussions, perhaps even a specialised AM consultant for the AEC industry. Similar to overall design where there is reliance on façade consultants to bridge the needs of several fields, the building industry would likewise benefit from specialty consultants for the use of AM. A consultant specialized in the design and fabrication of AM parts for the construction industry could represent the interests of each of the stakeholders, and support the node designer as a single point of contact to develop a solution that fits the needs of the design, and is efficient in terms of its structural behaviour, fabrication, and assembly. As AM is a relatively new in the construction industry, this field is not yet really present in the façade design and engineering. However, as the use of AM in the industry increases, the inherent complexity of designing AM parts with multidisciplinary requirements makes it likely that we will see the emergence of AM consultants for building applications.

6.6.1.3 Prototyping

First Prototype

The production of the first prototype is an instrumental part of the overall process that presents a few significant advantages. Even if the first prints are not satisfactory, this first prototyping provides a full picture of the node fabrication process, from CAM modelling and machine setup to post-processing, which avoids surprises during the final prototyping and production. It also gives direction for the print refinement process, which can then focus on specific aspects of the design or production in an informed way. This is particularly important because of the high cost of AM fabrication.

For the prototyping phase of this project, the team explored one AM node design and primary method of AM fabrication at a time. Each prototyping phase began by printing a full node prototype, with the exception of the DED-GMA node, for which only a partial prototype consisting of the primary arms and one secondary arm of the node was printed. Exploring one option at a time afforded the team the opportunity to learn from the mistakes of the previous iterations, and continually improve the next prototype, even across AM methods.

In some cases, overall printing efficiency can be improved by printing multiple parts simultaneously. For example, in DED-GMA printing, the required inter-layer cooling time is such that multiple nodes can be printed in about the same amount of time as it takes to print one. However, in printing multiple nodes at once, one loses the opportunity to refine the design, the printing parameters, the path planning, the model delivery, etc. between iterations.

Process/parameter refinement

The majority of the major steps involved in the development of AM structural nodes (for example node design, selection of the fabrication method, prototyping, final part dimensioning, digital fabrication design) would still be part of structural node development regardless of whether or not the nodes are being fabricated with AM. The refinement of fabrication parameters, however, is an integral part of the development of AM parts that is not typical in (or at least not so integral to) the development of non-AM structural nodes. More traditional structural node solutions are built from standardized materials that have standardized manufacturing procedures, standardized geometrical tolerances and standardized mechanical properties. The use of AM is fundamentally different in this sense. The shape of the final part has a significant impact on the manufacturing strategy and vice versa, which in turn will influence the mechanical properties and geometrical tolerances. In order to arrive at the desired design with the desired properties, and with reasonably short printing times, the right balance of print strategy and printing parameters is necessary. Arriving at that balance likely requires exploration – i.e. the iterative refinement of the printing process and parameters.

The iterative refinement of process parameters is important for both DED and PBF printing, although the focus for the two is likely to be different. In DED processes there are significantly more possibilities when it comes to path-planning. The printing sequence, the relative orientation of the substrate and the print head, the deposition pattern, the layer thickness, etc. will all have a significant effect on the efficiency of the fabrication process, as well as the aesthetic, tolerances, and mechanical behaviour of the nodes. In PBF printing, since the process is a relatively slow fabrication method, the process/parameter refinement phase is particularly helpful to find a balance between mechanical properties, printing speed, and surface quality. Increasing the printing speed by increasing layer height or scan speed will, as discussed in Chapter 4, negatively affect mechanical properties, which in the end will require a more robust node. It will also increase surface roughness which may require additional post-processing.

The advantages of the systemization of the AM solutions became particularly evident during the parameter refinement phase – a process which was both time-consuming and expensive. This particular project was exploratory and made allowances for the extra time, cost, and effort required for this phase. In cases where the design team wants a bespoke AM node solution, similar allowances will also have to be made. However, as different node solutions come to market, the systemization of node solutions will allow project teams to skip over this particular step, as the parameters will already be refined for the node in question.

6.6.1.4 Digital fabrication design

The responsibility for the generation of the fabrication data for the AM nodes in the Glasstec project belonged to the execution team, and was undertaken by the author on their behalf. An advantage of prescribing the ownership of the LPIF model used to generate node fabrication data to the execution team is that the node fabrication data is integrated with the fabrication data for the rest of the façade components. Combining all of the digital fabrication information in a single platform simplifies quality control and avoids potential modelling errors that might translate to fabricated parts.

6.6.1.5 Gasket node design

The process for the development of AM gasket nodes is much simpler than for AM structural nodes. Since the component does not contribute to the architectural aesthetic of the façade, input from the design team is not necessary. More importantly, since the component is not structural and has no life-safety implications, feedback loops with the structural engineer are also not necessary. This avoids the slow iterative process that restrains the structural node design. The development of gasket nodes is also unlikely to necessitate drastically different solutions across various projects, as the requirements for gasket designs and materials tend to exhibit less variation from one project to another compared to structural nodes.

The execution team is responsible for the design of a gasket node that has a suitable interface with the node below, the glass above, and the incoming extruded gasket profiles in order to maintain the continuity of the compressive seal and the internal drainage across the node to achieve good system performance. An advantage of the design and development of both the structural node and the node gasket being led by the execution team is that they can conveniently be made compatible with one another.

The most challenging part of the gasket development process faced during the Glasstec project was the identification of suitable materials, since high quality gaskets should adhere to a number of requirements – including information that is not readily available on technical data sheets such as resilience to long-term UV exposure, chemical compatibility with other system products, hydrophobicity, etc.. The materials identified in this study were suitable for a first proof-of-concept for an AM gasket, however more testing is needed before confirming whether the materials are suitable for long-term use in an actual façade.

6.6.2 Reflection on the proposed digital workflow

Working with digital models is an essential part of the process in the realization of freeform steel and glass façades, regardless of whether or not AM is being used. Digital workflows with clearly defined responsibilities, inputs and outputs, and interoperability strategies are an important part of project planning to enable the level of collaboration that is necessary to build interdisciplinary projects successfully. As such, the design and development of AM nodes should fit into a cohesive digital workflow for the realization of freeform steel and glass façades.

The digital workflow described in this chapter was ultimately successful. The collaboration progressed smoothly, and the end product was successfully constructed and completed on schedule. The workflow strategy also allows plenty of freedom down the road to adapt the definitions to a different architectural design, profile geometries, type of gasket etc. as the system design evolves and different projects are explored. Upon reflection, there are a few aspects of the digital workflow that stand out, either because they were particularly helpful, or because they should be improved upon.

One of the more successful aspects of the digital workflow was the separation of the Global and Local Parameter Integration Models. Upon reflection, there are three main advantages to organizing the workflow in this way. First, this strategy allows the LPIF model, which generates complex node geometry, to be non-project specific. The LPIF model is an algorithm - a defined sequence of instructions to process input variables. Each systemized node design requires its own algorithm. By separating the GPI and LPIF models, and by prescribing strict formatting requirements for the necessary LPIF model input variables, LPIF models can be easily be used in future projects, or interchanged for quick exploration of different node possibilities. For the Glasstec project, LPIF models for each of the node designs were being developed in tandem while the fabrication and evaluation of the benchmark nodes was underway. When the decision was made to move forward with the DED-L node, the geometrical output from the GPI model was plugged into the LPIF model for the DED-L node and the fabrication data for the structural nodes was rapidly generated.

Second, the division of the GPI and LPIF models enables the two phases of the project to have different owners. While the model ownership will not necessarily always be as defined in this workflow, it is a logical division of responsibilities. The architectural design team is responsible for the design model in such a way that they have maximum design freedom and control over the development of the overall design. The execution team, which is likely to work on a wide variety of projects using a similar façade typology, can build a library of LPIF models for future projects.

This strategy, however, depends on the clear definition of inputs, outputs, and requirements for data structures to be successful.

Lastly, this configuration compartmentalizes the overall algorithm for the façade and lightens the computational load in both phases. The GPI model generates only geometric primitives such as lines and surface, and avoids computationally demanding operations such as boolean operations. Because of this, the outputs of the GPI model can quite effectively be integrated into evolutionary algorithms to optimize the overall geometry or rationalization in an informed way. The simple output can also be used as a quick tool for visualization or inspection of the overall design for general detailing, clash detection, etc., in a light and flexible parametric model without significant computational effort. Once the overall geometry is settled, the LPIF model, which requires much heavier modelling operations, can then recompute the updated output geometry from the GPI model.

Another aspect of the digital workflow worth discussing is the configuration for the iterative refinement of the overall geometry and rationalization. In complex projects, it's common for the design optimization/rationalization phase and structural analysis to be subcontracted to a façade consultant since these two aspects of design are closely linked and have a significant impact on structural efficiency and constructibility. In this project, there was no separate façade consultancy and so the task of optimization relied on a close, iterative collaboration between the design team and the structural team. The design team maintained ownership of the parametric model for design exploration and visualization and the structural team maintained ownership of the structural analysis model. The SOFiSTiK AG Rhino/Grasshopper Interface tool [226] was used to share model updates between the two teams. This worked quite well for a situation where the optimization objectives were not structural. However the inability to facilitate multi-objective optimization integrating both structural optimization and AM optimization is a notable caveat of the digital strategy. In order to do so, a more integrated approach would be needed.

While the optimization phase was ultimately successful, upon reflection there is a notable shortcoming in the execution of this task for the Glasstec project. The rationalization optimization for the Glasstec project was undertaken, as is typical in freeform projects, at the early phases of the design. The final geometry for the façade was therefore frozen quite early in the overall process so that the team could move forward with other tasks. The optimization process focused on configuring the surface and rationalization to generate nodes that are as small as possible based on their overall bounding box dimensions. This was done with the general understanding that AM is costly and time-consuming and smaller nodes equate to less printing time and cost. Moving forward, it would be beneficial to optimize the

overall design and rationalization based on metrics specific to the node design rather than aiming for small nodes in general.

For example, for the final DED-L node design which was used, one could optimize the overall design to minimize total printing for all nodes by finding the right balance of node configuration for larger pipe sizes. Such an optimization would result in nodes that take up a larger volume, but require less printing effort due to the increase of pipe size and consequent void in the node centre. For the final DED-GMA node design, the minimum size of the node is less critical because the material deposition speed is relatively quick. Rather, the optimization could focus on distributing the arms as evenly as possible to avoid the tight spaces that drastically increased printing time and path-planning effort. For final PBF-L node design, a logical optimization metric would be to minimize the node size specifically with a similar distribution of arm lengths. This would reduce the necessary cross-bracing of the interior wall structure along the arm lengths, reduce the amount of material required to print the exterior walls, and it would reduce the node footprint which impacts the amount of support structure required, which accounts for a significant amount of the printing time.

The optimization of the overall geometry based on the actual node design could play a significant role in reducing the printing load for a project. In an exploratory project such as this one, this is difficult because the node design is not yet known at the beginning of the project when the original optimization takes place. Potentially, an additional round of overall optimization could be integrated into the end stage of the project, however this would require revalidating the overall structural design, recalculating structural actions, and ensuring that the connection capacities are not exceeded. However, in projects using previously developed system solutions where the key geometrical metrics impacting fabrication efficiency are known, targeted optimization could play a significant role in reducing the printing load.

Another notable weakness in the digital workflow was the amount of manual work required in the end to finalize the model. Throughout the project, Rhino/Grasshopper was used as the main platform for ODR, GPI and LPIF phases. While this tool was ideal for ODR and GPI phases, the level of detail required for LPIF was difficult to manage in this platform. Some of the more demanding geometrical operations required additional intervention to achieve. Filleting, for example, which can be a challenging geometrical feature to compute because “it involves not only geometrical calculations but also topological modifications”[\[227\]](#), and which was required often in the nodal components to match the base system geometries, was achieved by either roundabout-modelling approximating a true fillet in grasshopper, manual intervention in the Rhino environment, or even exporting to other platforms to

achieve. Similar issues were faced with Boolean operations. This step is shown in the digital workflow diagram (Figure 6.29) in dotted lines as "Final Touch Modelling". In future applications, several strategies could be implemented to avoid this. For example, the modelling strategy in grasshopper could be updated to circumvent these challenging operations, or other parametric modelling tools could also be explored either as a supplement to or as a replacement for Rhino/Grasshopper. Ultimately, the tool or collection of tools that is used should be able to undertake the modelling requirements of the specific node components, it should be compatible with the requirements, capabilities, and digital resource of the various stakeholders, and it should facilitate digital data exchange across platforms and stakeholders.

Additionally, the outputs generated from the definition, while providing a good basis for manufacturing, could have been developed further. Glass drawings consisted of the general dimensions, outlines and relative positions of the panes of glass, but lacked additional information such as line weights, layers, tolerances, additional IGU components and title blocks to create a quality fully automated fabrication drawing set. The node geometry consisted of closed solids and limited engraving data, but could in future projects be further developed to automate some of the CAM modelling for printing and machining. This is particularly relevant for DED printing because of the potential complexity of path planning. Finally, the assembly could be outputted to common Building Information Modelling (BIM) platforms. BIM models have become an important collaboration tool for multidisciplinary projects, and particularly for the execution team, contain information to facilitate various phases of the execution process for example procurement, stock management, fabrication, and assembly.

6.6.3 Recommendations for the interdisciplinary development of AM parts for buildings

The overall process and experience of the design and realization of the Glasstec façade offered a first-hand experience on the integration of AM in an architectural project. Many of the lessons learned over the course of the project are also relevant for the development of other AM projects in the built environment, not only nodes. In addition to the description of the different methods and digital workflow, this chapter offers the following recommendations based on the experience:

- In order to maximise fabrication efficiency, AM building component design benefits from starting with the selection of an AM process, which should be informed by specific requirements, including its relationship to other building components.

- The design development of AM parts should be a close collaborative effort between the design, engineering, execution, and AM-execution teams. Design workshops early involving all parties are recommended early in the design process. The emergence of consultancies specializing in the use of AM for architectural applications would be beneficial to the development of structural node solutions.
- All stakeholders who are affected by the design of the AM part should have a basic knowledge of the principles of DfAM and of how certain design decisions affect the responsibilities of the other stakeholders in order to have productive discussions and streamline design development.
- For the design of systemized structural parts, qualitative feedback on part topology by the engineering team in the early phases of the design can help drastically improve its structural efficacy, and reduce material usage and printing load in the end.
- An initial comprehensive AM prototype including post-processing followed by smaller prototypes for process refinement are a good strategy for identifying fabrication bottlenecks early, and having more focused prototyping efforts later, improving the design in an informed way.
- A dedicated phase during AM part development for refinement of the print strategy and printing parameters is an important, albeit time- and cost-intensive step in the development of structural AM parts to achieve a balance of print quality, good material properties and fabrication efficiency.
- Particularly for mass-customized products, the development of AM parts as system products could enable certain time- and cost-intensive phases of the project such as print parameter refinement and performance testing to be skipped in future applications.
- The definition of a digital workflow strategy with clearly defined inputs and outputs enables smooth interdisciplinary collaboration, facilitates design flexibility, establishes a good foundation for quality control measures, and can significantly reduce the digital modelling workload in future projects.
- If possible, an optimization phase that reduces the print load of mass-customized parts should be based on the most effective fitness values for the specific AM part design in order to maximize the impact of the optimization. If the optimization can only take place before the AM part is designed, optimization to minimize bounding box can also be moderately effective.

6.7 Conclusion

This chapter reviews the interdisciplinary collaboration that was conducted during the design and development of a freeform façade with AM structural and gasket node components, including an exploration phase undertaking the development and prototyping of several node designs and AM methods, and the construction of a mock-up and of a full-scale freeform façade. From this experience, a workflow is outlined for the design and development of AM components for freeform steel and glass façades that provides a roadmap for the iterative development of AM components with consideration for the responsibilities of the different stakeholders. It also outlines a strategy for the organization of a collaborative digital workflow that facilitates this development, and concludes with recommendations for future interdisciplinary AM construction projects.

The development of structural nodes, in particular the collaborative refinement of node design and the iterative process of printing parameter refinement, highlights the complexity of AM structural node design. This complexity stems from the importance of structural nodes in the design, structural performance, system performance, and constructibility of façades, and from the complex correlations impacting the design, fabrication, and mechanical properties of AM parts. The structural node design process can be expedited and design outcomes improved by enhancing stakeholder familiarity with DfAM principles and having a more integrated design development. In order to support the design development of structural nodes, this chapter provides a detailed list of key facets of structural node design in which decision-making impacts the tasks and responsibilities of several stakeholders, often in contrasting ways.

In contrast to the design and development process of structural nodes, in which the designer and structural engineer play pivotal roles, gasket nodes require a collaboration between only the execution team and AM fabricator. In the outlined workflow, the initial validation of material properties precedes node topology design, highlighting the importance of material selection in influencing gasket design. Integration with the base façade system guides the refinement of the node topology. Compatibility of the structural node and gasket nodes is made notably easier in this particular project by being the responsibility of same stakeholder.

This chapter also describes a digital workflow that supports the processes outlined for the overall façade development, structural node development, and gasket node development, enabling collaboration through clearly defined inputs and outputs.

The workflow is compartmentalized in modelling phases corresponding to the responsibilities of the stakeholders. It enables flexibility over the course of a design exploration, and also moving forward into other applications. Critical reflections on the digital workflow highlight areas for improvement, in particular facilitating multi-objective optimization that includes both structural optimization and AM optimization, and aligning AM optimization more closely with the specific demands of AM node designs.



Detail view of additively manufactured structural node in freeform façade (Image courtesy of Jansen AG)

7 Conclusion

This dissertation included an exploration of existing construction methods, a review of AM node precedents, an investigation into the properties of AM materials, the development and analysis of AM structural nodes and gaskets nodes, and culminated in the realization of a full-scale freeform steel and glass façade complete with additively manufactured components.

This final chapter summarizes and highlights the main findings of this research, and frames the different steps undertaken in the context of the main research question. This is done by first answering individually each of the sub-questions, which were subdivided as chapters in this book, and which, when taken as a whole, begin to provide a comprehensive answer to the main research question. The limitations of this research project are denoted, topics for future research are discussed, and final remarks are made on the role of additive manufacturing in the future of the construction industry.

7.1 Introduction

This dissertation aimed to facilitate the integration of AM into the design and construction of freeform steel and glass façades to improve current FFSGF detailed design strategies. In order to provide a comprehensive answer to the main research question, this research used a combination of literature review, an exploration of the design and fabrication of AM components, and a case study on the interdisciplinary realization of a FFSGF using AM components. This chapter provides answers to the supporting sub-questions and main research question, followed by general conclusions, limitations of the study, recommendations for further research, and final remarks.

7.2 Research Sub-questions

The main research question for this dissertation is the following:

How can additive manufacturing be effectively utilized to develop node solutions that support freeform steel and glass façade construction?

In order to answer the main research question, this dissertation first answered a series of sub-questions that each provide a partial outcome contributing to a comprehensive answer of the main research question. Each chapter consists of one main sub-question, while Chapters 4 and 5 also have additional sub-questions to gather supplementary background information required to answer the main sub-question for the chapter.

Opportunities to improve on current FFSGF construction practices through the use of AM (Chapter 2)

The first step in answering the main research question was to identify key challenges of FFSGF construction that can potentially be improved by the use of AM. In order to answer this sub-question, this chapter provides a comprehensive overview of structural nodes solutions and enclosure system solutions applied in FFSGF from 2000 to 2020. Information is collected on the overall design of freeform steel and façades, roofs, and canopies, the detailed design of their structural systems and enclosure systems, and the fabrication methods used for their realization. The different solutions are classified into general typologies. For each typology, the strengths and limitations in terms of their geometry, fabrication, and applicability are identified and subsequently discussed.

From the overview, four opportunities are identified from the study of existing FFSGF construction solutions that can potentially be improved by the freedom afforded by additive manufacturing. The first opportunity is to develop an AM structural node solution as a “system product”[19] that is applicable to a wide range of geometrical configurations and that can achieve material efficiency, fabrication efficiency, and geometrical flexibility without compromising design efficiency or assembly efficiency. The second is to use AM as a tool to design structural nodes that contribute with their appearance to the architectural expression of a façade, uninhibited by the limitations of traditional fabrication methods. The third is the potential development of additively manufactured mass-customized interior gasket nodes. The fourth

opportunity is to explore AM for the fabrication of exterior gasket nodes and a corresponding capture system that would enable the construction of a dry-dry, pressure equalized freeform façade system as a means of avoiding pressure-driven leakage and condensation.

In addition to the identified opportunities for AM intervention, the overview and discussion of construction strategies for both the structural system and enclosure system can be a useful resource for architects and building professionals during the early phases of the design process for a FFSGF.

State-of-the-art in the use of additive manufacturing for freeform façade construction (Chapter 3)

The next step in this research was to identify relevant research gaps in the use of AM for nodal components and connections in steel and glass façades. A literature review was used to present an overview of the use of AM in façades that includes the range of façade components under investigation and the AM printing methods and materials used to design and fabricate them. A more detailed review of the most relevant articles is also provided, namely those pertaining specifically to AM nodes and connections.

Since the use of AM in architecture is relatively new, there is only a small pool of relevant literature available. As such, several research gaps were identified: there is no precedent for the exploration of AM for gasket nodes; there is no precedent for a systemized AM structural node for a steel and glass façade system; there is no precedent exploring AM methods with higher deposition speeds such as DED printing for the fabrication of structural nodes; and there is no study exploring how the use of AM can practically be integrated into a complex interdisciplinary workflow.

The use AM to improve the design of structural nodes (Chapter 4)

Chapter 4 aims at answering the following question: To what extent can the use AM improve the design of structural nodes? This research question explores whether and to what extent structural nodes can be improved relative to existing solutions through the use of AM. Improvement to structural nodes is defined, based on the discussion in Chapter 2, as overcoming a compromise between geometrical flexibility, material efficiency, and fabrication efficiency without compromising assembly efficiency or design efficiency.

In order to answer this question, several AM nodes for different AM methods are designed, fabricated, and compared to a CNC milled node. However, a few preliminary steps were needed prior to the design and fabrication of nodes. The first was to provide an overview of different metal AM methods in order to refine the scope of the design exploration, from which two are selected as a basis for comparison. The second was to validate the material properties of AM metal for structural components in buildings. To do this, stainless steel 316L was used as a basis for exploration. In the final step, node designs are developed for three different AM methods guided by their respective design guidelines, fabricated, and compared to benchmark milled nodes in terms of material efficiency and fabrication efficiency.

The mechanical properties of the material under investigation displayed significant variation between printing methods and also within printing methods due to differences in the fabrication process, including printing parameters and post-processing. Minimum requirements for ductility, fatigue, and fracture toughness were met by AM materials, but not invariably so. This section confirms that the mechanical properties of AM parts produced with all three AM methods are in general quite promising since mechanical properties were shown to be able to approach, meet, or exceed benchmark values and Eurocode requirements in all cases where information was available. However, it also highlights the need for material testing based on the actual printing parameters and overall fabrication process of the end-use part, as the material properties are heavily impacted by orientation, printing parameters and post-processing.

The comparison of the AM structural nodes to the CNC milled nodes highlighted the strengths and weaknesses of the respective node designs and AM methods. In terms of fabrication efficiency, the complexity of path planning appeared to be a very significant factor in whether the printing time using DED was better or worse than the solid milled node. The complexity of the geometry was a significant factor in the material usage, particularly because of the specific end connection requirements of the node. For the PBF-L node, the fabrication time for a single node was significantly higher than all the other options. However, the use of industrial PBF-L technology could significantly improve its relative fabrication efficiency.

This chapter concludes that improvements to existing node solutions can potentially be made through the use of additive manufacturing, but this is not necessarily a given. Ultimately, the extent to which AM can be a more appropriate choice than more traditional structural node solutions, depends on a few key factors: the quality of the design of the AM node and its compatibility with the specific AM method and fabrication strategy; the compatibility of the AM node solution with the specific structural and geometrical requirements of the application; the potential for node

weight reduction and the extent to which weight reduction at nodes would positively impact the structure; and finally the design intent of the project and whether traditional fabrication methods are able to meet the node design ambitions.

In addition, this chapter provides an overview of the fabrication process and corresponding fabrication data to provide a realistic benchmark for future AM nodes. Reflections on the current node designs and fabrication strategies in combination with recommendations for the design of AM structural nodes provide insight for future projects to avoid similar inefficiencies and develop more optimal node solutions.

The use of AM to provide better solutions for node conditions in the interior drainage layer (Chapter 5)

Chapter 5 answers the following question: To what extent can AM provide better solutions for node conditions in the interior drainage layer? This research question explores the feasibility of an AM gasket node as a means of achieving a mass-customizable product that enables a wider range of geometrical configurations, standard connections, a high-quality air- and water-tight compressive seal, integrated hierarchical drainage, and avoids undesirable water pooling.

Four potential materials for four different AM methods were identified from material databases based on benchmark mechanical properties from a gasket material standard. A benchmark prototype was designed to incorporate geometrical features that are likely to be integrated in a gasket design. A preliminary prototype was printed using all four materials/methods. Finally, a full gasket prototype including all of the identified features for an AM gasket was fabricated.

During the course of this investigation, several materials were found within the range of the benchmark properties outlined in the material standard. While this is not sufficient to conclusively state that the AM materials adhere to Eurocode requirements, since these are based on façade assembly testing, it is sufficient to validate the materials for a proof of concept. All four AM materials/methods that were explored for the first round of prototyping were successful in printing complex AM parts integrating all of the outlined geometrical features with high fidelity.

For the second round of prototyping, a gasket node design was defined that incorporates all of the gasket features identified in Chapter 2: standard connection with incoming gasket profiles; cross-sectional change; hierarchical drainage; and a standard interface with structural nodes. The gasket node can also be mass-

customized through the use of AM and integration into a parametric modelling workflow. This gasket node design presents a qualitative improvement on current node solutions as it integrates the above-mentioned gasket features. These features serve to facilitate assembly and overcome the vulnerabilities of existing node solutions, which are largely attributed to difficult but critical workmanship and irregular, geometrically challenging settings.

Detailed fabrication data for the printed prototypes was not collected and therefore no information is available on the fabrication intensity of the proposed solution. The fabrication intensity of the AM nodes is almost necessarily significantly more demanding than the other gasket node solutions. However, one must consider how the advantages of facilitated assembly and mass customization would provide significant improvement in terms of on-site assembly efficiency and façade performance in geometrically complex conditions.

Integration of AM in an interdisciplinary collaboration for the realization of a FFSGF (Chapter 6)

Chapter 6 answers the following research question: How can additive manufacturing be effectively integrated into interdisciplinary workflows for the realization of freeform steel and glass façades? This last step in the study discusses the process of working with additive manufacturing technology in an interdisciplinary workflow typical of freeform steel and glass façade construction. The workflow is drawn from the experience of the realization of a FFSGF with AM node components by a multidisciplinary team.

The answer to the question is given in the form of an organized approach in which the tasks and responsibilities of the main project stakeholders, important flows of information and feedback, and iterative development phases are outlined. The method described is divided in 3 main phases: the overall architectural design and connection design; structural node development; and gasket node development. This approach is accompanied by a digital workflow that provides a framework for the necessary detailed design information and digital data exchanges of the three phases. This chapter also provides recommendations to facilitate AM product development for the built environment.

7.3 Main Research Question

The main research question for this dissertation is actually quite broad as it includes two relatively open terms. The first is additive manufacturing, which encompasses a range of different manufacturing methods that are different in terms of their possibilities, strengths, weaknesses, and design limitations. The second is the improvement of node solutions for FFSGF which consist of multiple layers and for which there are multiple possible avenues for improvement. To answer this question, this dissertation takes an approach in which the different possibilities are presented, and then a selection of the possibilities are selected for more detailed exploration. First a range of different FFSGF construction methods are reviewed to identify different opportunities where AM could potentially provide an avenue for improvement. From this review, two specific opportunities, namely structural nodes and gasket nodes, are selected for future exploration.

The next step is the development of AM solutions for each of these options. In order to do this, an overview of the available AM methods for the required materials is provided. Then, the material properties for a subset of materials for different AM methods is collected to explore whether the properties of the AM materials are practicably suitable for construction. The products are then designed, fabricated, and the extent to which they are able to improve on existing solutions is discussed. Finally, the entire product development process from the previous phase is made explicit in workflows that outline how AM can be effectively integrated into the interdisciplinary process of a FFSGF construction, and how this integration impacts the roles of the key stakeholders.

The dissertation as a whole functions as a process demonstration that can support the future development of AM structural nodes and gasket nodes. For future researchers following a similar path, recommendations and lessons learned from the experience are outlined along the way.

The development of AM nodal components as system products was hypothesized at the beginning of this study as a means of achieving a level of design efficiency, engineering efficiency, and assembly efficiency. This hypothesis was induced by the ubiquitousness of system products in the façade industry because of their benefits in design, digital modelling, engineering, fabrication, and assembly processes. The approach to systemize AM nodes revealed its advantages at nearly every step throughout the course of this study.

As discussed in Chapter 4, the mechanical properties of AM parts are dependent on a range of factors including the AM method used, the printing parameters, and the shape and orientation of the AM parts. This is particularly important because metal AM parts are susceptible to poor ductility. These factors are also key variables in the fabrication efficiency of AM parts. The systemization of node products supports the standardization of the printing process and its parameters which has several benefits. As discussed in Chapter 6, the refinement of printing properties is an important step, particularly in the design development of structural nodes. This process refinement works towards finding a balance of the right printing parameters and path planning to achieve the desired balance of surface quality, material properties, and fabrication efficiency, and to avoid printing defects and failures. While this step is crucial, it is also time-consuming and expensive, particularly because of the lack of AM norms and standards, and the lack of construction legislation supporting the use of AM. The systemization of node solutions allows future products using a previously developed systemized node to skip this step. Moreover, the certification of AM products for the building industry is an important next step in their proper integration into the built environment, and this will require the ability to produce parts with good, predictable, and reliable mechanical properties. The development of AM parts as system products with standardized printing processes is a logical strategy towards that end.

In addition, as systemized node solutions come to market, designers will have a library of interchangeable AM nodes to choose from. This will enable system providers to provide practical information to help designers make informed design decisions when selecting node products, for example regarding the structural capacity, cost, fabrication efficiency, and geometrical limitations of specific node products. Thus, designers will have the possibility to select from a range of pre-existing solutions with the knowledge of the extent to which these solutions are suited to their specific application, and how they compare to other more traditional node solutions. In addition, the selection of predefined system products during the early phases of a project enables the targeted optimization of the façade geometry and rationalization based on the key metrics of a specific node product. This can significantly improve material usage and fabrication efficiency compared to if the overall façade design and rationalization is fixed before the node design is selected.

Ultimately, while the additive manufacturing of nodes is undoubtedly a possible route for the production of AM nodes, whether it is capable of improving on traditional building methods will rely on optimizing as much as possible their design, material usage, and fabrication, an effort that is greatly supported by AM node systemization.

7.4 General Conclusions

7.4.1 Limitations of the research

The outcomes presented by this dissertation follow the focus and the aims outlined in the introduction chapter. While the results provide answers to the research questions, they should be interpreted as valid within a specific set of boundary conditions. These boundary conditions are expanded upon below.

The first limitation of this research relates to the choice of focusing on specific AM components, methods, and materials. This was due to the fact that the main research question explored steel and glass freeform façades and additive manufacturing, which both have a wide range of possibilities. In order to provide detailed information on the design and fabrication process of AM components, the scope of this research was narrowed to two key components, namely the structural node and gasket node. For each of these components, the detailed exploration was further narrowed to a specific range of AM materials and AM methods. Particularly for the structural node, the exploration is limited to only two AM methods (DED and PBF) and one material (Stainless Steel 316L). The selection of these two AM methods was made because the two technologies were very different in nature and would benefit from different facets of AM. The exploration was centred on only one material since it was felt that a broader exploration including multiple materials would be too exhaustive, and that focus on a single material would enable a clearer comparison of the different fabrication methods.

Another limitation in this research is the exclusion of cost as a metric in the evaluation of the provided solutions. Cost is unequivocally an important factor in the comparative analysis of AM products. However, as AM technology continues to develop rapidly and increase in popularity, the cost of AM will change significantly. As such, an evaluation of the cost is excluded as results would quickly become outdated. It was therefore decided to evaluate nodes based on qualities that impact their value as products, such as the ability to reduce dead load on the structure or improve assembly, and qualities from which costs are calculated such as material usage and fabrication time.

This dissertation covered many aspects of AM node components for freeform steel and glass façade construction. Along the way, a number of key areas for future development were identified. These can broadly be divided into four key objectives: (1) further exploration of AM methods and materials; (2) further development of AM components; (3) detailed investigations to support interdisciplinary DfAM of high-performance parts; and (4) analysis of the sustainability of the approach.

Future research for structural nodes

In Chapter 4, the material properties of Stainless Steel 316L were reviewed from literature to establish the extent to which its material properties are suitable for use in structural components in the built environment. The completeness of the study was limited to the included literature. While PBF-L printing is the only one of the three printing technologies for which values were reported that were either equal to or superior to the threshold requirements and/or properties of wrought equivalent SS316L, it should be noted that there were significantly more articles available on PBF-L compared to DED-L and DED-GMA. This is likely due to the fact that PBF-L technology is generally more established, and is also of-interest across a wide range of industries including aerospace and medicine. Additional studies on the mechanical properties of DED-L and DED-GMA are necessary to make a balanced comparison between the three printing technologies. A more comprehensive study exploring ductility, toughness, fatigue strength, and non-linear stress-strain behaviour of samples fabricated using consistent sets of fabrication variables is necessary in order to definitively ascertain whether such an AM structural part is suitable for use in architectural applications.

In addition, a broader exploration of AM materials should also be undertaken. Chapter 4 explored only the mechanical properties of AM SS316L. It is likely that future applications may require the use of a different stainless steel or carbon steel alloy. In this case, a similar study for the different alloys in question would be necessary. Notably, SS316L was selected as the basis for this study since it is a popular material in the AM industry. As such, it was readily available for prototype printing, and there was a good amount of literature available on the study of its mechanical properties when produced using AM. The popularity of this particular alloy in the AM industry is due in part to its good mechanical properties. Other materials may not present such favourable properties when 3D printed, and should be properly evaluated prior to being used with AM for the building industry.

Moreover, three different structural nodes were designed and printed using different AM technologies and compared in terms of fabrication time and material usage to a benchmark node using CNC milling, and the strengths and limitations of each node design were discussed. Since both of these metrics are very dependent on the node design, the further development of the proposed structural node designs and the exploration of alternative designs would provide a more comprehensive view of the extent to which AM is capable of improving on current solutions. In addition, the broader exploration of different AM methods would provide different opportunities for node development and potential improvement through the use of AM. This is because the design and development of AM parts requires a design strategy tailored to the specific AM method and would therefore require different DfAM approaches, and because the potential of AM as a means of improving on traditional fabrications depends heavily on the compatibility of the node design with its AM method. This is particularly relevant in the development of structural nodes where the possibilities for the design of the object are much broader than for gaskets, as they contributes significantly to the architectural expression of the project.

Future research for gasket nodes

In Chapter 5, AM was applied as a means of fabricating mass-customized AM gasket nodes, and a proof-of-concept node was fabricated. However there is much research to be done before this type of application is ready for market. First, AM materials should be tested to ensure that the properties are indeed suitable for this type of applications, and development in the field of material science may be necessary to develop specific AM materials for architectural gasket applications. While the quality of the prototypes was qualitatively assessed, further research should include façade performance testing to validate their performance in a façade assembly per building industry standards. Also, the suitability of the proposed design and different printing technologies should be evaluated in terms of fabrication time, cost, sustainability, and performance to get a better understanding of the extent to which the advantages of AM gaskets (namely improved performance and assembly) do or do not outweigh the consequent increase in design intensity, fabrication intensity, and fabrication cost that comes with the use of AM over existing solutions. The proposed gasket design should also be further developed based on the results of that research.

Further, in Chapter 2, current industry solutions for nodal conditions in the internal drainage layer were discusses and evaluated based on their integration of different features. The evaluation was done in this qualitative way since very limited information is available on the performance of such façade systems and products. The lack of information regarding the performance of different solutions is

a limitation in this study. The evaluation of air- and water-performance data either from mock-ups or from built precedents of current solutions would provide clearer benchmarks for the development of AM parts.

Future research for other aspects of freeform steel and glass construction

The research question for this dissertation focuses on a specific aspect of FFSGF, namely nodal conditions. As such, the work in this dissertation explored primarily two key components of FFSGF construction: structural nodes and gasket nodes. Notably, this study did not investigate the potential of AM for glass – an integral part of steel and glass façades. As was seen in Chapter 3, the use of 3D-printing technology for infill elements is a relatively common topic in studies related to additive manufacturing in façades, and amongst these were two examples of 3D printing for glass components. The first described a novel method for creating monolithic glass elements for buildings with customized colour, opacity, and relief, while the second explored rapid tooling sand moulds for custom glass parts.

Beyond these examples, there is also potential for the use of AM to improve glass infill elements for the construction of FFSGF. This research addressed the challenges of FFSGF primarily by implementing a few key strategies to node components: facilitating assembly and improving performance through improved connections and interfaces; minimizing dead loads through material efficiency; and optimizing fabrication and assembly of mass-customized components through digital fabrication. While these aspects were applied to structural nodes and gasket nodes, the strategies are also applicable to glazing units.

For example, in order to improve performance, glazing units could be fitted with edge conditions such that the interface between the glass and structural profile/gasket profiles is co-planar, improving the integrity of the seal. In order to reduce the panel weight, strategic reinforcements can be applied to glazing units such that much thinner panels can be used. Such a strategy has already been explored in [230], but can be further developed for freeform applications. To improve fabrication and assembly, components such as spacers or toggles can potentially be integrated directly using AM.

For all of the above, while it's possible that glazing units be printed in their entirety, additive manufacturing for glazing units would likely benefit most from hybrid manufacturing methods where AM material is deposited on mass-manufactured glass. In this way, since it will be nearly impossible for AM glass to compete with

float glass in terms of transparency, visual quality, and fabrication efficiency for large components, the end-product benefits from the speed, efficiency, and aesthetic of float glass, and the geometrical freedom and mass customization of AM.

In addition to additively manufacturing glass, exploration into how AM could potentially improve other components in freeform façade assemblies, for example printing mass-customized toggles, or printing exterior components to enable freeform dry-sealed systems could also yield interesting results.

Supporting information to make more informed decisions during the design of AM components

In addition to the above, the design development undertaken in the course of this research highlighted some of the areas in which further exploration would help in making more informed decisions during the design process with the goal of maximizing the potential of additive manufacturing, while minimizing its drawbacks.

One important example is the study of AM structural materials. The complex interactions between printing methods, printing parameters, AM materials and part shape and orientation and their impact on the physical and mechanical properties of AM parts is not entirely understood and is an actively evolving topic in the field of material science. At this point in time, working with AM in the built environment requires lots of quality control testing and conservative assumptions to ensure the safe and reliable performance of AM parts. Once the body of knowledge on this topic is sufficiently developed, AM norms and standards can be developed and adopted in legislation to support the design and engineering of structural AM parts for the built environment. The use of AM can then begin to take a more cemented role in the fabrication of complex parts for the construction industry, and designers can be bolder and less conservative in the design and engineering of AM parts, enabling further reduction of material in structural parts and ultimately making AM a more cost-competitive option.

Another aspect in which additional knowledge would be helpful in the development of AM nodes is the implications of detailed façade design decisions on the suitability of AM as a whole, or of specific AM methods. This topic was briefly discussed in Chapter 4 where it was noted that the fabrication efficiency and material efficiency of different node solutions can be quite sensitive to seemingly minor changes in the detailed design of a façade, such as its panelization strategy or profile proportions. A follow up study can be done to explore the extent to which different variables in the detailed design of FFSGF affect these metrics. This study would be helpful in

understanding the suitability of different solutions to support early design decision making in a FFSGF project, or could be used as fitness metrics in optimization algorithms to minimize material usage and fabrication times.

Sustainability

Lastly, because of the significant role of the built environment in the climate crisis, the building industry has a responsibility to improve current building practices. The building envelope is a key element in the overall sustainability of a building. On one hand, façade systems are responsible for a significant portion of the environmental impact of a building. According to Hartwell and Overend [231], embodied carbon for initial construction of modern-day façades is around 13–30% of the whole building footprint, and this number increases when on-going maintenance is taken into consideration. On the other hand, the carbon footprint of a building related to its operational performance is closely related to the design and quality of its façade [232]. These two facets of sustainability are often in tension with one another and have led to many different, often opposing approaches for the building envelope when it comes to sustainability.

That being said, there are many different paths to sustainable architecture. these include for example: the simplification of building assemblies to reduce embodied carbon; the design of buildings using renewable resources to decrease reliance finite resources like fossil fuels and non-renewable minerals; the introduction of “smart” technology to improve operational energy consumption [233]; the design of more robust building assemblies to increase building lifespan [234]; or the design of circular buildings and building systems that facilitate disassembly for reuse and enable more frequent refurbishment with state-of-the-art high-performance alternatives [235]. All of the above options present different paths to sustainable solutions, but each prioritizes the environmental impact in the product stage, construction stage, use stage, and end-of-life stage in different degrees.

While FFSGF are not an inherently sustainable choice in most applications, their place in sustainable construction can not be entirely rejected. For example, freeform steel and glass roofs are commonly applied as a refurbishment strategy for the conversion of historic courtyards to interior space [4, 27, 32, 52–55, 69–71, 101]. Refurbishment is often a more sustainable alternative to new construction. The use of structural form-finding for optimized gridshell geometry generally yields freeform results, and these structurally optimized geometries are a lighter imposition on the existing infrastructure compared to non-optimized geometries. This enables material savings in both the construction of the new enclosure as well as in the reinforcement

of the existing infrastructure. Insulated glazing units offer insulation, enable natural daylighting, and can be made operable for passive ventilation, while excessive solar heat gain can be mitigated with opaque insulated infill panels or shading devices. The use of freeform steel and glass façades as a retrofitted second skin around existing infrastructure is another avenue in which they may prove to be a solution in line with sustainability objectives. Ultimately, although freeform steel and glass façades may not be the first façade typology that emerges in discussions on sustainability, there exists in certain contexts a potential for the integration of these façade types within sustainable architectural practices. The application of these façades, however, should be supported by robust building simulations and Life Cycle Analysis (LCA) to validate their sustainability.

Moreover, the impact of AM in the overall sustainability of the façade remains to be explored. AM in general comes with environmental advantages and disadvantages when compared to other manufacturing methods. AM, particularly when it comes to metal AM, can be a very energy-intensive process. Its also a process that can potentially produce a significant amount of waste material. For example, support structures or failed prints and prototyping can negatively impact the environmental impact of seemingly sustainable solutions such as topologically optimized nodes.

On the other hand, AM can provide secondary environmental benefits related to the achievable complexity of AM parts such as those outlined in Figure 1.2. For example, complex part design can improve insulation performance. In addition, consolidating an assembly into a single AM part reduces the LCA impact of the product from the sum of all of its subcomponents (including raw material, transport, and manufacturing) to that of a single component built from a commercial material such as powder or wire. In the context of this work, the sustainability of the approach should be explored for both structural nodes and gasket nodes. A better understanding what the environmental impact is compared to more traditional manufacturing routes, and the extent to which any added environmental cost is compensated by the higher performance of AM products needs to be further investigated.

For structural nodes, future research should explore the environmental impact of AM nodes versus other structural node systems, and should consider the relative impact of different metal AM technologies and hybrid fabrication strategies. It would also be valuable to develop guidelines for sustainable AM, such as the identification of threshold buy-to-fly ratios beyond which different AM methods are a potentially more sustainable alternative to CNC-milling. It would also be interesting to assess the extent to which material savings can be achieved in a full scale case study, not only in the nodes themselves, but also consequently in the rest of the supporting

structure, and the resulting impact on the overall embodied carbon of the façade. In applications with many large nodes, this contribution may be rather significant. For gasket nodes, future research should compare the sustainability of AM gasket nodes versus existing solutions, taking into consideration operational energy savings from improved façade performance achieved through more geometrically suitable solutions.

Further, it is also worth noting the potential role of AM towards the realization of circular façades. For example, the additive manufacturing of exterior node gaskets could be leveraged to fabricate fully dry-sealed freeform façade systems instead of silicone joints, facilitating disassembly. This could be beneficial for façade-as-a-service models, or portable installations. AM can also provide a potential avenue for bridging the gap between modularized façade systems and the custom requirements of individual building projects. Computational methods could be developed linking design models to circular product databases, identifying local, suitable structural profiles, and generating nodes to fill the gaps according to the required building proportions and structural requirements. This strategy is not only relevant to FFSGF, which is a very specific subset of façade applications, but also to more standardized façade applications. The backup structure is a significant contributor to the environmental footprint in the LCA of curtain wall construction, of which a majority of the contribution is from stages A1-A3 (raw material extraction/processing; transport to the manufacturer; and manufacturing). Enabling the use of secondary products therefore has significant potential in this regard.

To conclude, façades are an integral part of overall building sustainability, and as there are many different approaches to sustainability, there is potential for FFSGF to be a sustainable solution under the right set of circumstances. The use of AM in FFSGF applications has the potential to improve environmental impact compared to existing construction strategies. In addition to this, the use of AM has the potential to contribute towards facilitating circular façade construction both for freeform and standard façade applications. However, while AM can be a very exciting proposition, in both of these instances, the extent to which AM impacts sustainability needs to be further explored in a quantifiable way through comprehensive building performance simulations and LCA.

7.5 Final Remarks

The emergence of AM into the construction industry presents a prospect that unleashes a myriad of possibilities for the built environment. This project explored the use of AM as a potential means of improving existing construction methods. Projects like the AM bridge by MX3D in Amsterdam [144] highlight the possibilities of AM at the intersection of technology, engineering, and craft. 3D-printed homes are being explored as a means of providing sustainable solutions for humanitarian crises like homelessness, housing scarcity, and displaced populations [228]. Advances towards using AM for construction on the moon and on Mars [229] bring us one step closer to monumental advances for mankind. On the whole, it is a very inspiring time to be exploring the possibilities of AM in architecture.

That being said, there is a tendency to perceive AM as a technology without limits and with which we can fabricate any conceivable object. Certainly, AM introduces new possibilities for fabrication that allow us to fabricate things that were simply not possible before, but the potential of AM is not limitless – and just because it's possible to fabricate a particular object with AM, this does not necessarily mean that it's practicable, or that improved performance will justify the increase in fabrication cost and/or complexity. While the aerospace industry can likely justify a sharp increase in fabrication time, cost, and complexity for an object that is lighter or has even marginally better performance, the architectural industry cannot – especially where the fabrication of dozens, hundreds or even thousands of mass-customized components is concerned.

This dissertation endeavours to enhance freeform steel and glass façades by concentrating on a specific aspect of the overall system that holds significant potential for AM intervention – an aspect with critical performance requirements, intricate geometries, diverse design possibilities, and for which existing solutions exhibit evident room for improvement and optimization. To this end, different AM technologies and materials were explored, AM systemized node products were designed and fabricated, and a full-scale construction using AM structural and gasket nodes was realized. This dissertation illustrates the promising potential of AM technology in freeform steel and glass façade applications. Furthermore, it contributes to the building industry's ability to fully embrace AM technology by advancing essential knowledge in this area.

Bibliography

- [1] Schlaich, M., et al., *Palacio de Comunicaciones – a single layer glass grid shell over the courtyard of the future town hall of Madrid*, in *Symposium of the International Association for Shell and Spatial Structures*, A. Domingo Cabo and C.M. Lázaro Fernández, Editors. 2009: Valencia.
- [2] Ney & Partners. *Glass Roof Dutch Maritime Museum*. 2011 [cited 2020 28/05/2020]; Available from: <https://ney.partners/project/glass-roof-dutch-maritime-museum/>.
- [3] Chadwick, A., et al., *PLATO – Gridshell Design Method for Chadstone Shopping Mall Roof*, in *IABSE Conference: Creativity and Collaboration – Instilling Imagination and Innovation in Structural Design*. 2017: Bath, United Kingdom.
- [4] Sischka, J., *Engineering the Construction of the Great Roof for the British Museum*, in *Widespan Roof Structures*. 2000. p. 199-207.
- [5] Jenkins, D. and N. Foster, *Norman Foster : works 5*. 2009, Munich; New York: Prestel.
- [6] van Nieuwamerongen, F. *New-generation motorway architecture*. 2005.
- [7] fuksas. *Admirant Entrance Building*. 2023/04/11; Available from: <https://fuksas.com/admirant-entrance-building/>.
- [8] *The Dalí Museum / HOK*. ArchDaily, 2011.
- [9] Schlaich, J.R., H. Schober, and K. Kürschner, *New Trade Fair in Milan — Grid Topology and Structural Behaviour of a Free-Formed Glass-Covered Surface*. *International Journal of Space Structures*, 2005. **20**(1): p. 1-14.
- [10] Knippers, J. and T. Helbig, *Recent Developments in the Design of Glazed Grid Shells*. *International Journal of Space Structures*, 2009. **24**(2): p. 111-126.
- [11] Anderson, D., et al., *Złote Tarasy, Warsaw, Poland*. *The Arup Journal*, 2008(1): p. 31-53.
- [12] Helbig, T., L. Giampellegrini, and M. Oppe, “*Carioca Wave*” – *A free-form steel-and-glass canopy in Rio de Janeiro, Brazil*. *Steel Construction*, 2014. **7**(4): p. 252-257.
- [13] Foster and Partners. <https://www.fosterandpartners.com/projects/smithsonian-institution-courtyard/>. [cited 2020 27/01/2020]; Available from: <https://www.fosterandpartners.com/projects/smithsonian-institution-courtyard/>.
- [14] Coop Himmelb(l)au. *Musée des Confluences The Crystal Cloud of Knowledge*. 2023/04/11; Available from: <https://coop-himmelblau.at/projects/musee-des-confluences/>.
- [15] Coop Himmelb(l)au. *BMW Welt in Munich Play of Dynamic Forces*. 2023/04/11; Available from: <https://coop-himmelblau.at/projects/bmw-welt/>.
- [16] Memari, A.M. and S. Architectural Engineering Institute. Committee on Curtain Wall, *Curtain wall systems : a primer*. 2013, American Society of Civil Engineers: Reston, Virginia.
- [17] Schittich, C. and A.-D. Institut für Internationale, *Glass construction manual*. 2nd, rev. and expanded ed. 2007, Basel, London: Birkhäuser.
- [18] Knaack, U., *Facçades : principles of construction*. 2007, Birkhäuser: Basel.
- [19] Eekhout, M. and I.O.S. Press, *Methodology for product development in architecture*. 2008, Delft University Press/IOS Press: Amsterdam.
- [20] ASTM International, *ASTM F2792-12a Standard Terminology for Additive Manufacturing Technologies*. 2013, ASTM International.
- [21] Kumke, M., et al., *Methods and tools for identifying and leveraging additive manufacturing design potentials*. *International Journal on Interactive Design and Manufacturing (IJIDeM)*, 2018. **12**(2): p. 481-493.
- [22] Paparo, I. and M. Overend. *Performance-based material selection and design f o r freeform building envelopes*. 2015.
- [23] Canada Mortgage and Housing Corporation, *Glass and metal curtain walls*, in *Best practice guide, building technology*. 2004, Canada Mortgage and Housing Corporation,: Canada.

- [24] Schober, H. and S. Justiz, *Cabot Circus, Bristol Ebene Vierecknetze für freigeformte Glasdächer*, in *Glasbau 2012*. 2012, Wiley-VCH Verlag GmbH & Co. KGaA : Weinheim, Germany. p. 28-42.
- [25] Helbig, T., F. Kamp, and M. Oppe, *An Eye to the Sky*. Steel Construction, 2015. **8**(2): p. 133-138.
- [26] Correa, C. and C. Schwitter, *Engineering an Icon Complex Structural Systems for the Jewel Changi Airport*, in *STRUCTURE magazine*. 2019. p. 36-39.
- [27] Sischka, J., et al., *Die Überdachung des Great Court im British Museum in London*. Stahlbau, 2001. **70**(7): p. 492-502.
- [28] Knippers, J. and T. Helbig, *The Frankfurt Zeil Grid Shel*, in *Symposium of the International Association for Shell and Spatial Structures*, A. Domingo Cabo and C.M. Lázaro Fernández, Editors. 2009: Valencia.
- [29] Stahr, A. and J.r. Ruth, *Das wohltemperierte Netz - Zum Konstruktiven Entwurf direkt verglaster Stabnetze auf Freiformflächen*. 2009, Professur Tragwerkslehre: Weimar.
- [30] Stephan, S.r., J. Sánchez-Alvarez, and K. Knebel, *Stabwerke auf Freiformflächen*. Stahlbau, 2004. **73**(8): p. 562-572.
- [31] Schober, H., *Transparent Shells*. 2015, Wiley.
- [32] Williams, C., *The analytic and numerical definition of the geometry of the British Museum Great Court Roof*. Proceedings of the the Third International Conference on Mathematics & Design, 2001: p. 434-440.
- [33] Sischka, J., *The use of steel and glass in complex geometry and free form façades and roofs concepts*, in *Glass Performance Days*, s.n., Editor. 2007, Glass performance days: Tampere. p. 210-212.
- [34] Weller, B., *Glass in building : principles, applications, examples*. 2009, Birkhäuser ; Edition Detail: Basel, Switzerland München.
- [35] Steel Construction Institute, *The Schubert Club Band Shell*. 2011, Steel Construction Institute: Ascot. p. 1-4.
- [36] McCormick, S., et al., *Schubert Club Band Shell, Saint Paul, Minnesota, USA*. Structural Engineering International, 2004. **14**(2): p. 140-141.
- [37] Tellier, X., et al., *Morphogenesis of curved structural envelopes under fabrication constraints*. 2020. p. 1 online resource.
- [38] Tellier, X., et al., *Surfaces with planar curvature lines: Discretization, generation and application to the rationalization of curved architectural envelopes*. Automation in Construction, 2019. **106**.
- [39] Schlaich Bergermann und Partner. *Schlüterhof Roof, German Historical Museum*. [cited 2020 28/01/2020]; Available from: <https://www.sbp.de/en/project/schlueterhof-roof-german-historical-museum/>.
- [40] Eekhout, M., *'Zappi' Structures And Constructions In 'Blob' Architecture*, in *EU COST C13 Glass and Interactive Building Envelopes : Final Report*, M. Crisinel, et al., Editors. 2007, IOS Press, Incorporated.
- [41] Eekhout, M. and I.O.S. Press, *Free form technology from Delft*. 2015, IOS Press: Amsterdam.
- [42] Gabriel, A.F., Norman; Kaltenbach, Frank; Thonger, James ; Glover, David; Shuttleworth, Ken, *City Hall in London*, in *Detail*. 2002. p. 1086-1109.
- [43] Merkel, J., *City Hall, London, England*. Architectural Record, 2003(02): p. 110-123.
- [44] Meyer Boake, T., *Diagrid structures : systems, connections, details*. 2014, Basel: Birkhäuser.
- [45] Cook, M., A. Palmer, and J. Sischka, *SAGE Music Centre, Gateshead – Design and construction of the roof structure*, in *The Structural Engineer*. 2006, The Institution of Structural Engineers. p. 23-29.
- [46] Meechan, S. *How the Sage turned a piece of Gateshead wasteland into a world-class venue*. 2017.
- [47] Meyer Boake, T., *Complex steel structures : non-orthogonal geometries in building with steel*. 2020, Basel: Birkhäuser, part of Walter de Gruyter GmbH, Berlin.
- [48] Pottmann, H. and J. Wallner, *Mathematics and Society*, W. König, Editor. 2016, European Mathematical Society Publishing House: Zürich, Switzerland.
- [49] den Hollander, J.P., *Een Script voor Staal*, in *Bouwen met Staal*. 2006. p. 20-25.
- [50] *Noise Wall and Car Showroom near Utrecht*, in *Detail*. 2007.
- [51] Mukerji, S., *Drapes of Glazing*, in *Glass Magazine*. 2005. p. 39-43.
- [52] Lother, K. and W. Rudolph, *The Canopy at the Smithsonian Institution's Kogod Courtyard in Washington D.C.*, in *Detail*. 2009. p. 84-90.
- [53] Menges, A., *Instrumental geometry*. Architectural Design, 2006. **76**(2): p. 42-53.
- [54] Peters, B. *The Smithsonian courtyard enclosure: A case-study of digital design processes*. in *ACADIA*. 2007. Halifax: Riverside Architectural Press.
- [55] Peters, B., *Personal Communication with Brady Peters*, L. Tramontini, Editor. 2020.
- [56] Lother, K., *Heating and Cooling Façades – the Steel Façade of BMW Welt in Munich*, in *Innovative Design + Construction*. 2007. p. 836-844.

- [57] Köppl, J., et al., *BMW-Welt München - die Stahlkonstruktion in der realen Umsetzung*. Stahlbau, 2005. **74**(7): p. 492-498.
- [58] S H Structures. *Cabot Circus, Bristol*. 14/02/2020]; Available from: <https://www.shstructures.com/projects/cabot-circus-bristol/>.
- [59] Sischka, J., et al., *Knoten zum Verbinden von Stäben eines Flächentragwerks*, E.P. Office, Editor. 2009, Waager-Biro Stahlbau AG: Austria.
- [60] Barf, H., *Innovative design + construction : manufacturing and design synergies in the building process*. 2010, Institut für internationale: München.
- [61] Stroetmann, R., R. Istel, and D. Hanek, *PalaisQuartier Frankfurt: Zeilforum - Planung und Ausführung der architektonischen Gebäudehülle*. Stahlbau, 2008. **77**(10): p. 696-707.
- [62] *MyZeil Shopping Centre in Frankfurt on the Main*, in *Detail*. 2011.
- [63] Post, N.M. *Salvador Dalí Museum by HOK Opens This Month in Florida*. Architectural Record, 2011.
- [64] Martin, S.D. *A Treasure Box for Dalí*. Structure Magazine, 2013.
- [65] Butler, C. and H. Hine, *New Dali Museum Construction*. 2010: Online.
- [66] García Page, C., *Palacio de Cibeles Cubierta con Gloria*, in *Boletín informativo de Arquitectos Técnicos Aparejadores*. 2011: Madrid. p. 29-41.
- [67] Waagner Biro Steel and Glass. *The Blob*. [cited 2023 19/01/2023]; Available from: <https://wb-sg.com/projects/blob/>.
- [68] Crone, J., *Een constructieve zeepbel*, in *Bouwwereld*. 2010. p. 40-47.
- [69] Vinnitskaya, I. *National Maritime Museum / Dok Architecten*. ArchDaily, 2012.
- [70] Adriaenssens, S., et al. *Finding the Form of an Irregular Meshed Steel and Glass Shell Based on Construction Constraints*. Journal of Architectural Engineering, 2012. **18**, 206-213 DOI: 10.1061/(ASCE)AE.1943-5568.0000074.
- [71] Info Steel. *Overkapping Nederlands Scheepvaartmuseum*. Available from: <https://www.infosteel.be/staal-bouw-project/22-overkapping-nederlands-scheepvaartmuseum.html>.
- [72] Novum Structures. *Shaw Centre*. [cited 2020 2020/03/23]; Available from: https://novumstructures.com/eu/novum_projects/shaw-centre/.
- [73] Seele. *Mansueto Library*. [cited 2019 14/06/2019]; Available from: <https://seele.com/references/mansueto-library/3/>.
- [74] Sobek, W. and L. Blandini, *The Mansueto Library - Notes on a glazed steel grid shell from design to construction*, in *Challenging Glass 2 - Conference on Architectural and Structural Applications of Glass, CGC 2010*, F. Bos, C. Louter, and F. Veer, Editors. 2010: Delft. Netherlands. p. 179-185.
- [75] University of Chicago Library, *Dome Construction - Structural Steel and Aluminum Frame*. 2010, Flickr.
- [76] WJE. *Glass Dome Building*. [cited 2023 2023/04/10]; Available from: <https://www.wje.com/projects/detail/glass-dome-building>.
- [77] McMeeken, R. *Giant glass panels arrive for the leaning tower of Abu Dhabi*. Building, 2009.
- [78] Meyer Boake, T., *the Emergence of the Diagrid - It's All About the Node*. International Journal of High-rise Buildings, 2016. **5**(4): p. 293-304.
- [79] Huzefa, A., *Rationalisation of freeform glass façades from concept to construction*, in *Department of Architecture and Civil Engineering*. 2013, University of Bath: Bath, UK.
- [80] Seele. *King's Cross Railway Station*. [cited 2023 20/01/2023]; Available from: <https://seele.com/references/kings-cross-railway-station>.
- [81] King, M. and A. Reddihough, *The Western Concourse Roof*. The Arup Journal, 2012(2): p. 12-19.
- [82] *King's Cross Station in London*, in *Detail*. 2012.
- [83] Schlaich Bergermann und Partner. *Glass roofs Höfe am Brühl*. 2023/04/10]; Available from: <https://www.sbp.de/en/project/glass-roofs-hoefe-am-bruehl/>.
- [84] Ranieri Da Re, G., *Personnal Communication with Guido Ranieri Da Re*, L. Tramontini, Editor. 2020.
- [85] Impresa CEV, *Il cantiere di Palazzo ex Unione Militare by Impresa Cev. Strutture, solai e restauro facciate*. 2012, YouTube. p. 6:01.
- [86] Info Steel. *Van Pallazo tot mega-boutique in Rome*. Available from: <https://www.infosteel.be/fuksas.html>.
- [87] Piscitelli, V. *Palazzo dell'Ex Unione Militare*. Ingenio, 2020.
- [88] Pichler. *H&M Flagshipstore and event location "La Lanterna"*. [cited 2023 20/01/2023]; Available from: <https://pichler.pro/en/references?project=125&kompetenz=Steel%2BGlass%20constructions>.
- [89] Schlaich, M. and M. Nier, *Die Plazaüberdachung des EY Headquarters in Luxemburg*. ce/papers, 2017. **1**(1): p. 61-74.

- [90] Metal Yapi. *Bory Mall*. 27/01/2021]; Available from: <http://www.metalyapi-eng.com/projects-bory-mall.html>.
- [91] Muharrem, C., *TEK KATMANLI VE SERBEST ŞEKİLLİ (TKSS)*, in Çelik Yapılar. 2016, Türk Yapısal Çelik Derneği: TUCSA.
- [92] Helbig, T., et al., *Free-form on every scale : "Tornado" roof structure for Bory Mall, Bratislava, Slovakia*. Steel Construction, 2016. **9**(3): p. 249-254.
- [93] Josef Gartner GmbH *Musée des Confluences – das neue Wahrzeichen von Lyon*. metall, 2015. 18-22.
- [94] Josef Gartner GmbH. *Musée Des Confluences*. [cited 2020 19/02/2020]; Available from: <https://josef-gartner.permasteelgroup.com/project-detail?project=1840>.
- [95] Studio Tjoa. *34th Street Canopy*. Available from: <https://www.studiotjoa.com/34th-street-canopy>.
- [96] Heydari, N., *Personal Communication with Nader Heydari*, L. Tramontini, Editor. 2020.
- [97] Chadwick, A., *Personal Communication with Aran Chadwick*, L. Tramontini, Editor. 2020.
- [98] Alba, C., *Dome Construction – Structural Steel and Aluminum Frame*. 2014, Behance.
- [99] Seele, *Steel glass gridshell roof for chadstone // Stahl-Glasdach für das Chadstone*. 2017, YouTube. p. 1:33.
- [100] Seele. *Glass Roof for Shopping Giant by Seele: Chadstone Shopping Centre*. [cited 02/07/2020; Available from: <https://seele.com/references/chadstone-shopping-centre/>].
- [101] Laganier, V. *Verrière technique de AIA, cour du Midi, Grand Hôtel-Dieu, Lyon*. Light Zoom Lumière, 2018.
- [102] Koos, F., et al. *Capital C, geometric optimization of a free-form steel gridshell towards planar quadrilateral glass units*. Challenging Glass Conference Proceedings. **7**, DOI: 10.7480/cgc.7.4493.
- [103] Crone, J., *The making of the Dome*, in *Bouwwereld*. 2019. p. 54-59.
- [104] Seele. *moynihan train hall*. [cited 2020 01/13/2020]; Available from: <https://seele.com/references/moynihan-train-hall>.
- [105] SOM. *Moynihan Train Hall*. [cited 2023 20/01/2023]; Available from: <https://www.som.com/projects/moynihan-train-hall/>.
- [106] *Moynihan Train Hall – Façade design to installation*. IGS Magazine, 2021.
- [107] Schlaich Bergermann und Partner. *Moynihan Train Hall*. Available from: <https://www.sbp.de/en/project/moynihan-train-hall/>.
- [108] *Jewel am Flughafen Singapur-Changi*, in *Detail Structure*. 2019. p. 40-45.
- [109] Correa, C., *Personal Communication with Cristobal Correa*, L. Tramontini, Editor. 2020.
- [110] Chandramohan, G. *Building the Jewel: A close-up look at the 9,000 pieces of glass used in Changi Airport's upcoming project*. Channel News Asia, 2018.
- [111] Vitro Architectural Glass. *Vitro Glass makes Jewel Changi Airport in Singapore sparkle*. Available from: <https://www.vitroglazings.com/about/news/vitro-glass-makes-jewel-changi-airport-in-singapore-sparkle/>.
- [112] Na, S., S. Kim, and S. Moon, *Additive manufacturing (3D Printing)-applied construction: Smart node system for an irregular building façade*. Journal of Building Engineering, 2022. **56**.
- [113] Ernst, J. and J. Gartner, *Das Edelstahl-Glas-Tragwerk eines Bankgebäudes in Berlin*, in *Edelstahl Rostfrei in der Architektur*. 2000, The European Stainless Steel Development Association: Berlin.
- [114] *Ekris Showroom | ONL*. ArchDaily, 2009. **2020**.
- [115] *CET Building | ONL*. 2012. **2020**.
- [116] Schuler, T.A. *The Lattice Roof of Crossrail Place at Canary Wharf*. Architect, 2016.
- [117] Novum Structures, *BK-System*, N. Structures, Editor.: Online.
- [118] Wikiarquitectura. *Ex Unione Militare Refurbishment*. [cited 2023 2023/01/31]; Available from: <https://en.wikiarquitectura.com/building/ex-unione-militare-refurbishment/>.
- [119] Liddell, I., *Frei Otto and the development of gridshells*. Case Studies in Structural Engineering, 2015. **4**: p. 39-49.
- [120] D'Amico, B., et al., *Timber gridshells: Numerical simulation, design and construction of a full scale structure*. Structures, 2015. **3**: p. 227-235.
- [121] Xylotec. *Gridshell - Sherborne GLAZED GLUE-LAMINATED OAK GRIDSHELL*. [cited 2023 2023/02/02]; Available from: <https://www.xylotec.co.uk/projects/sherborne-gridshell>.
- [122] Dombrowski, Q., *Filling the gap (cropped)*. 2010. p. <https://www.flickr.com/photos/quinnanya/4909536322/in/album-72157625003303438/>.
- [123] Pham, D. *Weymouth Discusses Designing the Hurricane-Resistant Salvador Dalí Museum*. inhabitat, 2014.
- [124] Patterson, M., et al., *Cassette Glazing Systems: Broadening the Façade Vocabulary Through the Use of Framed Glazing Panels*, in *Glass Performance Days*. 2013, Glass Performance Days: Finland.
- [125] Burry, J. and M. Burry, *The new mathematics of architecture*. 2010, London: Thames & Hudson.
- [126] Jenkins, D.S., *Norman Foster Works* 6. 2013, Munich :: Prestel.

- [127] Centre for Window and Cladding Technology, *CWCT Curtain Wall Installation Handbook*. 2001, Bath: University of Bath.
- [128] Taseva, Y., et al. *Large-scale 3D printing for functionally-graded façade*. in *25th International Conference on Computer-Aided Architectural Design Research in Asia, CAADRIA 2020*. 2020. The Association for Computer-Aided Architectural Design Research in Asia (CAADRIA).
- [129] Strauss, H., *AM Envelope: The Potential of Additive Manufacturing for façade constructions*, in *Architectural Engineering + Technology*. 2013, TU Delft: Delft.
- [130] Crolla, K. and N. Williams, *Smart Nodes: A System for Variable Structural Frames with 3D Metal-Printed Nodes*, in *ACADIA 2014: Design Agency*, D. Gerber, A. Huang, and J. Sanchez, Editors. 2014, Association for Computer Aided Design in Architecture: Los Angeles, United State. p. 311-316.
- [131] Prayudhi, B., *3F3D: Form Follows Force with 3D printing*, in *Architecture and The Built Environment department of Building Technology*. 2016, TU Delft: Delft, NL.
- [132] Crolla, K., et al. *Smartnodes pavilion*. in *22nd International Conference on Computer-Aided Architectural Design Research in Asia: Protocols, Flows and Glitches, CAADRIA 2017*. 2017. The Association for Computer-Aided Architectural Design Research in Asia (CAADRIA).
- [133] Seifi, H., et al., *Design optimization and additive manufacturing of nodes in gridshell structures*. *Engineering Structures*, 2018. **160**: p. 161-170.
- [134] Mohsen, A., *Design to Manufacture of Complex Building Envelopes*. *Mechanik, Werkstoffe und Konstruktion im Bauwesen*. Vol. 56. 2020, Wiesbaden, Germany: Springer Vieweg Wiesbaden. XIII, 230.
- [135] Altair, *Altair® OptiStruct®*. Retrieved June 18, 2016: <http://www.altairhyperworks.com/product/OptiStruct>.
- [136] Mohsen, A. and U. Knaack. *The imminent Future of Parametric Nodes*. in *39th IABSE Symposium in Vancouver 2017: Engineering the Future*. 2017. International Association for Bridge and Structural Engineering (IABSE).
- [137] Buchanan, C., et al., *Structural performance of additive manufactured metallic material and cross-sections*. *Journal of Constructional Steel Research*, 2017. **136**: p. 35-48.
- [138] European Committee for Standardization, *Stainless steels - Part 2: Technical delivery conditions for sheet/plate and strip of corrosion resisting steels for general purposes (EN 10088-2)*. 2014, European Committee for Standardization (CEN): Brussels.
- [139] Davis, J.R. and A. S. M. International Handbook Committee, *Stainless steels*. ASM specialty handbook. 1994, Materials Park, Ohio: ASM International.
- [140] Milewski, J.O., *Additive manufacturing of metals : from fundamental technology to rocket nozzles, medical implants, and custom jewelry*. 2017, Springer: Cham, Switzerland.
- [141] Thomas, D.S. and S.W. Gilbert, *Costs and Cost Effectiveness of Additive Manufacturing A Literature Review and Discussion*, U.S.D.o. Commerce, Editor. 2014, National Institute of Standards and Technology.
- [142] Weber, J., *Personal Communication with Juri Weber from MX3D*, L. Tramontini, Editor. 2022.
- [143] Lockett, H., et al., *Design for Wire + Arc Additive Manufacture: design rules and build orientation selection*. *Journal of Engineering Design*, 2017. **28**(7-9): p. 568-598.
- [144] Parkes, J. *Joris Laarman's 3D-printed stainless steel bridge finally opens in Amsterdam*. 2021.
- [145] Yu, H.Z. and R.S. Mishra, *Additive friction stir deposition: a deformation processing route to metal additive manufacturing*. *Materials Research Letters*, 2021. **9**(2): p. 71-83.
- [146] Senvol, *Senvol Database: Industrial Additive Manufacruing Machines and Materials*. Senvol: Online.
- [147] European Committee for Standardization, *Execution of steel structures and aluminium structures - Part 2: Technical requirements for steel structures (EN 1090-2)*. 2018, European Committee for Standardization (CEN).
- [148] European Committee for Standardization, *Eurocode 3: Design of steel structures - Part 1-1: General rules and rules for buildings (EN 1993-1-1)*. 2016, European Committee for Standardization (CEN).
- [149] European Committee for Standardization, *Eurocode 3: Design of steel structures - Part 1-4: General rules - Supplementary rules for stainless steels (EN 1993-1-4)*. 2006, European Committee for Standardization (CEN).
- [150] European Committee for Standardization, *Eurocode 3: Design of steel structures - Part 1-9: Fatigue (EN 1993-1-9)*. 2006, European Committee for Standardization (CEN).
- [151] European Committee for Standardization, *Eurocode 3: Design of steel structures - Part 1-1: General rules and rules for buildings (NEN-EN 1993-1-1+C2+A1/NB)*. 2016, European Committee for Standardization (CEN).
- [152] Afkhami, S., et al., *Effects of manufacturing parameters and mechanical post-processing on stainless steel 316L processed by laser powder bed fusion*. *Materials Science & Engineering A*, 2021. **802**.

- [153] Braun, M., et al., *Fatigue strength of PBF-LB/M and wrought 316L stainless steel: effect of post-treatment and cyclic mean stress*. Fatigue & Fracture of Engineering Materials & Structures, 2021. **44**(11): p. 3077–3093.
- [154] Li, X., et al., *Study on Mechanism of Structure Angle on Microstructure and Properties of SLM-Fabricated 316L Stainless Steel*. Frontiers in Bioengineering and Biotechnology, 2021. **9**.
- [155] Obeidi, M.A., et al., *Comparison of the porosity and mechanical performance of 316L stainless steel manufactured on different laser powder bed fusion metal additive manufacturing machines*. Journal of Materials Research and Technology, 2021. **13**: p. 2361–2374.
- [156] Cacace, S., et al., *The effect of energy density and porosity structure on tensile properties of 316L stainless steel produced by laser powder bed fusion*. Progress in Additive Manufacturing, 2022. **7**(5): p. 1053–1070.
- [157] Bertolini, R., et al., *The Effect Of The Building Direction And Surface Finish On The Mechanical Properties Of The Direct Energy Deposited AISI 316L Stainless Steel*. Manufacturing Letters: Supplement, 2022. **33**(Supplement): p. 109–116.
- [158] Pacheco, J.T., et al., *Laser directed energy deposition of AISI 316L stainless steel: The effect of build direction on mechanical properties in as-built and heat-treated conditions*. Advances in Industrial and Manufacturing Engineering, 2022. **4**.
- [159] Saboori, A., et al., *An investigation on the effect of powder recycling on the microstructure and mechanical properties of AISI 316L produced by Directed Energy Deposition*. Materials Science & Engineering A, 2019. **766**.
- [160] Saboori, A., et al., *An investigation on the effect of deposition pattern on the microstructure, mechanical properties and residual stress of 316L produced by Directed Energy Deposition*. Materials Science & Engineering A, 2020. **780**.
- [161] Wang, C., et al., *Study on microstructure and tensile properties of 316L stainless steel fabricated by CMT wire and arc additive manufacturing*. Materials Science & Engineering A, 2020. **796**.
- [162] Gowthaman, P., S. Jeyakumar, and D. Sarathchandra, *Influence of heat input on microstructure and mechanical behaviour of austenitic stainless steel 316L processed in wire and arc additive manufacturing*. Proceedings of the Institution of Mechanical Engineers, Part E: Journal of Process Mechanical Engineering, 2022.
- [163] European Committee for Standardization, *Eurocode 3: Design of steel structures - Part 1-10: Material toughness and through-thickness properties (EN 1993-1-10)*. 2005, European Committee for Standardization (CEN).
- [164] Kumar, D., et al., *Mechanisms controlling fracture toughness of additively manufactured stainless steel 316L*. International Journal of Fracture, 2021. **235**(1): p. 61–78.
- [165] Harvey, P.D. and American Society for Metals, *Engineering properties of steel*. 1982, American Society for Metals: Metals Park, Ohio.
- [166] Pauzon, C., et al., *Effect of argon and nitrogen atmospheres on the properties of stainless steel 316 L parts produced by laser-powder bed fusion*. Materials & Design, 2019. **179**: p. 107873.
- [167] Zhong, Y., et al., *Intragranular cellular segregation network structure strengthening 316L stainless steel prepared by selective laser melting*. Journal of Nuclear Materials, 2016. **470**: p. 170–178.
- [168] Kono, D., et al., *Effects of cladding path on workpiece geometry and impact toughness in Directed Energy Deposition of 316L stainless steel*. CIRP Annals - Manufacturing Technology, 2018. **67**(1): p. 233–236.
- [169] Ye, C., et al., *Microstructure and mechanical properties of the 316 stainless steel nuclear grade experimental component made by wire and arc additive manufacturing*. Proceedings of the Institution of Mechanical Engineers, Part C: Journal of Mechanical Engineering Science, 2020. **234**(21): p. 4258–4267.
- [170] Hatami, S., et al., *Fatigue Strength of 316 L Stainless Steel Manufactured by Selective Laser Melting*. Journal of Materials Engineering and Performance, 2020. **29**(5): p. 3183–3194.
- [171] Blinn, B., et al., *Process-influenced fatigue behavior of AISI 316L manufactured by powder- and wire-based Laser Direct Energy Deposition*. Materials Science & Engineering A, 2021. **818**.
- [172] Cegan, T., et al., *Effect of Hot Isostatic Pressing on Porosity and Mechanical Properties of 316 L Stainless Steel Prepared by the Selective Laser Melting Method*. Materials (Basel, Switzerland), 2020. **13**(19).
- [173] ASTM International, *ASTM 5291 1-1 Additive manufacturing — Design — Part 1: Laser-based powder bed fusion of metals*. 2019, ASTM International: Switzerland.
- [174] Ewald, A. and J. Schlattmann, *Design guidelines for laser metal deposition of lightweight structures*. Journal of Laser Applications, 2018. **30**(3): p. 032309.

- [175] Vastola, G., et al., *Design guidelines for suppressing distortion and buckling in metallic thin-wall structures built by powder-bed fusion additive manufacturing*. Materials & Design, 2022. **215**.
- [176] Weber, J. and F. Gilardi, *Personal Communication with Juri Weber and Filippo Gilardi from MX3D*, L. Tramontini, Editor. 2021.
- [177] Kazanas, P., et al., *Fabrication of geometrical features using wire and arc additive manufacture*. Proceedings of the Institution of Mechanical Engineers, Part B: Journal of Engineering Manufacture, 2012. **226**(6): p. 1042-1051.
- [178] Ely, L. *The Building Blocks of Directed Energy Deposition Design*. 2021.
- [179] Kokkonen, P., et al., *Design guide for additive manufacturing of metal components by SLM process*. 2016, VTT Technical Research Centre of Finland: Helsinki.
- [180] Mehnen, J.r., et al., *Design study for wire and arc additive manufacture*. International Journal of Product Development, 2014. **19**(1-2-3): p. 2.
- [181] European Committee for Standardization, *Eurocode 3: Design of steel structures – Part 1-8: design of joints (EN 1993-1-8)*. 2005, European Committee for Standardization (CEN): Brussels.
- [182] Siemens, *Siemens NX*.
- [183] Takemura, S., et al., *Design of powder nozzle for high resource efficiency in directed energy deposition based on computational fluid dynamics simulation*. The International Journal of Advanced Manufacturing Technology, 2019. **105**(10): p. 4107-4121.
- [184] Powell, D., et al., *Understanding powder degradation in metal additive manufacturing to allow the upcycling of recycled powders*. Journal of Cleaner Production, 2020. **268**: p. 122077.
- [185] DMG Mori, *CELOS*.
- [186] DMG Mori, *ReaLizer*.
- [187] Sartin, B., et al. *316L POWDER REUSE FOR METAL ADDITIVE MANUFACTURING*. in *Solid Freeform Fabrication (SFF) Symposium – An Additive Manufacturing Conference*. 2017. Austin: University of Texas in Austin.
- [188] Gilardi, F., *Personal Communication with Filippo Gilardi from MX3D*, L. Tramontini, Editor. 2021.
- [189] Andreau, O., et al., *A competition between the contour and hatching zones on the high cycle fatigue behaviour of a 316L stainless steel: Analyzed using X-ray computed tomography*. Materials Science & Engineering A, 2019. **757**: p. 146-159.
- [190] Scherz, C., et al., *Increasing productivity of laser powder bed fusion manufactured Hastelloy X through modification of process parameters*. Journal of Manufacturing Processes, 2022. **78**: p. 231-241.
- [191] Kostevsek, U., et al., *Development of productivity estimation model for mass-customized production by selective laser melting*. Rapid Prototyping Journal, 2018. **24**(3): p. 670-676.
- [192] Leicht, A., et al., *Increasing the Productivity of Laser Powder Bed Fusion for Stainless Steel 316L through Increased Layer Thickness*. Journal of Materials Engineering and Performance, 2021. **30**(1): p. 575-584.
- [193] Li, Y., et al., *Mechanical Properties and Constitutive Model of Selective Laser Melting 316L Stainless Steel at Different Scanning Speeds*. Advances in Materials Science and Engineering, 2022. **2022**: p. 2905843.
- [194] Khorasani, A., et al., *A review of technological improvements in laser-based powder bed fusion of metal printers*. The International Journal of Advanced Manufacturing Technology, 2020. **108**(1-2): p. 191-209.
- [195] DMG Mori launches new Lasertec 30 Dual SLM Additive Manufacturing machine. Metal AM, 2020.
- [196] Proto Labs Ltd. *Manufacturing Materials*. 2020-06-27]; Available from: <https://www.protolabs.com/en-gb/materials/comparison-guide/?category=rubber>.
- [197] materialise. *Materials*. 2020-06-11]; Available from: <https://www.materialise.com/en/industrial/3d-printing-materials>.
- [198] Shapeways Inc. *Materials for every stage of any project*. 2020-11-26]; Available from: <https://www.shapeways.com/materials>.
- [199] Sculpteo. *3D printing materials*. 26/11/2020]; Available from: <https://www.sculpteo.com/en/materials/>.
- [200] Spectroplast. *Materials*. 2020-11-22]; Available from: <https://spectroplast.com/materials/>.
- [201] Xometry. *Material Selection Guide*. 2020-11-27]; Available from: <https://www.xometry.com/materials/>.
- [202] European Committee for Standardization, *Curtain walling – Product standard (EN 13830)*. 2015, European Committee for Standardization (CEN).
- [203] European Committee for Standardization, *Building hardware – Gasket and weatherstripping for doors, windows, shutters and curtain walling – Part 1: Performance requirements and classification (EN 12365-1)*. 2003, European Committee for Standardization (CEN).
- [204] ASTM International, *ASTM C-864-05 Standard Specification for Dense Elastomeric Compression Seal Gaskets, Setting Blocks, and Spacers*. 2019, ASTM International: West Conshohocken, PA.

- [205] Spectroplast AG, *Spectroplast True Silicone A60*. 2020.
- [206] Spectroplast AG. *On-Demand Silicone Additive Manufacturing*. 26/11/2020]; Available from: <https://spectroplast.com/technology/>.
- [207] Wacker Chemie AG, *ACEO Silicone GP Shore A 60*. 2019.
- [208] Beamler BV. *Design Guidelines Printing with Silicone GP Shore A 20 - A 60*. 20/11/2020]; Available from: https://quote.beamler.com/assets/pdf/guides/Design-Guidelines-Silicone-GP-Shore-A20-A60.pdf?_ga=2.54392616.1678554696.1570434756-1257185474.1558356505.
- [209] pro3D GmbH. *Material-Details: Silikon Datenblatt*. 20/11/2020]; Available from: <https://www.fabb-it.de/material/details?material=silikon>.
- [210] Carbon Inc., *EPU 40*. 2020.
- [211] Carbon Inc., *EPU 41*. 2020.
- [212] Koslow, T. *3D Printing: The Stories We Missed This Week — November 5, 2016*. 2016.
- [213] Carbon Inc., *DLS™ Design Quick Guide*. 2021.
- [214] Proto Labs, I. *TPU 3D Printing*. 27/11/2020]; Available from: <https://www.protolabs.com/services/3d-printing/plastic/tpu/>.
- [215] Prodways, *Prodways Materials Selective Laser Sintering Powders*. 2019.
- [216] Proto Labs, I. *Design Guidelines for Selective Laser Sintering (SLS)*. 27/11/2020]; Available from: <https://www.protolabs.com/services/3d-printing/selective-laser-sintering/#design-guidelines>.
- [217] Çalışkan, C.İ. and Ü. Arpacioğlu, *Additive manufacturing on the façade: functional use of direct metal laser sintering hatch distance process parameters in building envelope*. Rapid Prototyping Journal, 2022. **28**(9): p. 1808-1820.
- [218] Carbon Inc. *What is Carbon Digital Light Synthesis ?* 27/11/2020]; Available from: <https://www.carbon3d.com/carbon-dls-technology>.
- [219] Hanson, K. *DLP 3D printing advantages, pros and cons*. The Additive Report, 2021.
- [220] Watkin, H. *ACEO to Reveal Silicone Multi-material 3D Printing at Formnext 2017*. 2017 [cited 2020 January 5]; Available from: <https://all3dp.com/aceo-reveal-silicone-multi-material-3d-printing-formnext-2017/#:~:text=Drop%20on%20Demand%3A%20ACEO's%203D,before%20the%20process%20begins%20again>.
- [221] Arbor, A., *ACEO® Launches U.S. Based Open Print Lab*. 2019: Online.
- [222] Proto Labs, I. *Selective Laser Sintering*. 27/11/2020]; Available from: <https://www.protolabs.com/services/3d-printing/selective-laser-sintering/>.
- [223] Jansen AG. *VISS Façade*. 01/05/2023]; Available from: <https://www.jansen.com/en/building-systems-profile-systems-steel/products/detail/viss-façade.html>.
- [224] Wang, S., et al. *Digital planting: Fabrication of integrated concrete green wall via additive manufacturing*. in *25th International Conference on Computer-Aided Architectural Design Research in Asia, CAADRIA 2020*. 2020. The Association for Computer-Aided Architectural Design Research in Asia (CAADRIA).
- [225] Wang, D., et al., *The Effect of a Scanning Strategy on the Residual Stress of 316L Steel Parts Fabricated by Selective Laser Melting (SLM)*. Materials, 2018. **11**(10).
- [226] SOFISTIK AG, *SOFISTIK Rhinoceros Interface*. 2020.
- [227] Chen, Y., et al. *Filleting and Rounding Using a Point-Based Method*. in *Design Automation Conference*. 2005.
- [228] Hughes, R.A. *In Italy, 3D Printers Are Making Eco-Friendly Emergency Housing*. Forbes, 2021.
- [229] Frazier, S., *NASA, ICON Advance Lunar Construction Technology for Moon Missions*. 2022, NASA.
- [230] Neeskens, T., *Thin glass composites: based on a structural efficiency increasing design strategy*, in *Architecture and The Built Environment department of Building Technology*. 2018, TU Delft: Delft, NL.
- [231] Hartwell, R. and M. Overend, *End-of-life Challenges in Façade Design: A disassembly framework for assessing the environmental reclamation potential of façade systems*. 2020.
- [232] O'Neill, R., et al., *Integrated operational and life-cycle modelling of energy, carbon and cost for building façades*. Journal of Cleaner Production, 2021. 286: p. 125370.
- [233] Habibi, S., O.P. Valladares, and D.M. Peña, *Sustainability performance by ten representative intelligent Façade technologies: a systematic review*. Sustainable Energy Technologies and Assessments, 2022. 52: p. 102001.
- [234] Marsh, R., *Building lifespan: effect on the environmental impact of building components in a Danish perspective*. Architectural Engineering and Design Management, 2017. 13(2): p. 80-100.
- [235] Azcárate-Aguerre, J.F., *Façades-as-a-Service: A cross-disciplinary model for the (re)development of circular building envelopes*. A+BE | Architecture and the Built Environment, 2023. 13(11): p. 1-270.
- [236] Galoffre, C. *L'Hôtel Dieu de Lyon se pare d'une verrière à double courbure*. batiactu, 2018

Appendix A

Freeform steel and glass façade
precedents detailed design
strategies

#	Project Info	Approximate Surface Area	Surface Qualification	Panelization	Profile Geometry	Profile Width/Diameter	Profile Depth	
1	British Museum Roof, 2000, UK	6 000	Form-Active	Tri	Rect. Tapered	80	80 – 200	
2	Schubert Club Band Shell Canopy, 2001, US	130	Revolution	Quad	Circular (curved)	48	N/A	
3	DZ Bank Berlin Roof, 2001, DE	-	Freeform	Tri	Rect. Solid	40	60	
4	Bosch Areal Roof, 2001, DE	-	Translation	Quad	Rect. Solid	60	60	
5	German Historical Museum Roof, 2002, DE	1 800	Translation	Quad	Rect. Hollow	60	140	
6	Alphen aan den Rijn Façade, 2003, NL	100	Rotational, Translation & Freeform	Tri/ Quad	Elliptical	75; 110	150; 220	
7	London City Hall Façade, 2002, UK	-	Freeform	Tri	Circular (curved)	324	N/A	
					T	75	180	
8	Uniq Tower Vienna Roof, 2004, AT	-	Scale-Translation	Quad	Rect. Solid	40	60	
9	The Sage at Gateshead Façade & Roof, 2004, UK	3 500	Revolution	Quad	I	-	800	
					Circular	455	N/A	
10	Hessing Cockpit Façade & Roof, 2005, NL	-	Freeform	Tri	Rect. Hollow	100	200	
					Circular	324	N/A	
11	New Milano Trade Fare (Logo) Canopy, 2005, IT	2 400	Form-Active	Tri/Quad	T	60 – 160	80 – 350	
12	New Milano Trade Fare (Vela) Canopy, 2005, IT	46 500	Freeform	Tri/Quad	T	60	160 – 200	
13	Smithsonian Courtyard Roof, 2007, US	2 601	Freeform	Quad	Special Built-up	-	555-1000	
14	BMW Welt Façade & Roof, 2007, DE	2 850	Freeform	Tri	Rect. Hollow	100	250; 300	
15	Cabot Circus Canopy, 2007, UK	5 800	Scale-Translation	Quad	Rect. Hollow	80	120	
16	Zlote Tarasy Façade & Roof, 2007, PL	10 240	Freeform	Tri	Rect. Hollow	100	200	
17	Westfield Shopping Center Roof	16 000	Freeform	Tri	Rect. Built-up	65	160	
18	MYZeil Façade, 2009, DE	13 000	Freeform	Tri/Quad	Rect. Built-up	60	120	
19	Salvador Dali Museum Façade & Roof, 2009, US	1 200	Freeform	Tri	Rect. Hollow	-	-	

	Profile End Condition	Structural Connection	Structural Node Typology	Structural Node Fabrication	Cables	Enclosure Typology	Gasket Joining Strategy	Sources
	NS: Cut/Mill	Welded	SAB	2D NC (Flame Cutting)	N	DG	CJS	[4, 27, 32]
	Continuous	Stacked	S	3D CNC and Standard Subcomponents, Assembly	Y	PS	None	[34-38]
	S: Notch	Bolted (Exposed, Splice)	MAS	cut from plate & CNC Milled	N	DG	C	[31]
	S: 90 Degree Cut	Welded	SAF	CNC Milled	Y	DG	-	[31]
	S: 90 Degree Cut	Continuous; Welded	MAH	Cast Subcomponents, Welded Assembly, CNC Milled Ends	Y	DG	-	[31, 39]
	Continuous	Continuous	DC	N/A	N	PS	None	[40, 41]
	NS: Cut/Mill	Welded						
	NS: Cut/Mill	Welded	DC	N/A	N	MPS	-	[42-44]
	NS: Cut/Mill	Welded	DC	N/A				
	S: 90 Degree Cut	Welded	SAF	CNC Milled	Y	-	-	[31]
	NS: Traditional Steel Framing	Typical Bolted Steel Frame	DC	None	Y	SP	- -	[5, 45-47]
	S: Exposed End Component	Bolted (Exposed, Splice)	MABU	Welded assembly or plate subcomponents	N	DG	-	[6, 49, 50]
	S: Concealed End Component	Bolted (Exposed, 2 Directions)				SP	-	
	S: Exposed End Component	Bolted (Exposed, from Node)	SAF	CNC milling of forged subcomponents	N	PS	None	[9, 31, 51]
	S: Exposed End Component	Bolted (Exposed, from Node)	SAF	CNC milling of forged subcomponents	N	DG	-	[9, 31, 51]
	NS: Cut/Mill	Welded	DC	None	N	CS	SV	[13, 52-55]
	NS: Cut/Mill	Welded	DC	None	N	DG	-	[47, 56, 57]
	S: 90 Degree Cut	Welded	SAF	CNC Milled	N	DG	-	[24, 31, 58]
	NS: Cut/Mill	Welded	SAB	NC Cutting	N	DG	-	[11, 59]
	S: Concealed End Component	Bolted (Concealed, From Member)	MAH	CNC cutting of subcomponents; manual welding of assembly; mechanical finishing of end faces	N	DG	-	[10, 60]
	S: 90 Degree Cut	Welded	MAS	CNC Milling	N	DG	-	[28, 61, 62]
	NS: Cut/Mill	Welded	SAB	Cut from plate				
	S: Exposed End Component	Bolted (Concealed, From Member)	SAF	CNC Machining	N	PS	None	[63-65]

>>>

#	Project Info	Approximate Surface Area	Surface Qualification	Panelization	Profile Geometry	Profile Width/Diameter	Profile Depth	
20	Cybele Palace Roof, 2009, ES	3 000	Form-Active	Tri	Rect. Hollow	80	80-120	
21	De Blob Façade & Roof, 2010 NL	2 940	Freeform	Tri	Rect. Built-up	60	75	
22	Dutch Maritime Museum Roof, 2011, NL	1 000	Form-Active	Tri/ Quad/ Pent	Rect.	40, 60	100-180	
23	Shaw Center Façade, 2011, CA	2 700	Freeform	Tri	Rect. Hollow	-	-	
24	Mansueto Library Roof, 2011, US	2 800	Translation	Quad	Circular	-	-	
25	Hyatt Capital Gate Façade, 2011, AE	23 000	Freeform	Tri	Rect. Hollow	-	-	
					Rect. Hollow	-	-	
					Triangular	-	-	
26	King's Cross Roof, 2012, UK	600	Revolution	Tri	Circular .	139-219	N/A	
					Rect.	150	150-450	
27	Paunsdorf Center Roof, 2012, DE	-	Translation	Quad	Rect. Hollow	40, 50	80, 90	
28	Höfe am Brühl Roof, 2012, DE	-	Freeform	Tri	Rect. Solid	50	70-100	
29	Gardens By The Bay Façade & Roof, 2012, SG	-	Revolution	Quad	Tapered Rectangle	-	-	
30	Carioca Wave Canopy, 2013, BR	1130	Freeform	Tri	Rect. Built-up	82	200	
31	Ex Unione Militare Façade & Roof, 2013, IT	2000	Freeform	Tri	Rect. Hollow	-	-	
32	Ernst & Young Plaza Roof Canopy, 2014, LU	-	Scaled Translation	Quad	Rect. Hollow	80	140	
33	Bory Mall Façade & Roof, 2014, SK	2500	Freeform	Tri	Rect. Hollow	70 -76	120-180	
34	Musée Des Confluences Façade & Roof, 2014, FR	3 500	Freeform	Tri	Rect. Hollow	80	180	
						250	450	
35	34th Street Canopy, 2015 US	-	Rotational	Quad	Rect. Solid	-	-	
36	Chadstone Shopping Center Roof, 2016, AU	7080	Form-Active	Quad	Rect. Hollow	82	220	
37	Grand Hotel Dieu Roof, 2018, FR	1050	Freeform	Tri	T Built-Up	-	Varies	
38	Capital C Façade & Roof, 2019, NL	-	Freeform	Quad	Rect. Hollow	100	200	
39	Moynihan Train Station Roof, 2019, US	5116	Form-Active	Quad	T	-	Varies	
40	Jewel Changi Airport Façade & Roof, 2019, SG	50 000	Rotational	Tri	Rect. Hollow	120	250 - 750	

End Condition: S = Standard; NS = Non-Standard; C/M = Cut/Mill;

Node Typology: MAH = Multi-Axis Hollow ; MAS = Multi-Axis Sull; MABU = Multi-Axis Built-Up; SAF = Single-Axis Faceted; SAC = Single-Axis Cylindrical; SAB = Single-Axis Bisecting; S = Stacked; DC = Direct Connection

	Profile End Condition	Structural Connection	Structural Node Typology	Structural Node Fabrication	Cables	Enclosure Typology	Gasket Joining Strategy	Sources
	S: Concealed End Component	Bolted (Exposed, Blind)	SAF	CNC Milling	N	DG	-	[1, 31, 66]
	NS: Cut/Mill	Welded	SAB	-	N	DG	-	[7, 59, 67, 68]
	NS: Cut/Mill	Welded	SAC	-	N	DG	C	[2, 69-71]
	S: Exposed End Component	Bolted (Concealed, From Member)	SAF	CNC Milled	N	PS	None	[47, 72]
	S: Concealed End Component	Bolted (Concealed, From Member)	MAH	CNC milling, welded assembly	N	SP	CJS	[73-75]
	NS: Cut/Mill	Welded	SAB	Built-up plates	N	MPS	-	[77-79]
	S: Exposed End Component	Bolted (Covered, Splice)						
	NS: Cut/Mill	Welded	DC	None				
	NS: Cut/Mill	-	SAC	-	N	SP	C	[47, 80-82]
	NS: Cut/Mill	Welded	DC	None				
	S: 90 Degree Cut	Welded	MAS	CNC milling	N	DG	-	[31]
	NS: Notch	Bolted (Exposed, Splice)	SAC	-	N	DG	-	[31]
	S: 90 Degree Cut	Welded	SAF	-	Y	DG	C	[47, 79]
	S: Concealed End Component	Bolted (Concealed, From Member)	MAH	CNC Milling & Welded Assembly	N	DG	-	[12]
	NS: Cut/Mill & Recessed End Component	Welded	SAC	-	N	DG	CJS	[84-88]
	S: 90 Degree Cut	Welded	MAS	CNC Milling	N	DG	-	[31, 89]
	S: Concealed End Component	Bolted (Concealed, From Member)	MAS	CNC Milling	N	DG	-	[90-92]
	S: 90 Degree Cut	Welded						
	-	-	DC	None	N	SP	-	[14, 93, 94]
	S: Notch	Bolted (Exposed, Splice)	MAS	CNC Machining	N	DG	IM	[95, 96]
	S: Concealed End Component	Bolted (Concealed, From Member)	MAS	CNC Machining	N	DG	CJH	[3, 97-100]
	-	Welded	SAC	-	N	DG	CJH	[101, 236]
	NS: Cut/Mill	Welded	DC	None	N	DG	CJH	[102, 103]
	-	Welded	SAF	-	Y	CS	-	[104-107]
	S: Concealed End Component	Bolted (Concealed, From Member)	MAS	5-Axis CNC Milling	N	DG	CJH	[26, 108-111]
	S: 90 Degree Cut	Welded						

Enclosure Typology: DG = Directly Glazed; SP = Secondary Profile; PS = Point Supported; CS = Cassette System; MPS = Mega-Panel System

Gasket Joining Strategy: CJS = Cut & Join Single Layer; CJH = Cut & Join Hierarchical Layers; IM = Injection Moulding; C = Circular; SV = Silicone Variform

Curriculum Vitae



Lia Tramontini

Contact:

Lia.Tramontini@gmail.com

- 1992** Born in Sudbury, Canada
- 2010-2015** Bachelor of Architectural Sciences, University of Waterloo, Canada
- 2014-2017** Façade Technical and Computational Designer, Walter P Moore, United States
- 2017-2019** Master of Building Technology, Technical University of Delft, the Netherlands
- 2017-2021** Quality Control and Research Lead, Neme Design Studio
- Since 2019** Member of the Façade Research Group, Technical University of Delft, the Netherlands
- 2020** Façade Design, knippershelbig GmbH
- Since 2023** Project Manager in Research & Development, Jansen AG

Publications

Journal Publication :

Oppe, M., L. Tramontini, and S. Thieme, *Additive Fertigung von freigeformten Stahl-Glas-Konstruktionen*, in *Glasbau 2023*. 2023, Ernst & Sohn GmbH : Berlin, Germany. p. 21-32.

Conference Publication :

Tramontini, L., S. Thieme, and L. Giampellegrini, *Towards the additive manufacturing of freeform steel and glass façades*, in *Advanced Building Skins*. 2022: Bern, Switzerland.

Towards the Integration of Additive Manufacturing for Freeform Steel and Glass Façade Construction

Lia Tramontini

The thesis, titled 'Towards the Integration of Additive Manufacturing for Freeform Steel and Glass Façade Construction,' explores the transformative role of additive manufacturing (AM) in enhancing the design and construction of Freeform Steel and Glass Façades (FFSGF). These façades involve intricate components, necessitating collaborative efforts among designers, engineers, and fabricators to achieve complex façade geometries with good performance while ensuring efficiency in design, material usage, fabrication, and cost. Recent advancements in AM technology have made it a potentially viable and increasingly accessible fabrication strategy, particularly for mass-customized components such as those used in freeform construction. The research aims to answer the central question of how AM can effectively contribute to developing node solutions supporting Freeform Steel & Glass Façade (FFSGF) construction. The study systematically examines opportunities for improvement in existing solutions. Chapters 2 and 3 provide a critical overview of FFSGF construction typologies and explore the current landscape of AM in façade applications. Chapters 4 and 5 delve into the design and development of crucial components—structural nodes and gasket nodes—utilizing different AM technologies. Prototypes are manufactured and evaluated in comparison to existing solutions. Chapter 6 provides a case study of integrating AM product development into a larger construction project, emphasizing interdisciplinary collaboration. The thesis underlines the advantages of the systemization of AM node design throughout the design and fabrication of AM nodes. This research contributes to the evolving knowledge at the intersection of design, engineering, construction, and AM, aiming to provide a valuable resource for building industry professionals navigating the complexities of incorporating AM into the fabrication of freeform steel and glass façades.

A+BE | Architecture and the Built Environment | TU Delft BK